



SNC • LAVALIN

# Inner Harbour Sediment Stability Study - Kingston Inner Harbour Transport Canada and Parks Canada Water Lot Kingston, Ontario

Public Services and Procurement Canada



Environment et Geoscience

March | 2020

Report  
Ref. Interne 653502-EG-L01-01



## Inner Harbour Sediment Stability Study – Kingston Inner Harbour Transport Canada and Parks Canada Water Lot Kingston, Ontario

Public Services and Procurement Canada

Prepared by:



**Patrick Verhaar, Ph.D.**  
Project leader - Fluvial and coastal geomorphologist  
*Environment & Geoscience*  
**Engineering, Design & Project Management**

Approved by:



**Stephane Lorrain, Geo., MSc.**  
Senior project director  
*Environment & Geoscience*  
**Engineering, Design & Project Management**

O/Reference No.: 653502  
O/Document No. : 653502-EG-L01-01

March 2020

Distribution : Mr. Paul Schiller (1 copy)

SNC-LAVALIN Environment & Geoscience. 2020. Report 653502-EG-L01-PA. Montreal, 97 pages. + app.



## NOTICE

This report has been prepared and the work referred to in this report has been undertaken by SNC-Lavalin Inc., for the exclusive use of PSPC (the Client), who has been party to the development of the scope of work and understands its limitations. The methodology, findings, conclusions and recommendations in this report are based solely upon the scope of work and subject to the time and budgetary considerations described in the proposal and/or contract pursuant to which this report was issued. Any use, reliance on, or decision made by a third party based on this report is the sole responsibility of such third party. SNC-Lavalin Inc. accepts no liability or responsibility for any damages that may be suffered or incurred by any third party as a result of the use of, reliance on, or any decision made based on this report.

The findings, conclusions and recommendations in this report (i) have been developed in a manner consistent with the level of skill normally exercised by professionals currently practising under similar conditions in the area, and (ii) reflect SNC-Lavalin Inc.'s, best judgment based on information available at the time of preparation of this report. No other warranties, either expressed or implied, are made with respect to the professional services provided to Client or the findings, conclusions and recommendations contained in this report. The findings and conclusions contained in this report are valid only as of the date of this report and may be based, in part, upon information provided by others. If any of the information is inaccurate, new information is discovered or project parameters change, modifications to this report may be necessary.

This report must be read as a whole, as sections taken out of context may be misleading. If discrepancies occur between the preliminary (draft) and final version of this report, it is the final version that takes precedence. Nothing in this report is intended to constitute or provide a legal opinion.

The contents of this report are confidential and proprietary. Other than by the Client, copying or distribution of this report or use of or reliance on the information contained herein, in whole or in part, is not permitted without the express written permission of the Client and SNC-Lavalin Inc.

## Project Team

### Client

Mr. Paul Schiller,	Project Manager
Mr. Javier Banuelos,	Project Manager

### SNC-Lavalin GEM Québec inc.

Melanie Siewert, M. Sc.	Project Manager
Stephane Lorrain, M. Sc.	Project Director
Patrick Verhaar, Ph.D.	Data processing and redaction
Sara Dubosq, eng. MSc.	Data processing and Stage 2 surveys
Veronique Proulx, B.eng.	Surveys
Romain Rosant, B.Sc.	Surveys
Pierre-David Beaudry,	Surveys
Sébastien Boyer-Levesque,	Surveys
Jérémie Desrosiers,	Surveys

### Edition

Mélanie Hunault	Administrative Assistant
-----------------	--------------------------

## Summary

As outlined in the PWGSC TOR, the goal for this project is to conduct a Harbour Wide Sediment Stability Study appropriate for the nature and size of sediment contamination and in the water lot to the south of Belle Island. In order to gain better understanding of the hydraulic circulation dynamics in the Kingston Inner Harbour (KIH) and sediment dynamics in the areas of concern, water lots TC-4; TC-2A; TC-RC and PC-W two stages of surveys were organized.

For stage one surveys, seasonal measurements of water velocity, turbidity and suspended sediment were undertaken at four key moments (late spring, summer, fall and spring) at 22 stations within the KIH basin. Time series of water levels, and weather conditions (wind speed, wind direction and atmospheric pressure) were collected from June 2018 until June 2019.

For stage two surveys, tubular core samples were collected at 6 locations to determine sedimentation rate and mixing conditions using radioisotopes ( $^{210}\text{Pb}$ ,  $^{137}\text{Cs}$ ). Four box-core samples, one within each water lot, were collected to determine onset of sediment mobilization and erosion rate using a Core Mini Flume (CMF).

The stage one results show that water velocities in the KIH basin are low and do not have a well-established circulation pattern. The suspended sediment and turbidity are low, and peaks in turbidity are observed during south to eastern wind induced wave events. The water levels in the KIH are controlled by Lake Ontario and the St-Lawrence River discharge. The analysis of water level confirms that KIH water level are closely following fluctuations in Lake Ontario water levels from wind setup and seiche events. The wavelet analytics show that long period oscillations in Lake Ontario water level propagate into the KIH.

Stage two results show very low sedimentation rates from the radio isotopic sediment dating. Towards the northern part, water lot PC-W and TC-1, sedimentation rates increase, most likely related to the adjacent landfill area. Erodibility experiments on the box-core samples show low near bottom water velocities for water lots TC-4; TC-2A and PC-W of around 0.06 m/s with water lot TC-RC being more resistant to re-suspension with a critical velocity of 0.16 m/s.

In the areas of interest, near-bottom velocities exceed critical water velocity for resuspension under easterly and south-easterly wind conditions. With regards to resuspension caused by boat traffic, namely pleasure crafts, it is likely very low or non-existent given that the whole area is covered by dense aquatic vegetation. The vegetation will limit the ability for boats to travel at high speed and will also attenuate any disturbance quickly. Finally, the hydraulic influence on water velocities and subsequent sediment re-suspension of the Cataraqui River is very limited.

Our study shows that the KIH is a quiescent environment which promotes sediment settling with the presence of aquatic plants that have a stabilizing effect on the fine organic sediments. Re-suspension of sediments does occur under East to South wind conditions, but overall low water velocities will limit the travel distance of resuspended sediments. Further attenuation of wind wave resuspension and sediment transport is expected with the extensive and dense macrophyte beds that cover over 80% of Kingston Inner Harbour.

## Table of Content

1	Introduction	1
2	Methodology	2
2.1	Stage One Surveys - Hydraulic Study	2
2.1.1	Seasonal Measurements	2
2.1.2	Time Series Measurements	7
2.2	Stage Two Surveys - Sediment Dynamics	7
2.2.1	Sediment Dating	7
2.2.2	Sediment Resuspension Experiment	9
3	Results	13
3.1	Stage One Surveys - Hydraulic Study	13
3.1.1	Seasonal Measurements	13
3.1.2	Time Series Measurements	15
3.1.3	Kingston Inner Harbour Wave Modeling	32
3.2	Stage Two Surveys - Sediment Dynamics	36
3.2.1	Sediment Dating	36
3.2.2	Sediment Resuspension Experiment	79
4	Discussion	85
4.1	Physical setting	85
4.2	Sediment type and distribution	88
4.3	Sediment rates	88
4.4	Sediment erodibility	91
4.5	Water Level	92
4.6	Aquatic Vegetation	93
4.7	Climate change	95
5	Conclusion	97
6	References	98

## List of Tables

Table 1	Wind statistics for 2018-2019 at the LaSalle Causeway	16
Table 2	Wind frequency distribution per direction at the LaSalle Causeway weather station (2018-2019)	17
Table 3	Wind velocity with 1-, 10- and 50-year return period for South, South-East and East direction.	20
Table 4	Wind and wave characteristics and bottom velocity and sampling locations within the Kingston Inner Harbour that generate the highest near-bottom water velocity	36
Table 5	Core 1A – Sample description	39
Table 6	Core 2A – Sample description	44
Table 7	Core 3A – Sample description	51
Table 8	Core 4A – Sample description	58
Table 9	Core 2B – Sample description	65
Table 10	Core 2B – Regression fit as a function of background subtracted	66
Table 11	Core 4B – Sample description	73
Table 12	Average sedimentation rates based on accumulation rate and density	78
Table 13	TSS – Tu linear regression results and offsets for the three turbidity sensors	81
Table 14	Threshold water velocity at 0.04 m above the bottom for each of the box cores.	81
Table 15	Estimated depth of post 1966 sedimentation and modern sedimentation rates	90
Table 16	Sediment accumulation rate ( $^{210}\text{Pb}$ ) and settling conditions inferred from $^{210}\text{Pb}$ and $^{137}\text{Cs}$ inventories	90
Table 17	Comparison of the near bottom orbital velocities obtained from the wave model and the erosion threshold velocities measured during the erodibility experiment for return periods of 1, 10 and 50 yr.	92
Table 18	Summary of the wavelet analysis for Kingston and LaSalle causeway stations showing the seasonal recurrence of oscillation events and range of corresponding water level variations.	93

## List of Figures

Figure 1	Calendar of all field survey activities	3
Figure 2	Location of sampling and monitoring stations	4
Figure 3	Representation of the gravity/percussion corer used to collect samples for the radio-isotopic analysis (left) and sample collection from the ice cover (right: February 2019).	9
Figure 4	Representation of the diver box core (top) and sampling from the ice cover using commercial divers (bottom March 2019)	10
Figure 5	Schematic of the CMF and example showing the apparatus installed in one of the box cores	12
Figure 6	Average flow speed and direction measured during the 4 field visits	14
Figure 7	Relationship of Total Suspended Solids concentration versus Turbidity measurements for visits 2, 3 and 8 combined	15
Figure 8	Wind data from the LaSalle Causeway weather station (2018/06/13 – 2019/06/08)	16
Figure 9	Weather station at the Kingston airport (1970/01/01 – 2019/12/31)	19
Figure 10	Return period of the wind depending on its direction.	19
Figure 11	Water level correlation between stations (period)	20
Figure 12	Water level comparison between LaSalle Causeway and Rideau Marina stations	21
Figure 13	Wavelet analysis results showing significant oscillation events of different period (black line) for the Kingston CHS and LaSalle Causeway stations, during autumn 2018 (a, b), winter 2018-2019 (c, d), and spring 2019 (e, f)	23
Figure 14	Wavelet analysis of water level time series from September 2018, observed only in the Kingston Inner Harbour (24 h period). Significant events (95% confidence) are identified with a black line	26
Figure 15	Near bottom water velocity and wave height from waves at the downstream water level station along the observed wind speeds	28
Figure 16	Turbidity and wave bottom velocity relationship	30
Figure 17	Bathymetry of the bay,	34
Figure 18	Significant wave height for winds with 50-year return period for the (a) East; (b) South-East; (c) South directions and the associated near bottom water velocities for (d) East (e) South-East (f) South directions	35
Figure 19	<sup>210</sup> Pb – Profile results of core 1A	40
Figure 20	<sup>137</sup> Cs - Profile results of core 1A	41
Figure 21	<sup>210</sup> Pb – Profile results of core 2A	45
Figure 22	<sup>137</sup> Cs - Profile results of core 2A	48
Figure 23	<sup>210</sup> Pb – Profile results of core 3A	52
Figure 24	<sup>137</sup> Cs - Profile results of core 3A	55
Figure 25	<sup>210</sup> Pb – Profile results of core 4A	59
Figure 26	<sup>137</sup> Cs - Profile results of core 4A	62
Figure 27	<sup>210</sup> Pb – Profile results of core 2B	67
Figure 28	<sup>137</sup> Cs - Profile results of core 2B	70
Figure 29	<sup>210</sup> Pb – Profile results of core 4B	74
Figure 30	<sup>137</sup> Cs - Profile results of core 4B	77
Figure 31	Regression suspended sediment and TU sensors for each core experiment	80

Figure 32	Suspended particle matter (left) and Erosion rates (right) for each core. The start of resuspension is indicated by the vertical dashed line and critical velocity by the horizontal dashed line	83
Figure 33	Total suspended solids versus applied velocity for all cores at 3 elevations	84
Figure 34	Bathymetry of Kingston Inner Harbour	85
Figure 35	Simulated water velocity in the Cataragui River according to HCCL, 2011	87
Figure 36	Google earth close-up of Navigation traces in macrophyte beds around the Kingston Rowing Club (3 September 2015)	94
Figure 37	Macrophyte beds in the KIH basin, delimitation from satellite image September 6, 2015 with color clustering, plus images from under water camera from field visit on February 2 <sup>nd</sup> 2019	96

## List of Appendices

Appendix 1	Time Series of Wind, Atmospheric Pressure and Water Level
Appendix 2	Input parameters and validation CMS wave model
Appendix 3	Results of wave simulation
Appendix 4	Radio Isotopic Analysis Core 1A
Appendix 5	Radio Isotopic Analysis Core 2A
Appendix 6	Radio Isotopic Analysis Core 3A
Appendix 7	Radio Isotopic Analysis Core 4A
Appendix 8	Radio Isotopic Analysis Core 2B
Appendix 9	Radio Isotopic Analysis Core 4B
Appendix 10	Core extraction forms and photos

## Definitions and Acronyms

ADCP:	Acoustic Doppler Current Profiler
ADV:	Acoustic Doppler Velocimeter
CMF:	Core Mini Flume
CRM:	Certified Reference Material
CRS:	Constant Rate of Supply
KIH:	Kingston Inner Harbour
MDL:	Method Detection Limit
POT:	Peak Over Threshold
TSS:	Total Suspended Solids
Tu:	Turbidity
H <sub>s</sub> :	Significant wave period, corresponding to mean wave height (trough to crest) of the highest third of the waves
T <sub>p</sub> :	Peak period, corresponding to the period of the maximum energy of the wave spectra.
u <sub>o</sub> :	bottom velocity generated by the water particle displacement of a given wave
k:	wave number ( $2\pi/L$ )
L:	wavelength
h:	water column height
I <sub>1</sub> :	<sup>210</sup> Pb inventory (DPM/cm <sup>2</sup> ) below depth 30.5 cm
I <sub>T</sub> :	total <sup>210</sup> Pb inventory (DPM/cm <sup>2</sup> ) in core (artificial)

## 1 Introduction

As outlined in the PWGSC TOR, the goal for this project is to conduct a Kingston Inner Harbour (KIH) Wide Sediment Stability Study and further inform the Conceptual Sediment Model (CSM) that has been established for the site (Golder, 2017):

- › appropriate for the nature and size of sediment contamination;
- › in the water lots to the south of Belle Island, and particularly within the four (4) areas identified for focused investigation;
- › to provide quantitative and descriptive information about the forcing agents contributing to sediment transport under site specific conditions (wind, wave, water level, boating, etc.).

Surveys were organized in two stages to gain a better understanding of:

- › Stage 1 surveys – Hydraulic Study
  - Hydraulic circulation and total suspended solids (TSS) variation;
  - Water level variations, wave regime and flushing conditions within KIH.
- › Stage 2 Surveys – Sediment Dynamics
  - Threshold for sediment stability;
  - Sediment deposition conditions within KIH.

The specific objectives were:

- › Seasonal hydraulics surveys:
  - Measure flow (speed and direction) on a network of stations across the KIH at different seasons to determine if there is a predominant circulation pattern;
  - Characterize weather conditions (wind speed and direction) and water level variations at the LaSalle Causeway and the Rideau Marina (water level only) to describe the wave regime and the possible seiche events that may contribute to increasing flushing within KIH;
  - Collect water samples for the determination of background TSS and correlation with turbidity (Tu) measurements to further describe sediment resuspension events.
- › Sediment dynamics:
  - Collect sediment cores to determine sedimentation rates using radioisotopes ( $^{210}\text{Pb}$ ,  $^{137}\text{Cs}$ ) in the areas of interest;
  - Determine onset of sediment mobilization and erosion rate using a Core Mini Flume (CMF) from box cores in the areas of interest.

A third stage which comprised a harbour-wide sediment sampling program<sup>1</sup> was removed from the scope of work.

---

<sup>1</sup> The sampling program using a grab sampler, aimed at collecting surface sediment samples at 276 stations. This would have been the first full-scale characterization of the sediment physical properties carried out in KIH and was key at informing the CSM. The results would have served as inputs in a Sediment Trend Analysis aimed at describing sediment pathways and identifying areas of sedimentation and erosion. Its purpose was to provide an understanding of the processes and dynamics of the harbor with respect to sediment sources, transport, and behavior.

## 2 Methodology

### 2.1 Stage One Surveys - Hydraulic Study

The stage one surveys are based on a combination of time series measurements of weather (wind speed and direction) and water levels, to infer the wave regime over the Kingston Inner Harbour, and seasonal surveys to characterize flow (speed and direction) and the concentration of suspended solids over one year (late Spring to early Spring). The calendar of field activities is presented in Figure 1.

#### 2.1.1 Seasonal Measurements

Seasonal measurements aim at characterizing the circulation pattern (flow speed and direction, discharge) in and out of the KIH study area. A network of 22 stations (Figure 2a) was visited 4 times during the 2018 – 2019 field season (Figure 1). The site was visited in late Spring/early Summer (June 2018: installation), late Summer (September 2018: low flow), late Fall (November 2018: Fall freshet) and Spring (June 2019: Spring freshet). Because the flow was so weak, at any season, the measurements were averaged over periods of 5 to 10 minutes.

Flow measurements were performed at each station using an acoustic doppler current profiler (ADCP) (Teledyne RiverPro). In November 2018, only stations where significant flow was observed previously were visited<sup>2</sup>. A turbidity profile was also performed at each station over the whole water column and water samples were collected for the determination of the TSS concentration near the surface and wherever possible near the bottom.

Discharge was measured at Belle Island and at the La Salle Causeway (Figure 2) using the ADCP. Again, low-flow conditions were a challenge in obtaining meaningful results.

Field visits were scheduled as follows:

- › Spring (June 2018):
  - Installation of monitoring stations
  - TSS & Tu profiling
  - ADCP profiling
- › Summer (September 2018):
  - TSS & Tu profiling
  - ADCP profiling
- › Fall (October 2018):
  - Install monitoring buoy
  - Reconfigure tide/wave sensor
- › Fall (November 2018):
  - TSS & Tu profiling
  - ADCP profiling
- › Spring (June 2019):
  - TSS & Tu profiling
  - ADCP profiling
  - Disassembling the monitoring stations

---

<sup>2</sup> The November 2018 field visit was supplementary to the planned program. Because of the harsh weather, a reduced number of stations were visited.



**Figure 2**      **Location of sampling and monitoring stations**







## 2.1.2 Time Series Measurements

Two hydrometric stations were installed upstream and downstream of the study area.

- › The downstream station was located at the LaSalle Causeway (Figure 2b). It comprised two data loggers (Campbell Scientific CR1000 and CR300) to measure weather parameters (wind speed<sup>3</sup> and direction, air temperature and atmospheric pressure) and water level respectively.
- › The upstream station was located at the Rideau Marina. It comprised a submerged pressure sensor<sup>4</sup> for water level measurement.
- › Sampling frequency for water level measurements was 10 min.

A submerged instrumented frame was initially planned to measure flow speed and direction, turbidity and wave height<sup>5</sup>. The proposed location for the frame was located just offshore of the Kingston Rowing Club, along the dredged channel which is free from aquatic vegetation. The bottom conditions proved too soft to support the weight of the frame which sank into the soft sediments at the time of deployment. Consequently, the instruments were installed along one of the Kingston Rowing Club's docks and at Molly Brant Point for a short time until a monitoring buoy was prepared (Figure 2b).

The complete time series are presented in Appendix 1. Quality control Matlab routines were applied to check for time consistency, coherent trends and to identify outliers. This was followed by a visual verification of all flagged data to confirm the results from the QAQC routines.

## 2.2 Stage Two Surveys - Sediment Dynamics

### 2.2.1 Sediment Dating

#### 2.2.1.1 Core Sampling

Undisturbed sediment cores were collected during the winter at 6 stations (Figure 2c) located in the following water lots: TC-4 (core 1A), TC-2A (core 2A), TC-RC (core 3A) and PC-W (core 4A). Two additional sites were sampled to obtain longer cores from deeper substrate, at locations where accumulation conditions would likely be better. Core 2B and core 4B were collected south and north of water lot TC-1, respectively (Figure 2c). The sampling location was also constrained by the ice cover thickness and thickness of the soft sediment horizon.

Sample collection was performed using a light gravity/percussion corer (Figure 3) using a clean, clear polycarbonate core barrel (68/71 mm id/od x 140 cm and 200 cm long). The cores were divided into subsamples every centimetre using an incremental core extruding apparatus to provide consistent subsamples using 10 mm disk spacers. These subsamples were kept in clean heavy walled polypropylene jars that were destined for the following analysis:

- › Physical parameters:
  - Specific weight,
  - Specific density,
- › Radio-isotopes:
  - <sup>210</sup>Pb, <sup>137</sup>Cs to measure sedimentation rate,

---

<sup>3</sup> Average speed (10 seconds and 2 minutes), wind gust using a RM Young Marine sensor.

<sup>4</sup> Self logging RBRduet T.D|wave.

<sup>5</sup> Nortek Vector single point current meter, RBR Concerto logger equipped with a Seapoint turbidity sensor, RBRduet T.D|wave submerged pressure sensor.

Care was taken to provide homogeneous samples without loss of water from the sample to provide representative dry bulk density results. The subsampling interval and the core diameter were adequate in providing enough sample volume for the respective analysis:

- ›  $^{210}\text{Pb}$ : > 0.5 – 1.0 g (equivalent dry wt.) per sample
- ›  $^{226}\text{Ra}$ : > 1.0 – 2.0 g (equivalent dry wt.) per sample
- ›  $^{137}\text{Cs}$ : > 5 g (equivalent dry wt.) per sample

### 2.2.1.2 Radio-Isotopic Determination

A certain number of samples were subsequently analyzed (Flett Research Ltd., Winnipeg) for the different radio isotopes  $^{210}\text{Pb}$ ,  $^{137}\text{Cs}$  and  $^{226}\text{Ra}$ . The  $^{210}\text{Pb}$  and  $^{137}\text{Cs}$  isotopes were used to determine the rate of sediment accumulation in lakes, oceans and other water bodies. It is typical to analyze 10 - 20 sections of a sediment core for  $^{210}\text{Pb}$  and  $^{137}\text{Cs}$ , covering an accumulation period of about 160 years. The age of the sediment from a depth in the sediment column can then be inferred.

The  $^{210}\text{Pb}$  results are normally modelled to obtain the best fit of the data using the constant rate of supply (CRS) model and/or the slope regression model are applied. Several  $^{226}\text{Ra}$  measurements are often required, usually 2 - 3 per core, to positively determine the  $^{210}\text{Pb}$  background level throughout the core length.

$^{137}\text{Cs}$  is used as an independent tracer to validate the  $^{210}\text{Pb}$  chronology. The  $^{137}\text{Cs}$  data is interpreted based on the 1959 and 1963 major input peaks or 1966 maximum inventory of the isotope in the northern hemisphere. The  $^{137}\text{Cs}$  peak input of 1963 or the maximum inventory of 1966 should correctly be predicted in the  $^{210}\text{Pb}$  model, for the latter to be valid. A plot of  $^{137}\text{Cs}$  activity vs. depth (cm) is supplied with the results.

Complete results are provided in Appendices 4 to 9 for cores: 1A; 2A; 3A; 4A; 2B and 4B respectively.

- ›  $^{137}\text{Cs}$  in sediment and soil is determined by counting the gamma emissions at 661.6 KeV that are emitted in 82.5% of the decays. The gamma radiation is relatively strong and therefore penetrates through several centimetres of sediment material with little attenuation. This procedure is modified from EML HASL-300 Method Ga-01-R (EML, 1997) and the method detection limit (MDL) with the HPGe (Germanium) detector is 0.3 DPM/g (95% confidence) for an 80,000 second counting period when measuring 9 g of dry samples. The method detection limit can be decreased to 0.1 DPM/g if 32 g of sample is used.
- ›  $^{210}\text{Pb}$  in sediment, soil and peat is by measurement of the  $^{210}\text{Po}$  granddaughter which is in secular equilibrium with  $^{210}\text{Pb}$  within 2 years of  $^{210}\text{Pb}$  deposition. This procedure is modified from Eakins and Morrison (1978). Samples are first spiked with a  $^{209}\text{Po}$  yield tracer, then digested in hot nitric acid. The digest is dried and made up in 1.5 N HCl and then the  $^{210}\text{Po}$  and  $^{209}\text{Po}$  alpha emitting isotopes are plated out on silver planchets followed by alpha spectrometry to determine the activity of the polonium isotopes. In the case of sediment and soil samples, an initial cleanup of samples may be done by distilling the polonium out of the samples at 500°C prior to nitric acid digestion. The detection limit (MDL) for 0.25 - 0.5 g (dry wt.) sample is between 0.1 - 0.2 DPM  $^{210}\text{Po}$ /g dry sample at a 95% confidence level for 60,000 second counting time. This can vary slightly and depends upon the amount of sample and the detector and recovery efficiency of each sample.
- ›  $^{226}\text{Ra}$  in sediment, soil and peat is determined by  $^{222}\text{Rn}$  emanation. This procedure is modified from that of Mathieu et al. (1988). The method detection limit (MDL) is dependent on the amount of sample analyzed. For a 60,000 second counting time the MDL @ 95% confidence for 2 g of dry samples is 0.1 DPM/g and for 0.5 g of dry samples is 0.5 DPM/g

**Figure 3** Representation of the gravity/percussion corer used to collect samples for the radio-isotopic analysis (left) and sample collection from the ice cover (right: February 2019).



## 2.2.2 Sediment Resuspension Experiment

### 2.2.2.1 Box Core Sampling

Large box cores were collected at 4 locations (Figure 2c) located in the water lots of interest (PC-W, TC-RC, TC-2A, TC-4) over the course of two days (March 19 and 20 2019). Cores 1A and 2A were collected about 90 m west of the planned point due to insufficient ice cover. Core 3A was difficult to collect because of the presence of sand and gravel which hindered pushing the box corer into the sediment. Eventually, the box corer was inserted deep into the sediment and fully closed with the sliding door with the assistance of the diver.

These undisturbed samples were destined for the sediment resuspension experiment using the CMF.

- › The CMF (Thompson et al. 2013) is a portable mini-flume that allows sediment stability and resuspension experiments to be undertaken on intact sediment cores rapidly after collection.
- › The CMF is built specifically to fit within a standard 300 mm (or larger) box core barrel. These large box corers could not be used as it requires heavy hoisting equipment aboard large vessels which cannot access the shallow waters of KIH.
- › Instead, a “diver box corer” was designed and built for the experiment (Figure 4).

**Figure 4 Representation of the diver box core (top) and sampling from the ice cover using commercial divers (bottom March 2019)**

No. article	Numéro de pièce	DESCRIPTION	Quantité
1	28390-1001	Boîtier échantillonneur	1
2	28390-1002	Panneau de côté	1
3	28390-1003	Glissière porte dessus	2
4	28390-1004	Porte dessus	1
5	28390-1005	Rail vertical porte tambour	2
6	28390-1007	Rail horizontal porte tambour	2
7	28390-1010	Renfort latéral	1
8	28390-1011	Panneau plexiglas	4
9	28390-1012	Rail courbe gauche porte tambour	1
10	28390-1013	Rail courbe droite porte tambour	1
11	28390-2000	Ass. Porte tambour	1
12	28390-1012	Lame de fond sédiment	2

NOUVELES MANIÈRES D'ÊTRE EN POUSSE SANS PRODIGES COMPANY TOUS SERVICES GÉNÉRALISÉS LEVAGE & DÉMONTAGE MAINTIEN PROTECTOR	<b>APR</b> ATELIER DE RÉVISION ROUILLER INC. TEL. (450) 467-5547 FAX (450) 467-3781 www.apr.ca	DESCRIPTION: Boîtier échantillonneur à sédiments QUANTITÉ: 19,42 kg APPROUVÉ PAR: M. G. B. B. B. DATE: 24-10-2018	NOM DU CLIENT: SNC Lavalin GEM PROJET: 28390 N° DE DROIT: 4 N° DE 0: 1 DE 2
---	---	--	--

a) Diver box core design



b) Diver box deployed from hoisting hut on the ice cover with support from professional divers



c) Overview of diver box

The “diver box corer” was based on the design of Carlton and Wetzel (1985). It is built of stainless-steel plates, with clear plexiglass windows and a polyethylene tambour door reinforced with SS rods and a cutting blade at the lower end. The surface area is 1,267 cm<sup>2</sup> (Figure 4).

The box core was lowered and raised using an electric winch from the diving hut which was installed on the ice cover and moved from station to station. Fieldwork was carried out in late March 2019 (Figure 1).

Close attention was paid not to disturb the collected sediment samples. The sampling method was designed to reduce any perturbation and the hoisting system used a davit and a winch to minimize shocks and vibrations of the samples. The experiment was carried out at the SNC-Lavalin office in Kingston, a short distance away from the sampling area to keep disturbance from transportation to a minimum. At the office, samples were preserved with an overlying layer of water which was oxygenated using an aquarium aerator to prevent decay. At the time of the experiment, care was taken to delicately remove the plant debris from the sediment surface, leaving the root system without reworking the sediments, such that the CMF could be inserted into the sediment without constraints.

#### 2.2.2.2 Core Mini Flume

The CMF (Figure 5) is a small annular flume based on the design of Thompson et al. (2013). It is itself based on the Mini Flume (Amos et al. 2000; Thompson and Amos 2002, 2004; Thompson et al. 2004; Widdows et al. 2007; Couceiro et al. 2013) and consists of two acrylic tubes 200 mm and 110 mm in diameter that form a measurement channel that is 40 mm wide. Four 2.5 cm<sup>2</sup> equidistantly spaced paddles generate a current. Paddle speed is controlled by a digital stepping motor (Intelligent Motion Systems, Inc.) commanded by a computer through a RS232 serial link.

The space within the core barrel allows a Nortek Vectrino ‘side looking’ Acoustic Doppler Velocimeter (ADV) to be fitted looking downwards to measure three components of flow velocity ( $u$  = azimuthal,  $v$  = radial, and  $w$  = vertical) at a height of 6 cm above the bed, with the sample cell being located approximately 4 cm above the bed. For comparisons to other systems, these velocities can be converted into bed shear stresses by the application of a power law (Soulsby, 1997):

$$u_* = 0.121 \left( \frac{D_{50}}{z} \right)^{1/7} U_z$$

And:

$$\tau_0 = \rho u_*^2$$

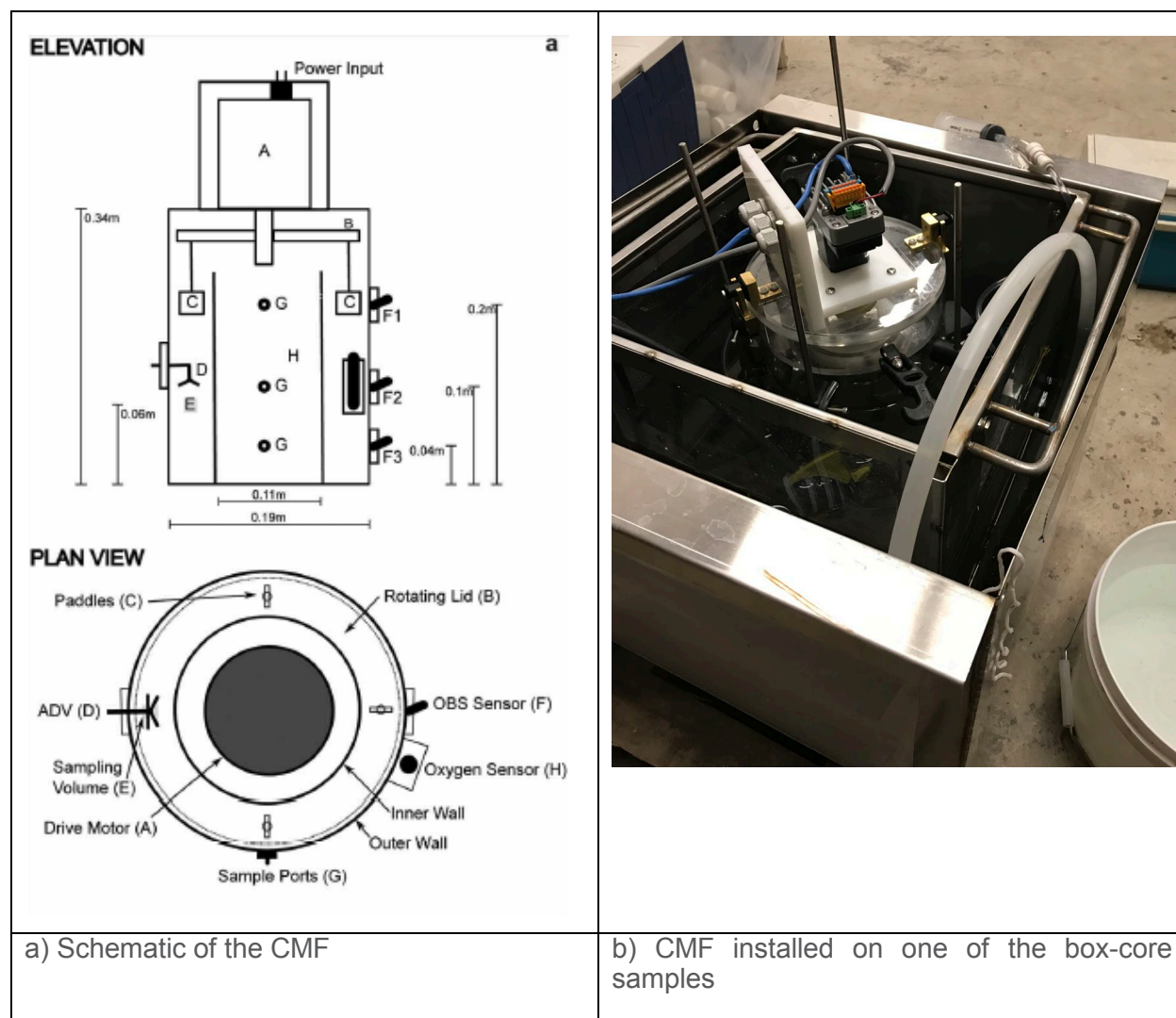
With the current design, the CMF will generate turbulent flow for the range of  $0.1 < u < 1$  m/s and transitional flow for the range  $0.04 < u < 0.6$  m/s under smooth bed conditions.

The CMF outer tube is equipped with three turbidity sensors (Seapoint Inc.) which detects light scattered by particles suspended in water, generating an output voltage proportional to turbidity or suspended solids. The sensors are placed at 4 cm, 10 cm and 20 cm from the bottom of the tube. Once inserted into the sediments, the bottom sensor is almost flush with the sediment / water interface. Beside each turbidity sensor, there is a sampling port to collect water samples throughout the experiment for the determination of the TSS concentration. The  $Tu - TSS$  relationship served to transform the turbidity data measured into TSS concentrations which are used in the calculation of the erosion rate.

The outer tube of the flume is initially placed into the sediment, away from the edges of the core barrel, which may have been disturbed during the core insertion. A plastic baffle is fitted 20 mm above the base on the outside the flume to act as an insertion guide. Three adjustable legs serve to keep the CMF apparatus at a constant level. This ensures consistent, flat placement of the flume into the bed while preventing it from sinking into the sediment under its own weight.

Once everything has settled and no turbidity or turbulence are observed in the tube, the experiment was started, and the paddle wheel speed of rotation was increased in steps. Each step lasted approximately 10 minutes or until the turbidity was decreasing. The steps were increased in small steps at the beginning to facilitate the identification of the threshold of sediment re-suspension. The experiments were conducted on the box core samples from April 4<sup>th</sup> to April 6<sup>th</sup> 2019, see Figure 1).

**Figure 5 Schematic of the CMF and example showing the apparatus installed in one of the box cores**



## 3 Results

### 3.1 Stage One Surveys - Hydraulic Study

#### 3.1.1 Seasonal Measurements

The flow velocities and directions measured during the four field visits are presented in Figure 6. The direction of the flow at any season does not demonstrate a clear circulation pattern in KIH (Figure 6). In addition, flow velocities averaged over the water column are weak with water velocities below 0.05 m/s for 90% of all measurements.

This indicates that the flow from the Catarauqui River does not have a significant influence on the entrainment of the water mass outside the navigation channel, where flow velocities are already weak. Furthermore, as the macrophyte beds develop during the open-water season, any circulation pattern would be further attenuated. In fact, the density of the aquatic plants was such at many of the sampling stations that flow velocities were often close to the detection limit of the ADCP.

Concomitant water samples and turbidity profiles were collected during ADCP profiling at each of the visits. The field visits were held at key hydrological moments during the open-water season (Figure 1):

- › Visit 1 – Late spring freshet early summer (mid-June 2018)
- › Visit 2 – Low flow conditions (September 2018)
- › Visit 3 – Fall freshet (November 2018)
- › Visit 8 – Spring freshet (early June 2019)

Measured TSS concentrations were very low<sup>6</sup> and showed a weak relationship with the turbidity. Concentrations were mostly below 6 mg/L with only two values reaching 12 mg/L and 14 mg/L during the Fall visit. There was a weak positive relationship between the turbidity and the TSS which show a high variability. The turbidity measurements were often difficult due to the high density of the aquatic plants which touched the lens of the turbidity sensor, generating outliers<sup>7</sup>. The linear regression is presented in Figure 7 for the combined data collected during visits 2, 3, and 8.

Summary:

Water velocities measured at 4 instances were very low. From the 22 stations no clear circulation pattern was observed. Sediment suspension and turbidity were very low and spikes in the turbidity were caused by the presence of plants and debris.

---

<sup>6</sup> During Visit 1, the detection limit was 1 mg/L and the resolution was 1 mg/L. The method was adapted for the next visits to increase the detection limit to 0.02 mg/L and the resolution to 0.01 mg/L.

<sup>7</sup> A MATLAB routine was applied to flag and filter any instantaneous increase larger than 10 NTU and outliers were removed when considered flawed.

**Figure 6 Average flow speed and direction measured during the 4 field visits**

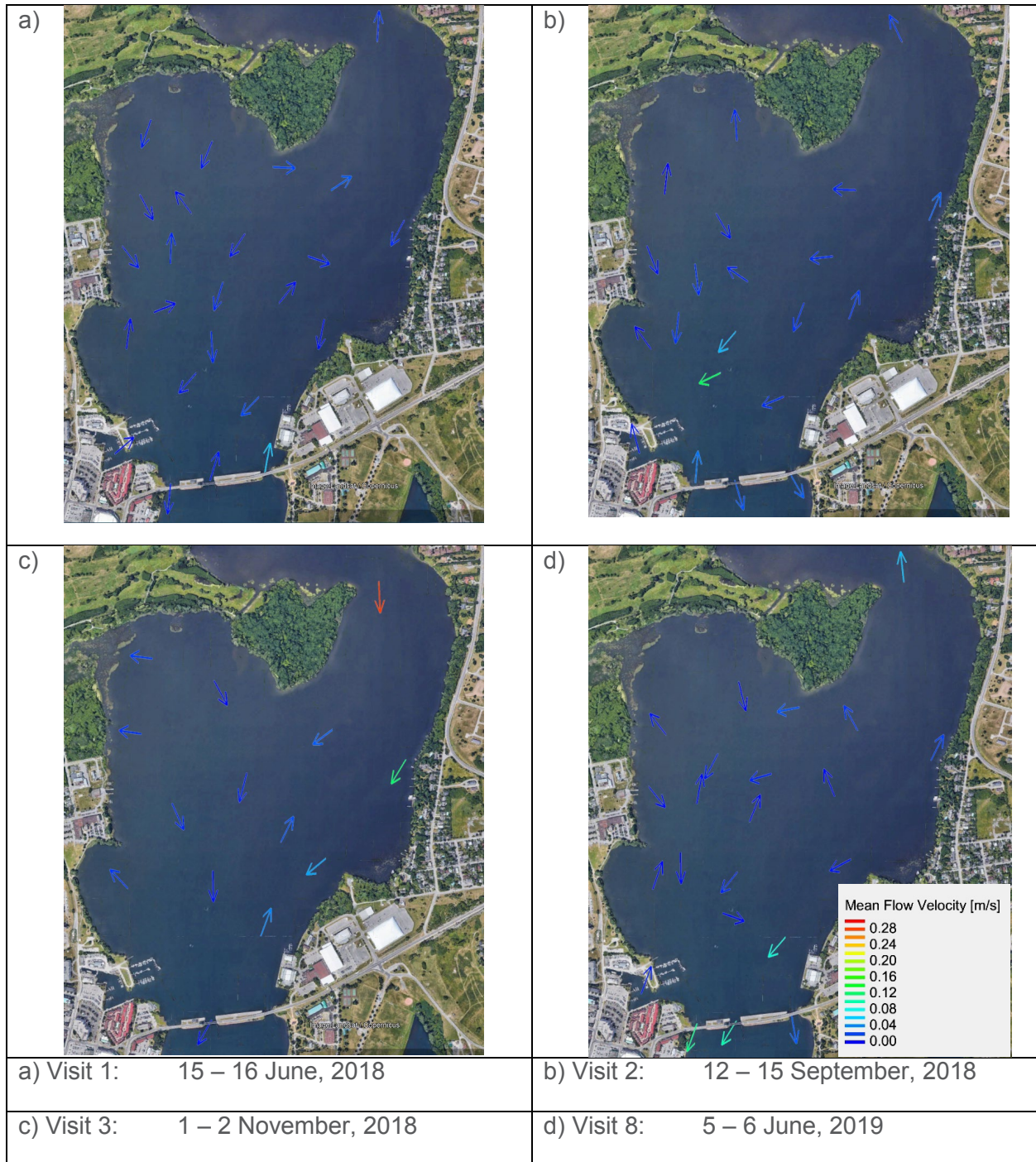
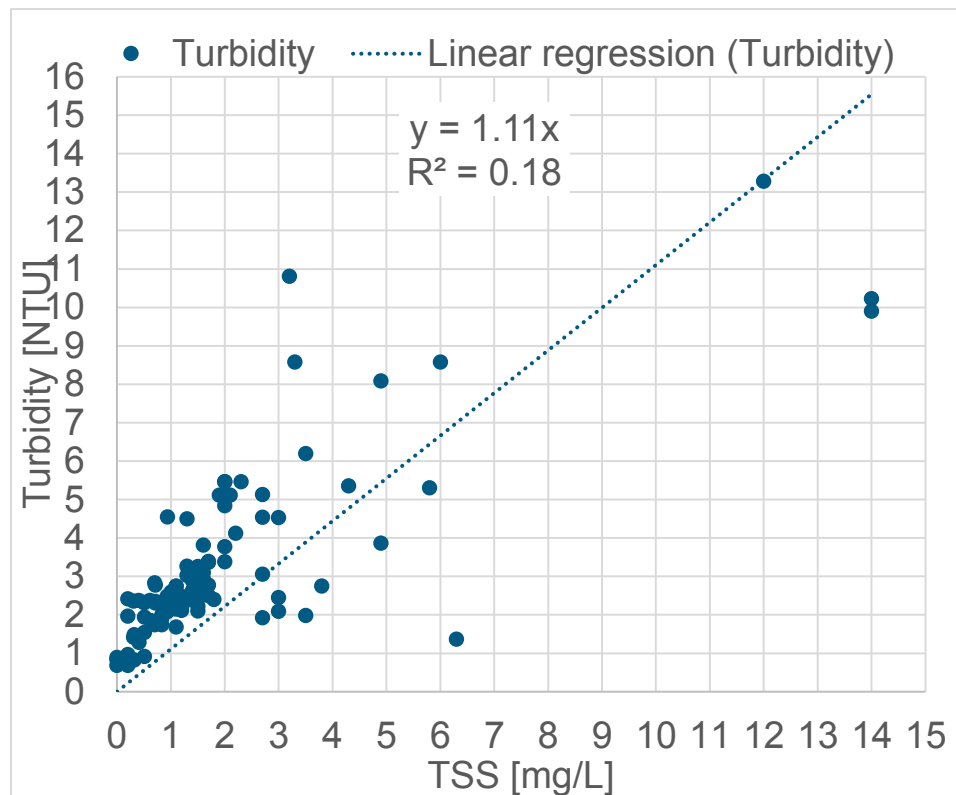


**Figure 7 Relationship of Total Suspended Solids concentration versus Turbidity measurements for visits 2, 3 and 8 combined**



Note: The analytical method for the determination of TSS was modified after the first visit to obtain a lower detection limit and higher resolution.

### 3.1.2 Time Series Measurements

#### 3.1.2.1 Wind Regime

During the monitoring period (June 13<sup>th</sup> 2018 to June 8<sup>th</sup> 2019), the prevailing winds blew from the NNE and the S-SSW. The strongest winds came from the south with a maximum wind speed of 67 km/h in winter (Figure 8). Monthly average wind speeds ranged between 11 km/h and 16 km/h (Table 1).

Given that the water lots of interest are located along the western shoreline of KIH, only winds blowing from the Eastern to Southern quadrants are of interest. Easterly winds occurred less often (< 10% of the time) and were generally below 30 km/h (Table 2). Southerly winds occurred slightly more often (13% of the time) and were generally stronger (up to 67 km/h, but typically below 40 km/h) (Table 2).

**Figure 8 Wind data from the LaSalle Causeway weather station (2018/06/13 – 2019/06/08)**

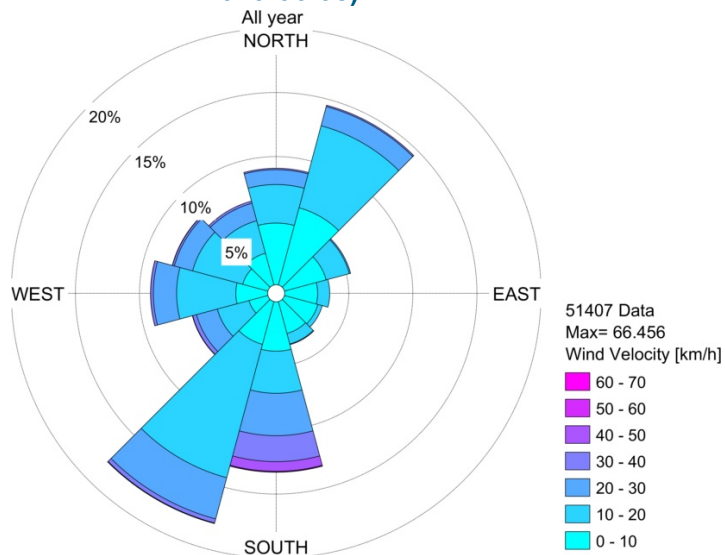


**Table 1 Wind statistics for 2018-2019 at the LaSalle Causeway**

Average wind velocity [km/h]	Maximum wind velocity [km/h]	Direction of the maximum wind velocity [deg N]	Period	
14	67	198	Annual	
12	39	301	June	2018
13	38	177	July	
13	49	178	August	
14	62	182	September	
14	45	183	October	
15	50	178	November	
12	41	343	December	
16	67	198	January	
14	47	194	February	
14	51	173	March	
14	46	179	April	
12	48	175	May	
11	31	216	June	

**Table 2 Wind frequency distribution per direction at the LaSalle Causeway weather station (2018-2019)**

		Wind velocity [km/h]								
		0	[0;10]	[10;20]	[20;30]	[30;40]	[40;50]	[50;60]	[60;70]	total
Wind direction	North		5%	3%	1%	0%				9%
	North-northeast		6%	7%	2%	0%				15%
	East-northeast		3%	2%	0%	0%				5%
	East		3%	1%						4%
	East-southeast		3%	0%	0%					3%
	South-Southeast		3%	1%	0%					3%
	South		4%	3%	3%	2%	1%	0%	0%	13%
	South-southwest		3%	11%	3%	0%	0%		0%	18%
	West-southwest		2%	3%	2%	0%	0%			6%
	West		2%	5%	2%	0%	0%			9%
	West-northwest		2%	4%	1%	0%	0%			8%
	North-northwest		3%	3%	1%	0%	0%			7%
Total		0.31%	38%	42%	16%	3%	1%	0%	0%	100%

The thick line indicates the 1% occurrence

### 3.1.2.2 Extreme Value Analysis

The time series of weather data collected during this project is too short (1 year) to perform an extreme value analysis and determine return periods. Therefore, data was obtained at the Kingston Airport for the period 1970 to 2019. The Kingston Airport is located approximately 11 km west of KIH, and close to Lake Ontario. Compared to KIH, it is more exposed to southerly and westerly winds. Nonetheless, daily wind data from Kingston Airport showed a similar distribution (Figure 9) as the weather station at the LaSalle Causeway (Figure 8). Data from the Kingston airport was therefore judged adequate to calculate the return periods.

The time series showed some limitations as from July 1995 to July 2008 no data is available during the nights. This means that storms happening during the night would be missed for the extreme value analysis, leading to an underestimation of the return period value of wind velocity. The constraint is likely not important since the remaining time series was almost complete (99.53% data return). In Figure 9 the wind rose is presented for the wind data from Kingston Airport. The maximum observed wind speed (83 km/h) came from the west. At Kingston Airport the strongest wind speeds observed from the east was 48 km/h, south-east was 57 km/h and south was 68 km/h.

Given the orientation of KIH, the location of the areas of interest and the topography surrounding the KIH, and taking inconsideration fetch length for different wind directions, only the wind blowing from the eastern, south-eastern and southern directions were considered in the extreme value analysis.

The extreme value analysis<sup>8</sup> (Figure 10, Table 3), indicated that the strongest winds for the 1-, 10- and 50-year return period, ranged from 53 km/h to 68 km/h (southern quadrant) , 43 km/h to 58 km/h (south-eastern quadrant) and 33 km/h to 45 km/h (eastern quadrant) respectively. These values are consistent with analysis by Hall Coastal Canada Ltd (HCCL, 2011) for the 1987 to 2007 period.

#### Summary:

Kingston Airport observations over the 1970 to 2019 period are used for extreme value analysis, with Southern to Western winds that are prevailing. Dominant observed wind directions at LaSalle Causeway are the South-West and North-East. For the areas of interest, the important wind directions are East, South-East and South, with the strongest wind coming from the South.

---

<sup>8</sup> The Peak over Threshold (POT) method was applied.

**Figure 9 Weather station at the Kingston airport (1970/01/01 – 2019/12/31)**

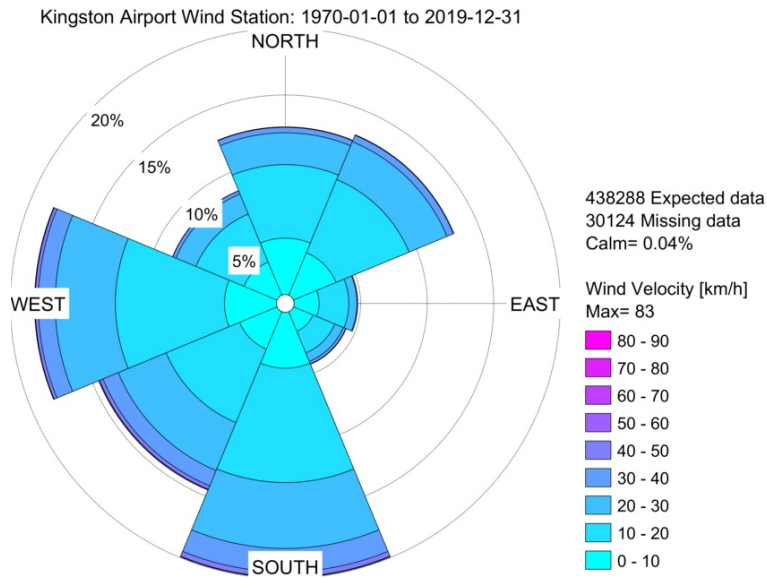


**Figure 10 Return period of the wind depending on its direction.**

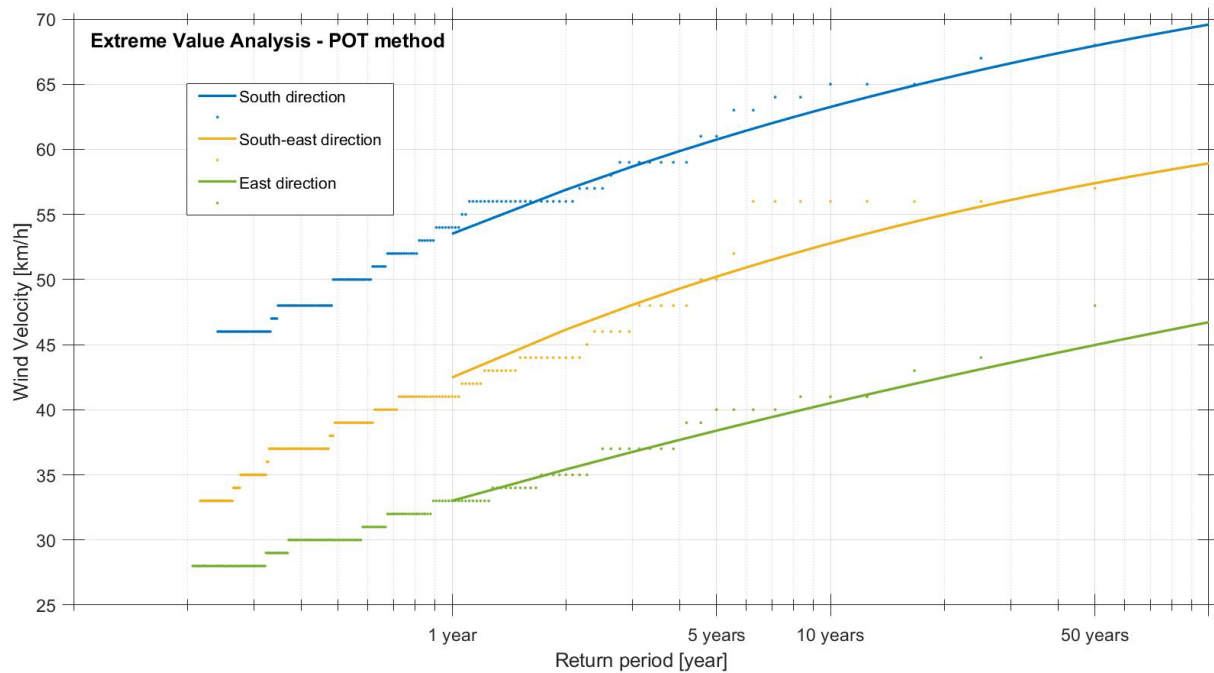


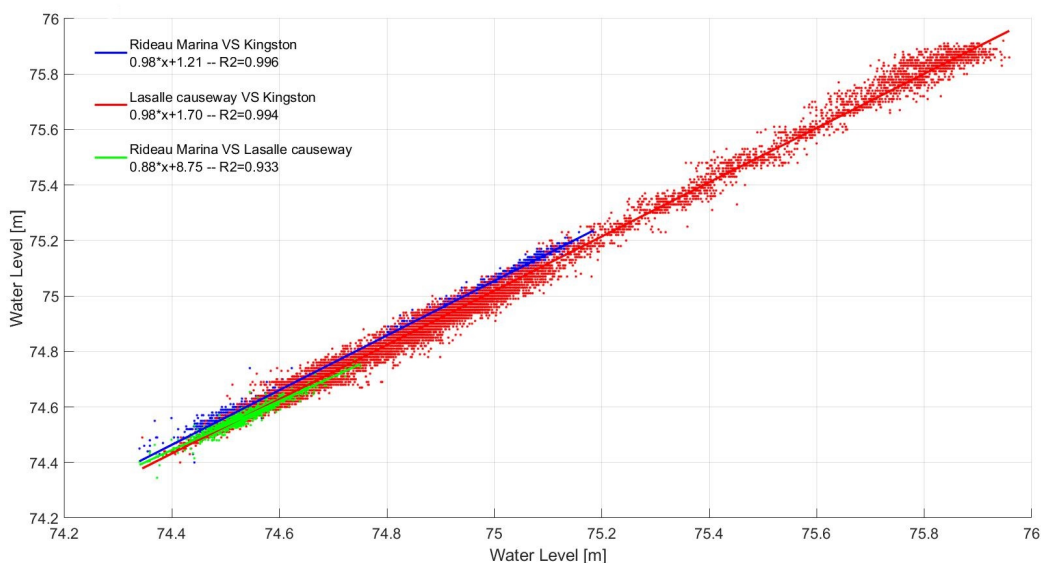
**Table 3 Wind velocity with 1-, 10- and 50-year return period for South, South-East and East direction.**

Wind Velocity [km/h]			
Wind direction [coming from]	Return Period		
	1 year	10 years	50 years
South	53.5 km/h	63.5 km/h	68.0 km/h
South-East	42.5 km/h	53.0 km/h	57.5 km/h
East	33.0 km/h	40.5 km/h	45.0 km/h

### 3.1.2.3 Water Level Measurements

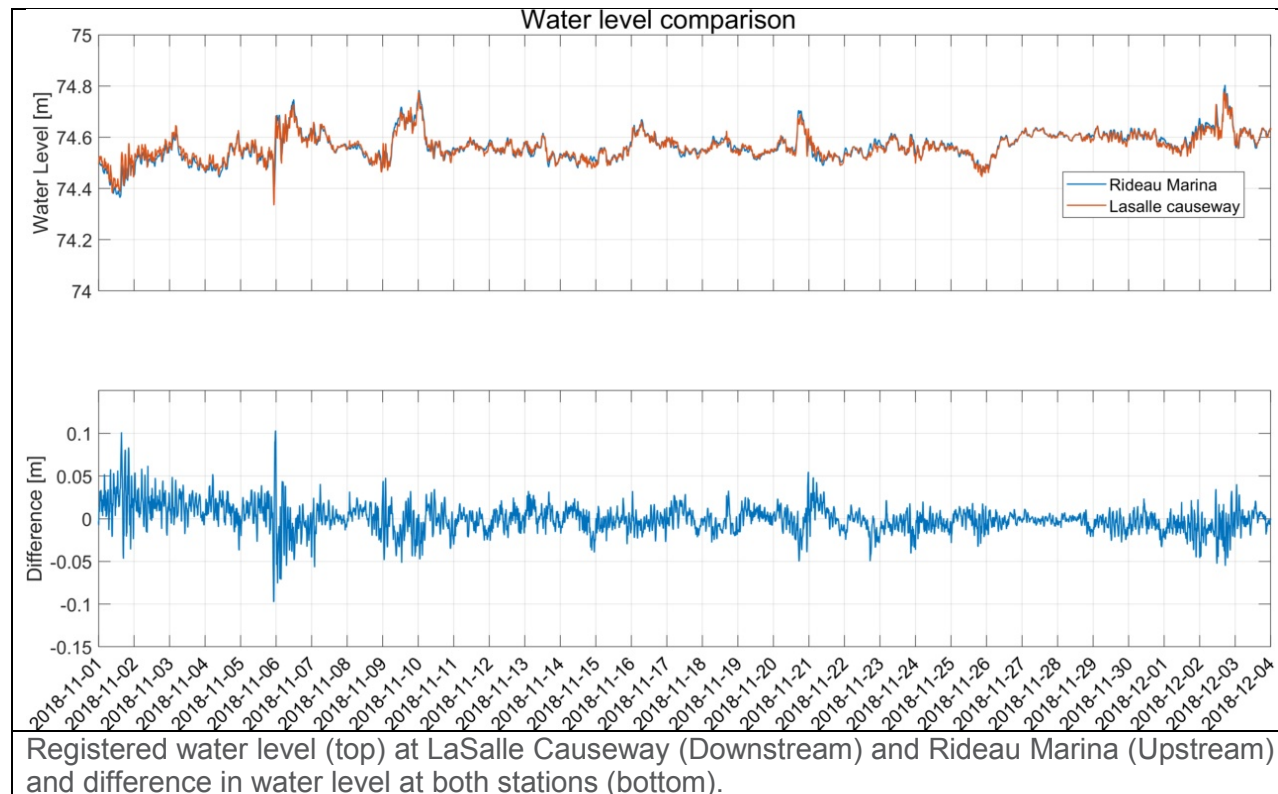
The water level time series from the two hydrometric stations located in KIH were compared to the water-level data obtained at the Kingston Canadian Hydrographic Service (CHS) station (13988), located in Lake Ontario. The purpose was to identify if Lake Ontario oscillations, such as seiches, were being propagated into KIH and if oscillations occurred specifically within KIH. The data is presented in Appendix 1. The data from all three stations is well correlated (Figure 11) and all stations show the same general seasonal fluctuations, with higher water levels during the spring freshet and lower water levels during winter.

**Figure 11 Water level correlation between stations (period)**



The water level data and difference in water level between the Rideau Marina and LaSalle Causeway station during the one-month concomitant records are presented in Figure 12. The differences are most of the time smaller than  $\pm 0.05$  m, this suggests that no time lag is observed between both stations and water levels rise and fall simultaneously with water level changes in Lake Ontario and changes in discharge in the Catarauqui River. Water levels at both stations closely follow the water levels in Lake Ontario, therefore the LaSalle Causeway is not considered to be a hydraulic obstruction between both water masses.

**Figure 12 Water level comparison between LaSalle Causeway and Rideau Marina stations**



Lake Ontario storms can initiate periodic low-frequency fluctuations of water level. Such oscillations, known as seiches, can potentially result in an unexpected rise in water level leading to increase flow within KIH with the sudden rise and fall of the water level. Sudden changes with large amplitude and short time period ( $>0.70$  m and  $< 3$  h) were not observed during our survey for which the LaSalle causeway might form an obstruction for this type of events.

Using wavelet analysis, we analyzed temporal patterns of the water level at the LaSalle Causeway and the Kingston CHS station (13988) for the nine-month time series during which the LaSalle Causeway water level station was operational (open water season). The purpose was to identify oscillations within the KIH which could be attributed to seiche or other oscillation events. A wavelet is a mathematical function used to divide a continuous-time series into different scale components. It can typically be visualized as a "brief oscillation" with a changing frequency which is applied as a filter, each pass identifying periodic events of a given period. The output is a 2D colour graph of energy peak with the period of the oscillation on the Y-axis and time of recording on the X-axis (Torrence and Compo, 1998). Significant events (95% confidence interval) are identified in the figures by a black line (Figure 13).

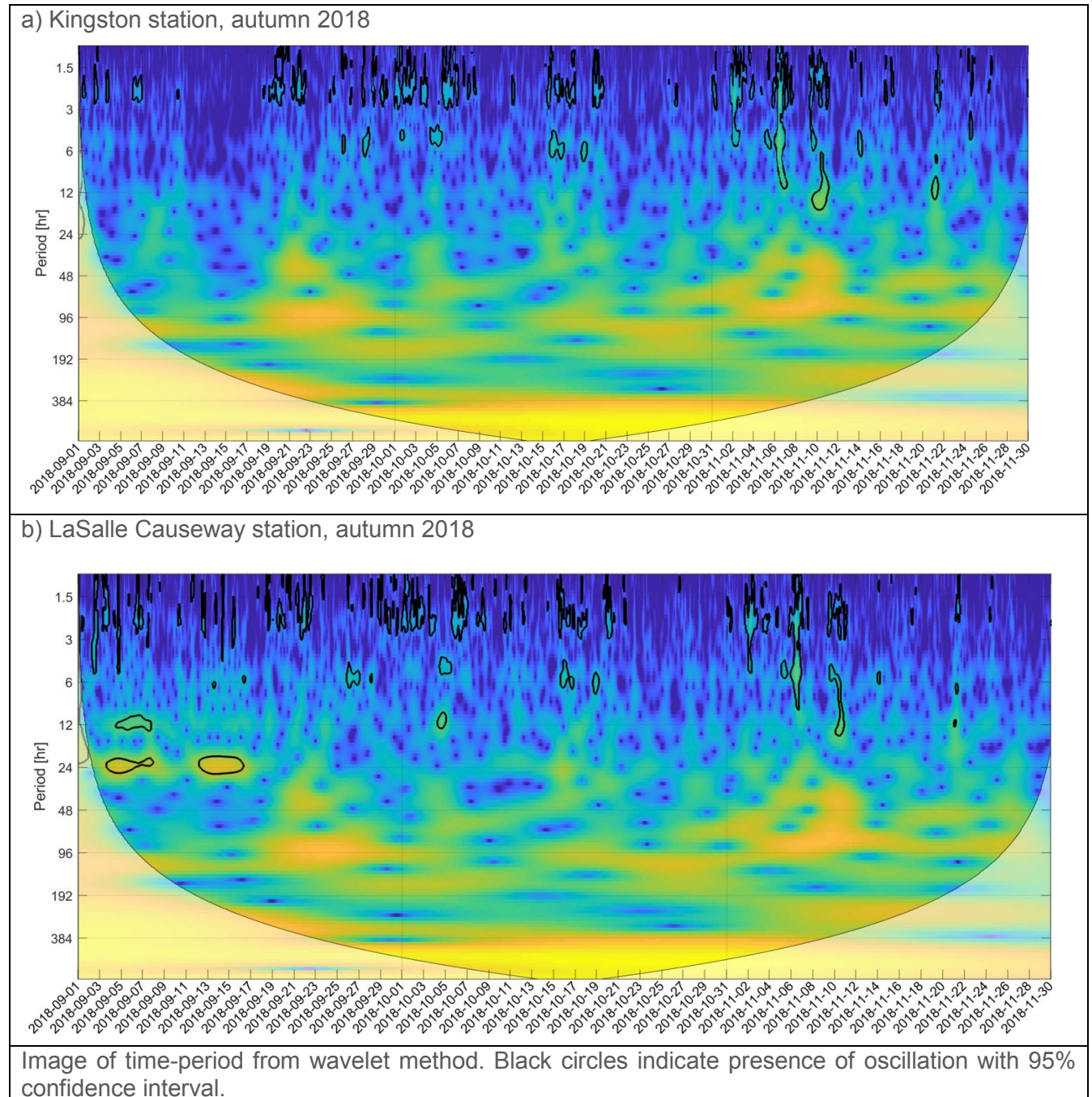
Seiches events have been identified at the Kingston CHS station in fall 2018, winter 2019 and spring 2019 (Figures 13a, 13c and 13e respectively). These events generated water level variations with different periods of 2 h, 5 h and 12 h during all three seasons. The 12 h period event was mostly observed in winter.

The Lake Ontario seiche events were also observed within KIH at the LaSalle Causeway with similar periods (Figures 13b, 13d and 13f). But a seiche with a 24 h period was only observed within the KIH and is locally generated. Figure 14 presents the observed water level in Lake Ontario and KIH for September 2018 and the results of the wave let analysis, 24 h oscillations with an amplitude of about 0.20 m is clearly visible in the KIH. During spring (Figures 13e and 13f) an oscillation with a 400 h period (more than 17 days) was identified at both stations, this marks the spring flood of the St-Lawrence River.

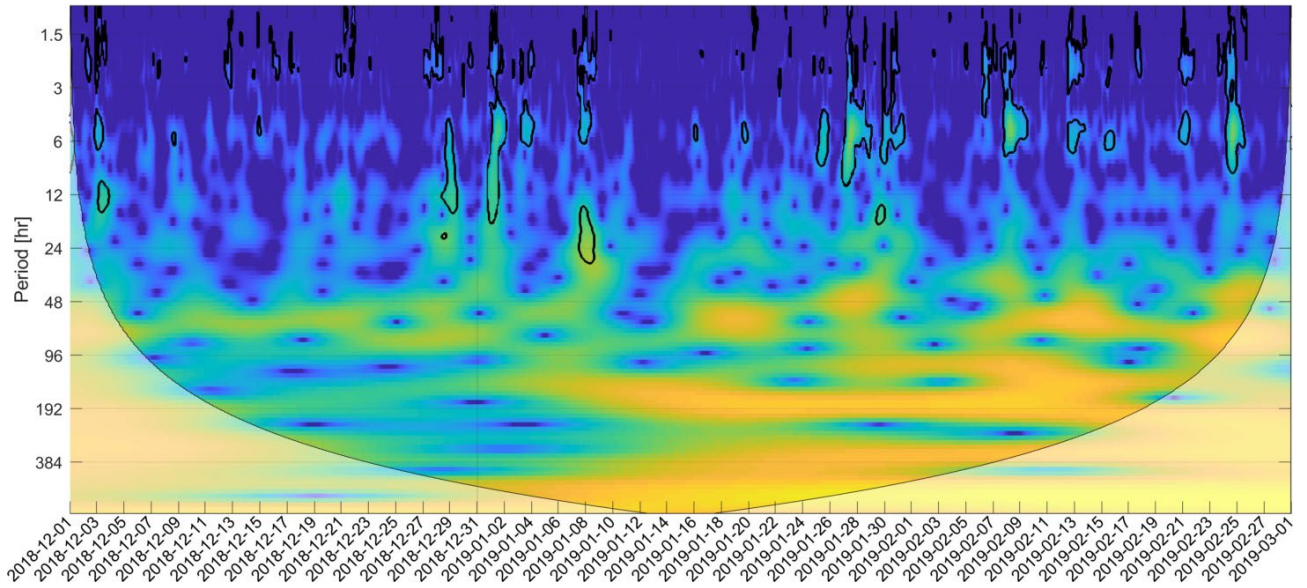
#### Summary:

Water levels in the KIH basin closely followed the Lake Ontario water levels. No significant differences were observed between water levels at Rideau Marina (upstream) and LaSalle Causeway (downstream), implying a simultaneous response of the bay. Any observed seiches in Lake Ontario water levels are also observed in the KIH. The wavelet analyses showed seiches with a period of 24 h only within the KIH basin, which did not show in Lake Ontario, therefore the seiches with 24 h period might be locally generated in the KIH basin.

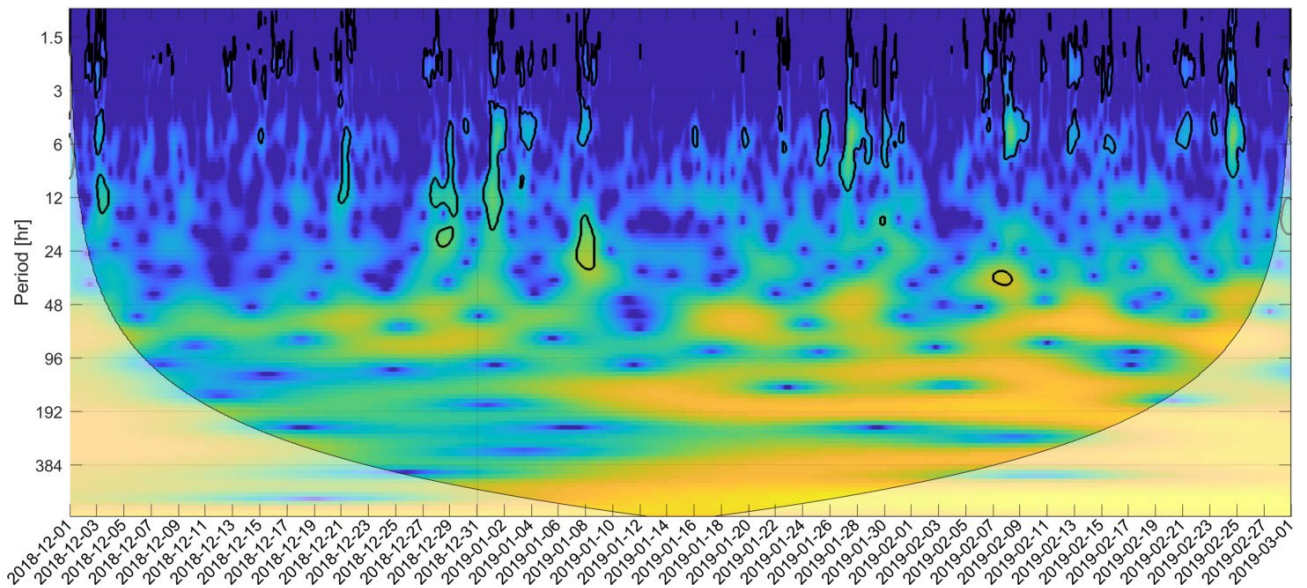
**Figure 13** Wavelet analysis results showing significant oscillation events of different period (black line) for the Kingston CHS and LaSalle Causeway stations, during autumn 2018 (a, b), winter 2018-2019 (c, d), and spring 2019 (e, f)



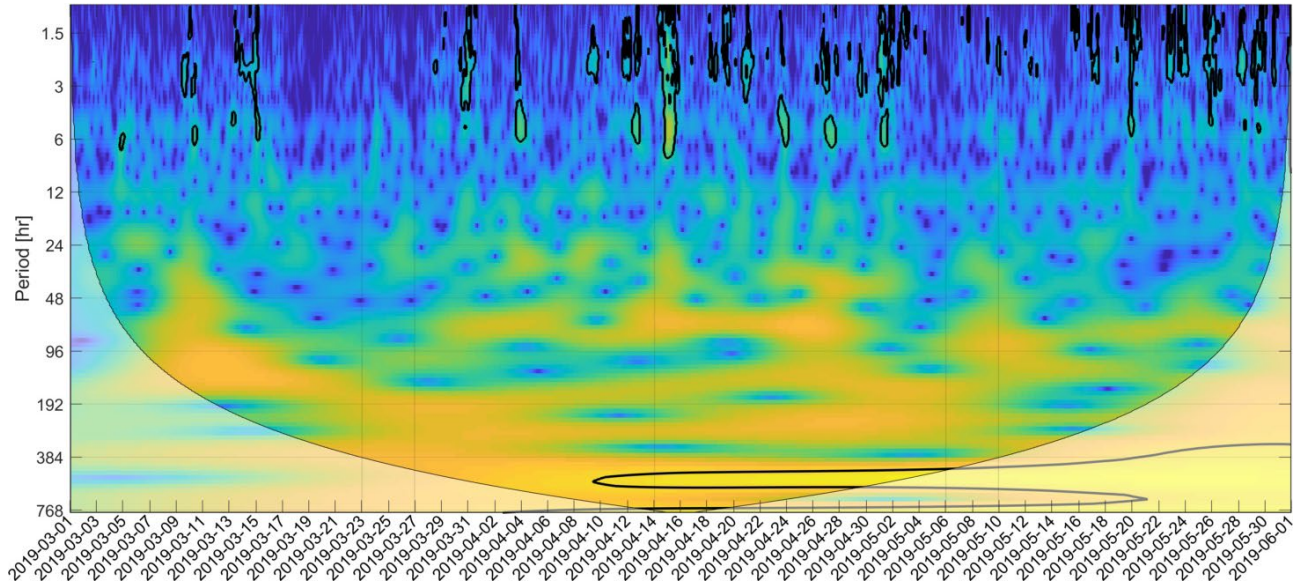
c) Kingston station, winter 2018-2019



d) LaSalle Causeway station, winter 2018-2019



e) Kingston station, spring 2019



f) LaSalle Causeway station, spring 2019

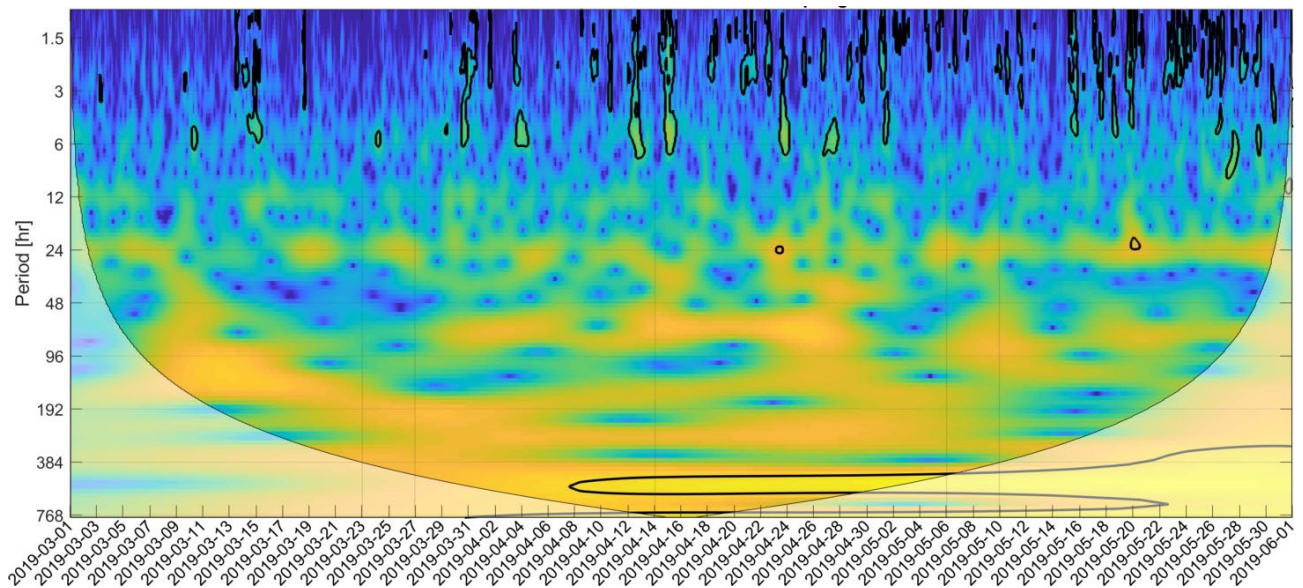
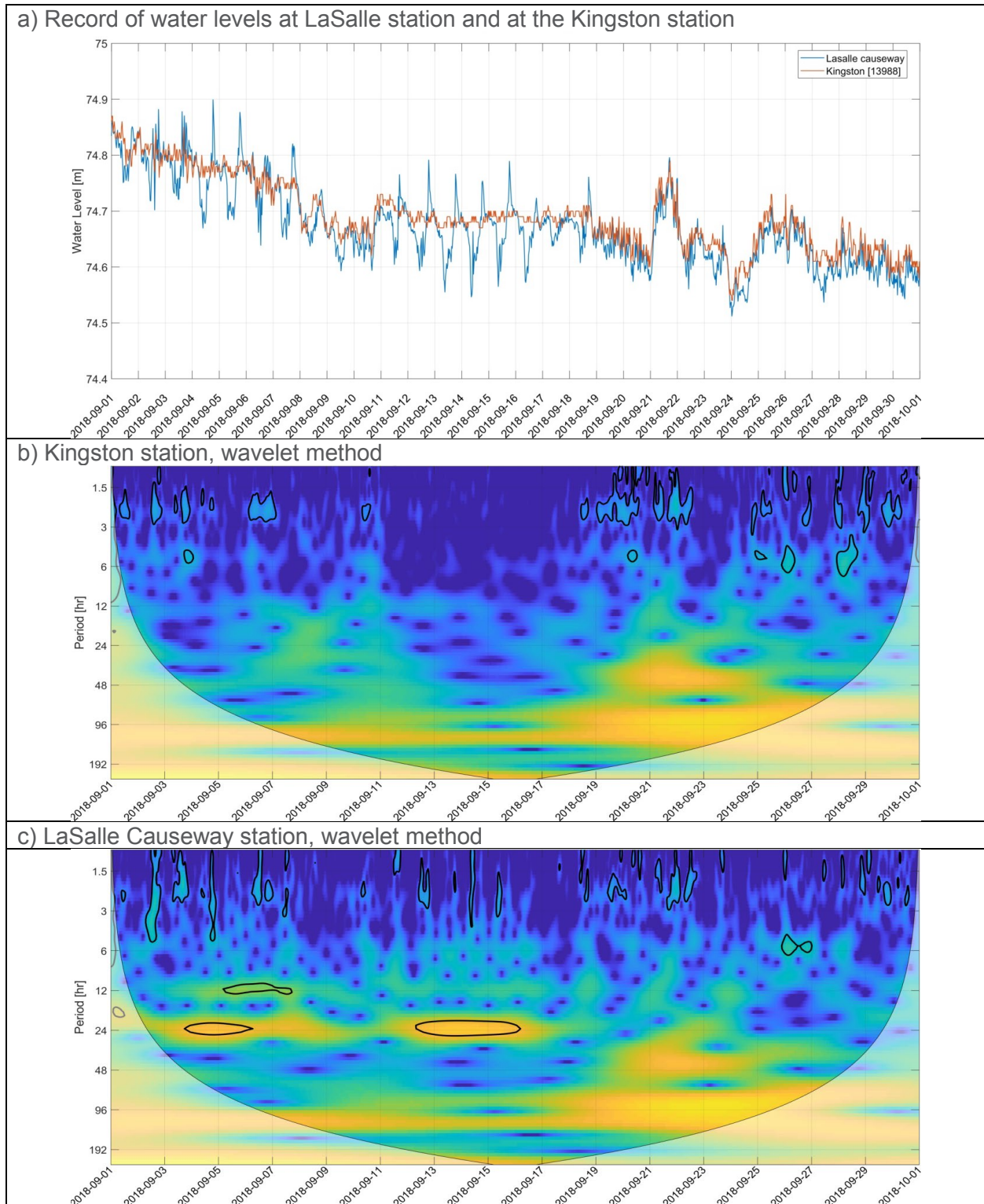


**Figure 14** Wavelet analysis of water level time series from September 2018, observed only in the Kingston Inner Harbour (24 h period). Significant events (95% confidence) are identified with a black line



### 3.1.2.4 Wave Regime

A spectral analysis was performed on the high frequency water level data recorded by the wave gauge (Figure 2) to describe the wave regime during the recording period. The significant wave height ( $H_s$ ) and period ( $T_p$ ) were calculated for wind waves.

The results of the spectral analysis were used to calculate bottom orbital velocity based on linear wave theory equation:

$$u_o = \frac{\pi H_s}{T_p \sinh kh}$$

With  $u_o$  particle bottom velocity

$H_s$  significant wave height

$T_p$  peak wave period

$k = \frac{2\pi}{L}$  where  $k$  is wavenumber and  $L$  is wave length

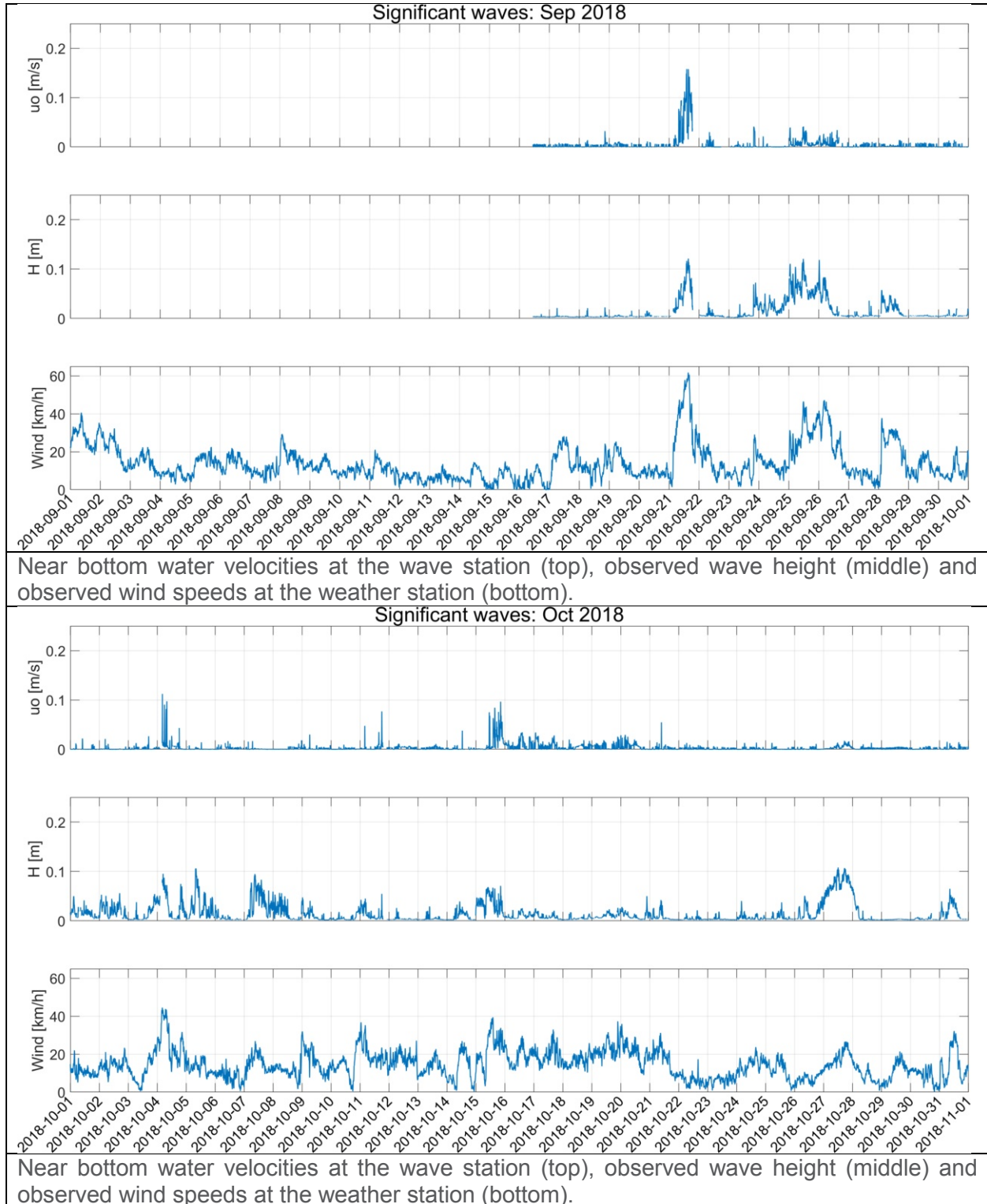
$h$  water depth

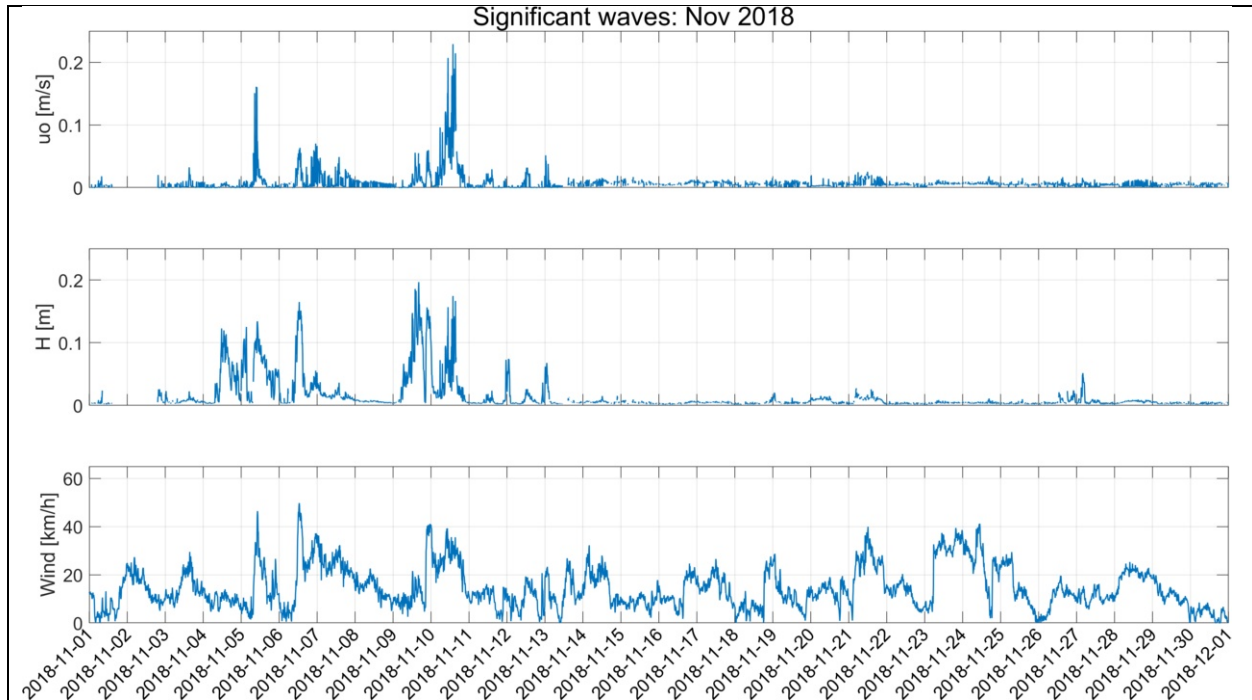
The time series of the near-bottom water velocity is presented in Figure 15 along with the wave height and wind speed. Wind direction is not presented in Figure 15 for clarity reasons, it was observed that higher near-bottom velocity occurred during winds from either the south or the south-east for which the fetch is longer. On November 13, 2018 the instrument was relocated from the old wharf to the Rowing Club, a location protected from southerly waves. After this date the recorded wave heights and thus near bottom velocity were reduced.

Summary:

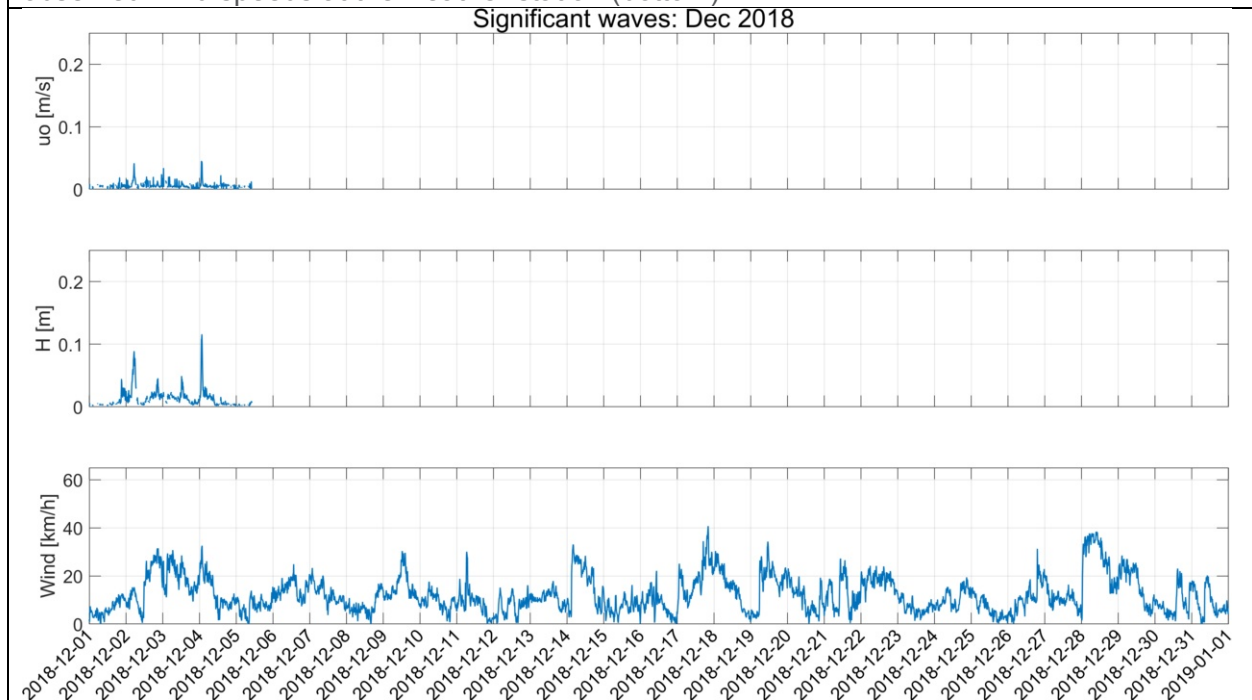
Within the three-month observation period, stronger winds generally led to significantly higher wave heights. Near-bottom velocities, however, are not directly correlated to stronger winds. Near-bottom velocity is related to wavelength with longer wave lengths generating stronger near-bottom velocities. Thus, a wave of with a given amplitude will interact with the bay floor depending on its wavelength (shallow versus deep water).

**Figure 15** Near bottom water velocity and wave height from waves at the downstream water level station along the observed wind speeds





Near bottom water velocities at the wave station (top), observed wave height (middle) and observed wind speeds at the weather station (bottom).



Near bottom water velocities at the wave station (top), observed wave height (middle) and observed wind speeds at the weather station (bottom).

### 3.1.2.5 Turbidity Measurements

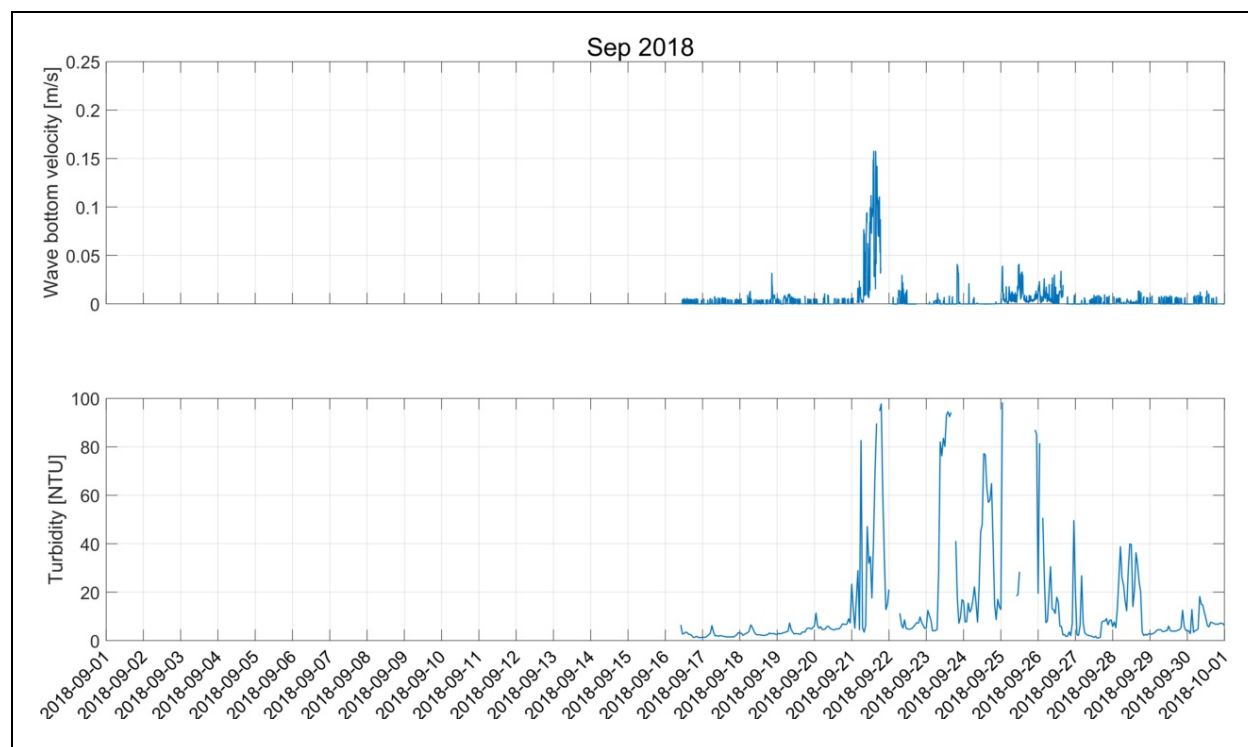
In general, the turbidity time series contain very low values, below 10 NTU, these low values are in accordance with the very low suspended sediment concentrations that were observed in the water samples and profiles. Although the turbidity is low, the signal is noisy, as mentioned in section 3.1.1. The noise within the time series could be explained by several different factors such as plants, fish, etc.

Wave bottom velocities calculated in section 3.1.2.3 are presented with the turbidity measurement (Figure 16). Velocity events coincided with peaks in turbidity suggesting re-suspension of bed material. At calmer moments, spikes in turbidity might be caused by either aquatic vegetation drifting in front of the sensor, (storm) runoff events directly to the KIH basin from the adjacent lands, or through higher turbidity of the Cataraqi River. Very high turbidity values (over 100 NTU, most certainly caused by plants or debris) are considered erroneous and were removed from the time series. Each wave event is followed by an increase of the turbidity exceeding 20 NTU, suggesting some sediments are re-suspended during these wave events. The duration of the turbidity events is unlikely related to boat traffic. The dense vegetation and shallow depths would not be attractive to pleasure crafts which are most likely cruising the main navigation channel. We suppose that the area is used mostly by the chase boat from the Kingston Rowing club and the od fisherman.

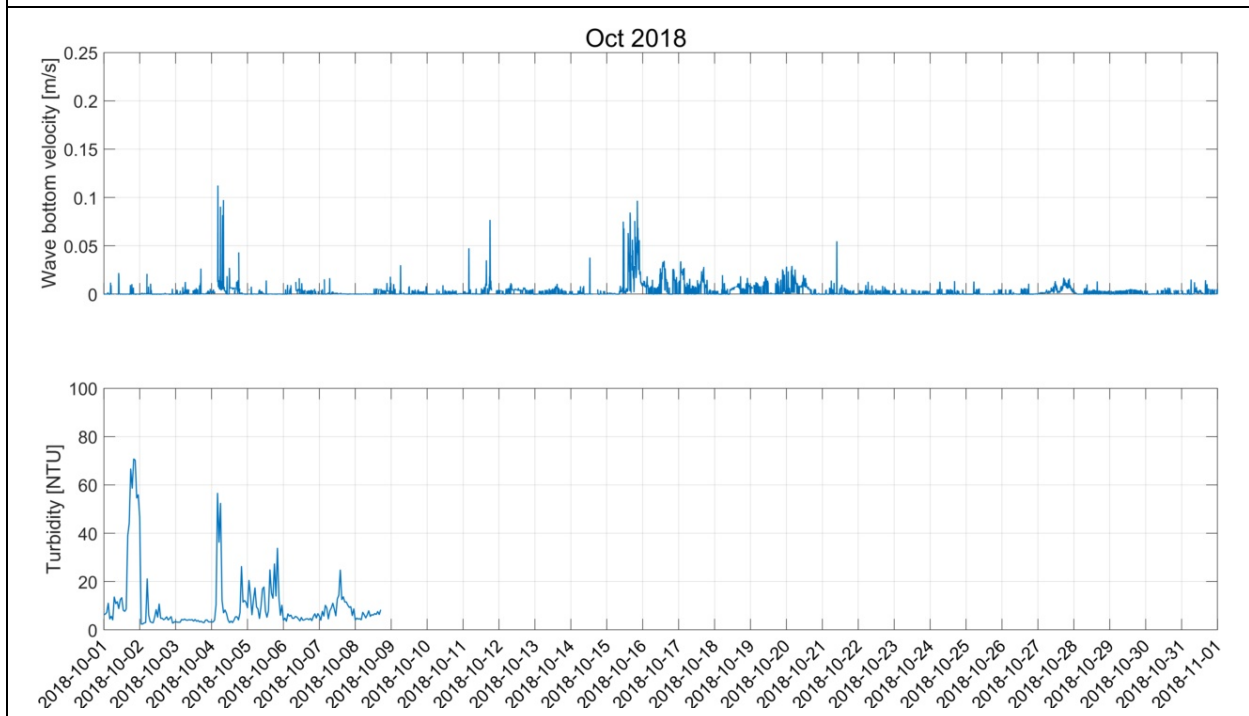
Summary:

Time series of turbidity show low values in general, which is consistent with the 4 field visits of suspended sediment sampling. Higher spikes in the time series are almost all related to plants and debris. Some of the turbidity events are linked to wind/wave episodes while others are likely linked to sediment inputs from run-off or the Cataraqi River.

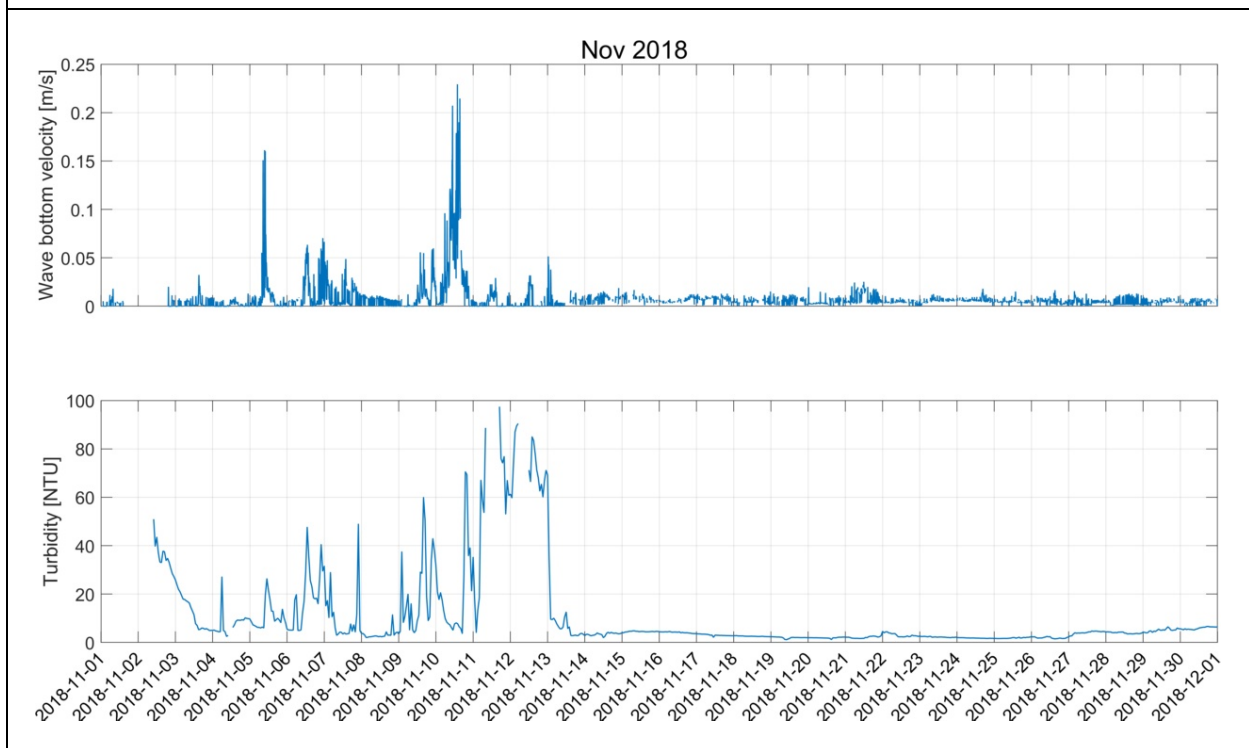
**Figure 16 Turbidity and wave bottom velocity relationship**



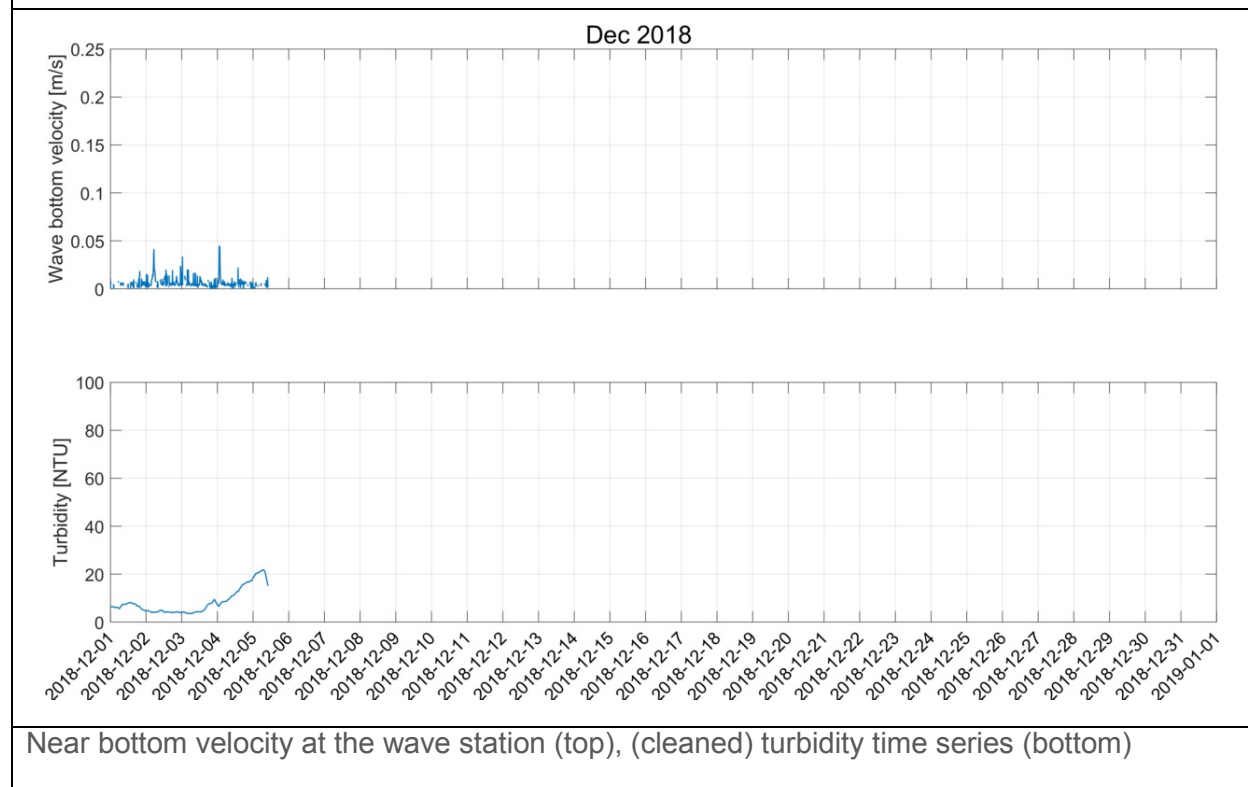
Near bottom velocity at the wave station (top), (cleaned) turbidity time series (bottom)



Near bottom velocity at the wave station (top), (cleaned) turbidity time series (bottom)



Near bottom velocity at the wave station (top), (cleaned) turbidity time series (bottom), note the instruments were moved on November 13<sup>th</sup>.



Near bottom velocity at the wave station (top), (cleaned) turbidity time series (bottom)

### 3.1.3 Kingston Inner Harbour Wave Modeling

A numerical model (CMS-Wave) to analyze wave generation and propagation was developed, details on inputs, parameter setting, and validation are provided in Appendix 2. The model is based on bathymetric data digitized from Navionics maps (Figure 17a). The data corresponds relatively well with a detailed bathymetry done by Monteith Ingram (Figure 17b), but the latter data was not available in any useful form to be incorporated in the model. Although less detailed, the available bathymetric data was representative of the morphology of the bay and adequate for wave modeling. Although necessary for wave propagation, the bathymetric data has less impact on wave development than the length of the fetch

From the recorded wind data, three critical wind directions were selected (Table 3), namely East, South-East and South with 1-, 10- and 50-year return periods, resulting in 9 simulation cases. The results are graphically presented in Appendix 3 for the significant wave height and near bottom velocity for each case. In Table A3-1 the near bottom velocities at the core sampling locations are presented.

The wave generation and propagation modelling are based on a constant wind acting with the fetch limited by the KIH boundaries. A cell size of 1 m is used for the wave propagation calculation, allowing for a good resolution. It's important to note that the model does not consider the presence of macrophyte beds that attenuate the wave propagation during its growing season (from July to September).

At the location of each core sampling location, the wave characteristics, the near-bottom water velocity generated by the waves were calculated (Table A3-1). In section 3.2.2 Erodibility experiment, these near bottom velocities were compared to threshold water velocity for re-suspension, see Table 13.

Waves in the bay were generated for those different extreme winds (Figure 18). Corresponding near-bottom velocity maps are presented in Figure 18 for the 50 years wind return period. The bottom velocity (linear formulation see section 3.1.2.4) was calculated at each node using water depth, wave period and amplitude from the wave modelling. Given the short fetch lengths in the KIH, the waves are not fully developed, and the wave period is therefore changing along the wave path. The irregularity visible in the near bottom velocities is due to the step size (resolution, 0.1 s) in the wave period of the model. In reality the velocity is more gradually increasing. Detailed waves characteristics for maximal near bottom velocities are given in Table 4 for each sampling location, results for all simulations are in Table 3A of Appendix 3. The maximum near-bottom velocity is 0.44 m/s at Box core 4A (water lot PC-W) during South-Eastern winds with 50-year return period. The other water lots (TC-4, TC-2A and TC-RC) the maximum near-bottom velocities are occurring during eastern winds, which are around 0.15 m/s.

#### Summary:

Wave characteristics are simulated for 3 critical wind directions for the KIH basin. The South-East wind direction seems the most critical as wave heights up to 0.57 m are expected with near-bottom water velocities reaching 0.44 m/s.

**Figure 17 Bathymetry of the bay,**

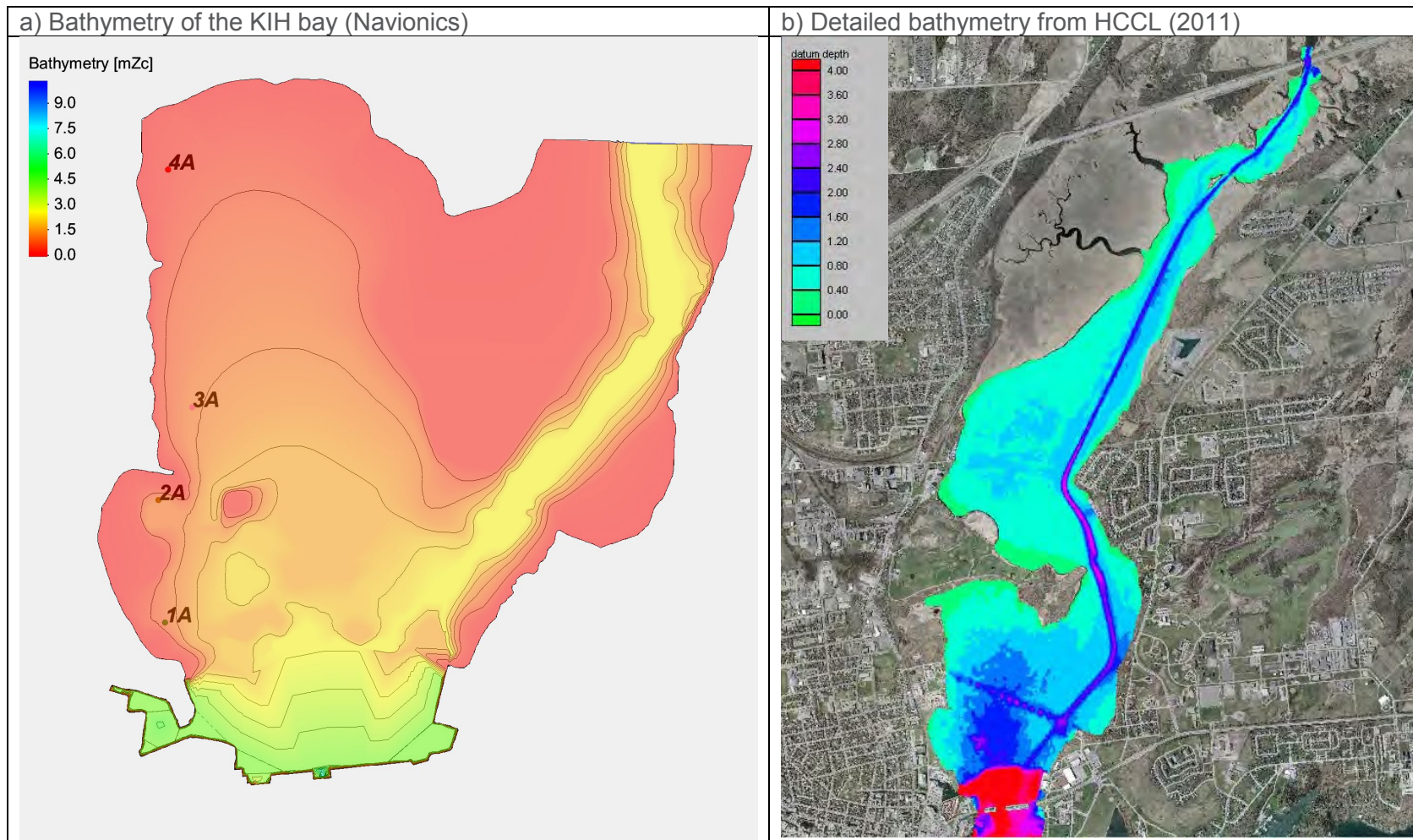
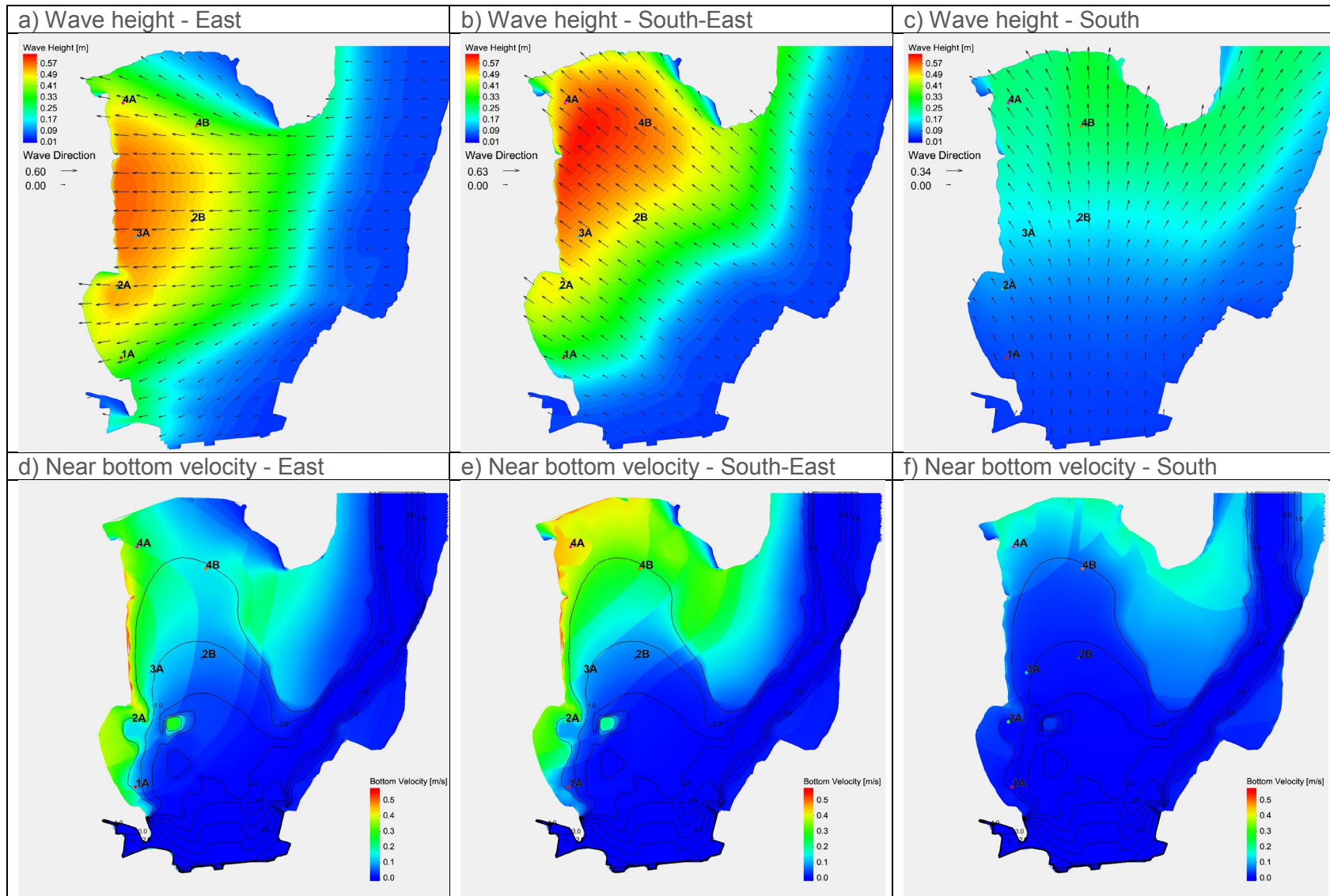


**Figure 18** Significant wave height for winds with 50-year return period for the (a) East; (b) South-East; (c) South directions and the associated near bottom water velocities for (d) East (e) South-East (f) South directions



Note: near-bed velocities are dependent on wave period, which is a function of the fetch length. Variation in wave period is high for short fetch length. The abrupt changes in near-bed velocities apparent on figures d, e and f are a result of this and show the limitations of numerical modelling for short fetch areas.

**Table 4 Wind and wave characteristics and bottom velocity and sampling locations within the Kingston Inner Harbour that generate the highest near-bottom water velocity**

Sampling Location	Wind Direction	Return Period [yrs]	Wave Height [m]	Wave Period [s]	Bottom Velocity [m/s]
1A	East	50	0.393	1.56	0.09
2A	East	50	0.524	1.72	0.14
3A	East	50	0.555	1.82	0.18
4A	South-East	50	0.540	1.92	0.44
2B	East	50	0.491	1.64	0.08
4B	South-East	50	0.570	1.82	0.28

## 3.2 Stage Two Surveys - Sediment Dynamics

### 3.2.1 Sediment Dating

#### 3.2.1.1 General Observations

Full reports from sediment dating for each core are provided in Appendices 4, 5, 6, 7, 8 and 9 for the cores 1A, 2A, 3A, 4A, 2B and 4B respectively. Photos and description of the stratigraphy for each core before extraction are available in appendix 10. Core stratigraphic description is limited to the horizon that was sub sampled for the radio isotopic analysis.

Key observations for the six cores are:

- › the  $^{210}\text{Pb}$  profiles exhibit an irregular but approximately exponential decrease in total  $^{210}\text{Pb}$  activity as a function of depth;
- › and the  $^{210}\text{Pb}$  activity barely exceeded the  $^{226}\text{Ra}$  activity measured in the cores (and the  $^{210}\text{Pb}$  activity is less than the  $^{226}\text{Ra}$  activity in core 2B), indicating that the background level of  $^{210}\text{Pb}$  may have been achieved in all the cores.

The CRS model assumes constant input of  $^{210}\text{Pb}$  and a core that is long enough to include a complete  $^{210}\text{Pb}$  inventory (all the measurable atmospheric source  $^{210}\text{Pb}$ ). Although the assumption was not respected for all the cores, the CRS model was applied to all the cores assuming the lowest total  $^{210}\text{Pb}$  activity was at background level. This suggests that the study area is very close to the main sediment input sources and that sediment settling conditions are affected by different forcing agents. Therefore, any change in sediment input rates and occurrence of resuspension events will affect the sediment settling rate. The CRS model is likely still the best compromise to interpret the radio isotope profiles.

When applying the linear regression model of Unsupported  $^{210}\text{Pb}$  activity, it is assumed that the input of  $^{210}\text{Pb}$  and the sediment accumulation rate are constant. The model was applied to the core interval where these assumptions may be satisfied to estimate the average sediment accumulation rate for the core interval. These assumptions were met for (part of) the cores 3A, 4A, 2B and 4B. Even though variations in the rate are apparent, the average rate will be estimated reasonably well. The age at the bottom of any core section can be estimated by dividing the cumulative dry weight/cm<sup>2</sup> by the accumulation rate. For example, in core 3A: the age at the bottom of section 12 (extrapolated depth 12.5 cm) is calculated as  $2.658 / 0.1185 = 22.4$  yrs. In general, the CRS model is to be preferred because it can provide valid predictions over the entire length of the modelled core, even though the sediment accumulation rate is changing with time.

The average sediment accumulation rate, from core surface to the extrapolated bottom depth of any section, can be calculated by dividing the cumulative dry mass at the bottom of the

extrapolated section by the calculated age at that depth. Except for core 1A, this was done for all the cores. For example, for core 2A: the average sediment accumulation rate can be calculated, from the core surface to the bottom of section 10 (depth 10 cm) by:  $1.459 / 41.4 = 0.0352 \text{ g/cm}^2/\text{yr}$

Overall, the analytical quality of radioisotope data (based upon the recovery of spike, the recovery of certified reference material (CRM), the results of repeat analyses and blanks) is considered good for all the six cores.

### 3.2.1.2 Water Lot TC-4 - Core 1A

The core sample description is shown on Table 5. Sediments at site 1A consisted primarily of silty sand near the surface with a decreasing size fraction down core to clay. The maximum activity of 9.05 DPM/g observed in section 6 – 7 cm is about 8 times the lowest activity of 1.07 DPM/g observed in section 50 – 51 cm (Table A4-1 and Figure 19a). The  $^{210}\text{Pb}$  activities in upper 2 sections (extrapolated depth 0 – 5 cm) are slightly lower than section 6 – 7 cm, and this probably represents increasing sediment accumulation rates, and/or physical mixing, and/or diffusion of  $^{210}\text{Pb}$  across a redox gradient, and/or incomplete diagenesis of surface sediment, and/or incomplete ingrowth of the  $^{210}\text{Po}$ , granddaughter of  $^{210}\text{Pb}$ , actually being measured.

- › The dry bulk densities generally increased with depth ranging between  $0.175 \text{ g/cm}^3$  and  $0.664 \text{ g/cm}^3$ .
- › The dry bulk densities decreased beginning 25 cm to 33.5 – 39 cm (Table A1-1 and Figure 19b).
- ›  $^{226}\text{Ra}$  activity 1.23 (11 – 12 cm), 1.31 (26 – 27 cm) and 1.05 DPM/g (58 – 59 cm)
- ›  $^{210}\text{Pb}$  activity (50 – 51 cm) barely exceeded  $^{226}\text{Ra}$  activity (58 – 59 cm)

$^{137}\text{Cs}$  was measured in 10 sections in the 0 – 31 cm core interval. Activities in the 0 – 29 cm portion of the core are significantly above background, ranging between 0.58 - 3.19 DPM/g (Table A4-2 and Figure 20). The shape of  $^{137}\text{Cs}$  profile in the 0 – 27 cm core interval suggests that the majority of the  $^{137}\text{Cs}$  is probably from external erosion sources (soils or sediments contaminated with bomb testing radionuclides). Below 27 cm, we expect to see the  $^{137}\text{Cs}$  activity gradually decline with depth. This tailing of  $^{137}\text{Cs}$  into deeper depths with  $^{210}\text{Pb}$  dates prior to 1954 is commonly seen and is attributed to downward diffusion of the isotope. However, in this core the tailing into deeper depths is not seen, rather, we see a sharp and sudden decrease immediately below the highest  $^{137}\text{Cs}$  activities and then a non-detect at section 30 – 31 cm. This is unexpected and suggests that part of the  $^{137}\text{Cs}$  profile may have been disturbed or is missing from the core.

CRS model of Age at bottom of Extrapolated section in years vs. Depth of bottom edge of current section in cm:

- › If one assumes that the  $^{210}\text{Pb}$  activity of 1.07 DPM/g (in the 50 – 51 cm section) is the background level, then it should be possible to apply the CRS model. The model predicted an age of 78 years at the bottom of the 26 – 27 cm section, an age too old to agree with the significant presence of  $^{137}\text{Cs}$  in the same section. This leads to the assumption that the  $^{210}\text{Pb}$  inventory is probably incomplete and the core cannot be processed by the CRS model.

Regression model of Unsupported  $^{210}\text{Pb}$  activity vs. Cumulative Dry Weight ( $\text{g/cm}^2$ ):

- › The shape of the  $^{210}\text{Pb}$  profile suggests that the input of  $^{210}\text{Pb}$  and the sediment accumulation rate may be constant in the core interval of sections 7 - 22 (extrapolated depth 5 - 22.5 cm) the regression model was applied to this interval and predicted ( $R^2 = 0.9496$ ) an average sediment accumulation rate of  $0.0610 \text{ g/cm}^2/\text{yr}$  when the unsupported  $^{210}\text{Pb}$  activity was calculated by subtracting the nearest neighboring  $^{226}\text{Ra}$  measurement from each total  $^{210}\text{Pb}$

value. However, the regression model predicted an age of 102 years at the bottom of section 22, an age too old to agree with the significant presence of  $^{137}\text{Cs}$  at this depth, and the continuing presence of significant  $^{137}\text{Cs}$  activities into deeper depths. It was concluded that the linear regression model should not be applied to this core.

- › Moreover, when the CRS model was applied it predicted that the sediment accumulation rates are variable throughout the core i.e. significant changes throughout the core length and increasing sediment accumulation rates towards the surface.

#### Summary:

The rapid decline in  $^{137}\text{Cs}$  activity below 27 cm, combined with the sudden termination in exponential decay of  $^{210}\text{Pb}$  at section 27 (extrapolated depth 25 - 27.5 cm) and the sharp decrease in dry bulk density in the same section, suggests that this core may have been disturbed or that a significant portion of the core may be missing.

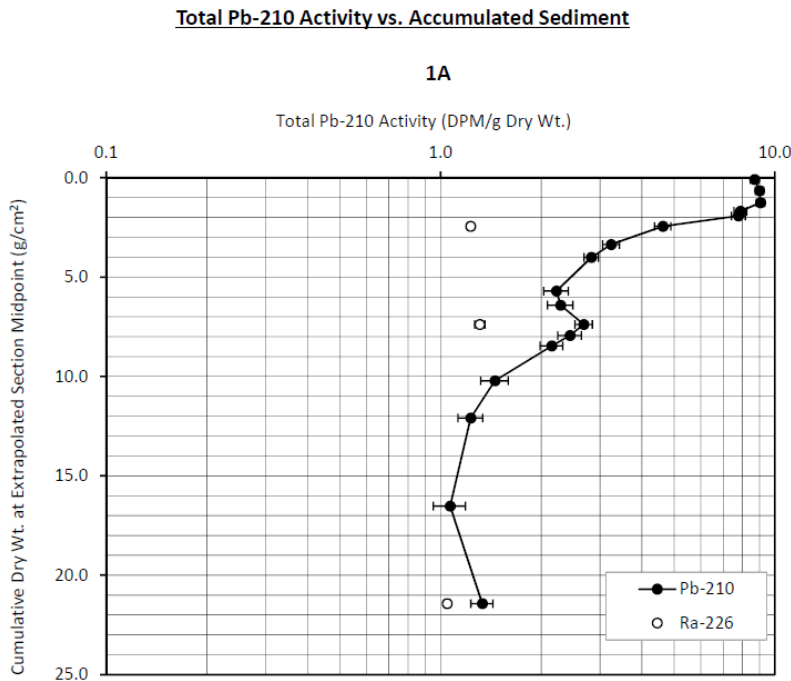
However, with the significant presence of  $^{137}\text{Cs}$  and unsupported  $^{210}\text{Pb}$  found in the 0 – 27 cm core interval, we can conclude that in general all sediments in this core interval likely represent post 1966 sediment accumulation.

**Table 5 Core 1A – Sample description**

Sample number	Interval [m]		Nature	Texture	Colour	Odour	Notes	Notes	
	top	bottom							
1A-2/2-1	0.0	1.0	sand/silt	watery	brown		vegetation (little)	small shell fragments	
1A-2/2-4	3.0	4.0	sand/silt	less watery	brown		vegetation (little)	small shell fragments	
1A-2/2-7	6.0	7.0	sand/silt	less watery	brown		vegetation (little)	small shell fragments	
1A-2/2-9	8.0	9.0	silt/sand	less watery	brown		vegetation (little)	small shell fragments	
1A-2/2-10	9.0	10.0	silt/sand	less watery	brown		vegetation (little)		
1A-2/2-12	11.0	12.0	silt/sand	little thick	brown	smell hydrocarbon	of	vegetation (little)	
1A-2/2-15	14.0	15.0	silt/sand	little thick	brown	smell hydrocarbon	of	vegetation (little)	
1A-2/2-17	16.0	17.0	clay/sand	thick	brown	smell hydrocarbon	of		Iron oxide forming on bottom of container
1A-2/2-22	21.0	22.0	clay/sand	thick	brown	smell hydrocarbon	of		Iron oxide forming on bottom of container
1A-2/2-24	23.0	24.0	clay/sand	thick	brown	smell hydrocarbon	of		Iron oxide forming on bottom of container
1A-2/2-27	26.0	27.0	clay	thick	brown	smell hydrocarbon	of		Iron oxide forming on bottom of container
1A-2/2-29	28.0	29.0	clay	thick	brown	smell hydrocarbon	of		Iron oxide forming on bottom of container
1A-2/2-31	30.0	31.0	clay	thick	brown	strong smell hydrocarbon	of		Iron oxide forming on bottom of container
1A-2/2-37	36.0	37.0	clay	thick	brown				Iron oxide forming on bottom of container
1A-2/2-42	41.0	42.0	clay	thick	brown				
1A-2/2-51	50.0	51.0	clay	thick	brown				
1A-2/2-59	58.0	59.0	clay	thick	brown				

**Figure 19** <sup>210</sup>Pb – Profile results of core 1A

a) Total <sup>210</sup>Pb activity vs accumulated sediments



b) Dry bulk density and % loss on drying vs accumulated sediment

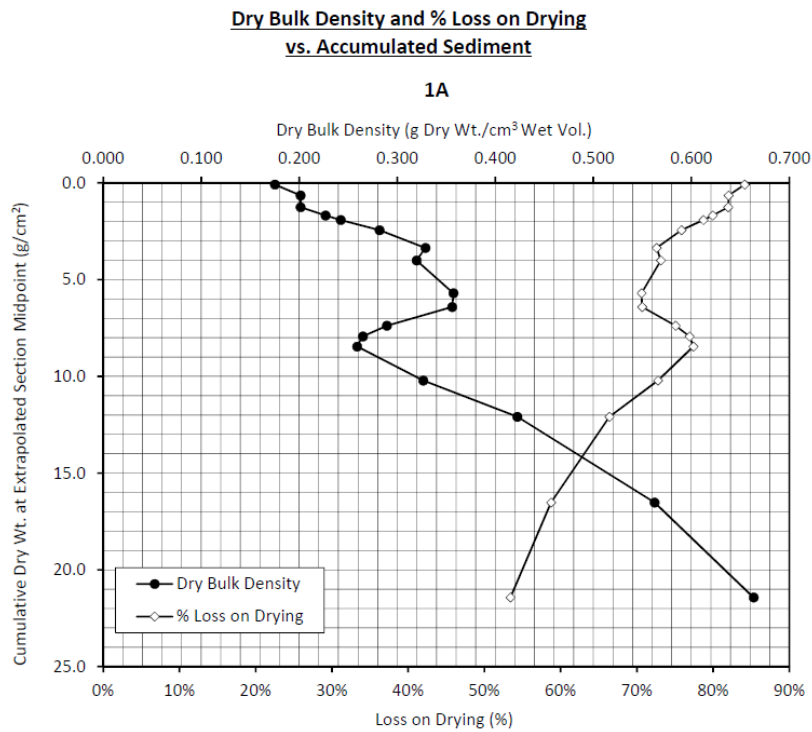
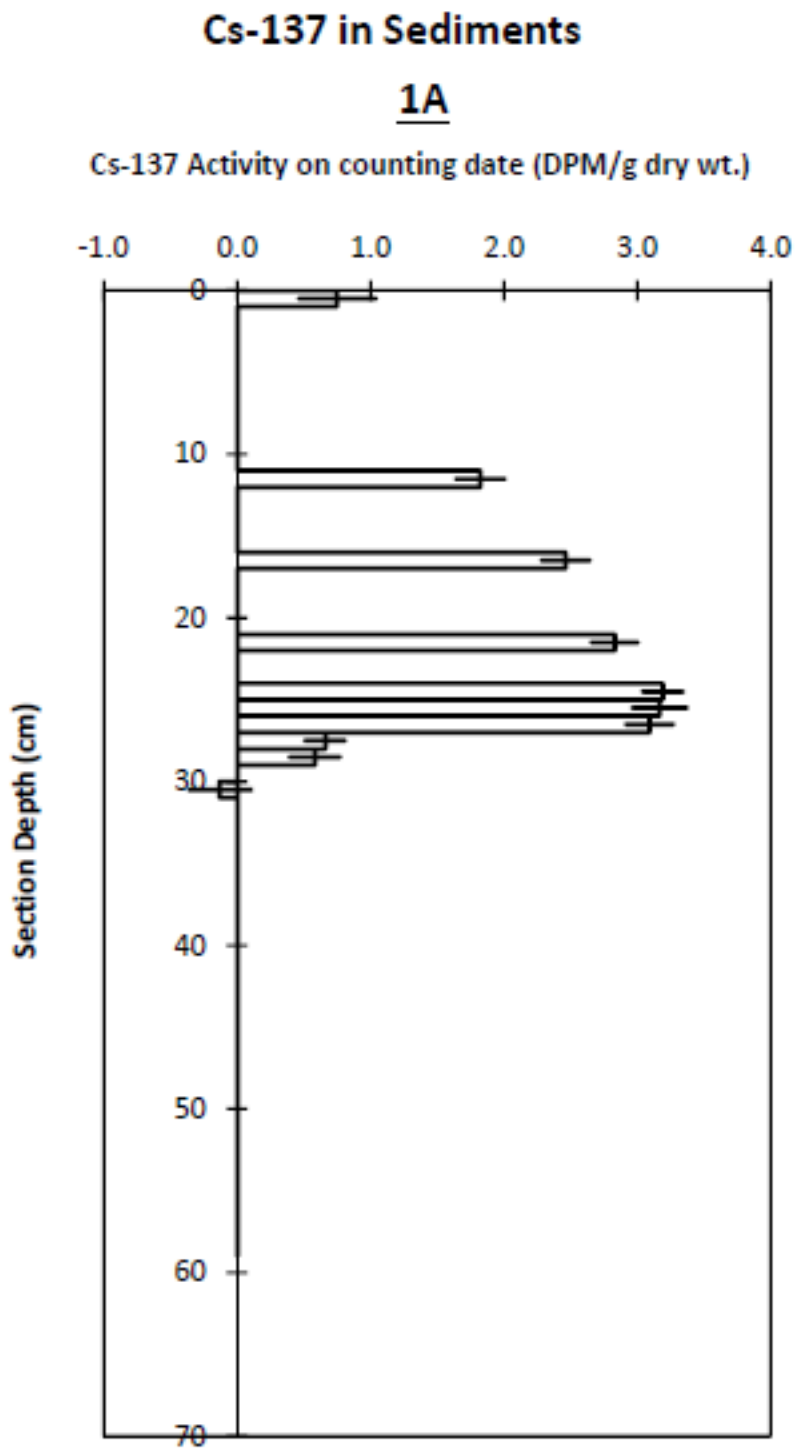


Figure 20 <sup>137</sup>Cs - Profile results of core 1A



Note: The bar plotted at the midpoint depth of each section represents +/- 1 standard deviation of the Cs-137 counting error.

### 3.2.1.3 Water Lot TC-2A - Core 2A

The core sample description is shown on Table 6. Sediments at site 2A consist primarily of silty sediments at the top, coarsening to sandy silt below and then sandy clay at the bottom of the core. The maximum activity of 11.99 DPM/g observed in section 0 – 1 cm is about 8 times the lowest activity of 1.57 DPM/g observed in section 26 – 27 cm (Table A5-1 and Figure 21a).

- › The dry bulk densities generally increased with depth ranging between 0.019 g/cm<sup>3</sup> and 0.431 g/cm<sup>3</sup> (Table A5-1 and Figure 21b).

<sup>226</sup>Ra was measured at 1.34, 1.22 and 1.48 DPM/g in sections 7 – 8 cm, 17 – 18 cm and 37 – 38 cm, respectively (Appendix 5). The <sup>210</sup>Pb activity in the 22 – 23 cm section barely exceeded the <sup>226</sup>Ra activity measured in the 37 – 38 cm section.

- › <sup>226</sup>Ra activity 1.34 (7 - 8 cm), 1.22 (17 – 18 cm) and 1.05 DPM/g (37 – 38 cm)
- › <sup>210</sup>Pb activity (22 – 23 cm) barely exceeded <sup>226</sup>Ra activity (37 – 38 cm)

<sup>137</sup>Cs was measured in core interval of 0 – 14 cm. The <sup>137</sup>Cs activities in this core interval are significantly above background in the upper 11 cm, ranging between 2.25 - 3.63 DPM/g. The shape of <sup>137</sup>Cs profile in the 0 – 11 cm core interval suggests that the majority of the <sup>137</sup>Cs is probably from external erosion sources. The <sup>137</sup>Cs activity then declines gradually with depth below 11 cm (Table A5-2 and Figure 22). The tailing of <sup>137</sup>Cs into deeper depths with <sup>210</sup>Pb dates prior to 1954 is commonly seen and is attributed to downward diffusion of the isotope.

CRS model of Age at bottom of Extrapolated section in years vs. Depth of bottom edge of current section in cm:

- › If one assumes that the activity in section 23 (1.61 DPM/g) is at the background <sup>210</sup>Pb level, then the model can be applied. The measured total activity results (DPM/g) are shown in Table A5-1. The estimated age at the bottom of each section and the individual sedimentation rate for each section are shown in Table A5-1. Plots of age vs. depth, sediment accumulation rate vs. depth and sediment accumulation rate vs. age are shown in Figures 22c, 22d and 22e, respectively.

Regression model of Unsupported <sup>210</sup>Pb activity vs. Cumulative Dry Weight (g/cm<sup>2</sup>):

- › Due to the sudden decrease in total <sup>210</sup>Pb activity at section 10 – 11 cm and the rapid decrease in dry bulk density occurring in the 11 – 12 cm and 14 – 15 cm sections, it is concluded that the model cannot be applied to the core.

### Summary:

In core 2A, the sediment accumulation rates are variable, ranging between 0.0198 g/cm<sup>2</sup>/yr and 0.0448 g/cm<sup>2</sup>/yr, with a large transient increase at section 11 (depth 10 – 11 cm) to 0.0832 g/cm<sup>2</sup>/yr (by the CRS model) (Table A5-1, Figures 22d and 22e).

The elevated <sup>137</sup>Cs activities in the core interval of 0 – 12 cm suggests that the majority of the <sup>137</sup>Cs is probably from external erosion sources, rather than direct deposition from the atmosphere. It is assumed that the 10 – 11 cm section represents the attaining of maximum <sup>137</sup>Cs terrestrial inventory which occurred in 1966, 53 years before the core was obtained. To have confidence that the <sup>210</sup>Pb models are functioning correctly, we typically hope to see the age predicted for the <sup>137</sup>Cs maximum be within 5 years of its known 1966 deposition. In this core, the CRS model indicates an age of 45.3 yrs at 11 cm depth. This age is about 7 years different from what we would expect when it is assumed that <sup>137</sup>Cs maximum inventory has been recorded at 10 – 11 cm. Despite this difference and the uncertainty associated with the unknown sedimentary processes occurring in the 10 – 15 cm core interval, the CRS results are considered compatible with the <sup>137</sup>Cs results, and therefore, it is concluded that the CRS model is providing reasonable estimates of age in this core.

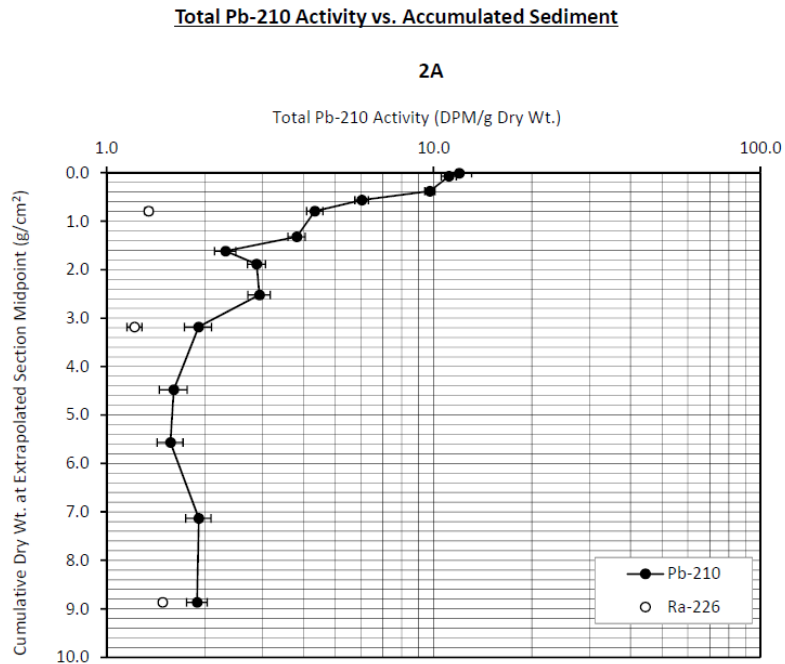
It is cautioned that predicted ages greater than 80 years in this core are gross approximations only.

**Table 6 Core 2A – Sample description**

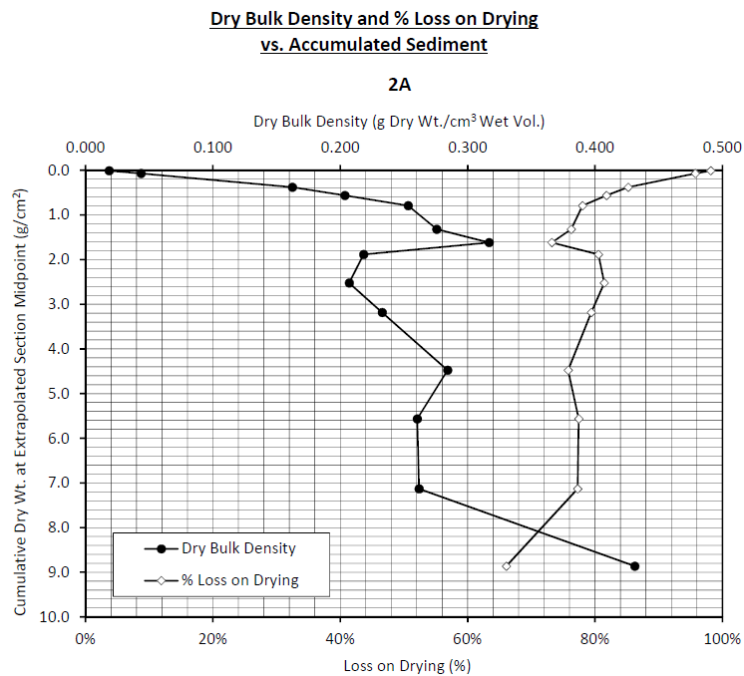
Sample number	Interval [m]		Nature	Texture	Colour	Odour	Notes	Notes
	top	bottom						
2A-2/2-1	0.0	1.0	silt	very watery	brown		vegetation (plenty)	Large quantity of vegetation
2A-2/2-3	2.0	3.0	silt	very watery	brown		vegetation (plenty)	Large quantity of vegetation
2A-2/2-6	5.0	6.0	silt/sand	less watery	brown		vegetation (little)	
2A-2/2-7	6.0	7.0	silt/sand	less watery	brown		vegetation (little)	
2A-2/2-8	7.0	8.0	silt/sand	less watery	brown			
2A-2/2-10	9.0	10.0	silt/sand	less watery	brown			
2A-2/2-11	10.0	11.0	clay/sand	little thick	brown	smell hydrocarbon	of	
2A-2/2-12	11.0	12.0	clay/sand	little thick	brown	smell hydrocarbon	of	
2A-2/2-15	14.0	15.0	clay/sand	little thick	brown	smell hydrocarbon	of	
2A-2/2-18	17.0	18.0	clay/sand	little thick	dark brown	faint smell hydrocarbon	of	
2A-2/2-23	22.0	23.0	clay/sand	little thick	dark brown	faint smell hydrocarbon	of	
2A-2/2-27	26.0	27.0	clay/sand	little thick	dark brown			vegetation (little)
2A-2/2-33	32.0	33.0	clay/sand	little thick	dark brown			
2A-2/2-38	37.0	38.0	clay/sand	little thick	dark brown			vegetation (little)

**Figure 21** <sup>210</sup>Pb – Profile results of core 2A

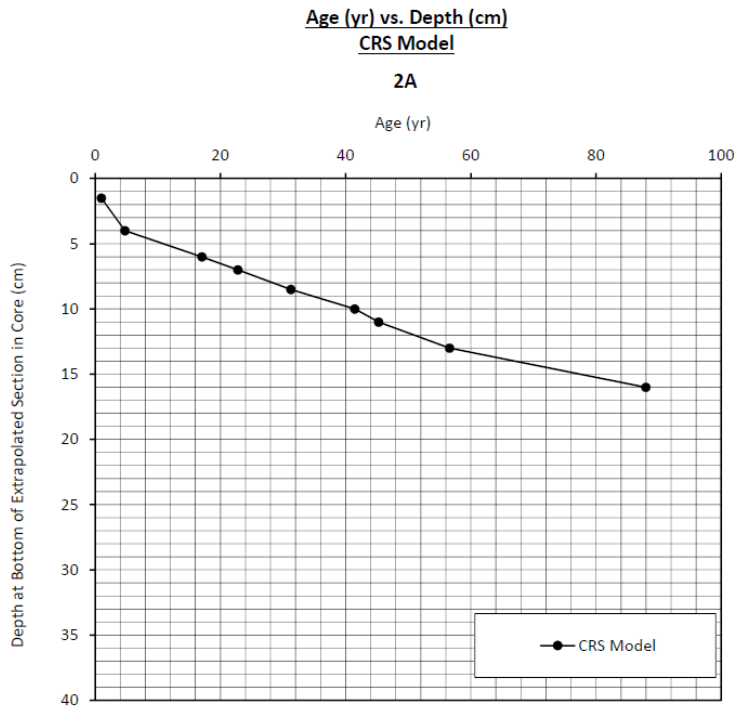
a) Total <sup>210</sup>Pb activity vs accumulated sediments



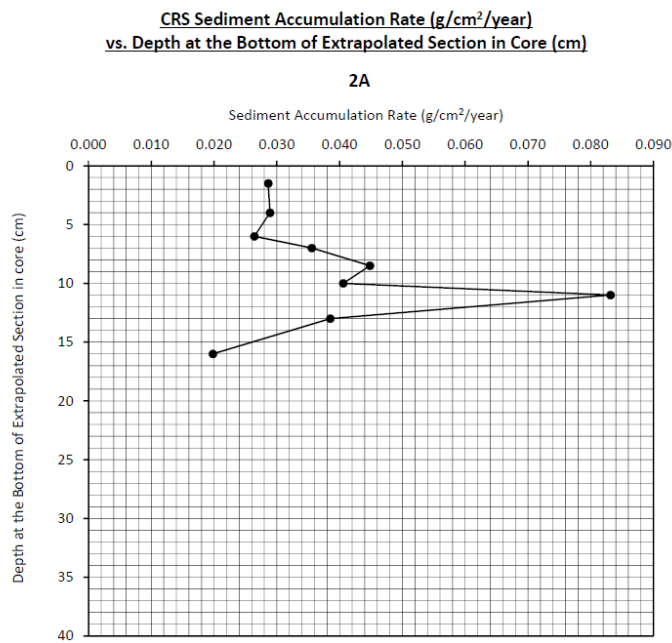
b) Dry bulk density and % loss on drying vs accumulated sediment



c) Age (yr) vs depth (cm) – CRS model vs Linear Regression Model



d) CRS sediment accumulation rate (g/cm<sup>2</sup>/year) vs depth at the bottom of extrapolated



section in core (cm)

e) CRS sediment accumulation rate ( $\text{g}/\text{cm}^2/\text{year}$ ) vs age at bottom of extrapolated section (yr)

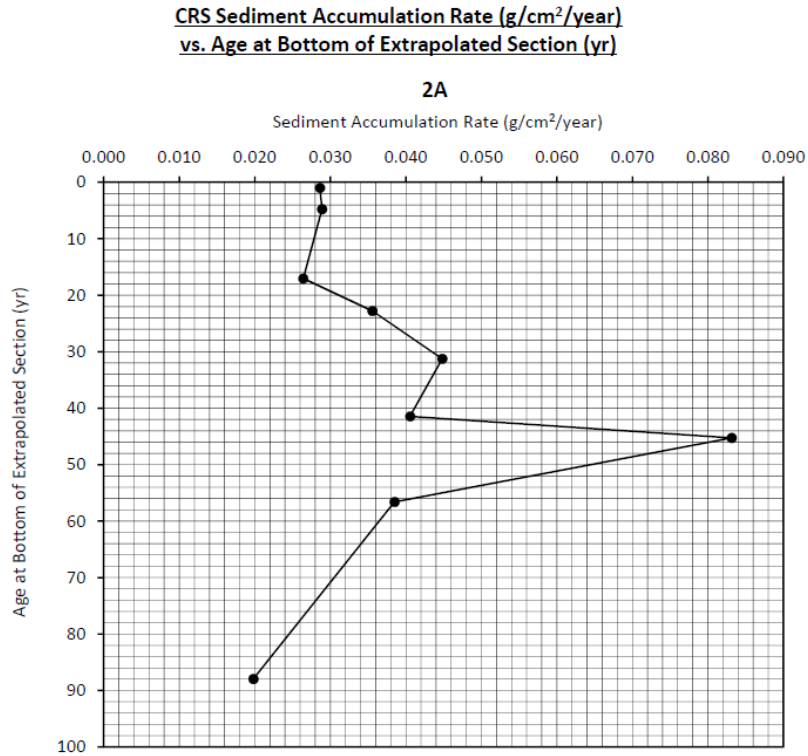
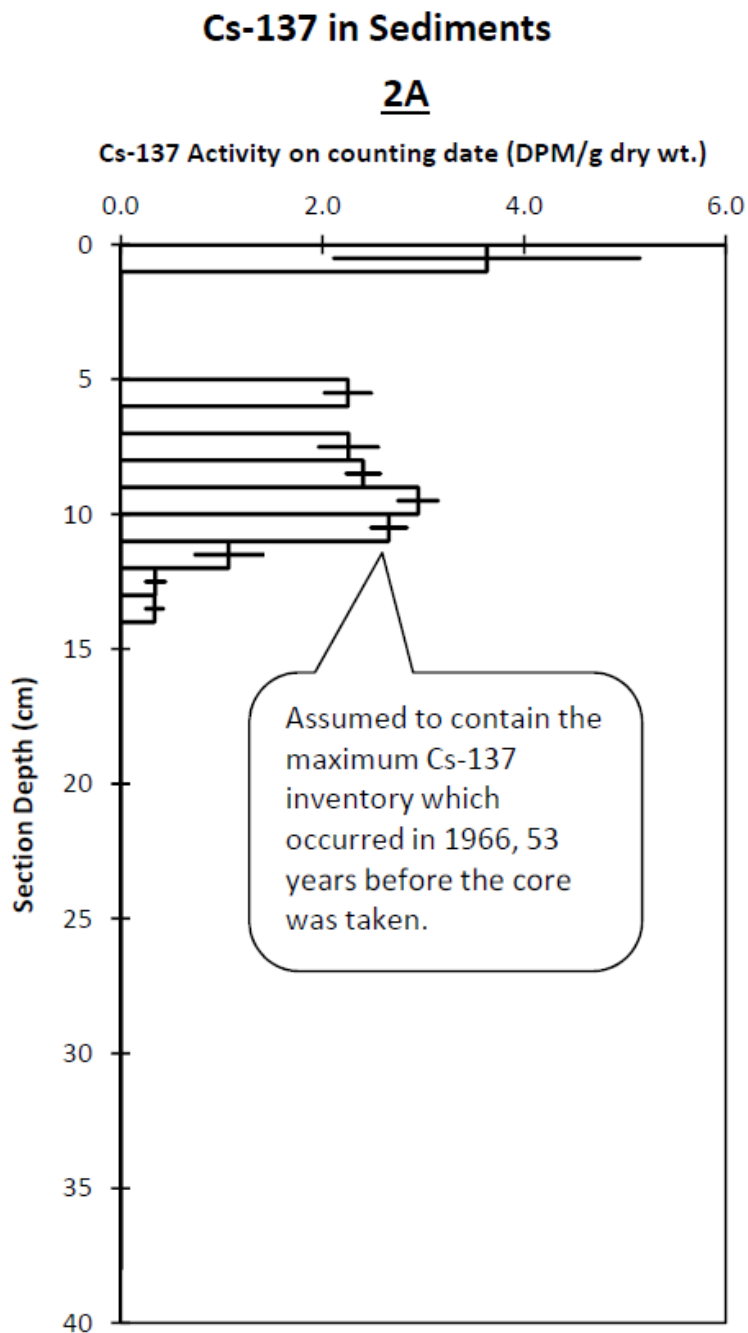


Figure 22 <sup>137</sup>Cs - Profile results of core 2A



Note: The bar plotted at the midpoint depth of each section represents +/- 1 standard deviation of the Cs-137 counting error.

### 3.2.1.4 Water Lot TC-RC - Core 3A

The core sample description is shown on Table 7. Sediments at site 3A consist primarily of silty sediments at the top, overlying sandy clay and clay at the bottom of the core. The maximum activity of 9.07 DPM/g observed in the surface section is about 10 times the lowest activity of 0.91 DPM/g observed in section 19 – 20 cm (Table A6-1 and Figure 23a).

- › The dry bulk densities gradually increased with depth ranging from 0.074 g/cm<sup>3</sup> to 1.411 g/cm<sup>3</sup>. (Table A6-1 and Figure 23b).

<sup>226</sup>Ra was measured at 1.24, 1.31 and 1.28 DPM/g in sections 7 – 8 cm, 17 – 18 cm and 20 – 21 cm, respectively (Appendix 6). The <sup>210</sup>Pb activity in the 20 – 21 cm section is similar to the <sup>226</sup>Ra activity measured in the same section.

- › <sup>226</sup>Ra activity 1.24 (7 – 8 cm), 1.31 (17 – 18 cm) and 1.28 DPM/g (20 – 21 cm)
- › <sup>210</sup>Pb activity (20 – 21 cm) is similar to <sup>226</sup>Ra activity (20 – 21 cm)

<sup>137</sup>Cs was measured in 10 sections in the 1 – 20 cm core interval. Activities in the 1 – 18 cm portion of the core are all significantly above background, ranging between 0.92 - 2.03 DPM/g (Table A6-2 and Figure 24). Below 18 cm, the <sup>137</sup>Cs activity declines with depth. The shape of <sup>137</sup>Cs profile in the 1 – 18 cm core interval suggests that the majority of the <sup>137</sup>Cs is probably from external erosion sources.

CRS model of Age at bottom of Extrapolated section in years vs. Depth of bottom edge of current section in cm:

- › The suspicious sudden termination in exponential decay of the <sup>210</sup>Pb profile in section 19 (depth 18 – 19 cm) as well as the sudden and rapid increase in dry bulk density in the same section are possible causes for us to discard the deeper portion of the core (i.e. truncate the core) due to the increasing uncertainty of the sedimentation process.
- › The <sup>226</sup>Ra activity indicates that the background <sup>210</sup>Pb activity level has not been achieved at 18 cm, leaving us with an incomplete truncated core that normally cannot be processed by the CRS model. In order to allow use of the CRS model, an artificial <sup>210</sup>Pb inventory of 32.105 DPM/cm<sup>2</sup> has been chosen such that the CRS model predicted exactly the same average sediment accumulation rate (0.1185 g/cm<sup>2</sup>/yr) as the linear regression model over the 0 – 18 cm segment of the core. With the CRS model calibrated, it has been used to calculate ages for the core interval of 0 – 18 cm.
- › The measured total activity results (DPM/g) are shown in Table A6-1. The estimated age at the bottom of each section plus the individual sediment accumulation rate for each section are shown in Table A6-2. Plots of age vs. depth, sediment accumulation rate vs. depth and sediment accumulation rate vs. age are shown in Figures 24d, 24e, 24f, respectively.

Regression model of Unsupported <sup>210</sup>Pb activity vs. Cumulative Dry Weight (g/cm<sup>2</sup>):

- › The linear regression model was applied to sections 1 - 18 (depth 0 – 18 cm) and the estimate of sediment accumulation rate was used to calibrate the CRS model.
- › The regression results are shown in Figure 24c. The model predicts ( $R^2 = 0.9502$ ) an average sediment accumulation rate of 0.1185 g/cm<sup>2</sup>/yr when the unsupported <sup>210</sup>Pb activity was calculated by subtracting the nearest neighbouring <sup>226</sup>Ra measurement from each total <sup>210</sup>Pb value. The age estimate at the bottom of each section is shown on Table A6-1 and Figure 24d.

#### Summary:

In core 3A, the significant presence of  $^{137}\text{Cs}$  in the 0 – 18 cm core interval indicates that these sections are less than 56 years old (post 1963). Based upon the shape of the  $^{210}\text{Pb}$  and dry bulk density profiles and the ages predicted by the  $^{210}\text{Pb}$  models, it is suspected that a portion of the core is missing, and it is likely that the 1966 maximum  $^{137}\text{Cs}$  inventory could be recorded in the suspected missing portions of the core. However, the CRS model indicates an age of 38.1 yrs at 18 cm depth, an age compatible with the presence of  $^{137}\text{Cs}$ .

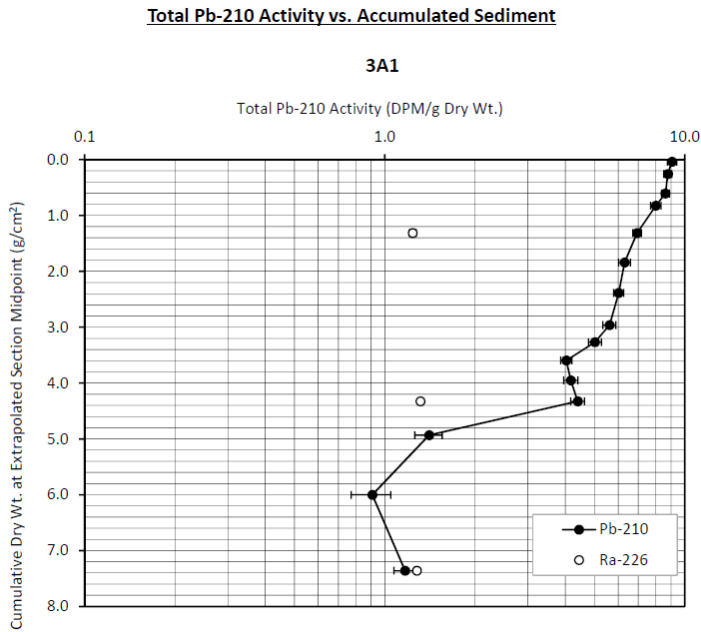
Over the entire core, the average sediment accumulation rate estimated by the CRS model has been forced to exactly coincide with the linear regression estimate of 0.1185 g/cm<sup>2</sup>/yr.

**Table 7 Core 3A – Sample description**

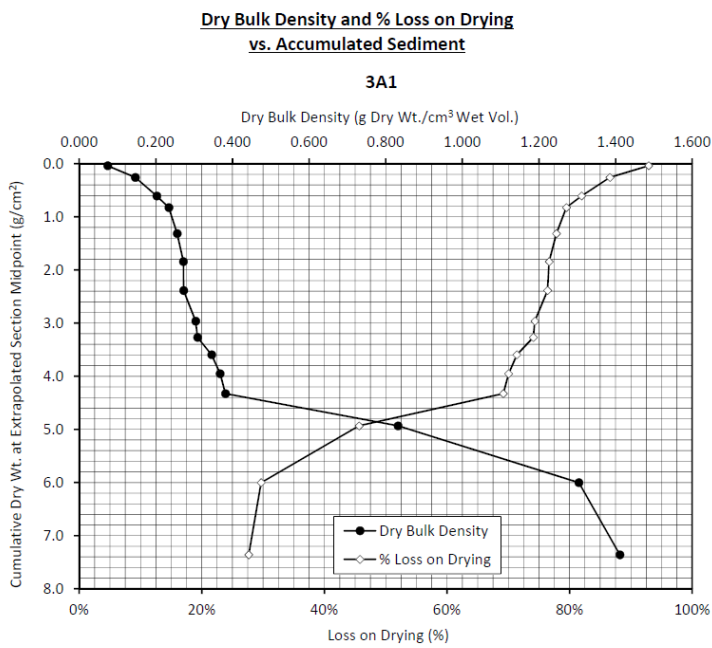
Sample number	Interval [m]		Nature	Texture	Colour	Odour	Notes	Notes
	top	bottom						
3A1-2/2-1	0.0	1.0	silt	very watery	light brown			
3A1-2/2-3	2.0	3.0	clay/silt	watery	light brown		vegetation (plenty)	
3A1-2/2-5	4.0	5.0	sand/clay	watery	light brown		vegetation (little)	
3A1-2/2-6	5.0	6.0	sand/clay	watery	light brown		vegetation (little)	Shell fragments
3A1-2/2-8	7.0	8.0	sand/clay	less watery	light brown		vegetation (little)	
3A1-2/2-10	9.0	10.0	sand/clay	less watery	light brown		vegetation (little)	
3A1-2/2-12	11.0	12.0	sand/clay	little thick	light brown			
3A1-2/2-14	13.0	14.0	sand/clay	little thick	light brown			
3A1-2/2-15	14.0	15.0	sand/clay	little thick	light brown			
3A1-2/2-16	15.0	16.0	sand/clay	little thick	light brown			
3A1-2/2-17	16.0	17.0	sand/clay	little thick	light brown			
3A1-2/2-18	17.0	18.0	sand/clay	little thick	light brown			
3A1-2/2-19	18.0	19.0	clay	very thick not much water	grey			
3A1-2/2-20	19.0	20.0	clay	very thick not much water	grey			
3A1-2/2-21	20.0	21.0	clay	very thick not much water	grey			

**Figure 23** <sup>210</sup>Pb – Profile results of core 3A

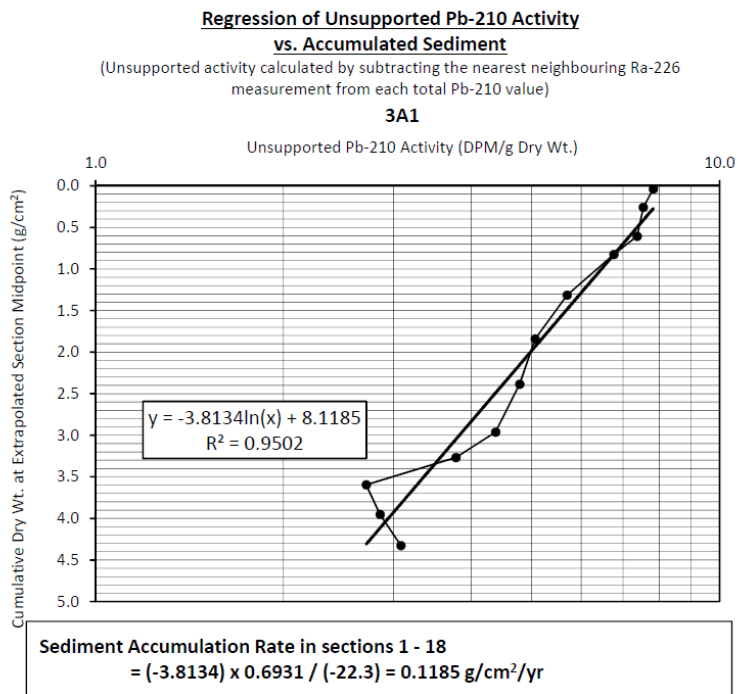
a) Total <sup>210</sup>Pb activity vs accumulated sediments



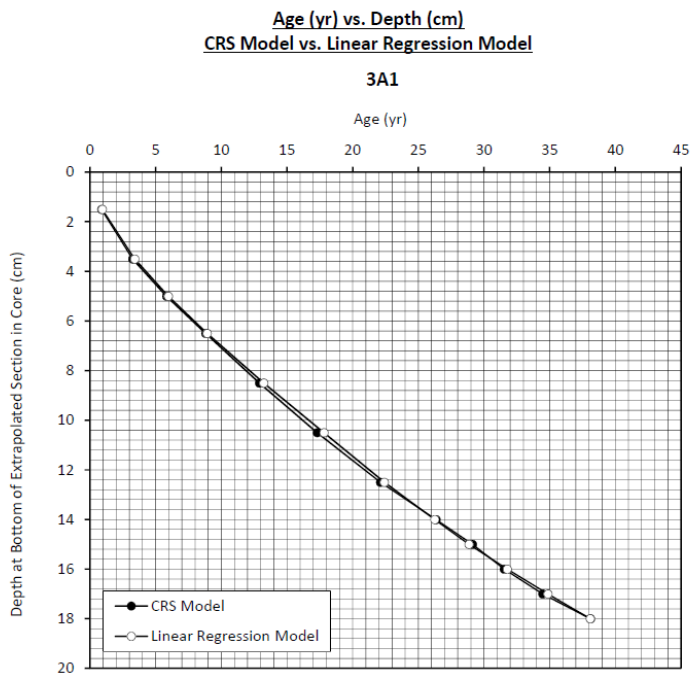
b) Dry bulk density and % loss on drying vs accumulated sediment



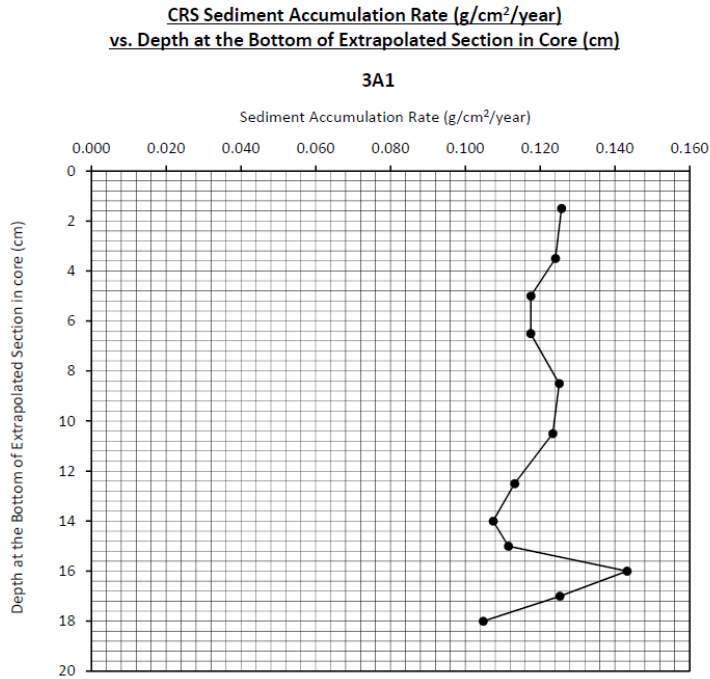
c) Regression of unsupported  $^{210}\text{Pb}$  activity vs accumulated sediment



d) Age (yr) vs depth (cm) – CRS model vs Linear Regression Model



- e) CRS sediment accumulation rate ( $\text{g}/\text{cm}^2/\text{year}$ ) vs depth at the bottom of extrapolated section in core (cm)



- f) CRS sediment accumulation rate ( $\text{g}/\text{cm}^2/\text{year}$ ) vs age at bottom of extrapolated section (yr)

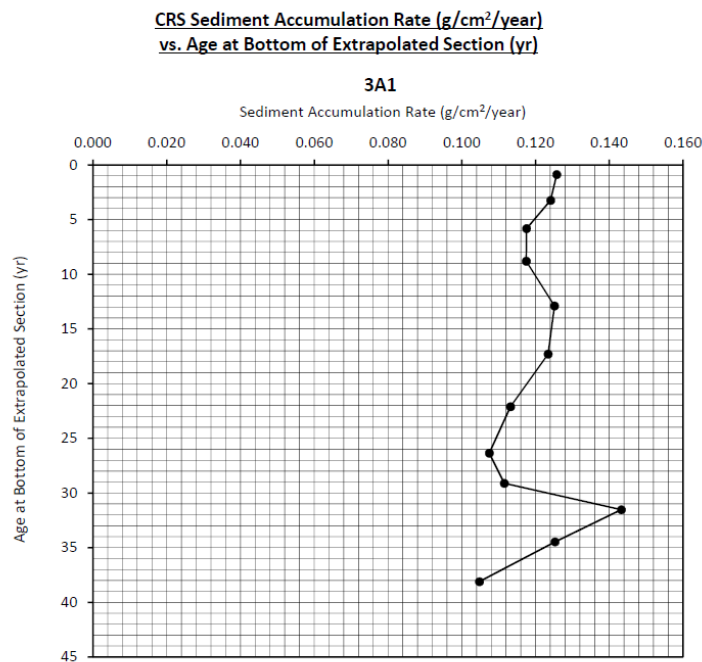
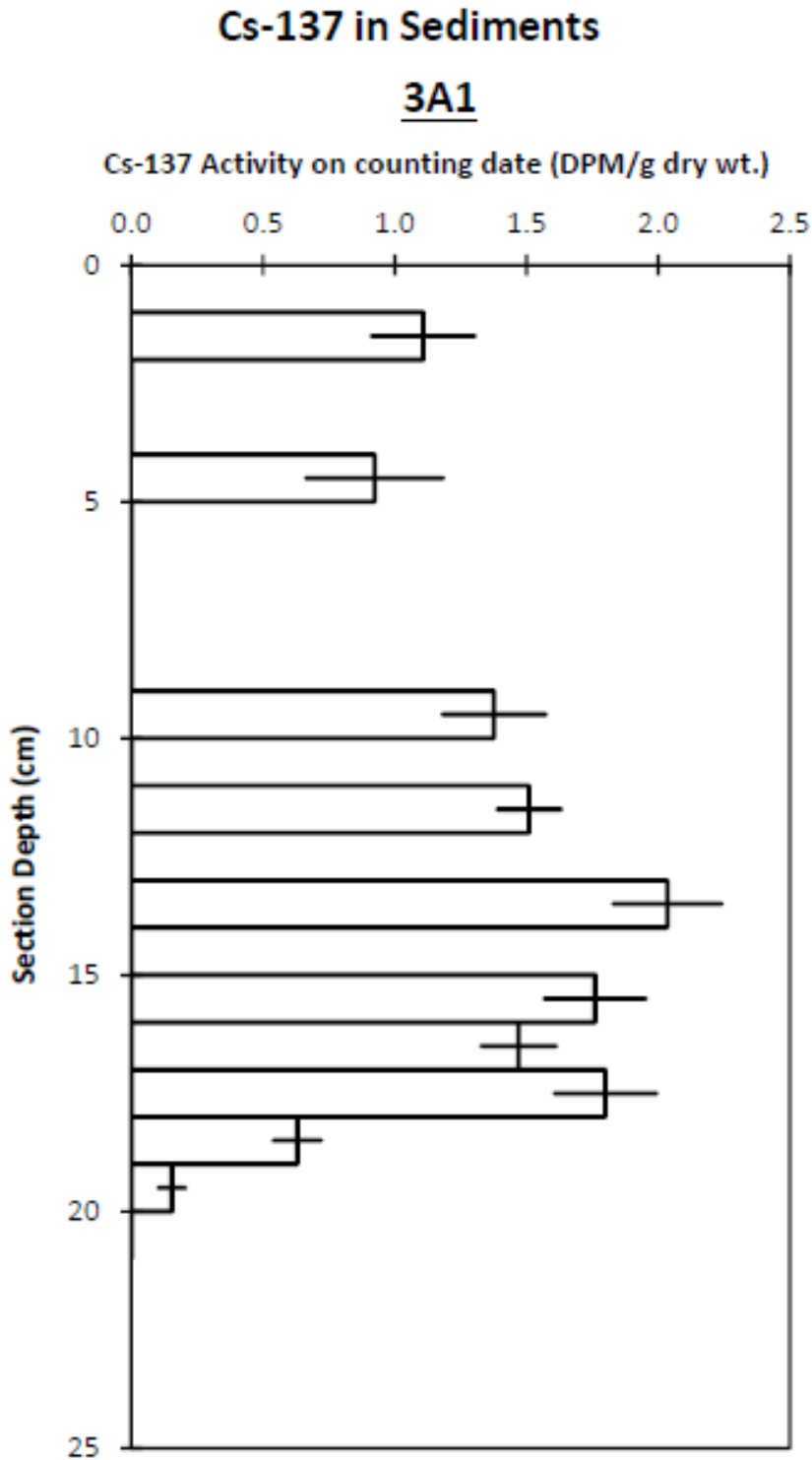


Figure 24 <sup>137</sup>Cs - Profile results of core 3A



Note: The bar plotted at the midpoint depth of each section represents +/- 1 standard deviation of the Cs-137 counting error.

### 3.2.1.5 Water lot PC-W - Core 4A

The core sample description is shown on Table 8. Sediments at site 4A consist primarily of coarser silty sand to sandy silt for the top half of the core, fining downward to sandy clay and clay at the bottom of the core. The maximum activity of 11.20 DPM/g observed in the surface section (extrapolated depth 0 - 1.5 cm) is about 35 times the lowest activity of 0.32 DPM/g observed in section 38 – 39 cm (Table A7-1 and Figure 25a).

- › The dry bulk densities gradually increase ranging from 0.162 g/cm<sup>3</sup> at the surface to 0.454 g/cm<sup>3</sup> at depth 30.5 cm then decreasing to 0.146 g/cm<sup>3</sup> at the bottom of the core (Table A7-1 and Figure 25b).
- › <sup>226</sup>Ra activity 0.83 (5 – 6 cm), 0.91 (17 – 18 cm) and 0.20 DPM/g (38 – 39 cm)
- › <sup>210</sup>Pb activity (38 – 39 cm) barely exceeded <sup>226</sup>Ra activity (38 – 39 cm)

<sup>137</sup>Cs was measured in 10 sections in the 0 - 34 cm core interval. Activities in the 14 - 33 cm portion of the core are all significantly above background, ranging between 0.45 - 1.33 DPM/g (Table A7-1 and Figure 25d).

CRS model of Age at bottom of Extrapolated section in years vs. Depth of bottom edge of current section in cm:

- › The rapid decrease in dry bulk density at section 32 (depth 31 - 32 m) as well as the significant change in <sup>226</sup>Ra activity at the bottom of the core are reasons to discard the deeper portion of the core. The <sup>226</sup>Ra activities indicate that the background <sup>210</sup>Pb activity level has not been achieved at 31 cm, leaving us with an incomplete truncated core that normally cannot be processed by the CRS model. However, in this core it is possible to calibrate the CRS model against the 1963 maximum <sup>137</sup>Cs input, and therefore allow the CRS model to be used (see details in appendix 7).
- › The measured total activity results (DPM/g) are shown in Table A7-1. The estimated age at the bottom of each section as well as the individual sedimentation rate for each section are shown in Table A7-1. Plots of age vs. depth, sediment accumulation rate vs. depth and sediment accumulation rate vs. age are shown in Figures 25d, 25e and 25f respectively.

Regression model of Unsupported <sup>210</sup>Pb activity vs. Cumulative Dry Weight (g/cm<sup>2</sup>):

- › The linear regression model was applied to sections 1 - 30 (depth 0 – 30 cm) and the estimate of sediment accumulation rate was used to validate the CRS model.
- › The regression results are shown in Figure 25c. The model predicts ( $R^2 = 0.9485$ ) an average sediment accumulation rate of 0.2037 g/cm<sup>2</sup>/yr when the unsupported <sup>210</sup>Pb activity was calculated by subtracting the nearest neighbouring <sup>226</sup>Ra measurement from each total <sup>210</sup>Pb value. The age estimation at the bottom of each section is shown on Table A7-1 and Figure 25d.

Summary:

It is assumed that the 1963 peak input of atmospheric <sup>137</sup>Cs has been recorded in the 30 – 31 cm section (Pages 13 and 17), where the maximum <sup>137</sup>Cs activity of 1.33 DPM/g was observed. The CRS model has been forced to predict an age of 56 years to the midpoint depth of this section (30.5 cm). With the CRS model calibrated, section ages down to a depth of 31 cm have been calculated.

Over the interval of sections 1 - 30 (depth 0 – 30 cm), the CRS model predicts an average sediment accumulation rate of 0.1894 g/cm<sup>2</sup>/yr, while the regression model predicts an average rate of 0.2037 g/cm<sup>2</sup>/yr. These results are relatively close and suggest that the CRS model is functioning correctly.

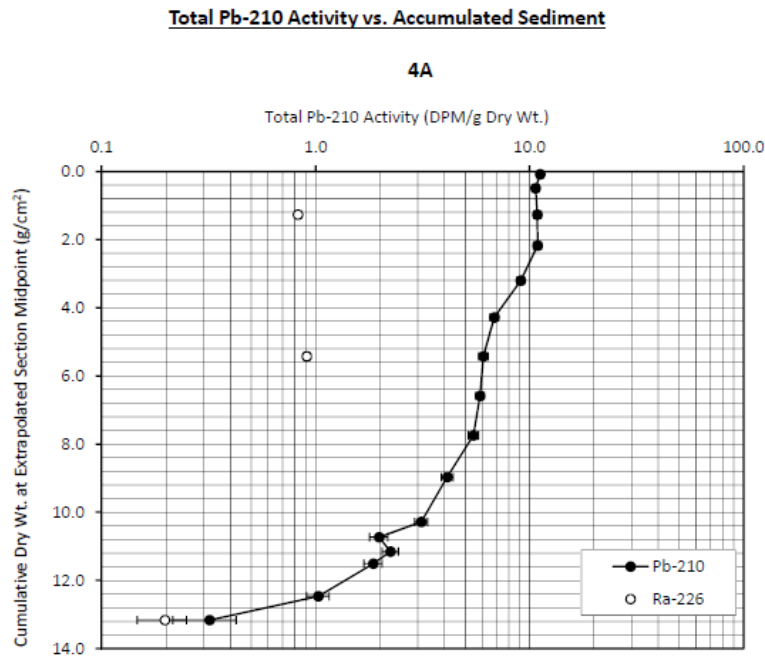
The sediment accumulation rates are variable in this core, ranging between 0.1558 g/cm<sup>2</sup>/yr and 0.2343 g/cm<sup>2</sup>/yr in 0 – 30 cm core interval, with a large increase at section 31 (depth 30 – 31 cm) increasing to 0.4041 g/cm<sup>2</sup>/yr (by the CRS model) (Table A7-1, Figure 25a and 25e).

**Table 8 Core 4A – Sample description**

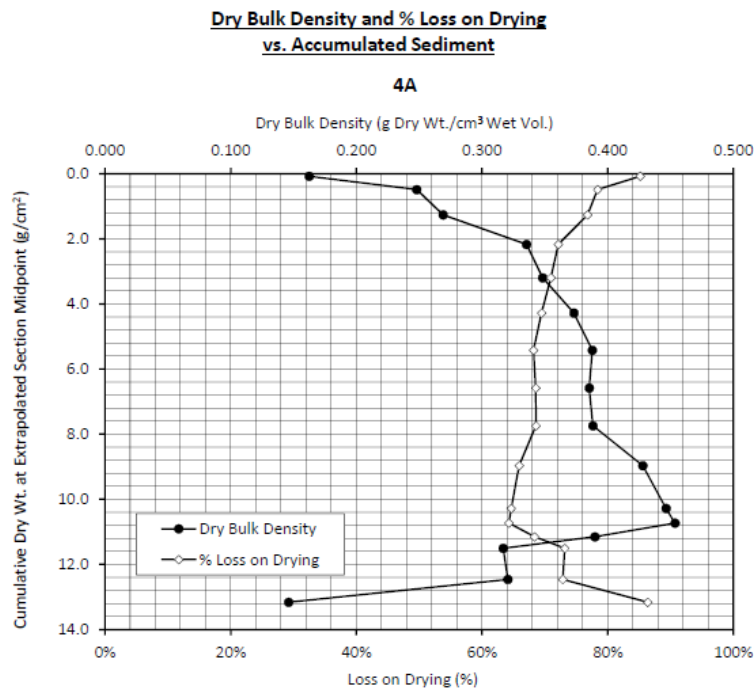
Sample number	Interval [m]		Nature	Texture	Colour	Odour	Notes	Notes
	top	bottom						
4A-2/2-1	0.0	1.0	silt	very watery	dark brown		vegetation (little)	
4A-2/2-3	2.0	3.0	silt/clay	less watery	dark brown	faint smell of decomposed vegetation	vegetation (little)	
4A-2/2-6	5.0	6.0	silt/clay	less watery	dark brown	See above	vegetation (little)	
4A-2/2-9	8.0	9.0	silt/clay	less watery	dark brown	See above		
4A-2/2-12	11.0	12.0	clay/silt	little thick	dark brown	See above		
4A-2/2-15	14.0	15.0	clay/silt	little thick	dark brown	See above		
4A-2/2-18	17.0	18.0	clay/silt	thick	dark brown			
4A-2/2-21	20.0	21.0	clay/silt	little thick	dark brown	See above		
4A-2/2-24	23.0	24.0	clay/silt	little thick	dark brown			
4A-2/2-27	26.0	27.0	clay/silt	thick	dark brown		shell (fragments)	
4A-2/2-30	29.0	30.0	clay/silt	thick	dark brown		shell (fragments)	
4A-2/2-31	30.0	31.0	clay/silt	thick	dark brown			
4A-2/2-32	31.0	32.0	clay/silt	thick	dark brown			
4A-2/2-33	32.0	33.0	clay/silt	thick	dark brown			
4A-2/2-36	35.0	36.0	silt	thick	black		vegetation (plenty)	Fluffy dark organic material, not a lot of water so fairly thick. Large pieces of wood present in sample. Tried to avoid when sub-sampling
4A-2/2-39	38.0	39.0	silt	thick	black		vegetation (plenty)	Fluffy dark organic material, not a lot of water so fairly thick

**Figure 25** <sup>210</sup>Pb – Profile results of core 4A

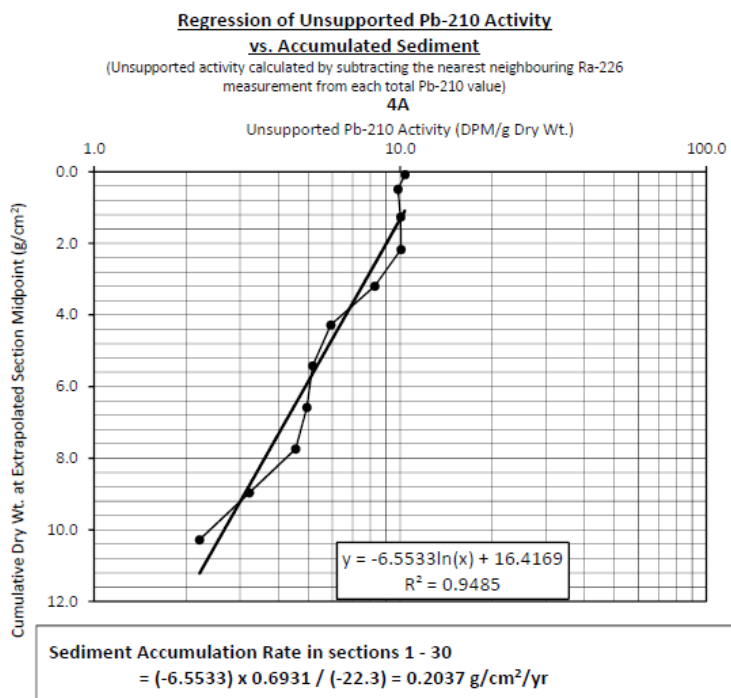
a) Total <sup>210</sup>Pb activity vs accumulated sediments



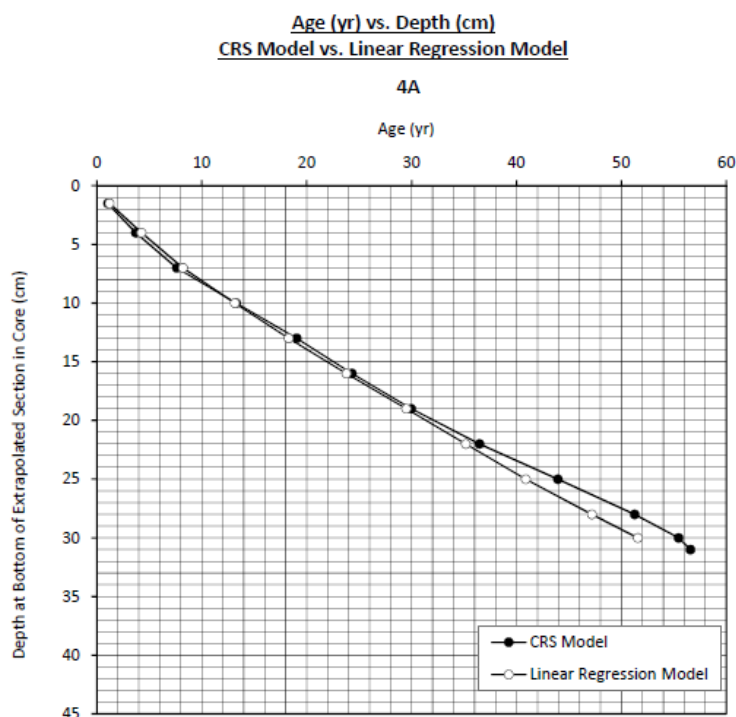
b) Dry bulk density and % loss on drying vs accumulated sediment



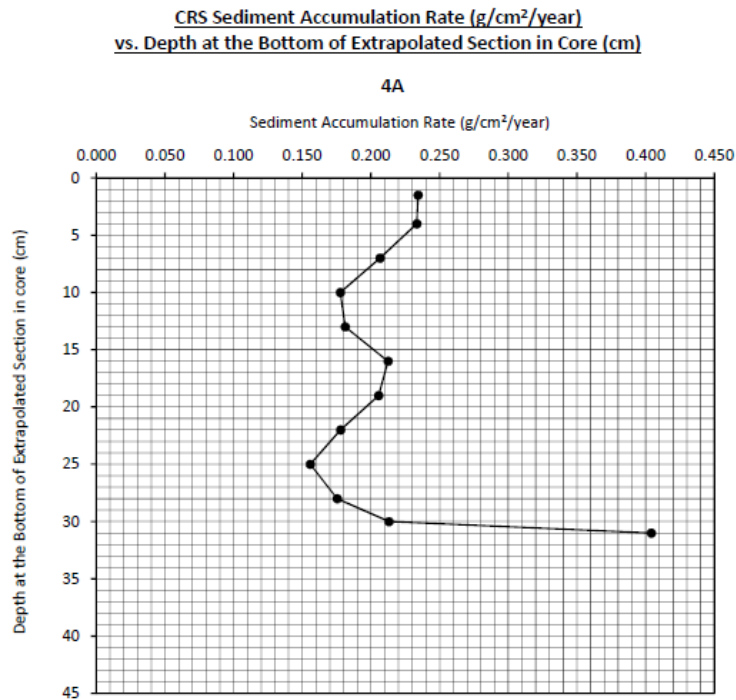
c) Regression of unsupported  $^{210}\text{Pb}$  activity vs accumulated sediment



d) Age (yr) vs depth (cm) – CRS model vs Linear Regression Model



- e) CRS sediment accumulation rate ( $\text{g}/\text{cm}^2/\text{year}$ ) vs depth at the bottom of extrapolated section in core (cm)



- f) CRS sediment accumulation rate ( $\text{g}/\text{cm}^2/\text{year}$ ) vs age at bottom of extrapolated section (yr)

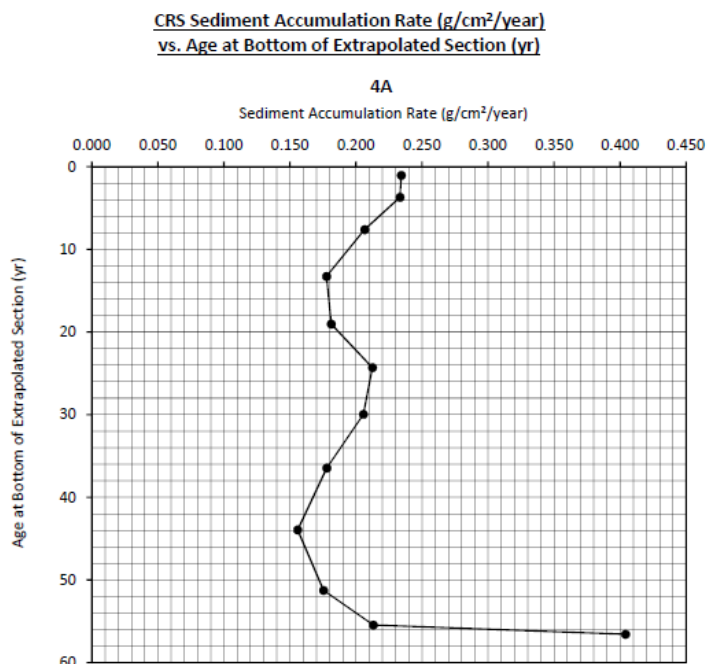
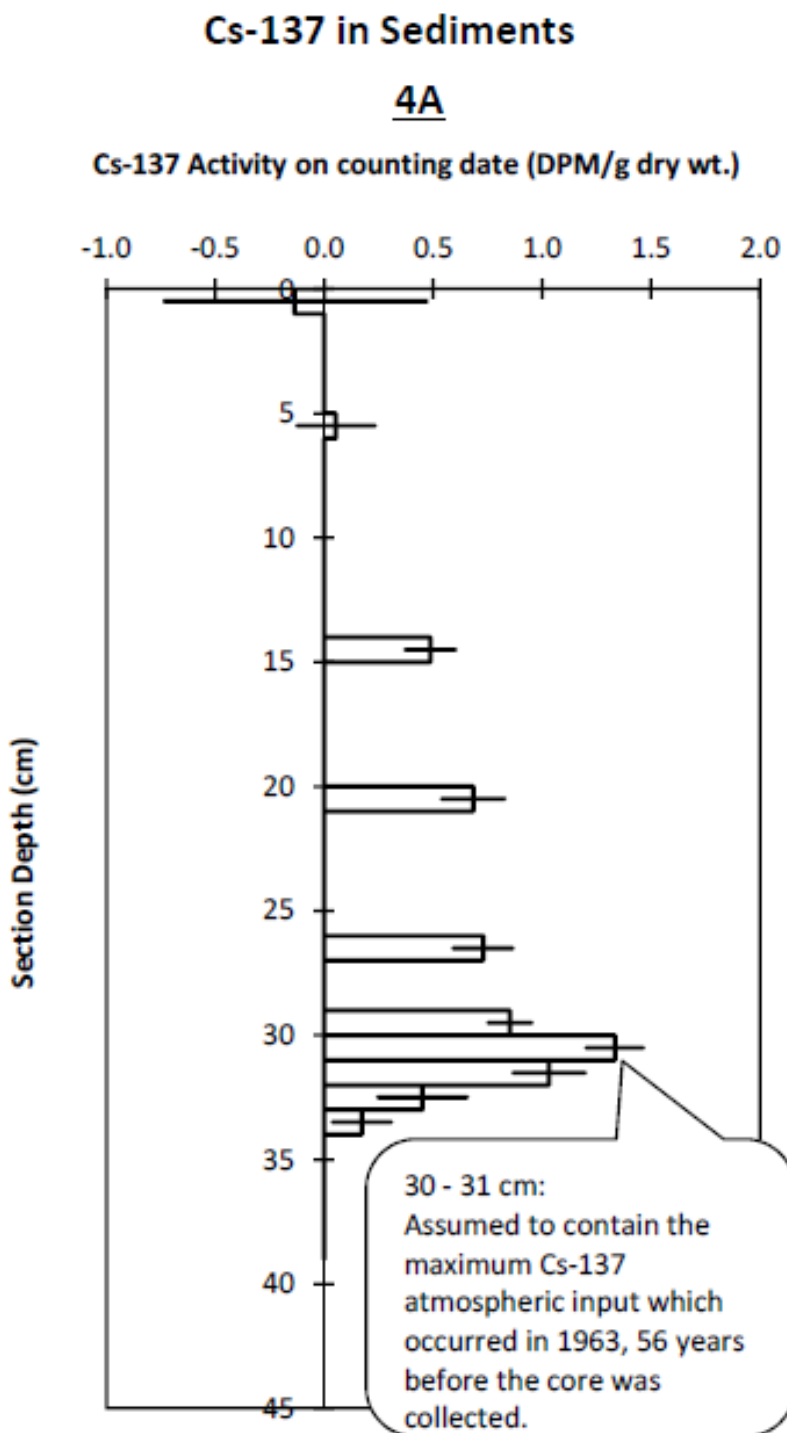


Figure 26 <sup>137</sup>Cs - Profile results of core 4A



Note: The bar plotted at the midpoint depth of each section represents +/- 1 standard deviation of the Cs-137 counting error.

### 3.2.1.6 Water Lot TC-2A - Core 2B

The core sample description is shown on Table 9. Sediments at site 2B are homogeneous and consist primarily of silt material with a slight increase in finer clay size fraction near the bottom of the core. The maximum activity of 12.23 DPM/g observed in section 3 (extrapolated depth 1.5 - 3.5 cm) is about 15 times the lowest activity of 0.84 DPM/g observed in section 51 (extrapolated depth 47.5 - 54.5 cm) (Table A8-1 and Figure 27a). The  $^{210}\text{Pb}$  activity in the surface section (extrapolated depth 0 - 1.5 cm) is slightly lower than the  $^{210}\text{Pb}$  activity in section 3 (extrapolated depth 1.5 - 3.5 cm), and this probably represents increasing sediment accumulation rates, and/or physical mixing, and/or diffusion of  $^{210}\text{Pb}$  across a redox gradient, and/or incomplete diagenesis of surface sediment, and/or incomplete ingrowth of the  $^{210}\text{Po}$ , granddaughter of  $^{210}\text{Pb}$ , actually being measured.

- › The dry bulk densities generally increased with depth, ranging from 0.101 g/cm<sup>3</sup> to 0.924 g/cm<sup>3</sup>
- › The maximum dry bulk density is at 47.5 - 54.5 cm (Table A8-1 and Figure 27b).
- ›  $^{226}\text{Ra}$  activity 1.36 (6 – 7 cm), 1.62 (28 – 29 cm) and at 1.411 g/cm<sup>3</sup> 1.62 DPM/g (67 – 68 cm)
- › Net unsupported  $^{210}\text{Pb}$  activity in core interval of 0 - 17.5 cm was calculated by subtracting the  $^{226}\text{Ra}$  activity measured at 6 – 7 cm section from each total  $^{210}\text{Pb}$  value
- ›  $^{210}\text{Pb}$  activity (67 – 68 cm) is less than  $^{226}\text{Ra}$  activity (67 – 68 cm)

$^{137}\text{Cs}$  was measured in 7 sections in the 12 – 21 cm core interval. Activities in this portion of the core are all significantly above background, ranging between 0.43 - 2.53 DPM/g (Table A8-2 and Figure 28). Below 17 cm, the  $^{137}\text{Cs}$  activity declines with depth. The shape of  $^{137}\text{Cs}$  profile in the 12 – 17 cm core interval suggests that the majority of the  $^{137}\text{Cs}$  is probably from external erosion sources.

CRS model of Age at bottom of Extrapolated section in years vs. Depth of bottom edge of current section in cm:

- › The suspicious sudden termination in exponential decay of the  $^{210}\text{Pb}$  profile in section 19 (extrapolated depth 17.5 - 19.5 cm) as well as the sudden decrease in dry bulk density beginning at section 19 and the continuing decrease in dry bulk density down to section 25, are reasons to discard the deeper portion of the core.
- › The  $^{226}\text{Ra}$  activity indicates that the background  $^{210}\text{Pb}$  activity level has not been achieved at 17.5 cm (extrapolated depth), leaving us with an incomplete truncated core that normally cannot be processed by the CRS model. In order to allow use of the CRS model, an artificial  $^{210}\text{Pb}$  inventory of 30.740 DPM/cm<sup>2</sup> has been chosen such that the CRS model predicted exactly the same average sediment accumulation rate (0.0803 g/cm<sup>2</sup>/yr) as the linear regression model over the 0 - 17.5 cm (extrapolated depth) segment of the core. With the CRS model calibrated, it has been used to calculate ages for the core interval of 0 - 17.5 cm (extrapolated depth).
- › The measured total activity results (DPM/g) are shown in Table A8-1. The estimated age at the bottom of each section and the individual sediment accumulation rate for each section are shown in Table A8-1. Plots of age vs. depth, sediment accumulation rate vs. depth and sediment accumulation rate vs. age are shown in Figures 28d, 28e, 28f, respectively.

#### Regression model of Unsupported $^{210}\text{Pb}$ activity vs. Cumulative Dry Weight ( $\text{g}/\text{cm}^2$ ):

- › The linear regression model was applied to sections 1 - 17 (extrapolated depth 0 - 17.5 cm) and the estimate of sediment accumulation rate is used to calibrate the CRS model over the same core interval.
- › The regression results are shown in Figure 28c and Table 10. The model predicts ( $R^2 = 0.9715$ ) an average sediment accumulation rate of  $0.0803 \text{ g}/\text{cm}^2/\text{yr}$  when a  $^{210}\text{Pb}$  background of  $1.3608 \text{ DPM}/\text{g}$  (closest to the  $^{226}\text{Ra}$  activity of  $1.36 \text{ DPM}/\text{g}$  measured in the 6 – 7 cm section) is chosen from the regression table. The age estimate at the bottom of each section is shown on Table A8-1 and Figure 28d.

#### Summary:

The significant presence of  $^{137}\text{Cs}$  in the 12 – 17 cm core interval indicates that the sediments in these sections are less than 56 years old (post 1963). Based upon the shape of the  $^{210}\text{Pb}$  and dry bulk density profiles and the ages predicted by the  $^{210}\text{Pb}$  models, it is suspected that a portion of the core is missing and it is likely that the 1966 maximum  $^{137}\text{Cs}$  inventory could be recorded in the suspected missing portions of the core (below 17.5 cm, extrapolated depth). However, the CRS model indicates an age of 45.6 yrs at 17.5 cm extrapolated depth, an age compatible with the presence of  $^{137}\text{Cs}$ .

The water level at Kingston Harbour monitor station dropped to a historic low level of  $-0.47 \text{ m}$  below datum on January 23, 1965. [See worksheet 'water level Kingston H'.] It is possible that this low-water level may be related to the disturbance of the shallow water sediments, from which this core was obtained. The modelling results indicate that the disturbance probably occurred about 46 years ago (i.e. in 1973). This is compatible with our belief that a number of years of sediment may be missing from the core below 17.5 cm (extrapolated depth) prior to 1973.

Over the core interval of 0 - 17.5 cm (extrapolated depth), the average sediment accumulation rate estimated by the CRS model has been forced to exactly coincide with the linear regression estimate of  $0.0803 \text{ g}/\text{cm}^2/\text{yr}$ .

**Table 9 Core 2B – Sample description**

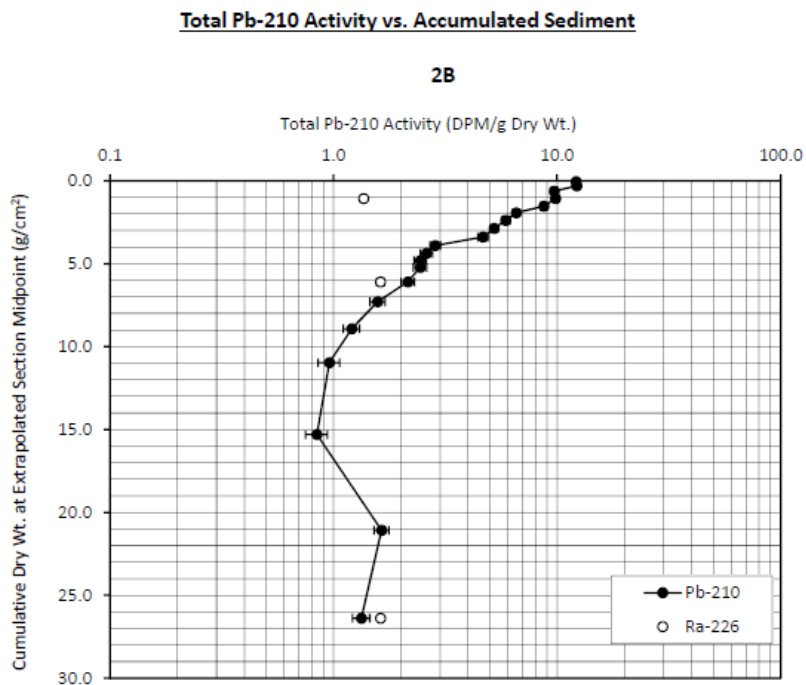
Sample number	Interval		Nature	Texture	Colour	Odour	Notes	Notes
	top	bottom						
2B-2/2-1	0.0	1.0	silt	very watery	dark brown		vegetation (little)	Shell fragments and vegetation.
2B-2/2-3	2.0	3.0	silt	very watery	dark brown		vegetation (little)	Shell fragments and vegetation.
2B-2/2-5	4.0	5.0	silt	very watery	dark brown		vegetation (little)	Shell fragments and vegetation.
2B-2/2-7	6.0	7.0	silt	little thick	dark brown		vegetation (little)	
2B-2/2-9	8.0	9.0	silt	watery	dark brown		vegetation (little)	
2B-2/2-11	10.0	11.0	silt	watery	dark brown		vegetation (little)	Shell fragments and vegetation.
2B-2/2-13	12.0	13.0	silt	watery	dark brown		vegetation (little)	
2B-2/2-15	14.0	15.0	silt	less watery	dark brown		vegetation (little)	
2B-2/2-17	16.0	17.0	silt	little thick	dark brown		vegetation (little)	
2B-2/2-19	18.0	19.0	silt	less watery	dark brown	smell hydrocarbon of		
2B-2/2-21	20.0	21.0	silt	less watery	dark brown	smell hydrocarbon of		
2B-2/2-23	22.0	23.0	silt	less watery	dark brown	smell hydrocarbon of		
2B-2/2-25	24.0	25.0	silt/sand	little thick	dark brown		vegetation (little)	
2B-2/2-29	28.0	29.0	silt	less watery	dark brown			
2B-2/2-34	33.0	34.0	silt	little thick	dark brown			
2B-2/2-40	39.0	40.0	silt	little thick	dark brown			
2B-2/2-45	44.0	45.0	clay/silt	little thick	light brown	not noticeable	shell (fragments)	
2B-2/2-51	50.0	51.0	clay/silt	little thick	light brown	not noticeable	shell (fragments)	
2B-2/2-59	58.0	59.0	clay/silt	little thick	light brown	not noticeable	shell (fragments)	
2B-2/2-68	67.0	68.0	clay	thick	grey/black	not noticeable		

**Table 10 Core 2B – Regression fit as a function of background subtracted**

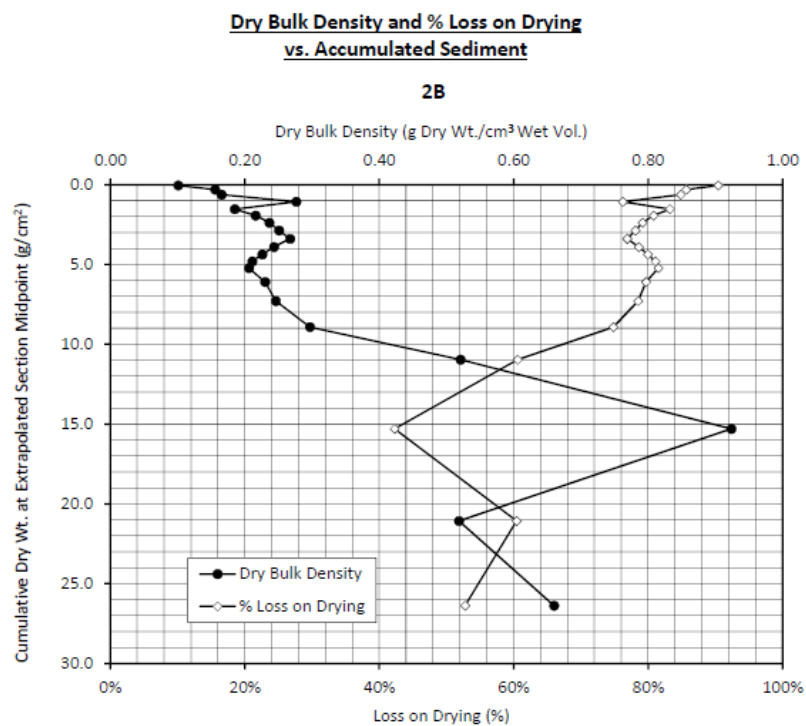
Background (DPM/g)	R <sup>2</sup>	Sediment Accumulation Rate (g/cm <sup>2</sup> /yr)	Slope 'm'	Y intercept 'b'
0.0000	0.9703	0.0986	-3.171	8.119
0.1508	0.9704	0.0966	-3.107	7.923
0.3020	0.9706	0.0946	-3.042	7.727
0.4533	0.9707	0.0925	-2.978	7.532
0.6045	0.9709	0.0905	-2.913	7.338
0.7558	0.9711	0.0885	-2.847	7.144
0.9070	0.9712	0.0865	-2.782	6.951
1.0583	0.9713	0.0844	-2.716	6.759
1.2095	0.9714	0.0824	-2.650	6.568
1.3608	0.9715	0.0803	-2.584	6.377
1.5120	0.9716	0.0782	-2.517	6.187
1.6633	0.9717	0.0761	-2.450	5.997
1.8145	0.9717	0.0740	-2.382	5.809
1.9658	0.9717	0.0719	-2.314	5.621
2.1170	0.9717	0.0698	-2.245	5.433
2.2683	0.9716	0.0676	-2.175	5.246
2.4195	0.9715	0.0654	-2.105	5.059
2.5708	0.9712	0.0632	-2.034	4.873
2.7220	0.9709	0.0610	-1.962	4.687
2.8733	0.9704	0.0587	-1.889	4.501
3.0245	0.9698	0.0564	-1.815	4.315

**Figure 27** <sup>210</sup>Pb – Profile results of core 2B

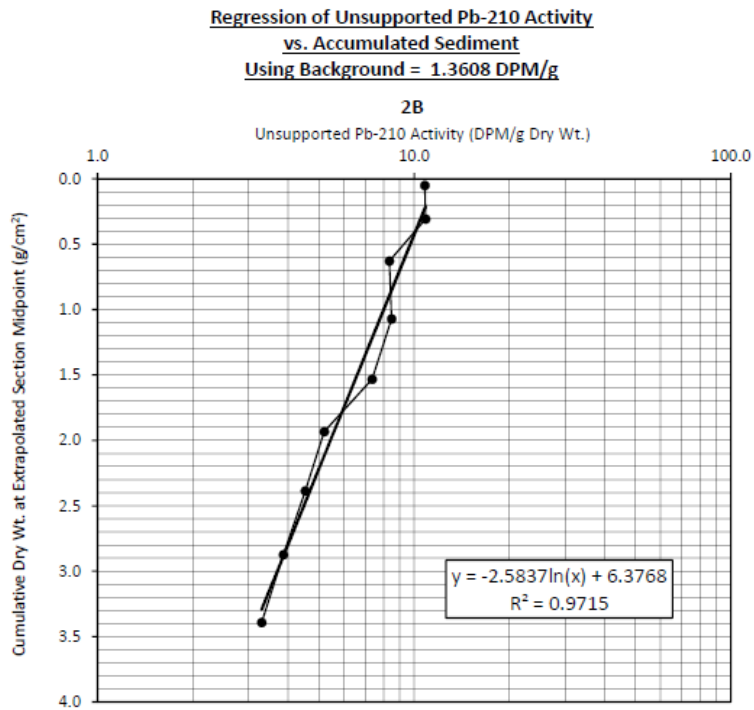
a) Total <sup>210</sup>Pb activity vs accumulated sediments



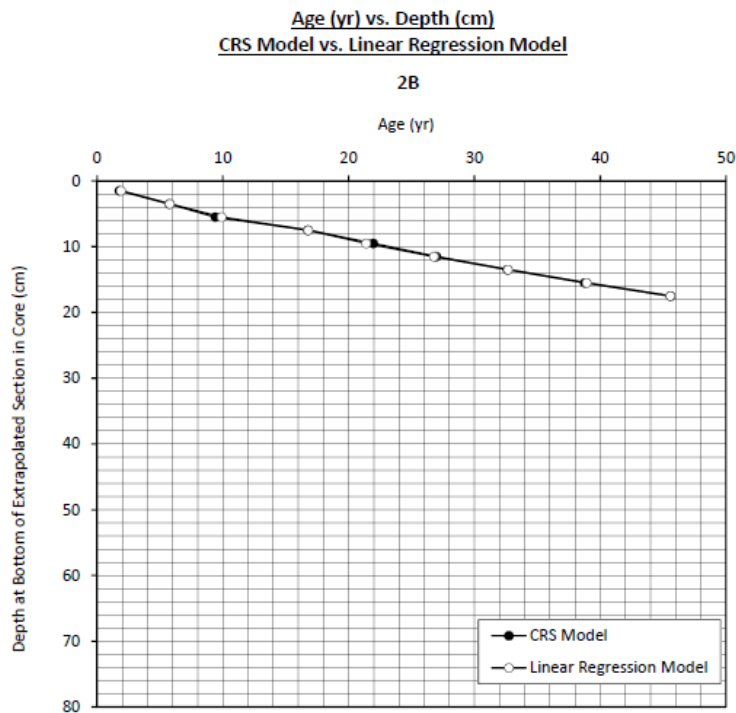
b) Dry bulk density and % loss on drying vs accumulated sediment



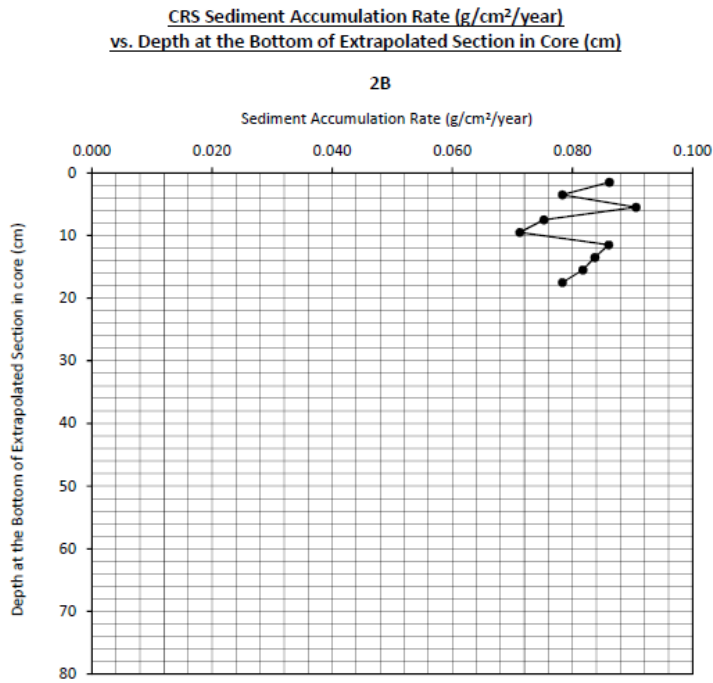
c) Regression of unsupported  $^{210}\text{Pb}$  activity vs accumulated sediment



d) Age (yr) vs depth (cm) – CRS model vs Linear Regression Model



- e) CRS sediment accumulation rate ( $\text{g}/\text{cm}^2/\text{year}$ ) vs depth at the bottom of extrapolated section in core (cm)



- f) CRS sediment accumulation rate ( $\text{g}/\text{cm}^2/\text{year}$ ) vs age at bottom of extrapolated section (yr)

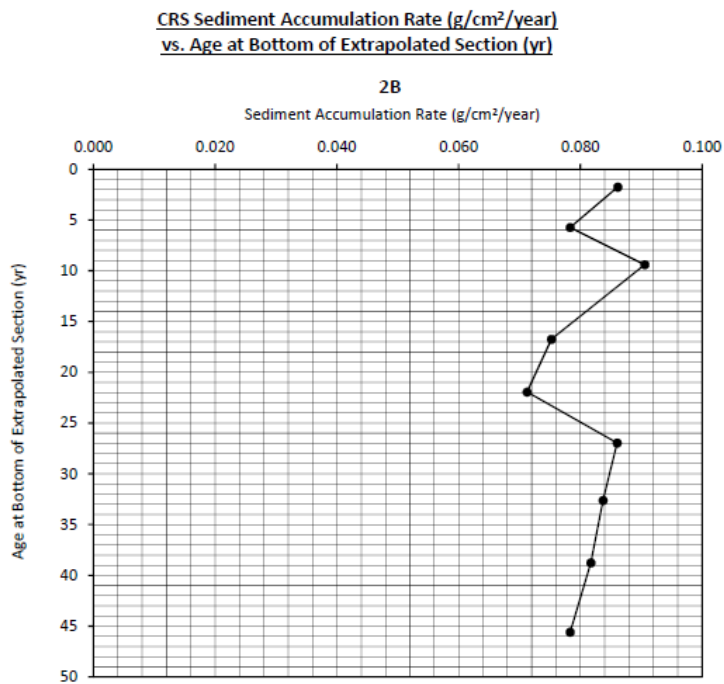
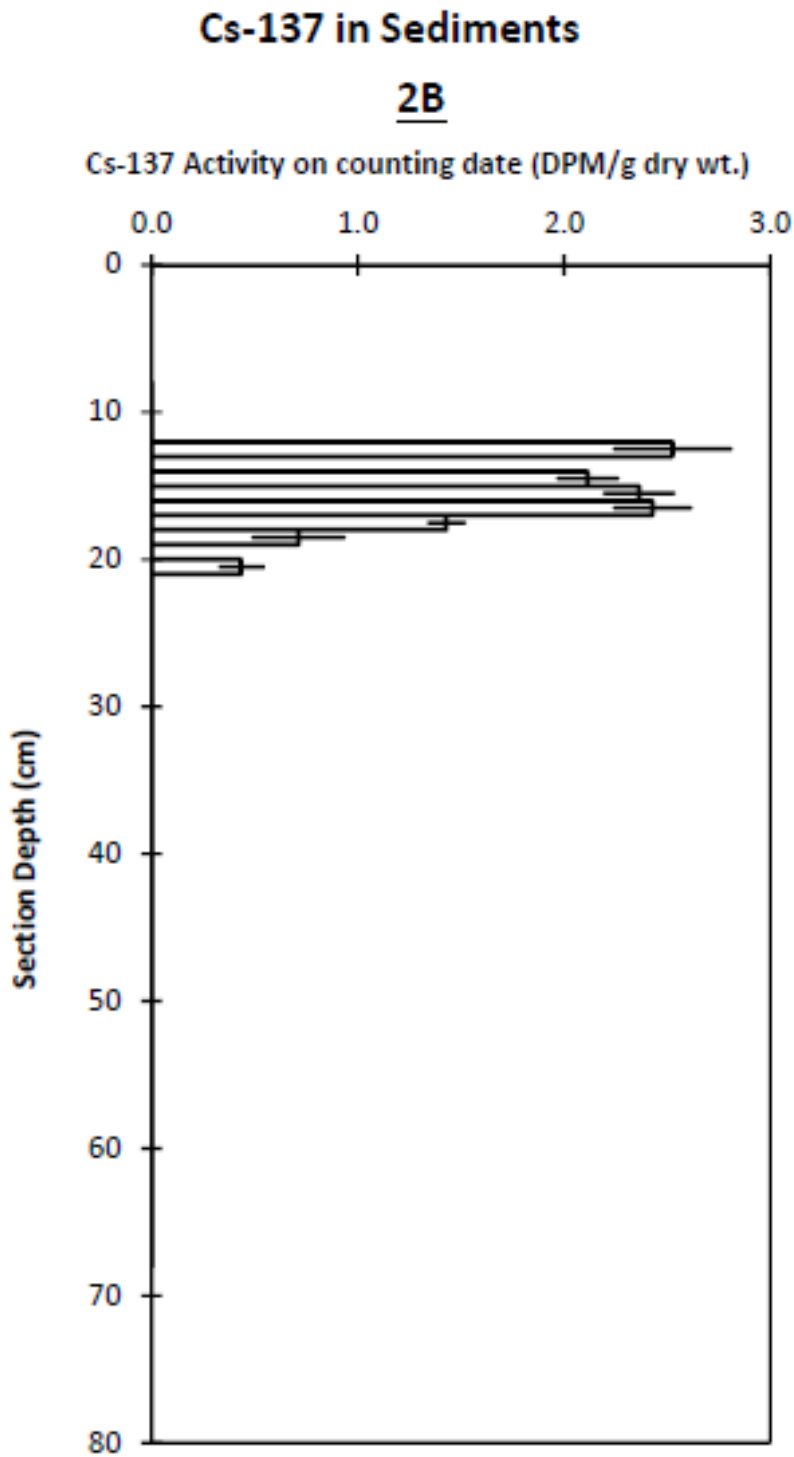


Figure 28 <sup>137</sup>Cs - Profile results of core 2B



Note: The bar plotted at the midpoint depth of each section represents +/- 1 standard deviation of the Cs-137 counting error.

### 3.2.1.7 Water Lot PC-W - Core 4B

The core sample description is shown on Table 11. Alike core 2B, sediments at site 4B are homogeneous and consist primarily of silt material with a slight increase in sand between interval 16 to 23 near the bottom third of the core. The maximum activity of 9.63 DPM/g observed in section 5 (extrapolated depth 3.5 - 5.5 cm) is about 30 times the lowest activity of 0.32 DPM/g observed in section 31 (extrapolated depth 29 - 31 cm) (Table A9-1 and Figure 29a). The  $^{210}\text{Pb}$  activities in sections 1 and 3 (extrapolated depth 0 - 3.5 cm) are slightly lower than the  $^{210}\text{Pb}$  activity in section 5 (extrapolated depth 3.5 - 5.5 cm), and this probably represents increasing sediment accumulation rates, and/or physical mixing, and/or diffusion of  $^{210}\text{Pb}$  across a redox gradient, and/or incomplete diagenesis of surface sediment, and/or incomplete ingrowth of the  $^{210}\text{Po}$ , granddaughter of  $^{210}\text{Pb}$ , actually being measured.

- › The dry bulk densities generally increased with depth, from 0.117 g/cm<sup>3</sup> to 0.934 g/cm<sup>3</sup>
- › The maximum dry density is at 19.5 – 21 cm below which it decreased to 0.178 g/cm<sup>3</sup> at the bottom of the core (Table A9-1 and Figure 29b).
- ›  $^{226}\text{Ra}$  activity 1.07 (6 – 7 cm), 1.05 (16 – 17 cm), 0.93 (18 – 19 cm), 0.52 (20 – 21 cm), 0.50 (21 – 22 cm), 0.47 (23 – 24 cm) and 0.35 DPM/g (30 – 31 cm)
- › Net unsupported  $^{210}\text{Pb}$  activity in core interval of 0 - 24.5 cm (extrapolated depth) was calculated by subtracting the nearest neighbouring  $^{226}\text{Ra}$  activity from each total  $^{210}\text{Pb}$  value, unless note otherwise
- ›  $^{210}\text{Pb}$  activity (30 – 31 cm) is very close to  $^{226}\text{Ra}$  activity (30 – 31 cm)

$^{137}\text{Cs}$  was measured in 10 sections in the 14 – 28 cm core interval. Activities in the 14 – 26 cm core interval are all significantly above background, ranging between 0.40 - 1.24 DPM/g (Table A9-2 and Figure 30). Below 23 cm, the  $^{137}\text{Cs}$  activity declines with depth. The shape of  $^{137}\text{Cs}$  profile in the 14 – 24 cm core interval suggests that the majority of the  $^{137}\text{Cs}$  is probably from external erosion sources.

CRS model of Age at bottom of Extrapolated section in years vs. Depth of bottom edge of current section in cm:

- › The  $^{210}\text{Pb}$  activities in sections 25 – 26 cm, 27 – 28 cm and 30 – 31 cm are not significantly different from the  $^{226}\text{Ra}$  activities measured in sections 23 – 24 cm and 30 – 31 cm, and therefore, it is suspected that the bottom 3 sections are likely an older basement sediment overlaid with different more recent sediment accumulation. This is possible cause for us to exclude the sections below 25 cm from the CRS calculation, due to the increasing uncertainty of the sedimentation process.
- › The  $^{226}\text{Ra}$  activity indicates that the background  $^{210}\text{Pb}$  activity level has not been achieved at 24.5 cm (extrapolated depth), leaving us with an incomplete truncated core that normally cannot be processed by the CRS model. In order to allow use of the CRS model, an artificial  $^{210}\text{Pb}$  inventory of 35.740 DPM/cm<sup>2</sup> has been chosen such that the CRS model predicted exactly the same average sediment accumulation rate (0.1121 g/cm<sup>2</sup>/yr) as the linear regression model over the 3.5 - 24.5 cm (extrapolated depth) segment of the core. With the CRS model calibrated, it has been used to calculate ages for the core interval of 0 - 24.5 cm (extrapolated depth).
- › The measured total activity results (DPM/g) are shown in Table A9-1. The estimated age at the bottom of each section as well as the individual sediment accumulation rate for each section are shown Table A9-1. Plots of age vs. depth, sediment accumulation rate vs. depth and sediment accumulation rate vs. age are shown in Figures 30d, 30e and 30f, respectively.

#### Regression model of Unsupported $^{210}\text{Pb}$ activity vs. Cumulative Dry Weight ( $\text{g}/\text{cm}^2$ ):

- › The linear regression model was applied to sections 5 - 17 (extrapolated depth 3.5 - 17.5 cm) and the estimate of sediment accumulation rate is used to calibrate the CRS model over the same core interval.
- › The regression results are shown in Figure 30c. The model predicts ( $R^2 = 0.9667$ ) an average sediment accumulation rate of  $0.1121 \text{ g}/\text{cm}^2/\text{yr}$  when the unsupported  $^{210}\text{Pb}$  activity was calculated by subtracting the nearest neighbouring  $^{226}\text{Ra}$  measurement from each total  $^{210}\text{Pb}$  value. The age of 3.7 years previously calculated for the bottom of section 3 (extrapolated depth 3.5 cm) by the CRS model must be added to the age estimate at the bottom of any core section. For example, the age at the bottom of section 9 (extrapolated depth 10 cm) is calculated as  $3.7 + (1.856 - 0.499) / 0.1121 = 15.8 \text{ yrs}$ . The age estimate at the bottom of each section is shown on Table A9-1 and Figure 30c.

#### Summary:

In core 4B, the sediment accumulation rates remain relatively constant in section 1 - 17 (extrapolated depth 0 - 17.5 cm), ranging between  $0.1026 \text{ g}/\text{cm}^2/\text{yr}$  and  $0.1400 \text{ g}/\text{cm}^2/\text{yr}$ . Below 17.5 cm the sediment accumulation rates start to increase with depth, peaking at  $0.6029 \text{ g}/\text{cm}^2/\text{yr}$  in section 22 (extrapolated depth 22.5 cm), and then decrease to  $0.3462 \text{ g}/\text{cm}^2/\text{yr}$  in section 24 (extrapolated depth 22.5 - 24.5 cm by the CRS model) (Table A9-1 and Figures 30d and 30e).

The elevated  $^{137}\text{Cs}$  activities in the core interval of 14 – 24 cm suggests that the majority of the  $^{137}\text{Cs}$  is probably from external erosion sources, rather than direct deposition from the atmosphere. It is assumed that the 23 – 24 cm section represents the attaining of maximum  $^{137}\text{Cs}$  terrestrial inventory which occurred in 1966, 53 years before the core was obtained. To have confidence that the  $^{210}\text{Pb}$  models are functioning correctly, we typically hope to see the age predicted for the  $^{137}\text{Cs}$  maximum be within 5 years of its known 1966 deposition. In this core, the CRS model indicates an age of 52.9 yrs at 24.5 cm (extrapolated depth). This age is very close to what we would expect when it is assumed that  $^{137}\text{Cs}$  maximum inventory has been recorded at 23 - 24 cm. Despite the small difference and the uncertainty associated with the unknown sedimentary processes occurring below 24.5 cm (extrapolated depth), the CRS results are considered compatible with the  $^{137}\text{Cs}$  results, and therefore, it is concluded that the CRS model is providing reasonable estimates of age in this core.

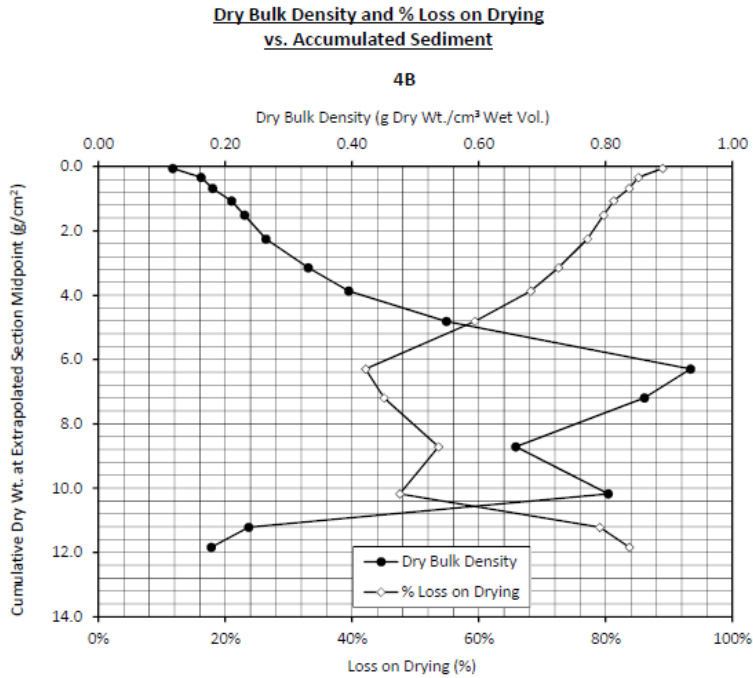
Over the core interval of 3.5 - 17.5 cm (extrapolated depth), the average sediment accumulation rate estimated by the CRS model has been forced to exactly coincide with the linear regression estimate of  $0.1121 \text{ g}/\text{cm}^2/\text{yr}$ .

**Table 11 Core 4B – Sample description**

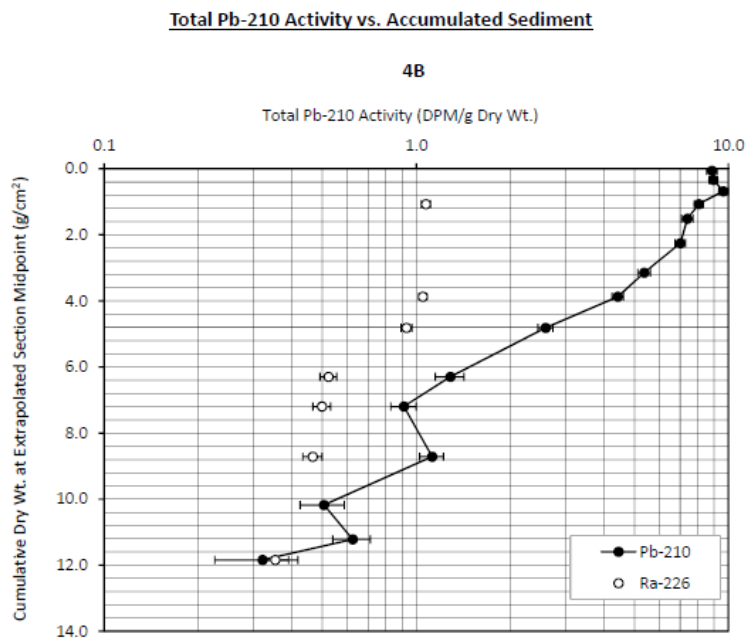
Sample number	Interval [m]		Nature	Texture	Colour	Odour	Notes	Notes
	top	bottom						
4B-2/2-1	0.0	1.0	silt	very watery	brown	not noticeable	vegetation (plenty)	
4B-2/2-3	2.0	3.0	silt	very watery	brown	not noticeable	vegetation (plenty)	
4B-2/2-5	4.0	5.0	silt	very watery	brown	not noticeable	vegetation (plenty)	
4B-2/2-7	6.0	7.0	silt	very watery	brown	not noticeable	vegetation (plenty)	
4B-2/2-9	8.0	9.0	silt	less watery	brown	not noticeable	vegetation (plenty)	
4B-2/2-12	11.0	12.0	silt	watery	brown	not noticeable	vegetation (little)	
4B-2/2-15	14.0	15.0	silt	little thick	brown	not noticeable	vegetation (plenty)	
4B-2/2-17	16.0	17.0	silt/sand	little thick	brown	not noticeable	vegetation (plenty)	
4B-2/2-19	18.0	19.0	silt/sand	little thick	brown	not noticeable	shell (fragments)	
4B-2/2-21	20.0	21.0	silt/sand	thick	brown	not noticeable	shell (fragments)	Shell fragments
4B-2/2-22	21.0	22.0	silt/sand	thick	brown	not noticeable	shell (fragments)	Shell fragments
4B-2/2-24	23.0	24.0	silt/sand	thick	brown	not noticeable	shell (fragments)	Shell fragments
4B-2/2-26	25.0	26.0	silt	thick	brown	not noticeable	vegetation (plenty)	Shell fragments
4B-2/2-28	27.0	28.0	silt	thick	brown	not noticeable	vegetation (plenty)	
4B-2/2-31	30.0	31.0	silt	thick	brown	not noticeable	vegetation (plenty)	

**Figure 29** <sup>210</sup>Pb – Profile results of core 4B

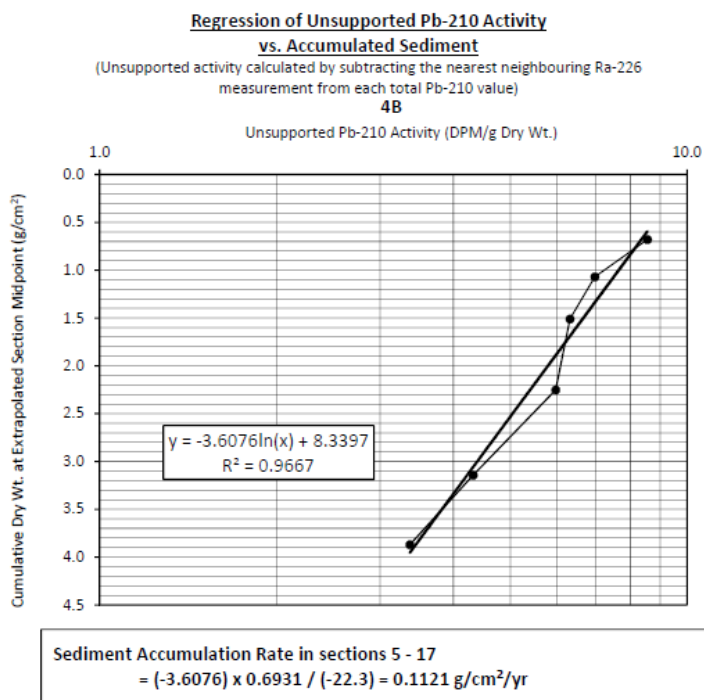
a) Total <sup>210</sup>Pb activity vs accumulated sediments



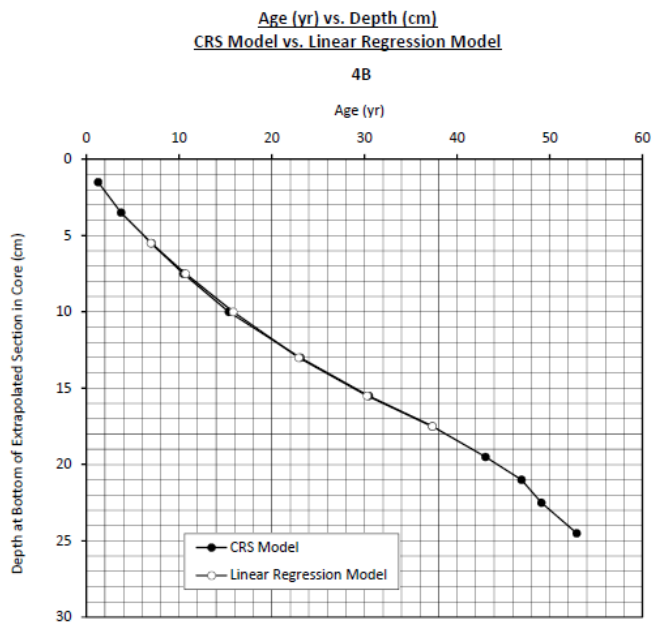
b) Dry bulk density and % loss on drying vs accumulated sediment



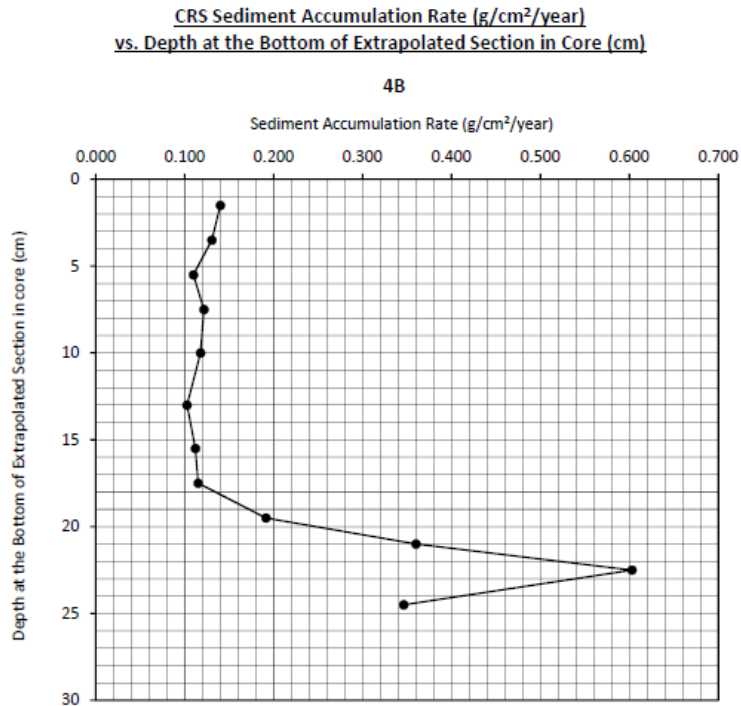
c) Regression of unsupported <sup>210</sup>Pb activity vs accumulated sediment



d) Age (yr) vs depth (cm) – CRS model vs Linear Regression Model



- e) CRS sediment accumulation rate ( $\text{g}/\text{cm}^2/\text{year}$ ) vs depth at the bottom of extrapolated section in core (cm)



- f) CRS sediment accumulation rate ( $\text{g}/\text{cm}^2/\text{year}$ ) vs age at bottom of extrapolated section (yr)

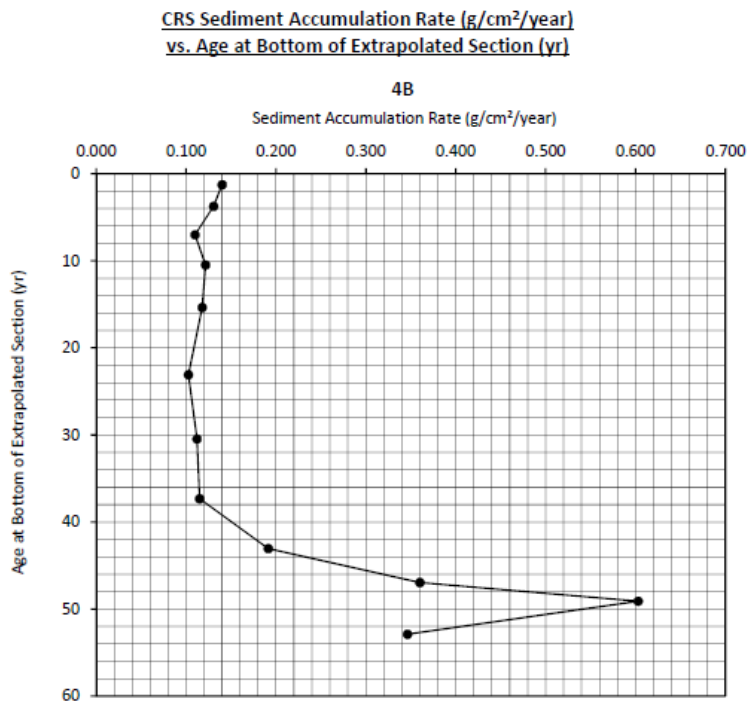
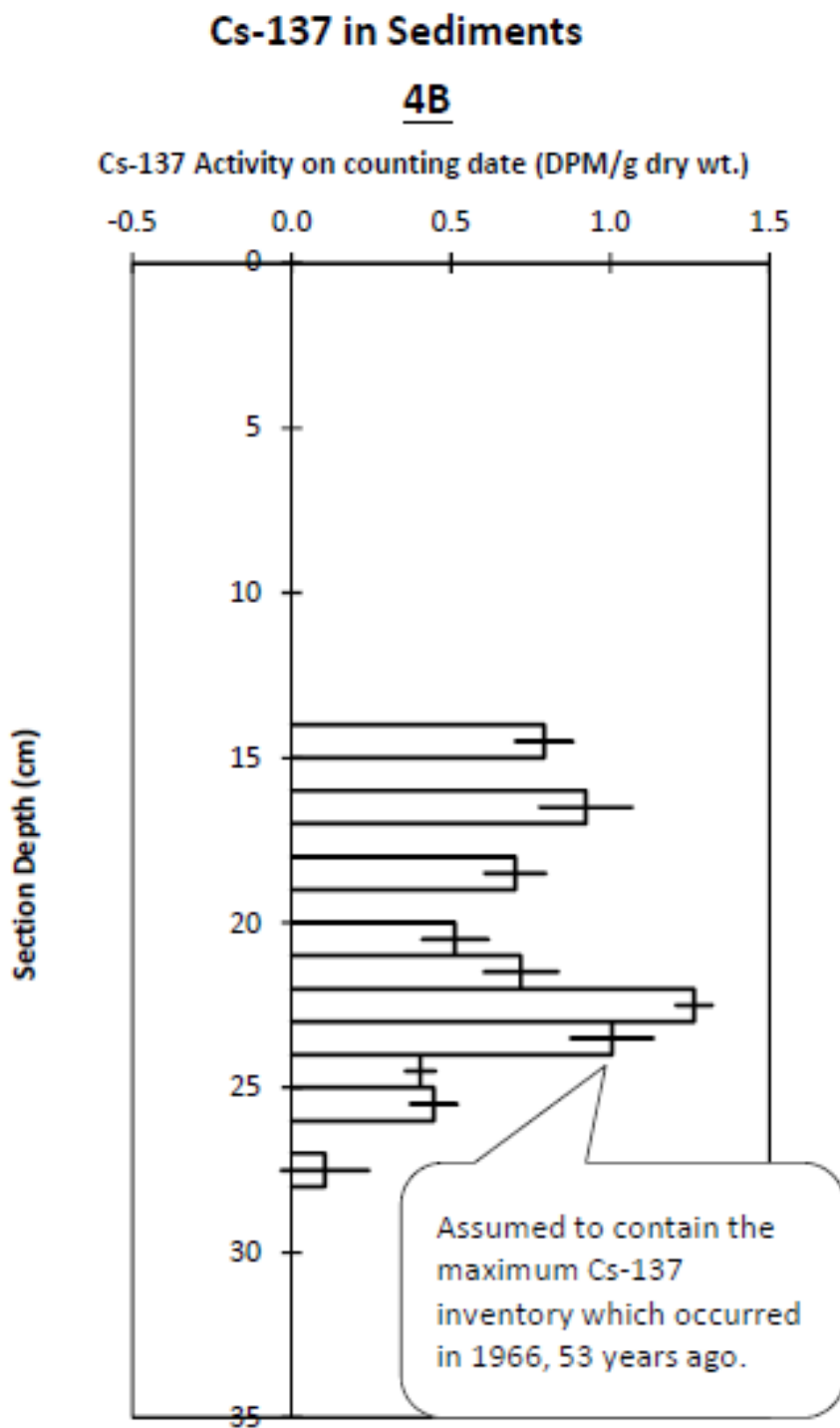


Figure 30 <sup>137</sup>Cs - Profile results of core 4B



Note: The bar plotted at the midpoint depth of each section represents +/- 1 standard deviation of the Cs-137 counting error.

For each core the average sedimentation rate was calculated using the accumulation rate, density and thickness from the isotopic analysis. The per core average values are presented in Table 12. For core 1A the average accumulation rate was used as per depth rates were not available.

$$S = \frac{\sum \frac{A}{\rho} d}{\sum d}$$

With: S Sedimentation rate [m/yr]  
 A Accumulation rate [g/m/yr]  
 $\rho$  Density [g/m<sup>3</sup>]  
 d Thickness of core sample [m]

**Table 12 Average sedimentation rates based on accumulation rate and density**

Core	Average accumulation rate [g/cm <sup>2</sup> /yr]	Average density [g/cm <sup>3</sup> ]	Total thickness [m]	Sedimentation rate [mm/yr]
1A	0.0610	0.369	0.590	1.9
2A	0.0345	0.177	0.160	3.7
3A	0.1199	0.251	0.180	5.8
4A	0.2014	0.353	0.310	6.1
2B	0.0811	0.209	0.175	4.2
4B	0.1864	0.383	0.245	5.3

### 3.2.2 Sediment Resuspension Experiment

The CMF experiments were carried out on each of the four box cores with 13 to 20 increment steps of the mixer motor speed. Water velocities increased from 0.01 m/s up to 0.21 m/s with the average increment corresponding to roughly 0.01 m/s. The rate of rotation was increased after the threshold of erosion was confirmed. Throughout the experiment for each core, 4 to 5 water samples were collected for TSS analysis at each Tu-sensor. Maximum suspended sediment concentration varied from 240 mg/L up to 2200 mg/L.

The relationship between TSS and Tu was established by linear regression for each Tu-sensor at each of the four core samples. The suspend sediment values were taken from four water samples for cores 2A and 4A and from five water samples for cores 1A and 3A. The linear regressions were established after correcting for the sensor offsets based on clear water background testing. In Figure 31 the suspended sediment concentrations from water sampling are plotted against the corrected turbidity for each of the instruments at each core. The linear regressions for each sensor, the obtained slope and regression parameter  $R^2$ , are given in Table 13.

In general, the suspended sediment calculated from the linear regressions overestimate the lower suspended sediment concentrations. The slope of the linear regression is different at each of the cores (Table 13), note the different vertical scale on Figure 31 and therefore less visual. The slope at each core is similar for each of the instruments, suggesting the variation is caused by difference in sediment composition (size and matter). Only sediments from the top layer were collected for the grain size distribution and resulted in small volumes. Because of the high water content of the samples sent for analysis and the small volumes, the determination of the grain size distribution could not be performed. Based on visual observations, core 3A had the coarsest sediments. This indicates that finer sediments will have a steeper slope, meaning for finer material a given TSS concentration lead to lower NTU values then coarser sediments at the same concentration.

**Figure 31 Regression suspended sediment and TU sensors for each core experiment**

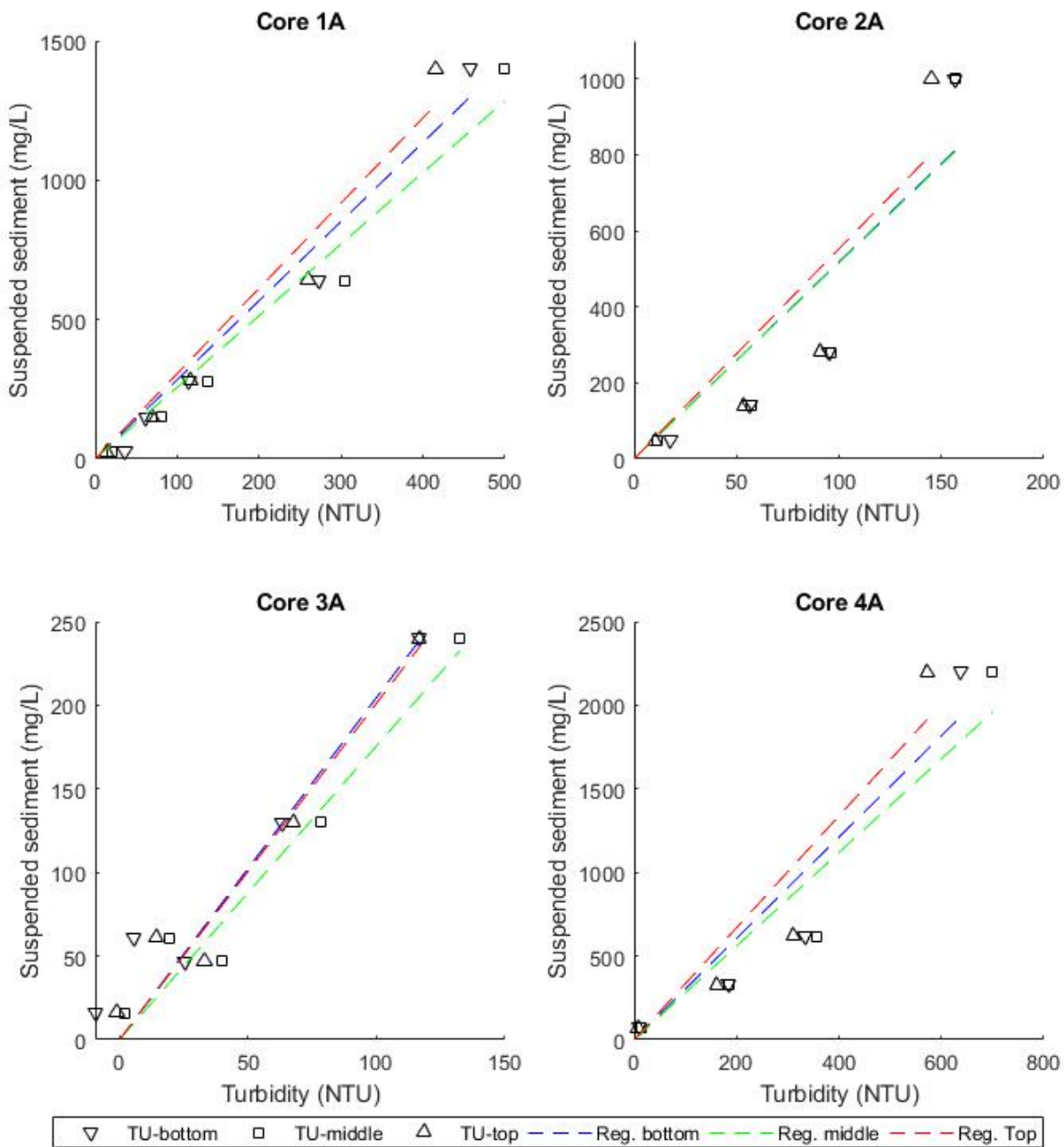


**Table 13 TSS – Tu linear regression results and offsets for the three turbidity sensors**

	Bottom		Middle		Top	
Offset	45.82		26.99		32.16	
Core	Slope	R <sup>2</sup>	Slope	R <sup>2</sup>	Slope	R <sup>2</sup>
1A	2.84	0.97	2.57	0.97	3.06	0.96
2A	5.18	0.81	5.16	0.81	5.53	0.80
3A	2.05	0.88	1.76	0.95	2.01	0.94
4A	3.03	0.90	2.80	0.91	3.35	0.90

The recorded time series of turbidity from each sensor are converted into a suspended sediment time series using the regression parameters and offsets (Table 13). The suspended sediment time series were smoothed using 20 s mobile mean averaging. The erosion rates, being the difference between suspended sediment at the end and the beginning divided by the time period, were calculated over 60 s interval based on the suspended sediment 20 s average time series. Both the suspended sediment time series and the erosion rates are presented in Figure 32 along with the water velocity at 0.04 m above the bed for the duration of each experiment. Experiments on core 1A and core 2A each have two discontinuities within the time series at the times the experiment was interrupted due to motor temperature issues. Experiments were restarted at the same previous motor speed they were stopped at, this causes spikes within the suspended sediment time series as sedimented particles are resuspended instantaneously and consequently within the erosion rate time series as well.

The threshold erosion water velocity is determined at the onset of the first distinct and stable increase in suspended sediment, which occurs at the first peak in erosion rates. The critical velocities for each core are indicated on Figure 32 and presented in Table 14. Figure 33 presents the suspended sediment for each of the water velocity at all cores and turbidity sensors.

**Table 14 Threshold water velocity at 0.04 m above the bottom for each of the box cores.**

Core	Threshold Velocity [m/s]
1A	0.07
2A	0.06
3A	0.16
4A	0.09

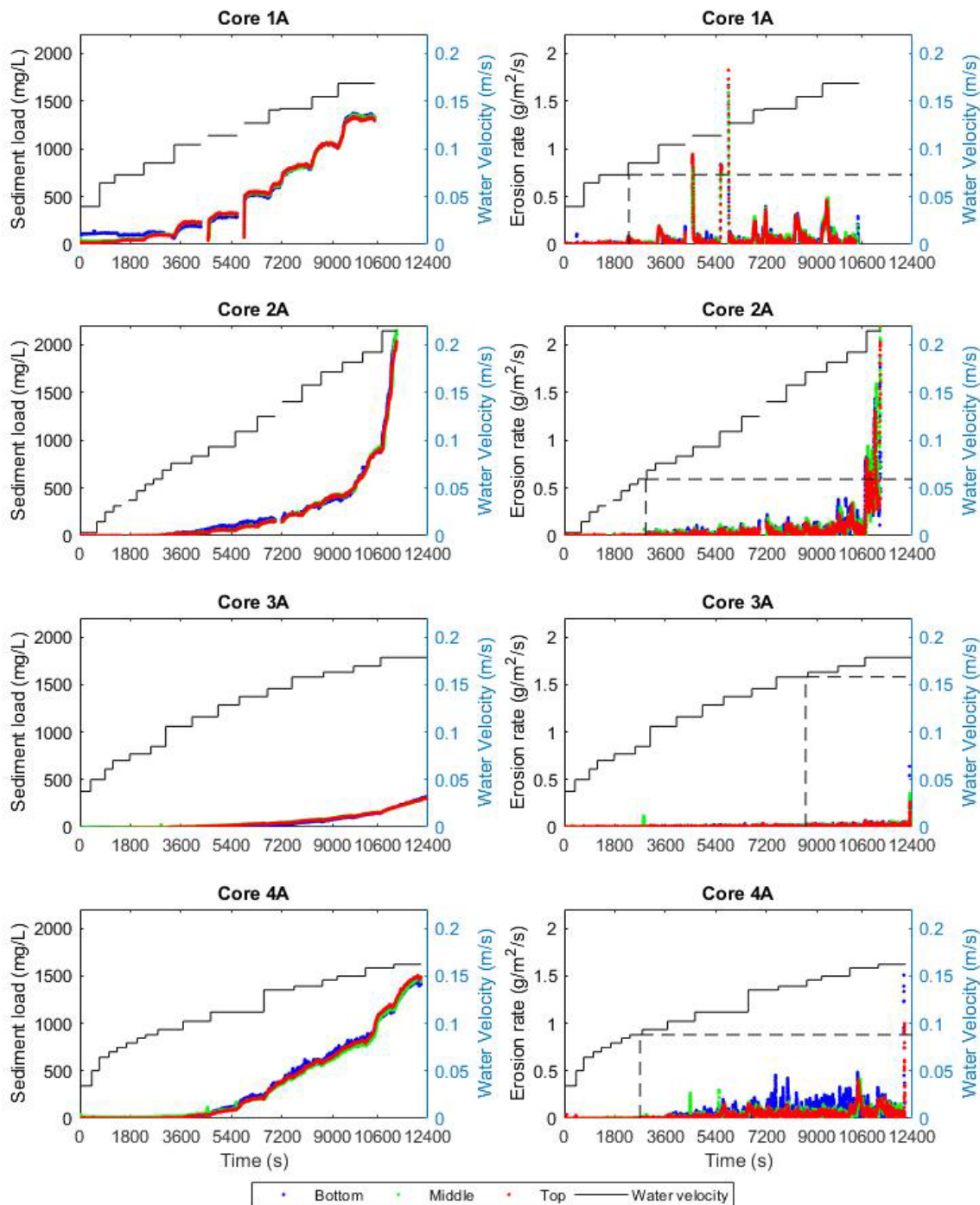
The erosion trend is different at core 3A (Figure 32) with lower suspended sediment and elevated critical erosion velocity, the threshold is two-fold in comparison with the other sites, which is probably related to the presence coarser bed material, however, this has not been demonstrated. Sediment load at the lowest sensor is elevated for core 1A at low water velocities in the flume which is possibly caused by some sediments being stuck on the sensor from the previous experiment and washed away at higher speeds, from that moment onwards the sediment load becomes comparable to the two higher sensors again. The lowest threshold water velocity for resuspension within the experiments is 0.06 m/s at 0.04 m above the bed.

All experiments, except for core 3A, demonstrated a typical response to stepwise increased water velocities with stepwise increase in suspended sediment concentration and a spiked erosion rate. This means that sediments are picked up from the bottom at the beginning of the increased water velocity and remain in suspension, the erosion takes place at the beginning of the step and erosion gradually diminishes to zero as suspended sediment concentration reach equilibrium. At the end of each step the sediment deposits at the bottom remain stable. Core 3A, on the other hand, is not reaching this equilibrium state at each velocity step. Suspended sediment concentration keeps rising while erosion rate remains almost zero until the threshold velocity is surpassed. Suspended sediment concentration keeps increasing after surpassing the threshold velocity and no levelling is observed at the end of each interval. The coarser substrate in core 3A (as indicated by the difficulty to collect enough material and closing the box corer and as observed in the isotopic analysis, see appendix 10) underlying the thin veil of fine sediment is likely the dominant component of the bottom sediments at that site.

#### Summary:

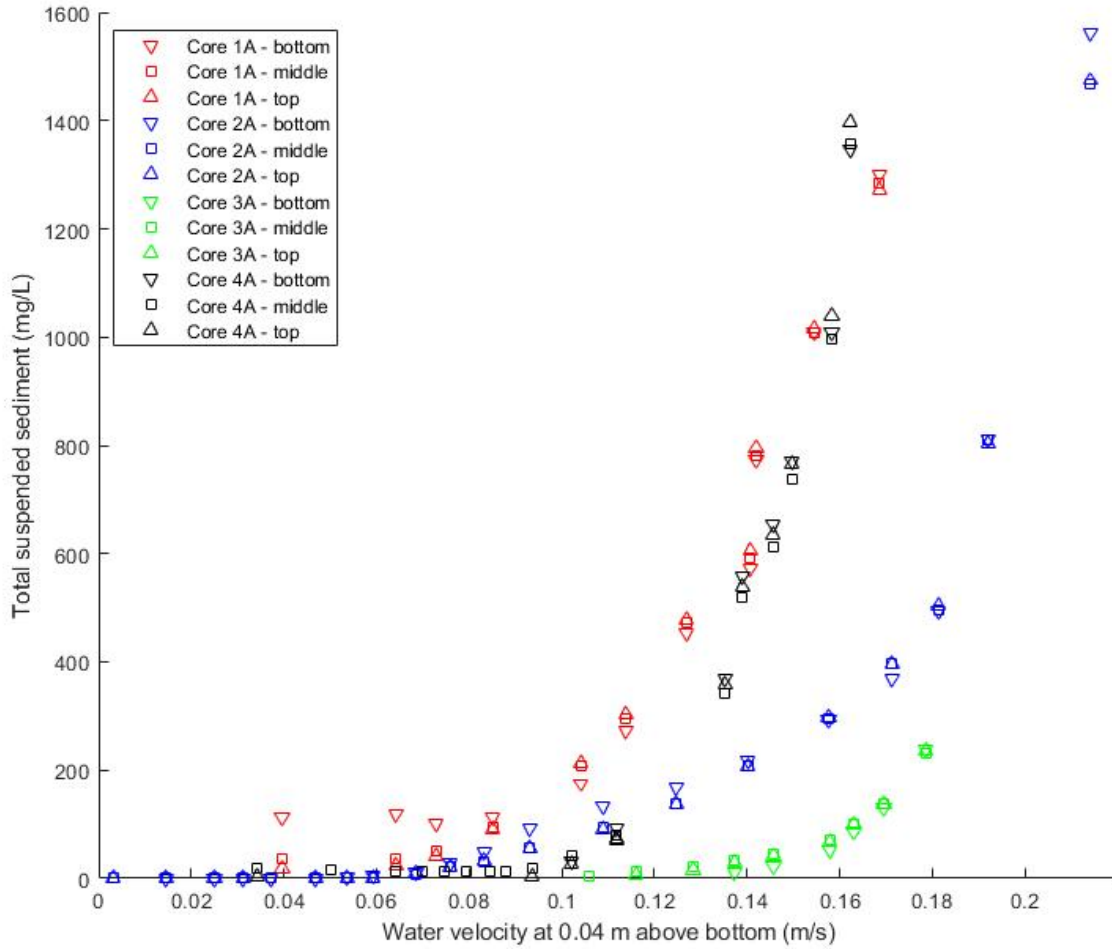
Results from the CMF experiments are showing a typical response at all cores, except for core 3A. Critical velocities for resuspension are similar between sites, except for core 3A where they are significantly higher. Due to the lack of grain size distribution no critical shear stress could be established. This was caused by the high organic content of the surficial sediments that were subsampled within the box cores. This is not unexpected given that most of the study area is covered by dense aquatic vegetation, even in winter when a thick veil of plants and plant debris is observed at the bottom.

**Figure 32** Suspended particle matter (left) and Erosion rates (right) for each core. The start of resuspension is indicated by the vertical dashed line and critical velocity by the horizontal dashed line



Suspended sediment rate, 20-second average (left) and erosion rate for 1-minute interval (right) for the duration each of the resuspension experiments, along with the water velocities at 0.04 m.

**Figure 33** Total suspended solids versus applied velocity for all cores at 3 elevations



Average sediment suspension rates for each water velocity interval from the resuspension experiments.

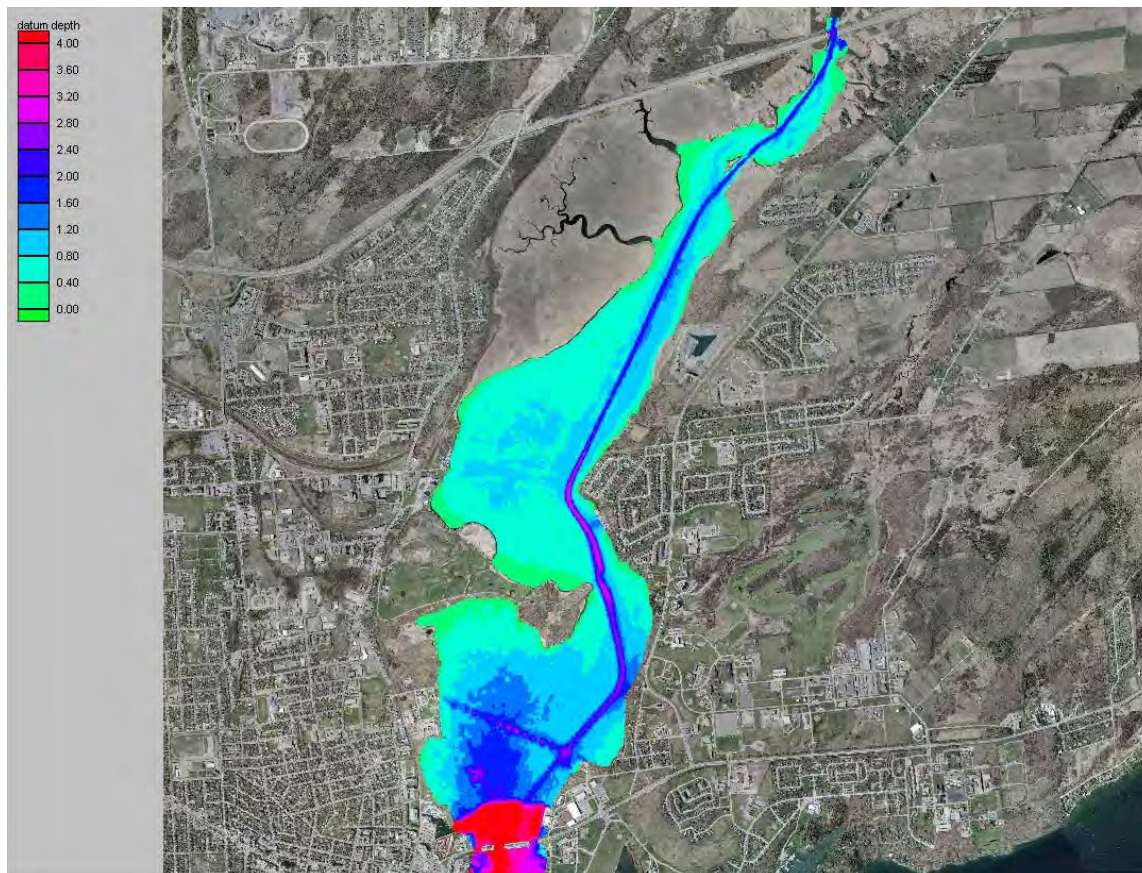
## 4 Discussion

### 4.1 Physical setting

Kingston Inner Harbour (KIH) is located at the mouth of the Cataraqui River. The downstream part of the River is a wide and relatively shallow water body that flows into Lake Ontario (Figure 34). It is divided into an upstream and downstream area, separated by Belle Island and Belle Park. Belle Park is an old landfill area, where currently the Belle Park Municipal Golf course is located. Further mention of KIH in the text will refer to the downstream section that connects with Lake Ontario, south of Belle Island.

The river mouth consists of a distinct narrow navigation channel, which was maintained by dredging<sup>9</sup>, and a wide shallow embayment. Outside of this approximately 4.5 m deep navigation channel, the riverbed is generally flat with typical depths in the order of 1.5 m. The river flows into Lake Ontario (upper St. Lawrence River) via three openings in the LaSalle Causeway, spanned by two fixed bridge structures and one bascule lift bridge in the centre opening. The three openings are about 40 m in width and the centre opening is about 6 m deep, the west and east opening are about 3 m deep (HCCL, 2011).

**Figure 34 Bathymetry of Kingston Inner Harbour**



<sup>9</sup> The dredging frequency is unknown. But it appears that the last dredging occurred in 1970 (City of Kingston – Kingston Environmental Advisory Committee Agenda – Meeting 03 2017 Schedule B). Website consulted 20-03-2020: [www.cityofkingston.ca/documents/10180/19309936/KEAF\\_A0317-SchedB.pdf](http://www.cityofkingston.ca/documents/10180/19309936/KEAF_A0317-SchedB.pdf)

Note: As surveyed by Monteith Ingram in 2009 (HCCL, 2011)

Currents within KIH have not been well studied (Golder, 2017), but observations from different references indicate this is a quiescent and lentic environment, where the circulation pattern will easily be modified depending on the relative importance of forcing agents such as wind, river discharge and surge. The Cataraqi River discharge will typically range between 4 m<sup>3</sup>/s to 17 m<sup>3</sup>/s at normal flow conditions with a 1:100 yr flood discharge of 50 m<sup>3</sup>/s. Discharge measurements carried out within this study ranged between 1 to 3 m<sup>3</sup>/s, which confirms the lentic character of KIH. These discharge conditions generated very low water velocities (<0.05 m/s 90% of the time) at the 22 stations spread across KIH and where ADCP profiling was performed in 2018 and early 2019 during the open water season (section 3.1.1).

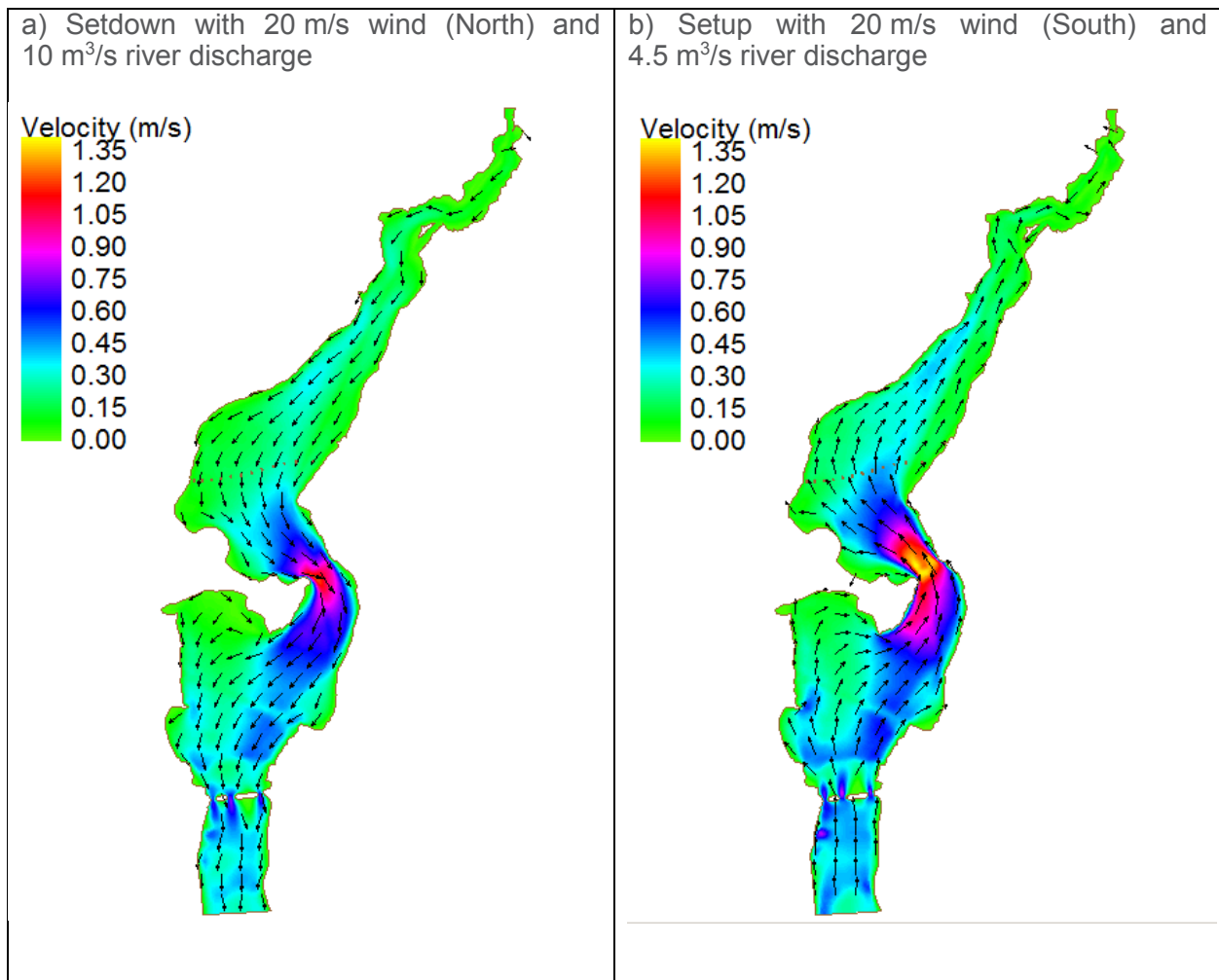
The low discharge of the Cataraqi River is such that flushing of the KIH is estimated to occur approximately 76 times per year (RMC, 2014 in Golder, 2017). This number is possibly overestimated given that the flow is likely channelized along the eastern shoreline and that there is extensive macrophyte beds in the shallow areas.

HCCL (2011) performed a hydrodynamic model for the entire KIH (upstream and downstream of Belle Island) in the context of the hydrotechnical analysis for the construction of the Third Crossing. Their report is focused mainly on the upstream KIH area and only low-resolution figures were available to describe the circulation pattern in the downstream KIH. The scenarios included different river discharges, wind and lake water level conditions. A subset of two cases is presented in Figure 35 (higher discharge, northerly wind and falling water level; lower discharge, southerly wind and rising water level). The former case (wind and flow aligned) shows an eddy close to Belle Island and a regular distribution of the flow across the KIH directed toward Lake Ontario (Figure 35). The latter case shows that wind is a significant forcing agent as the flow is fully diverted upstream (Figure 35). In both cases, water velocity remains small. This is fully inline with the ADCP water velocity measurements carried out in this study. Simulated (HCCL, 2011) and measured (this study) water velocities are typically too low to re-suspend the bed sediments observed within KIH as reported by Golder (2017) based on Shield's criterion. Based on our results and HCCL (2011) modeling results, we can conclude that KIH behaves more like a shallow lake than a river and that flow conditions are influenced by:

- > 1) the river discharge (hydraulic conditions and runoff contributions from upstream areas);
- > 2) wind generated stresses;

This suggests that wind-wave resuspension is probably a more important process for sediment re-suspension. As the sediments are resuspended, they would be subject to the prevailing current regime at that time. But the prevailing current regime would likely be of short duration (hours) as would the wave regime. These phenomena will occur during the open-water season and flow conditions will quiet down importantly during the ice-covered season. On average, the ice cover will set in from late December to mid to late April depending on the severity of the winter. This will contribute to the stabilization of the sediments at the bottom.

**Figure 35 Simulated water velocity in the Cataraqui River according to HCCL, 2011**



## 4.2 Sediment type and distribution

The sediment composition in the Cataraqi River mouth has been described in various studies in the area, namely Dalrymple and Carey (1990), HCCL (2011) and Golder (2017). Dalrymple and Carey (1990) have characterized the top soft sediment layer, upstream of Belle Island, as either peat or gyttjas. The gyttjas are soft, water-rich (generally >80%), muds with a wide range of organic contents (20-70%). Gyttjas with high organic contents (40-70% organic material), contain abundant root material, and commonly have a mottled appearance due to bioturbation by the roots. These fine soft sediments are observed over most of KIH where water velocities are low. The peat, which are those fine-grained or coarse and fibrous sediments that contain more than 70-75% organic detritus, are found in the shallow areas along the shoreline.

HCCL (2011) also reports a recent soft organic matter deposit at the surface, underlain by a soft to very stiff clay or silty clay over a thin layer of glacial till or very dense silty sand with some gravel. Based on core sediment stratigraphy, the soft organic matter surface deposit has a thickness of about 20 to 60 cm (Dalrymple and Carey, 1990). This is consistent with the thickness of the recent soft sediment horizon in the cores collected in this study, which ranged between 20 to 70 cm. Refusal when coring was generally associated to the presence of a thick and dense peat deposit, which correspond to the stratigraphy reported by Dalrymple and Carey (1990). The origin of this recent sediment deposit has been attributed to historical changes in the sediment inputs due to anthropogenic changes in land use within the watershed (Dalrymple and Carey, 1990). However, due to the presence of several large lakes in the watershed and along the Rideau Canal system, the sediment contribution from the watershed is probably low.

Golder (2017) presented (Figure 4) a map of bottom sediment grain size based on work from RMC (2014). The map is based on less than 20 sampling stations, unequally spaced. Therefore, important interpolation artefacts will result (lack of stations, no constraint from bathymetric changes or presence of macrophyte beds). But the figure suggests that the deeper sediment within the middle of KIH consist mostly of clayey silt with pockets of silty clay. Sediments found in shallower waters along the western shoreline consist of silty sand (1 station). Coarsening of the bottom sediments along the shoreline may indicate reworking and sorting due to the action of wave shoaling. There are not enough stations to draw further conclusion about the spatial distribution of bottom sediment types and assess sediment transport patterns within the harbour.

Taking into considerations the hydrodynamic conditions and sedimentary characteristics within KIH, the study area is likely a sediment limited environment as reported by Golder (2017). Sediment inputs to KIH will consist of a combination of alluvial sediments delivered by the Cataraqi River, resuspension and re-circulation of local bed sediments by waves and contribution from local storm water outfalls.

## 4.3 Sediment rates

As part of this study, a total of 6 cores were collected for radio-isotopic determination to calculate sedimentation rates within KIH. The description of the cores (section 3.2.1) provides an insight on the sedimentary conditions within the study area. The first series of cores (1A to 4A) are distributed along the western shoreline from south to north, and the remaining two other cores (2B and 4B) were in the north central area of KIH (Figure 1c). The sediment composition in the deeper offshore cores (2B and 4B) was relatively homogeneous consisting of silt to clayey silt. These cores also showed the thickest recent sediment horizon (59 and 31 cm respectively). Although fine sediments were observed in the other cores, the presence of sand was noteworthy in cores 1A, 2A and 3A, located further south in KIH, exposed to more open water and longer fetch. Core 4A, located in the far northwestern corner of KIH, although in shallow water as the

others, was composed mostly of silt and clayey silt. This suggests this site is better protected by Belle Island to the east, and less exposed to wave action.

The sedimentation rates were calculated from the vertical distribution of  $^{137}\text{Cs}$  and excess  $^{210}\text{Pb}$  in the sediment cores. The depth of the  $^{137}\text{Cs}$  peak activity is indicative of 1966 when the fallout from nuclear weapons testing during the Cold War was at its maximum.  $^{137}\text{Cs}$  first reached detectable levels in 1954. The depth of the peak (observed and interpreted)  $^{137}\text{Cs}$  activity is shown in Table 15. Based on the  $^{137}\text{Cs}$  profile, an approximate sedimentation rate has been calculated which ranged between 2 to 6 mm/y between all 6 cores. A more representative sedimentation rate using the CRS model is presented in Table 16. Overall, we observe that the sedimentation rate increases toward station 4A in the more protected north western part of KIH (Tables 15 and 16).

Based on the depth for  $^{137}\text{Cs}$  peak in the 6 cores, ranging from 12 cm to 30 cm dating back 53 yrs, the modern sedimentation rate is estimated around 2 mm/yr to almost 6 mm/yr within the KIH (Table 16). Kemp and Harper (1976) have estimated sedimentation rate around Lake Ontario ranging from as low as 0.3 mm/yr to 2.2 mm/yr, with the highest rate occurring in the Rochester and Kingston basins. These values are comparable with rates obtained in previous studies around the KIH (Dalrymple and Carey, 1990, Manion et al. 2010 and RMC, 2014). However, sedimentation rates are extremely small compared to other regions of the St-Lawrence River between Cornwall and Trois-Rivières where sedimentation rates are in the order of cm/yr (i.e. Carigan and Lorrain, 2000).

The results were generally coherent and justified the application of the CRS model to determine the age of the sediments for most cores, except for core 1A. The linear and CRS models of core 1A differed significantly and reported an age at the bottom of the core which was not coherent with the presence of  $^{137}\text{Cs}$  at the corresponding depth. It is likely that the resulting sedimentation rate of 0.0610 g/cm<sup>2</sup>/yr is not representative (Table 17). Furthermore, the  $^{137}\text{Cs}$  activity profile and sudden termination in exponential decay of  $^{210}\text{Pb}$  at 27 cm as well as the sharp decrease in dry bulk density in the same section, suggests that this core may have been disturbed or that a significant portion of the core may be missing. However, with the significant presence of  $^{137}\text{Cs}$  and unsupported  $^{210}\text{Pb}$  found in the 0 – 27 cm core interval, we can conclude that in general all sediments in this core interval likely represent post 1966 sediment accumulation.

The sedimentation rates calculated from the  $^{210}\text{Pb}$  CRS model show that it can vary greatly at a given site by a factor of 2 (core 4A) to 5 (core 4B) when compared to the average sedimentation rate (Table 16). This is indicative of changing settling conditions within KIH which may be attributed to change in sediment inputs. In addition, local hydrodynamic conditions may disturb the sediments, resulting in missing sections possibly attributed to resuspension events (core 3A and 2B).

For example, the water level at the Kingston Harbour hydrometric station dropped to a historic low level of -0.47 m below datum on January 23, 1965. It is possible that this low-water level condition may be related to the disturbance observed below the 17.5 cm depth in core 2B. The radio-isotopic modelling results indicated that the disturbance probably occurred about 46 years ago (i.e. in 1973) which is compatible with the 1965 event. The low water level event may have exposed the shallow water sediments to increase reworking and erosion by waves as indicated by the number of years of sediment that may be missing from the core below 17.5 cm prior to 1973. These events are unlikely nowadays given the newer regulations on the water levels.

The more regular profiles observed at stations 2A, 4A and 4B are indicative of a more stable settling environment.

**Table 15 Estimated depth of post 1966 sedimentation and modern sedimentation rates**

Core	1966 <sup>137</sup> Cs depth [m]	Modern sedimentation rate [mm/yr]
1A	0.27	5
2A	0.12	2
3A	0.18	3
4A	0.30	6
2B	0.18	3
4B	0.23	3

**Table 16 Sediment accumulation rate (<sup>210</sup>Pb) and settling conditions inferred from <sup>210</sup>Pb and <sup>137</sup>Cs inventories**

Core	Accumulation rate CRS ( <sup>210</sup> Pb) [g/cm <sup>2</sup> /yr]	<sup>137</sup> Cs depth [m]	Origin of Cs	Note
1A	0.0610	0.27	External erosion sources	Core may have been disturbed throughout or a portion is missing from the core. All sediments in this core interval likely represent post 1966 sediment accumulation.
2A	0.0323 (0.0198 to 0.0448)	0.12	External erosion sources	accumulation rates are variable. 1966 <sup>137</sup> Cs peak is present
3A	0.1185	0.18	External erosion sources	suspected portion of the core inclusive of the 1966 <sup>137</sup> Cs peak, is missing
4A	0.1894 (0.1558 to 0.4041)	0.30	--	accumulation rates are variable 1966 <sup>137</sup> Cs peak is present
2B	0.0803	0.18	External erosion sources	suspected portion of the core inclusive of the 1966 <sup>137</sup> Cs peak, is missing
4B	0.1121 (0.1026 to 0.6029)	0.23	External erosion sources	accumulation rates are variable 1966 <sup>137</sup> Cs peak is present

The maximum of <sup>137</sup>Cs inventory which occurred in 1966 is in general in agreement with the <sup>210</sup>Pb age from the CRS model.

The northern part of KIH is a settling environment with higher sedimentation rate. However, the site is not necessarily under steady conditions as settling rate varies. Sediments accumulate further south, but the disturbed top layer of some cores is indicative of a more dynamic environments where episodes of resuspension (core 1A and 3A) and re-deposition at nearby site (core 2A) occurs. Wave action is likely contributing to the mixing of the upper layer, transport and dilution with a coarser size fraction, resulting in a thinner recent sediment deposit as one move from the TC-RC to TC-4 water lots.

#### 4.4 Sediment erodibility

The determination of the threshold flow velocity for the onset of erosion was determined on all four cores during the CMF experiment. The critical near bed velocities observed for the KIH (around 0.05 - 0.16 m/s at 0.04 m above the bed) are relatively small. Thompson et al. 2013, using the same equipment on deep marine sediments, reported critical bed velocities about twice (0.2 m/s, at 0.06 m above the bed) what was measured for KIH.

Although the shear stress could not be calculated, due to the lack of grain size distribution data, the experiment conditions in the Thompson study were comparable to those from this study. The sediment granulometry and rheological properties are thus the only parameters that could explained the low threshold velocities measured. Although not demonstrated, finer sediment with a higher organic content in the upper layer of the horizon are likely easier to remobilize.

Combining the information from the radio-isotopic analysis and erodibility experiment, the water lots can be grouped into four areas within KIH:

- › Easily remobilized sediment – quieter settling conditions: PC-W
- › Easily remobilized sediment – re-deposition from external sources: TC-2A
- › Easily remobilized sediment – evidence of disturbance: TC-4
- › Less easily remobilized sediment – evidence of disturbance: TC-RC

Using the weather data from Kingston Airport for the period of 1970 to 2019, an extreme value analysis was performed on the wind data susceptible to affect the western part of KIH (East, South-East and South directions). It is important to observe that the dominant winds are blowing from the South-West and North-East directions but will have little to no impact on the area of concern. Using the resulting wind speeds and directions, the near bottom wave orbital velocities were calculated for 1-, 10- and 50-year return periods. The wave orbital velocities are then compared to the threshold velocities obtained from the erodibility experiment. Results are summarized in Table 17 for the location of all 4 sites.

**Table 17 Comparison of the near bottom orbital velocities obtained from the wave model and the erosion threshold velocities measured during the erodibility experiment for return periods of 1, 10 and 50 yr.**

	CMF results	Wave model results					
	Threshold Velocity [m/s]	East		South-East		South	
Core		Return Period [yr]	Velocity [m/s]	Return Period [yr]	Velocity [m/s]	Return Period [yr]	Velocity [m/s]
1A	0.07	50	0.09	>50	(0.03)	>50	(0.00)
2A	0.06	1	0.09	10	0.07	>50	(0.01)
3A	0.16	50	0.18	>50	(0.13)	>50	(0.01)
4A	0.09	1	0.28	1	0.37	10	0.10

Table 17 shows from which direction and return period when and at which station the sediment at the four locations would be potentially resuspended.

- › In water lot PC-W (station 4A), resuspension of bottom sediments would be expected from easterly and south easterly winds with a 1 yr return period, and from southerly winds with a 10 yr return period.
- › In water lots TC-2A (station 2A), resuspension is more likely to occur from easterly winds with a 1 yr return period, less often from south easterly winds with a 10 yr return period and rarely from southerly winds with a 50 yr return period.
- › In water lots TC-4 and TC-RC (stations 1A and 3A), resuspension events from wave activity are less likely as it requires winds with a return period of 50 yr or more.

Because the near-bottom velocities generated by wind waves are orbital and by nature not the driving force for erosion and transport, and because depth average water velocities are low, resuspended sediments should not travel far.

## 4.5 Water Level

Water levels within the KIH bay are generally controlled by Lake Ontario water levels and the St-Lawrence River discharge. Because Lake Ontario is susceptible to wind setup and seiche events, it was necessary to analyse water level variations within KIH to determine if such sudden and important changes in water level could induced a significant increase in flow velocity when compared to the base case. Previous studies had observed seiche events creating sudden water level fluctuations of up to 0.7 m (HCCL, 2011) with periods between 2 h and 5 h (Schwab, 1977 and Hamblin, 1982) in Lake Ontario.

Seiches events were identified at the Kingston CHS station which generated water level variations with periods of 2h, 5h and 12h during all three seasons. These Lake Ontario seiche events reverberate into KIH, but locally generated oscillations of longer period (24 h) were also observed within KIH only. Summary of the wavelet analysis results is shown in Table 18.

The water level time series were further compared to the turbidity time series to qualitatively assess if variations in turbidity, indicative of resuspension events, were correlated with the seiche events. No such correlation was observed, our data thus suggest no resuspension by seiche occurred within the scope of this study.

**Table 18 Summary of the wavelet analysis for Kingston and LaSalle causeway stations showing the seasonal recurrence of oscillation events and range of corresponding water level variations.**

Season	Period	Lake Ontario		Kingston Inner Harbour	
		n	Amplitude (m)	n	Amplitude (m)
Autumn 2018	2	45	0.05 – 0.26	60	0.05 – 0.35
	5	12		17	
	12	3		4	
	24	0		2	
Winter 2018-19	2	38	0.05 – 0.33	47	0.05 – 0.36
	5	17		22	
	12	5		6	
	24	2		2	
Spring 2019	2	45	0.05 – 0.41	41	0.05 – 0.37
	5	15		17	
	12	0		0	
	24	0		2	

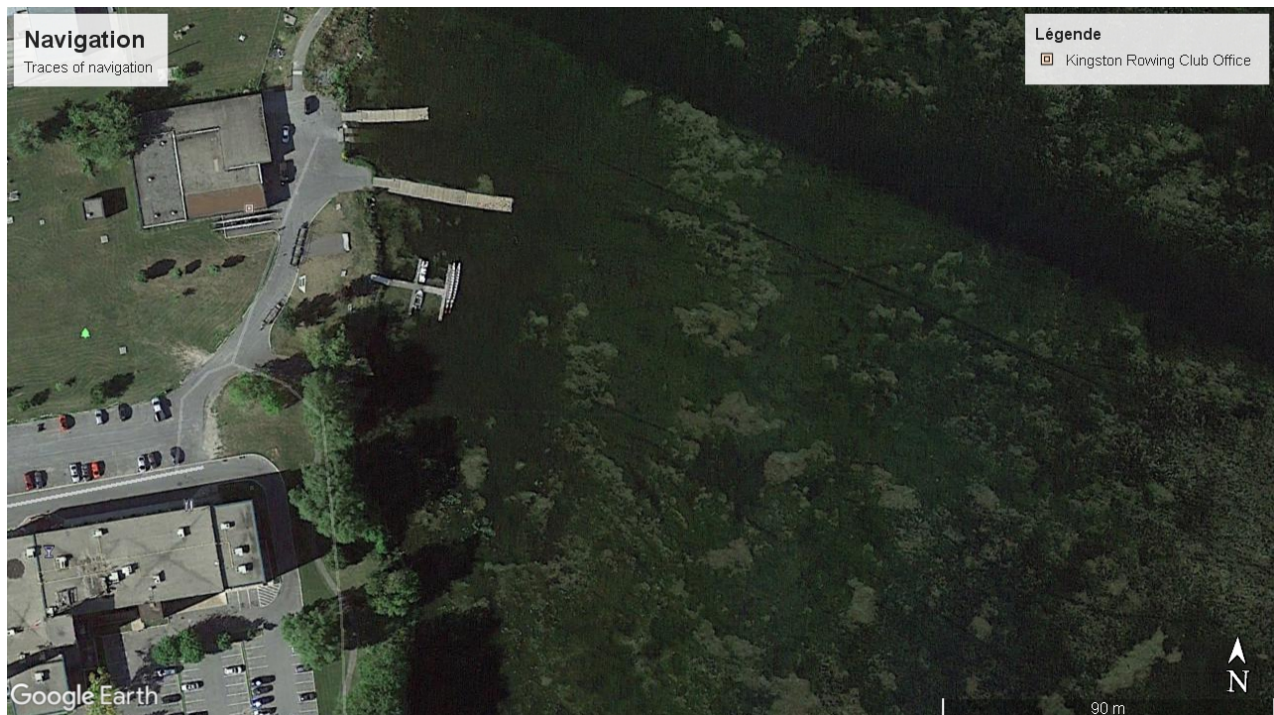
To further evaluate if the observed seiche events could generate sufficiently high water velocities to remobilize bottom sediments, the velocity at the LaSalle Causeway, resulting from the water mass entering or exiting the KIH was calculated using the event observed on May 5<sup>th</sup> 2018, which had the highest rate of change (amplitude over period). Based on the amplitude (0.72 m) and duration (3.1 h) of the oscillation, the maximum horizontal velocity was 0.28 m/s within the opening of the LaSalle Causeway. The cross-section area of the KIH is about 4.7 times larger than the LaSalle Causeway openings, the average water velocity in KIH cross-section will be 0.06 m/s, within the deeper navigation channel higher water velocities are expected and water velocities in the shallow section are expected to be lower (<0.06 m/s) and therefore a seiche will not cause sediment resuspension in the area of interest. However, during such an event, sediment that would have been resuspended due to wave action could be transported some distance away.

## 4.6 Aquatic Vegetation

The impact of the aquatic vegetation on reducing the fluvial flow and attenuating wave energy in the summer months has been well documented. This in turn may help to stabilize bed sediments (USEPA, 2006) with their root systems. Mentions of the extensive macrophyte beds in KIH have been reported by HCCL (2011) and Golder (2017). Our own observations during the open water season in 2018 indicated significant difficulties in navigating the study area, west of the navigational channel with repetitive clogging and fouling of the propeller by the aquatic vegetation.

Google earth imagery where aquatic vegetation is visible shows navigation traffic occurs mainly between the navigation channel and the Kingston Rowing Club (dark lines in Figure 36). Few trace lines are observed elsewhere within the rest of the study area. Based on the difficulties experienced by our field crew while conducting the measurements, it is assumed that navigation is limited in the area and prop wash is not an issue as boats cannot navigate at high speed.

**Figure 36** Google earth close-up of Navigation traces in macrophyte beds around the Kingston Rowing Club (3 September 2015)



To document the extent of the aquatic vegetation, a mapping exercise was conducted using free satellite imagery. The interpretation is based on a combination of visual delineation and image processing (colour histogram classification). A recent image (September 3<sup>rd</sup>, 2015) was processed and the results classified into three classes, namely floating vegetation, submerged vegetation and mixed (floating-submerged). No classification of the emergent vegetation was done as this is strictly limited to the shoreline which is not considered as a settling area. Results are shown on Figure 37 which also shows underwater images collected during the coring campaign from the ice cover.

Based on the analysis of satellite images, the northern two thirds of KIH and west of the navigation channel was well covered with aquatic vegetation. The water lots in KIH cover a total surface area of 83 ha. Of this, 83 % (69 ha) is covered by extensive macrophyte beds (floating: 14 ha, submerged: 9 ha; Mixed: 46 ha). The only water lots which are less or not affected by the presence of vegetation, are those located in the deeper reaches at the south end of KIH (TC-5, TC-AB and part of TC-4). The extent and density of the vegetation are such that very little boat activity was observed during the field visits.

Golder (2011) reported that the increased presence of cattails and Eurasian watermilfoil are associated with the accumulation of sediments related to human-induced hydrological changes. The major plant species present are: Eurasian watermilfoil, coontail, pondweeds and eelgrass.

The stabilizing effect of the aquatic plants is likely not limited to the open water summer season. Indeed, even following the fall senescence period, there is still a significant vegetal mat on the bottom (Figure 37, underwater camera screenshots). Wind wave events occurring during the winter will have little to no effect because of the presence of the ice cover. But, during the inter-season (fall, spring), strong storms may occur. Although the macrophytes beds will have decrease

in biomass following the fall senescence period, the plant mat found at the bottom will act as a significant stabilizing agent against wave induced currents.

The presence of aquatic plants was not considered in the wave model or during the erodibility experiment (root systems were preserved, but all plants were cut at the stem). So, despite being easily resuspended with corresponding wind events with a return frequency of 1, 10 and 50 yr or more, depending on origin (Table 15), the macrophyte beds will limit sediment resuspension and transit. The presented instances of exceeding threshold water velocities are likely over estimated.

## 4.7 Climate change

Climate change can affect a wide range of physical parameters, like water level, discharge, waves and ice cover, through changes in precipitation, temperature and wind. What is being observed in the recent past are rapid transitions between extreme high and low water levels in the Great Lakes. This seesawing pattern is likely the “new normal” driven by changing interactions between global climate variability and the components of the regional hydrological cycle (Gronewold and Rood, 2019).

Undoubtedly, the effects of a warming climate are being observed in the Great Lakes. Precipitation increases in winter and spring are consistent with the fact that a warming atmosphere can transport more water vapor. As a result, increased atmospheric moisture contributes to more precipitation during extreme events. Therefore, wet weather patterns are becoming very wet. By the same token, changes in seasonal cycles of snowmelt and runoff align with the fact that spring is coming earlier and climate models project that this trend will continue. Similarly, rising lake temperatures contribute to increased evaporation. Therefore, dry weather patterns when they occur will lead to lower lake levels.

As stated before, the KIH has low water velocities and river discharge, therefore any change in timing and magnitude of river discharge caused by change in precipitation will likely have minor impact on the water velocities. But increase in precipitation events may generate higher sediment loadings from the watershed and consequently, increase in sediment settling rates. Shorter winters could lead to reduction of the ice cover, exposing the KIH to more wind induced wave events and sediment resuspension events, all this depending on the wind direction. Increase in south westerly prolonged wind events may also lead to an increase in seiche events, but these have been shown to have little effect on the sediment resuspension within the KIH. Nevertheless, as water velocities by discharge are negligible it remains unlikely resuspended sediments will be flushed out of the KIH.

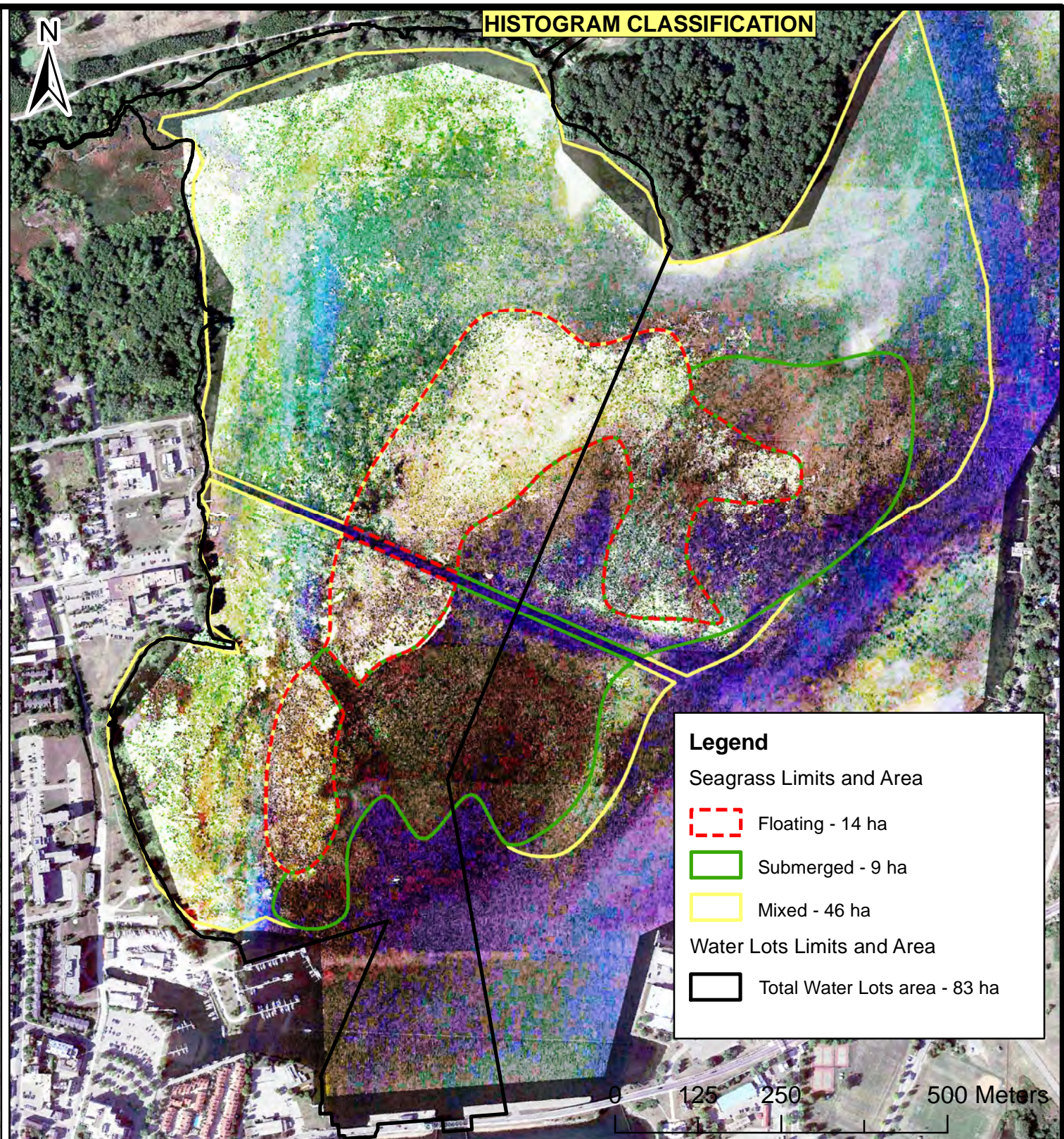
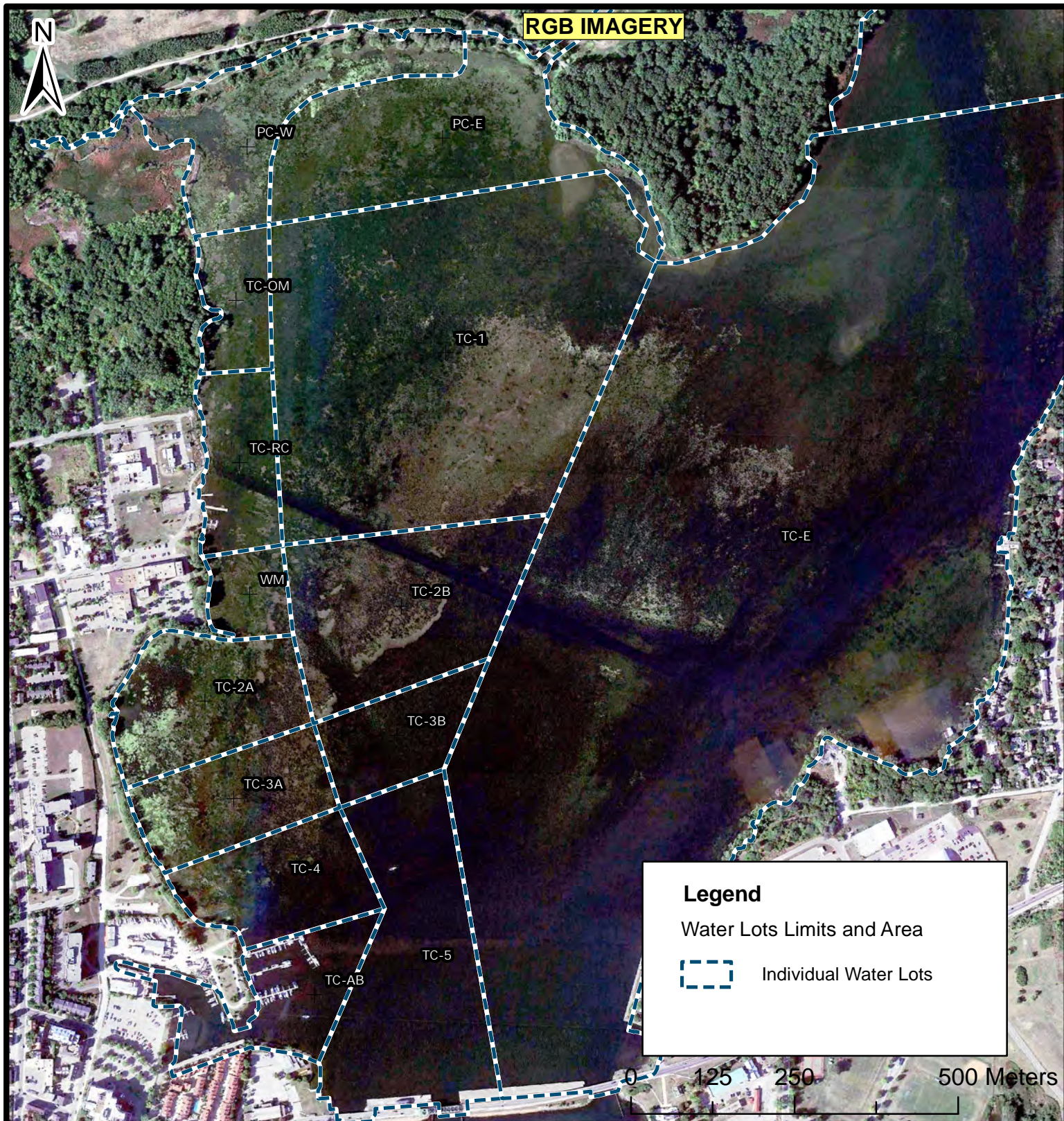


Image Reference:  
 - Google Earth, 2020 Maxar Technologie image acquisition, 20 cm pixel resolution, September 3rd 2015

## 5 Conclusion

Results have shown that the Kingston Inner Harbour does not have a well-established circulation pattern and that wind events and, to a lesser extent, fluvial discharge from the Cataraqui River will drive the circulation. The base case circulation pattern (fluvial influence only), will be easily reverse by wind. Nonetheless, the resulting water velocities are always low and not enough to resuspend bottom sediments. This suggest that KIH is a generally quiescent environment suitable for sediment settling, albeit with low sediment loadings and where sediment mobility is low and limited locally.

Indeed, fine organic watery sediments accumulate throughout most of the shallow embayment. Results from the radio isotopic analysis have demonstrated that settling rates increase toward the northern part of KIH with thicker recent sediment deposits in water lots PC-W and TC-1, but that sedimentation is not a steady process with varying sedimentation rates and missing sediment horizons when looking at the  $^{210}\text{Pb}$  and  $^{137}\text{Cs}$  inventories.

During four field visits water velocity, turbidity, suspended sediment and discharge data were collected. Time series of water elevation, weather conditions (wind speed and direction), waves and turbidity were also collected. This data was used to better understand the hydraulic dynamics in the KIH bay, stage 1 of the proposal. Sediment samples, box cores and tubular cores, were collected and analyzed to determine re-suspension velocity and sedimentation rates, to obtain insight on past and present sediment dynamics, stage 2 of the proposal. The box core sampling provided useful information about re-suspension water velocities, unfortunately sediment contained high amounts of organic matter that sample volume was insufficient for grain size analysis.

Re-suspension at the site occurs under wave generated currents as shown from the field measurement analysis and the wave generation and propagation simulation. Although, episodes during which water velocities exceeded re-suspension threshold occur frequently (5 observations in a three-month period), large erosion events are unlikely as mean water velocities remain low. The influence of the Cataraqui River on the hydraulic dynamic is very limited.

### **Water lot TC-4 (core 1A)**

The critical water velocity for re-suspension is 0.07 m/s, which is approached under Eastern winds with a 50-year return period. Re-suspension of contaminated sediments is rare.

### **Water lot TC-2A (core 2A)**

The critical water velocity for re-suspension is 0.06 m/s, wind with 1- and 10-year return period from the East and South-East, respectively, exceed the threshold. Radioisotope analysis shows deposition of sediment from previous deposited sediments. Re-suspension of contaminated sediments is likely with relative frequent events.

### **Water-lot TC-RC (core 3A)**

The critical water velocity for re-suspension is 0.16 m/s, the wind and wave analysis indicate that these water speeds are only reached by wind from the East with 50-year return period. Radioisotope analysis shows disturbance of the top layer indicating re-suspension of contaminated sediments can occur.

### **Water lot PC-W (core 4A)**

The critical water velocity for re-suspension is 0.09 m/s, which is approached under Eastern and South-Eastern winds with a 1-year return period as well as Southern winds with 10-year return period. Re-suspension of contaminated sediments can occur and is more frequent than the other sites.

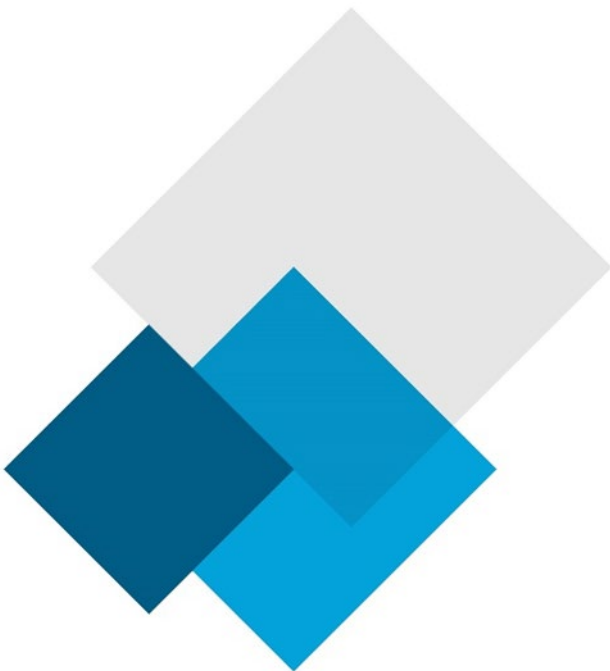
## 6 References

- Amos, C. L., T. F. Sutherland, D. Cloutier, and S. Patterson. 2000. Corrasion of a remoulded cohesive bed by saltating littorinid shells. *Cont. Shelf Res.* 20:1291-1315 [doi:10.1016/S0278-4343(00)00024-8].
- Carigan, R. and S. Lorrain, 2000, Sediment dynamics in the fluvial lakes of the St. Lawrence River: accumulation rates and characterization of the mixed sediment layer. *Can. J. Fish. Aquat. Sci.* 57(Suppl. 1): 63–77.
- Carlton, R. G. and R. G. Wetzel, 1985. A box corer for studying metabolism of epipellic microorganisms in sediment under in situ conditions. *Limnol. Oceanogr.*, 30(2), 1985, 422-426.
- Couceiro, F., G. R. Fones, C. E. L. Thompson, P. J. Statham, D. B. Sivyer, R. Parker, B. A. Kelly-Gerrey, and C. L. Amos. 2013. Impact of resuspension of cohesive sediment at the Oyster Grounds (North Sea) on nutrient exchange across the sediment-water interface. *Biogeochemistry* [doi:10.1007/s10533-012-9710-7].
- Dalrymple, R. W. and Carey, J. S., 1990. Water-level fluctuations in Lake Ontario over the last 4000 years as recorded in the Cataraqui River lagoon, Kingston, Ontario. *Canadian Journal of Earth Sciences*, 27(10), pp.1330-1338.
- Environmental Measurements Laboratory (EML), US Department of Energy - HASL-300 Method Ga-01-R Gamma Emitters in the Environment by Energy, HASL EML Procedures Manual, 28th Edition, February 1997.
- Eakins, J. D. and R. T. Morrison. 1978. A new procedure for the determination of lead-210 in lake and marine sediments. *International Journal of Applied Radiation and Isotopes.* 29, 531-536.
- Golder, 2017, Preliminary Sediment Transport Study – Kingston Inner Harbour, Kingston, Ontario. Report number: 1661792-002-R-Rev0-3000.
- Gronewold D. and Rood Richard B. 2019. Climate change is driving rapid shifts between high and low water levels on the Great Lakes. *The Conversation*, June 8, 2019.
- Hamblin, P. F., 1982, On the free surface oscillations of Lake Ontario. *Limnol. Oceanogr.* 27(6), 1029-1049.
- HCCL, 2011, Hydrotechnical Analysis in Support of Environmental Assessment for Third Crossing of Cataraqui River. Prepared for the City of Kingston. 20 December 2011.
- Kemp, A. L. W., and N. S. Harper, 1976, Sedimentation Rates and a Sediment Budget for Lake Ontario, *Journal of Great Lakes Research* 2(2):324-339, DOI: 10.1016/S0380-1330(76)72296-2.
- Mathieu, G.G., P.E. Biscaye, R.A. Lupton and D.E. Hammond. System for measurement of <sup>222</sup>Rn at low levels in natural waters. 1988. *Health Physics.* 55, 989 – 992.
- Manion, N.C., Campbell, L. and Rutter, A., 2010. Historic brownfields and industrial activity in Kingston, Ontario: Assessing potential contributions to mercury contamination in sediment of the Cataraqui River. *Science of the total environment*, 408(9), pp.2060-2067.

- RMC-ESG. 2014. Application of the Canada-Ontario Decision-Making Framework for Contaminated Sediments in the Kingston Inner Harbour. Prepared by Environmental Sciences Group, Royal Military College, Kingston, Ontario. February 2014.
- Soulsby, R. L. 1997. The dynamics of marine sands: a manual for practical applications. Thomas Telford Applications.
- Schwab, D. J. 1977. Internal free oscillations in Lake Ontario. Great Lakes Environmental Research Laboratory, National Oceanic and Atmospheric Administration, Ann Arbor, Michigan.
- Thompson, C. E. L., and C. L. Amos. 2002. The impact of mobile disarticulated shells of *Cerastoderma edulis* on the abrasion of a cohesive substrate. *Estuaries* 25(2):204-214 [doi:10. 1007/ BF02691308].
- Thompson, C. E. L., C. L. Amos, M. Lecouturier, and T. E. R. Jones. 2004. Flow deceleration as a method of determining drag coefficient over roughened flat beds. *J. Geophys. Res.* 109(C03001).
- Thompson, C.E.L., Couceiro, F., Jones, G.R. and Amos, C.L. 2013 Shipboard measurements of sediment stability using a small annular flume—Core Mini Flume (CMF). *Limnol. Oceanogr.: Methods* 11, 2013, 604–615.
- Torrence, C and G. P. Compo. 1998. A practical guide to wavelet analysis. *Bull. Am. Meteorol. Soc.* 79(1): 61–78.
- United States Environmental Protection Agency (USEPA). 2006. Great River Ecosystems Field Operations Manual. Report No. EPA/620/R-06/002.
- Widdows, J., J. S. Lucas, M. D. Brinsley, P. N. Salkeld, and F. J. Staff. 2002. Investigation of the effects of current velocity on mussel feeding and mussel bed stability using an annular flume. *Helgoland Mar. Res.* 56(1):3-12 [doi:10. 1007/s10152-001-0100-0].

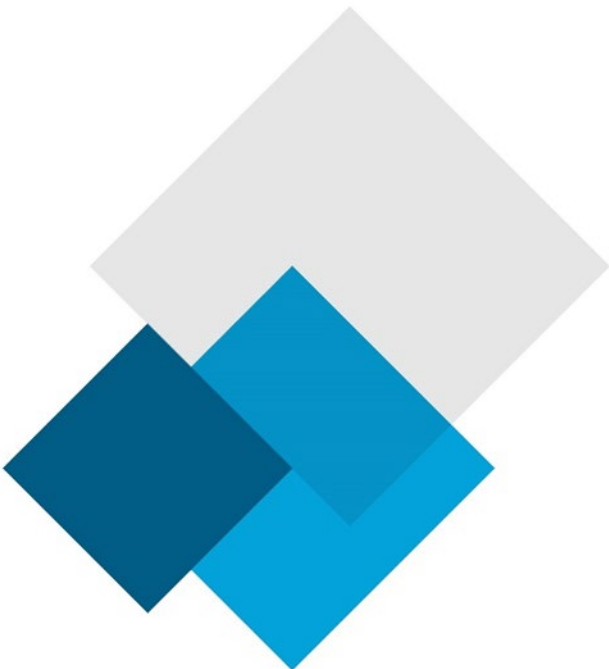
# Appendix 1

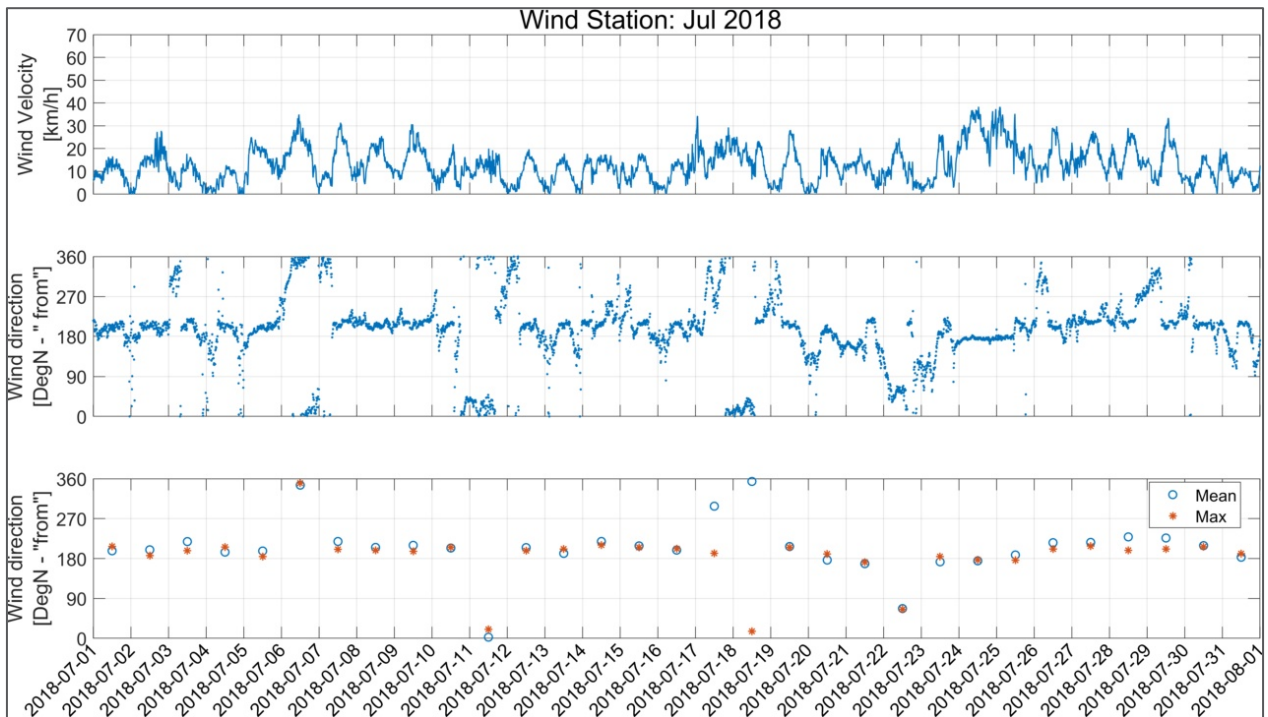
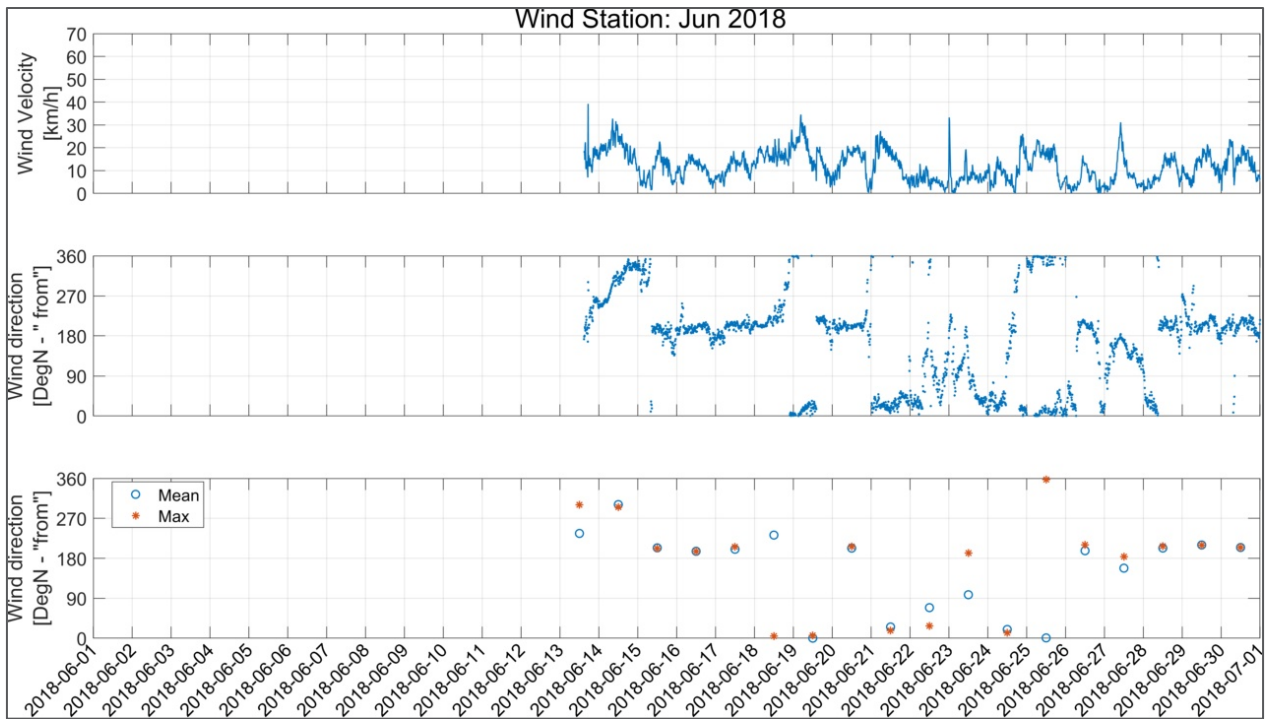
Time Series of Wind, Atmospheric Pressure and Water Level

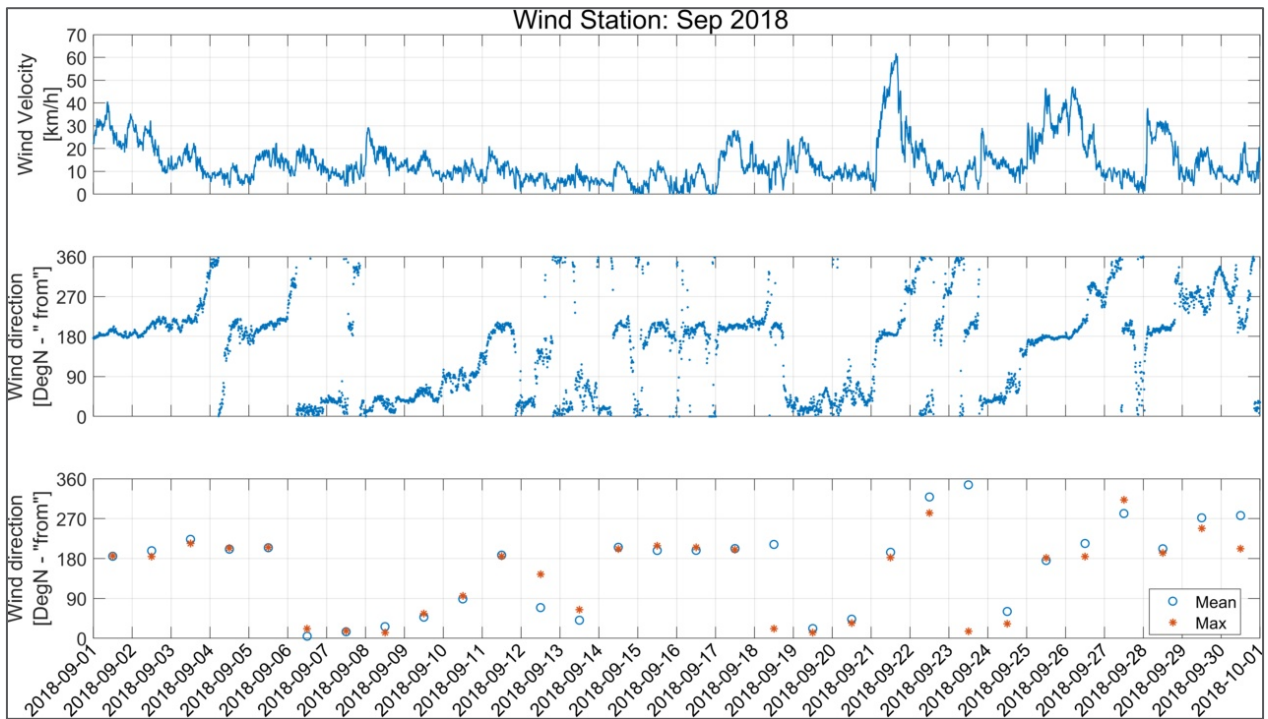
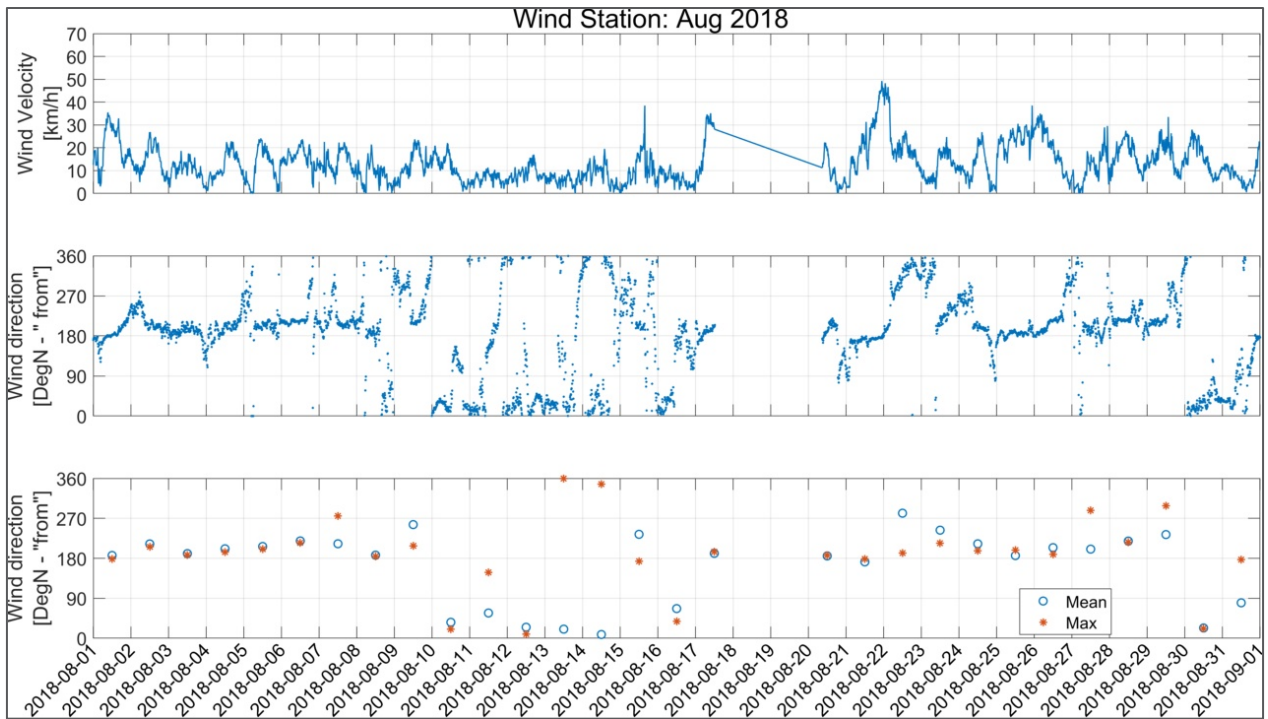


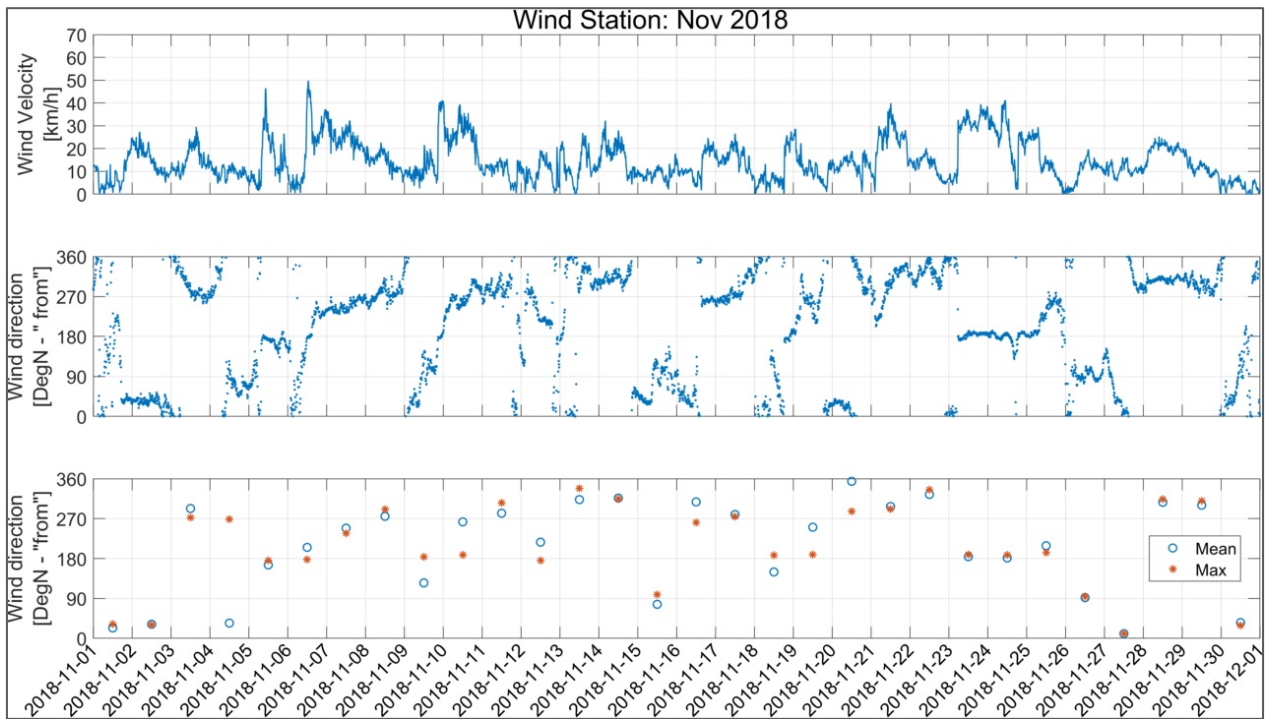
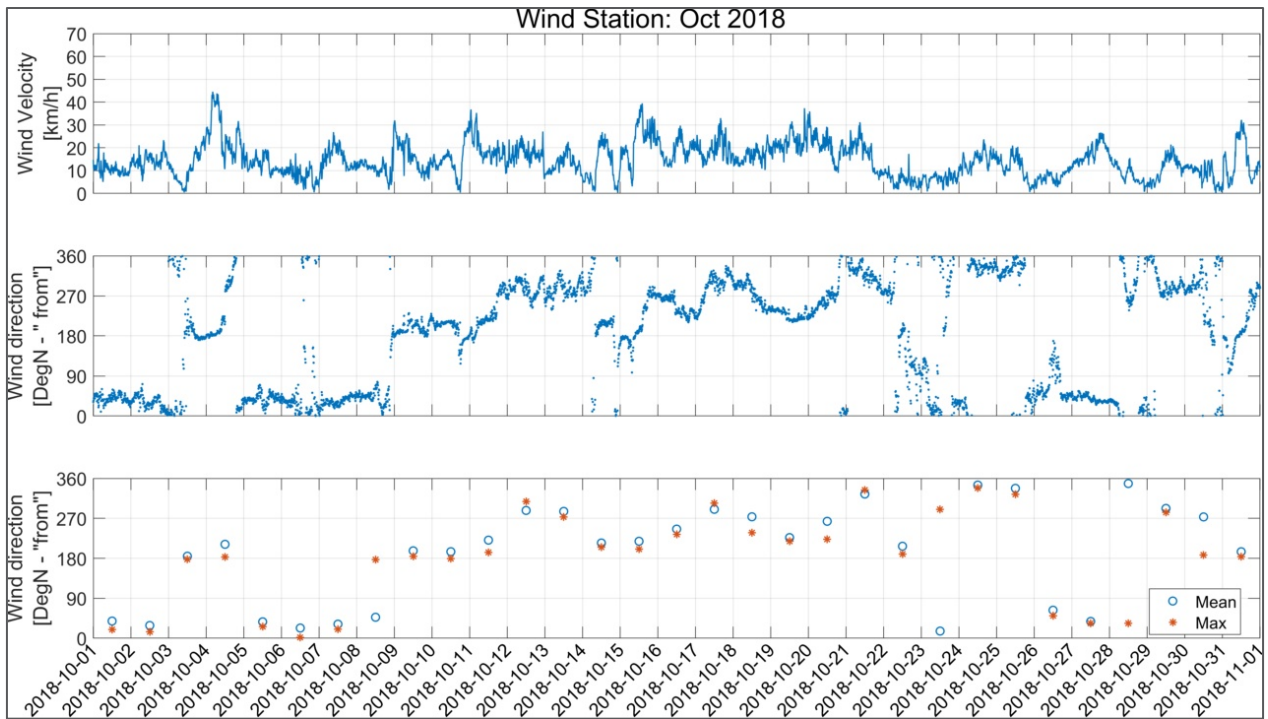
# Appendix 1-1

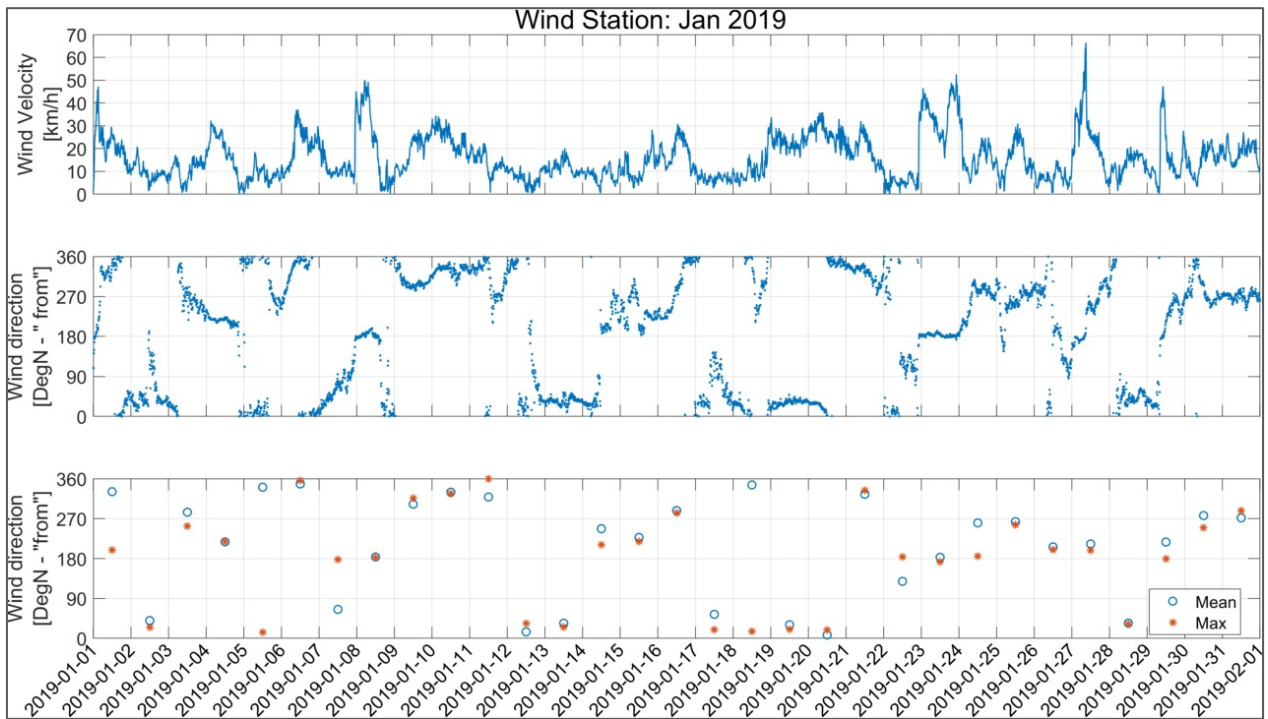
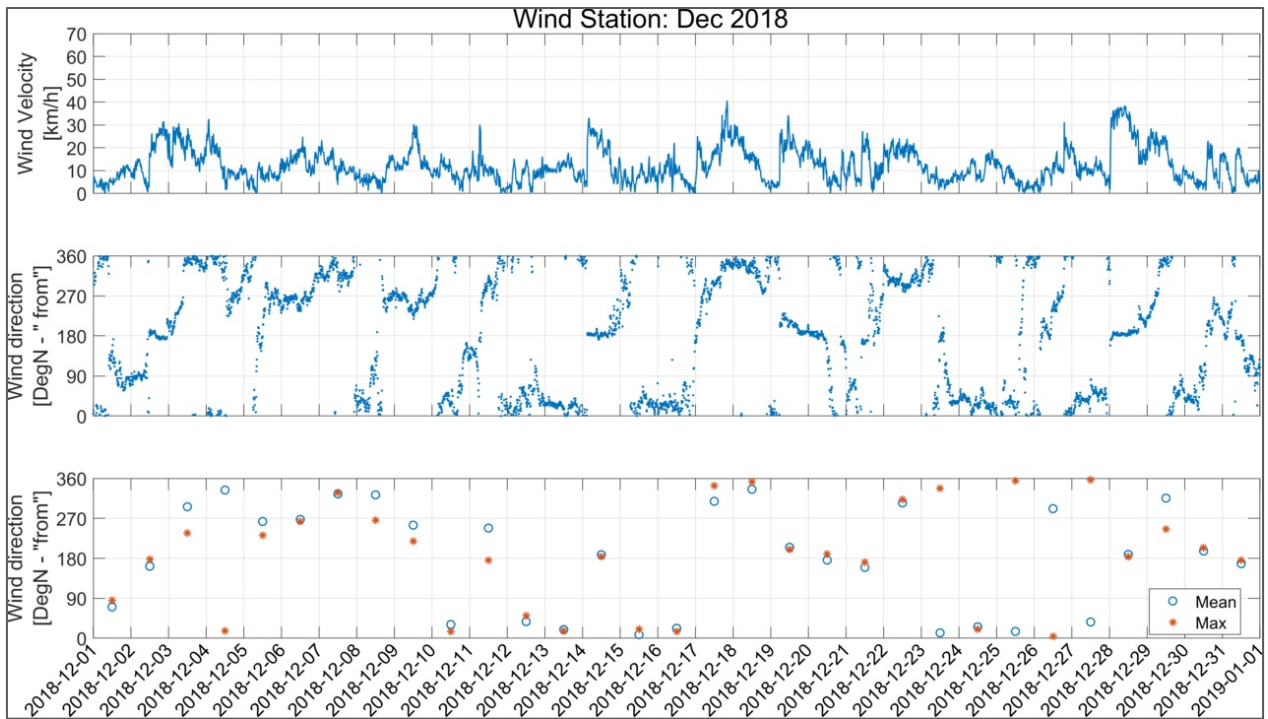
Wind

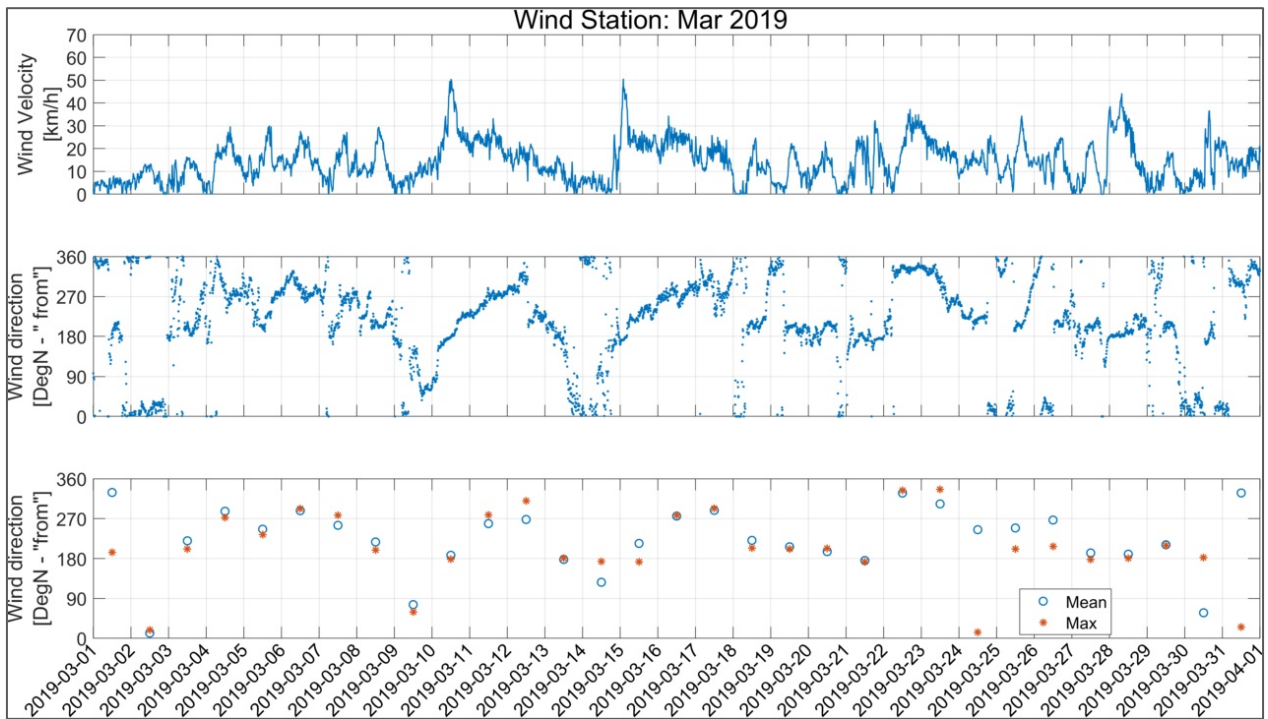
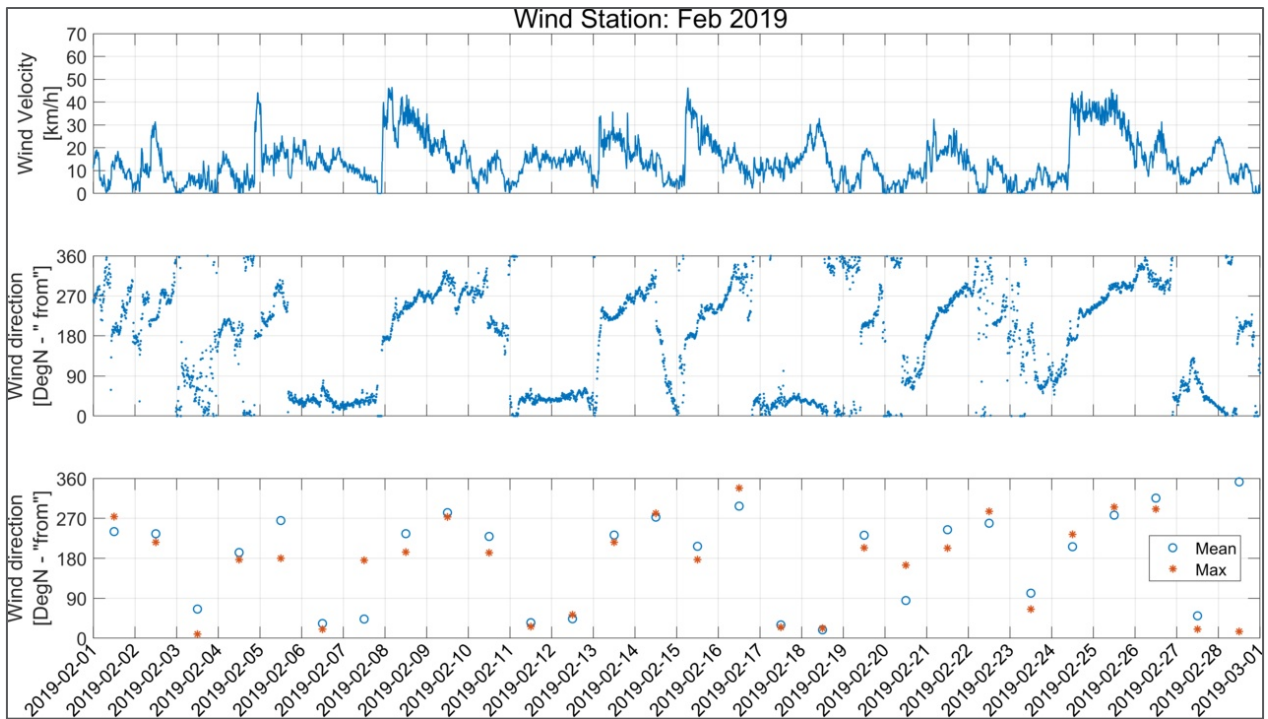


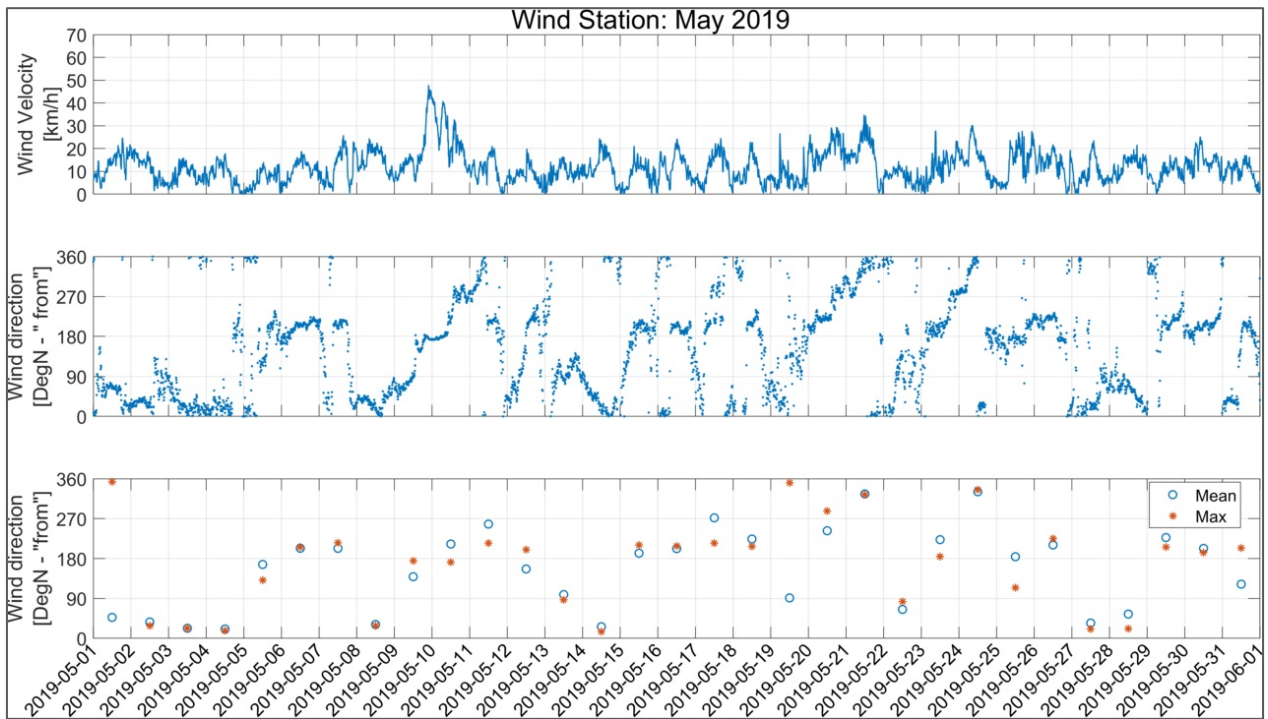
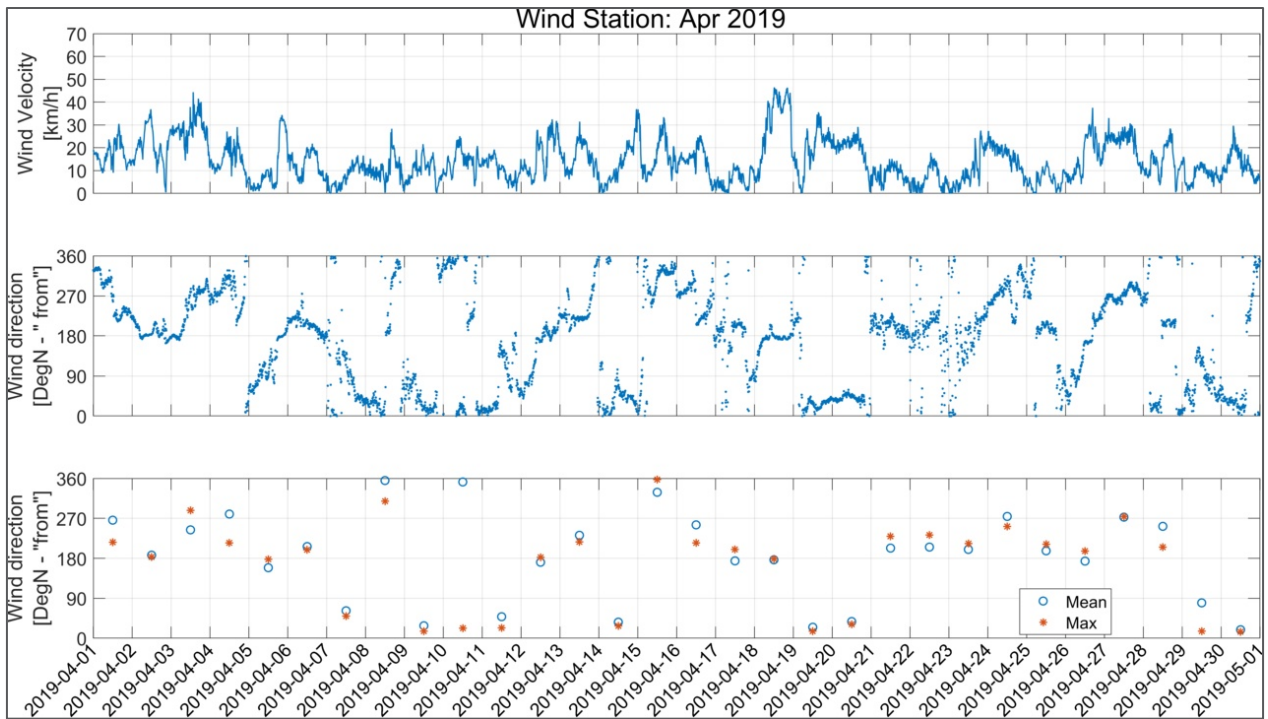












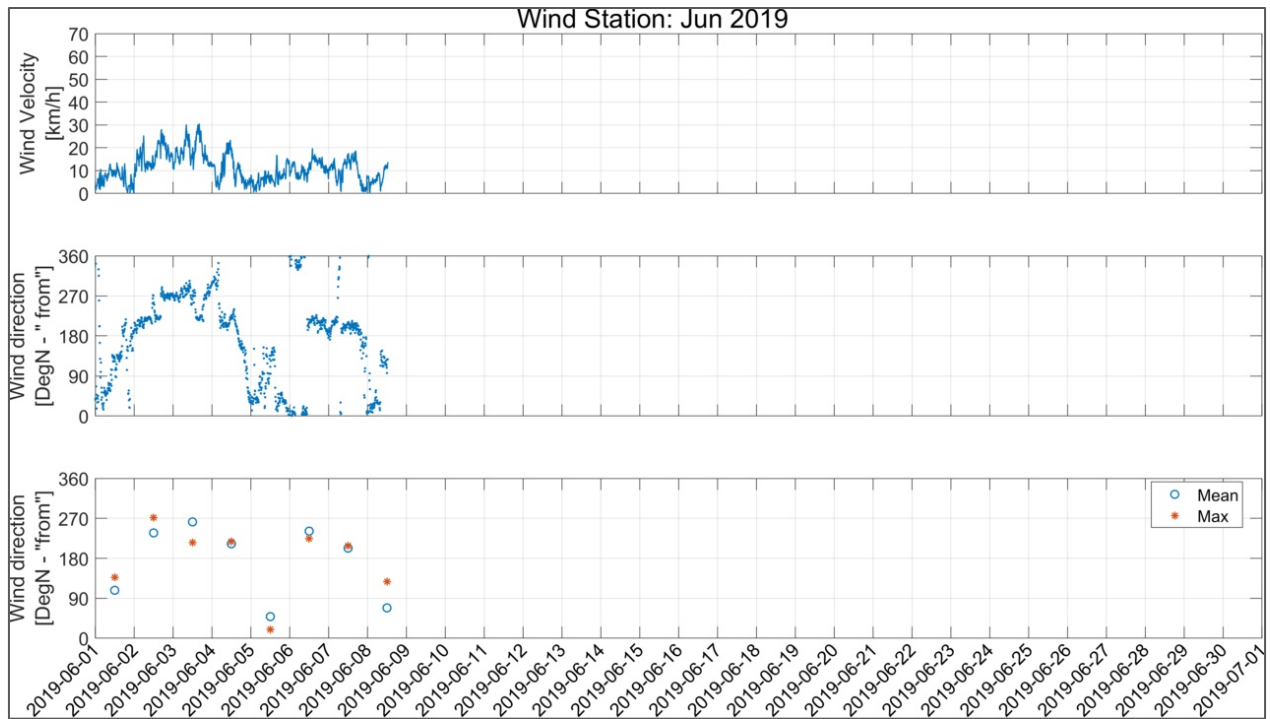


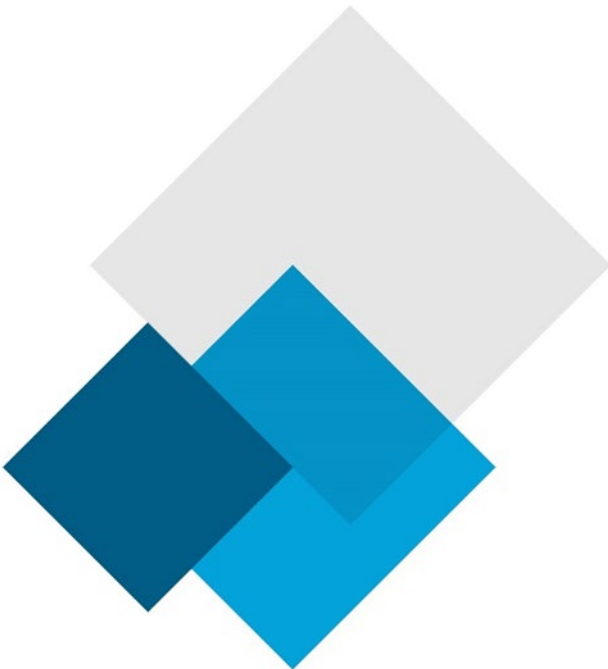
**Table A1-1 Wind frequency distribution at the LaSalle causeway weather station (2018-2019)**

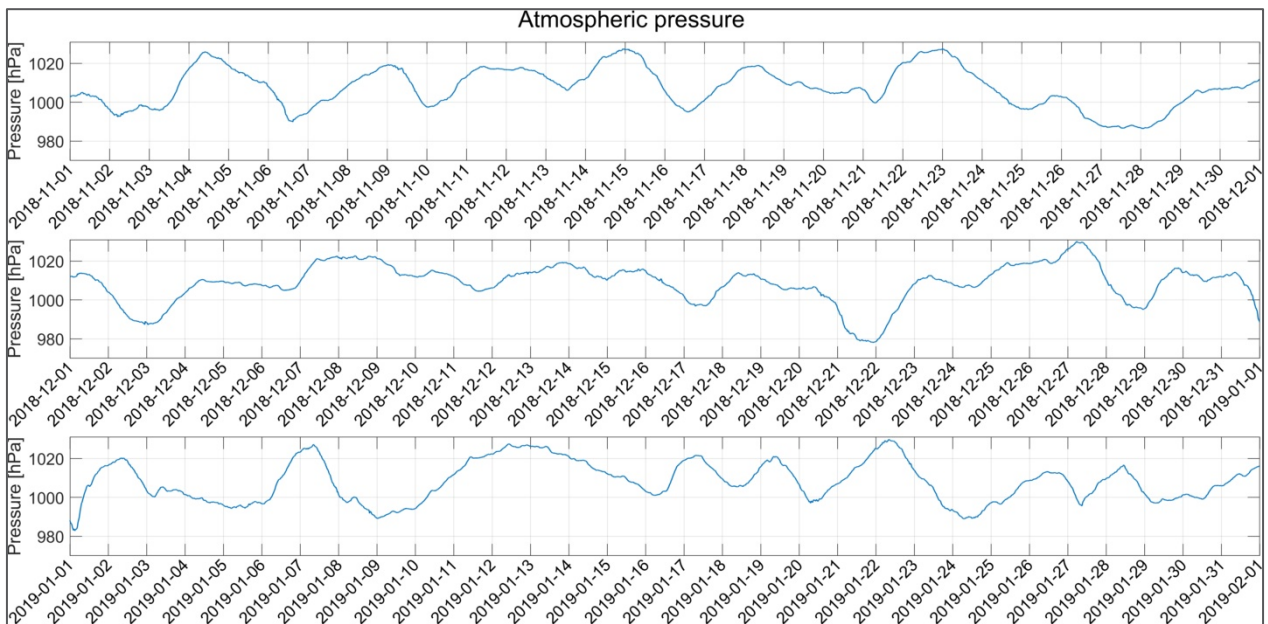
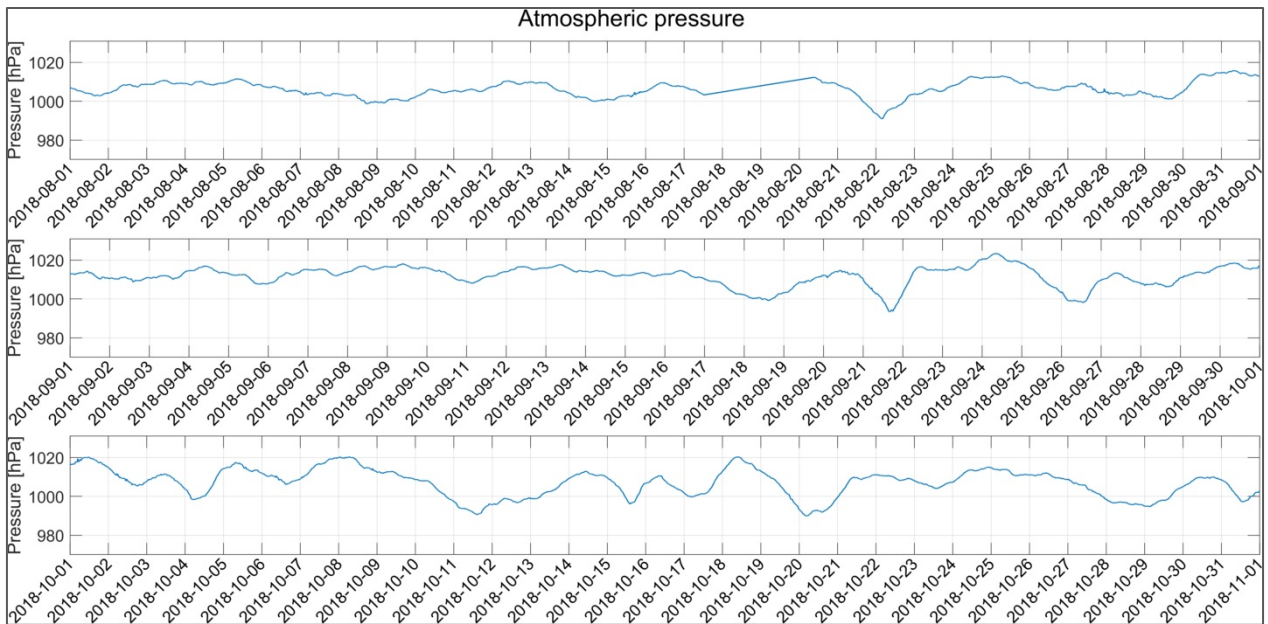
			Wind velocity (km/h)							total
			0	[0;10]	[10;20]	[20;30]	[30;40]	[40;50]	[50;60]	
Wind blowing from [deg N]	[-15;15]	N	2325	1546	600	57				4528
		%	5%	3%	1%	0%				9%
	[15;45]	N	3203	3407	796	58				7464
		%	6%	7%	2%	0%				15%
	[45;75]	N	1733	965	52	1				2751
		%	3%	2%	0%	0%				5%
	[75;105]	N	1319	482						1801
		%	3%	1%						4%
	[105;135]	N	1385	182	1					1568
		%	3%	0%	0%					3%
	[135;165]	N	1320	439	28					1787
		%	3%	1%	0%					3%

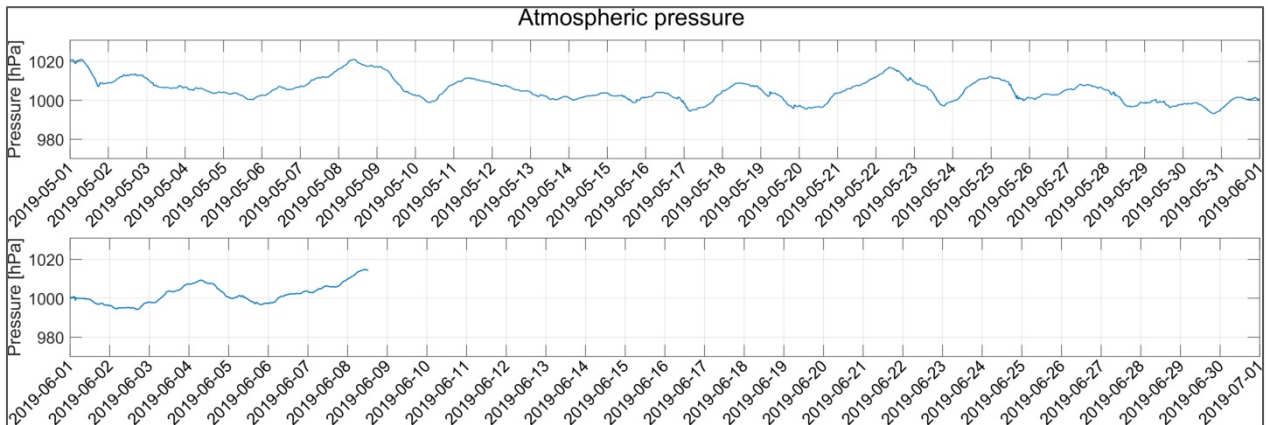
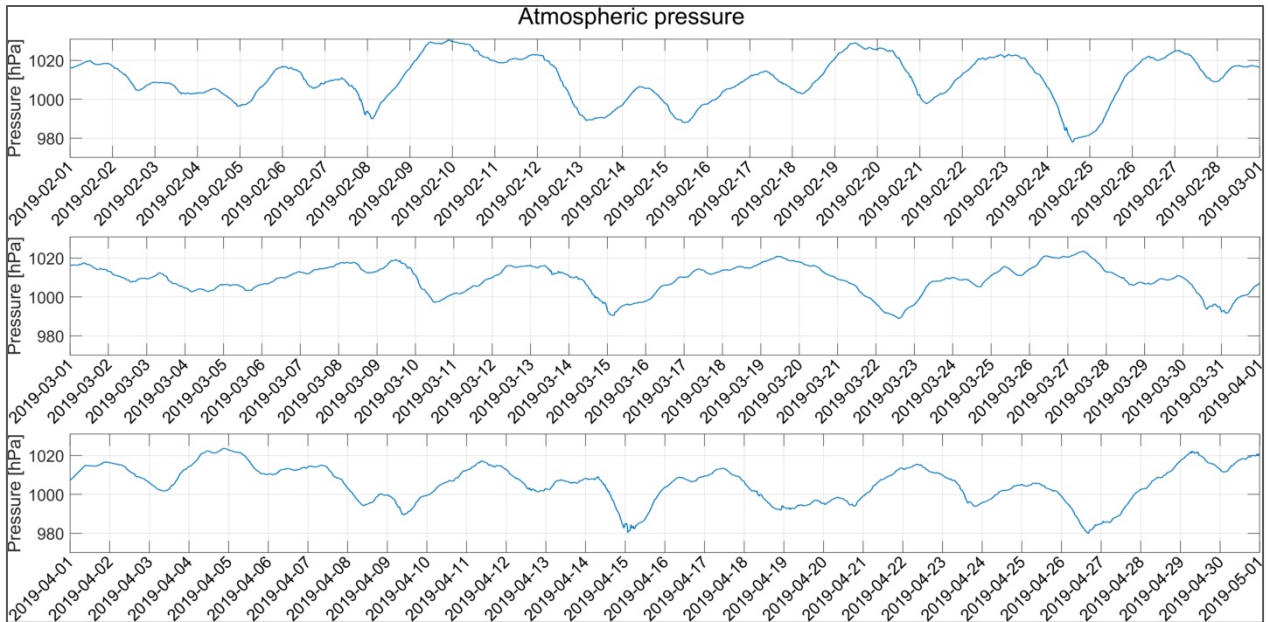
		Wind velocity (km/h)								total
		0	[0;10]	[10;20]	[20;30]	[30;40]	[40;50]	[50;60]	[60;70]	
[165;195]	N		1982	1679	1697	1039	387	31	7	6822
	%		4%	3%	3%	2%	1%	0%	0%	13%
[195;225]	N		1779	5545	1715	170	23		1	9233
	%		3%	11%	3%	0%	0%		0%	18%
[225;255]	N		784	1316	863	158	16			3137
	%		2%	3%	2%	0%	0%			6%
[255;285]	N		1280	2369	934	110	5			4698
	%		2%	5%	2%	0%	0%			9%
[285;315]	N		1041	2093	757	78	12			3981
	%		2%	4%	1%	0%	0%			8%
[315;345]	N		1315	1350	721	89	1			3476
	%		3%	3%	1%	0%	0%			7%
Total	N	161	19466	21373	8164	1760	444	31	8	51407
	%	0.31%	38%	42%	16%	3%	1%	0%	0%	100%

# Appendix 1-2

Atmospheric Pressure

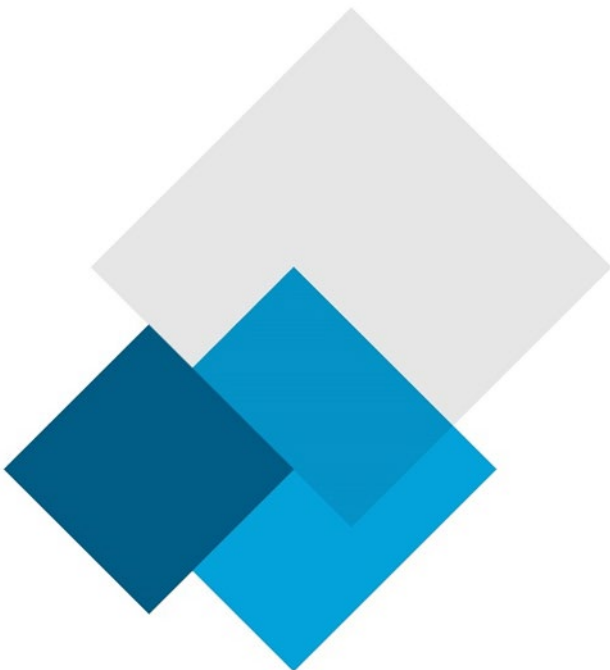




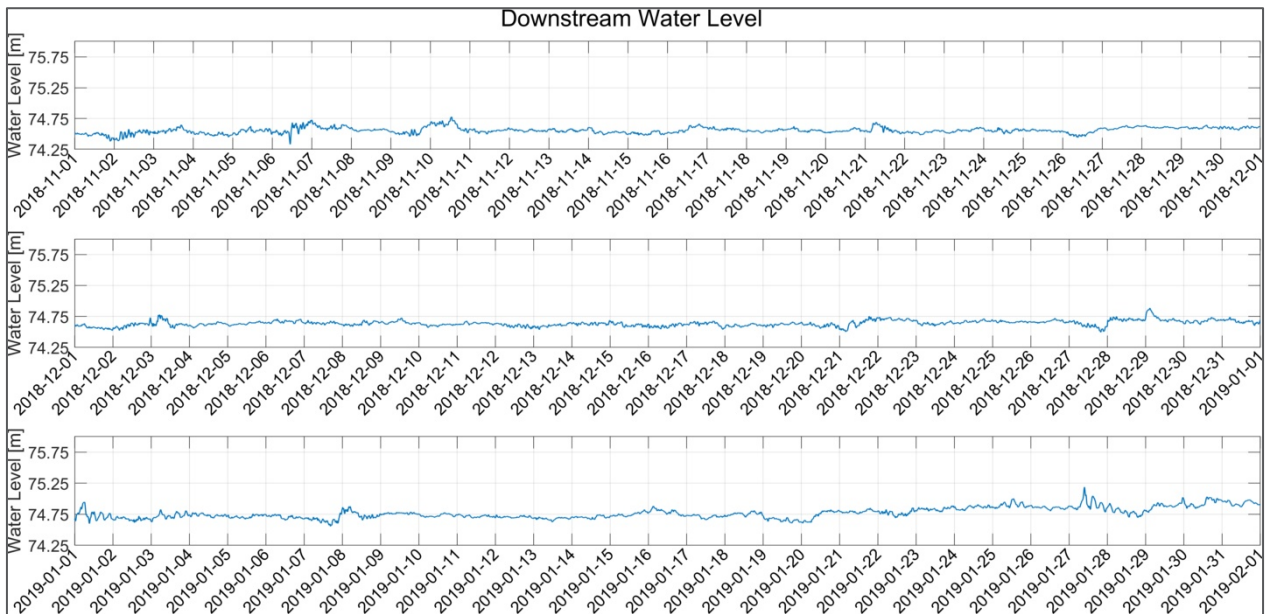
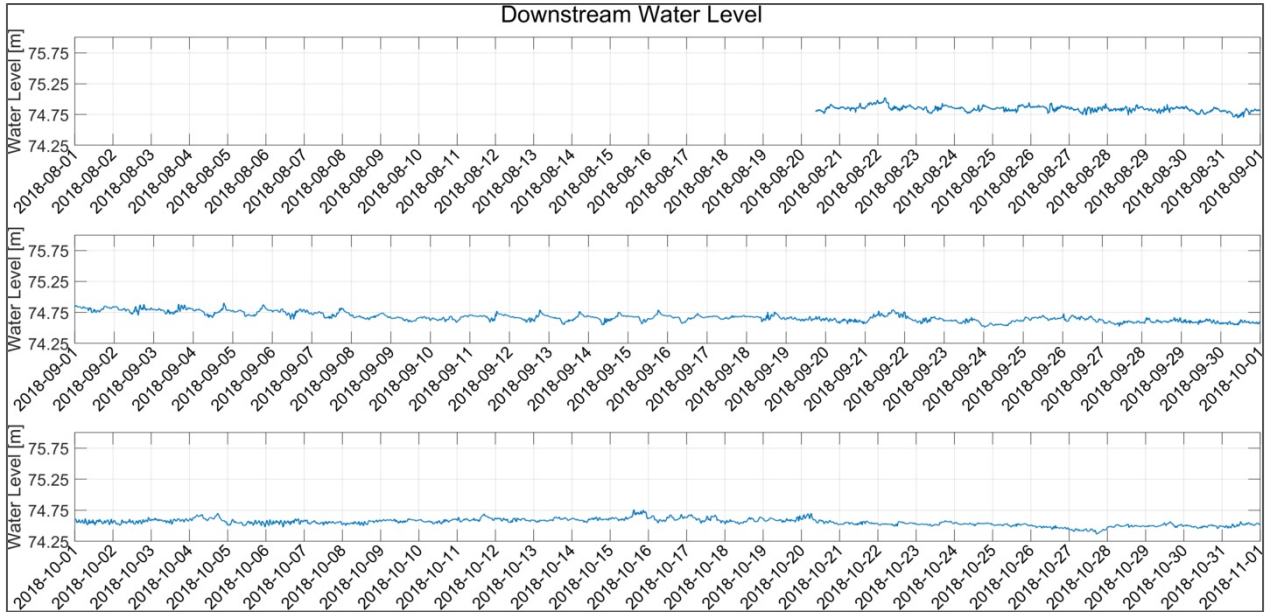


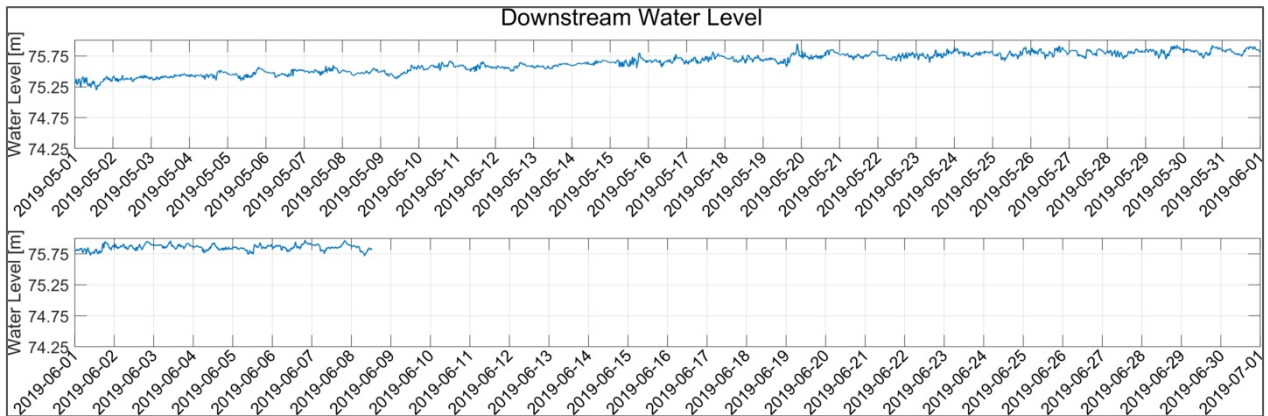
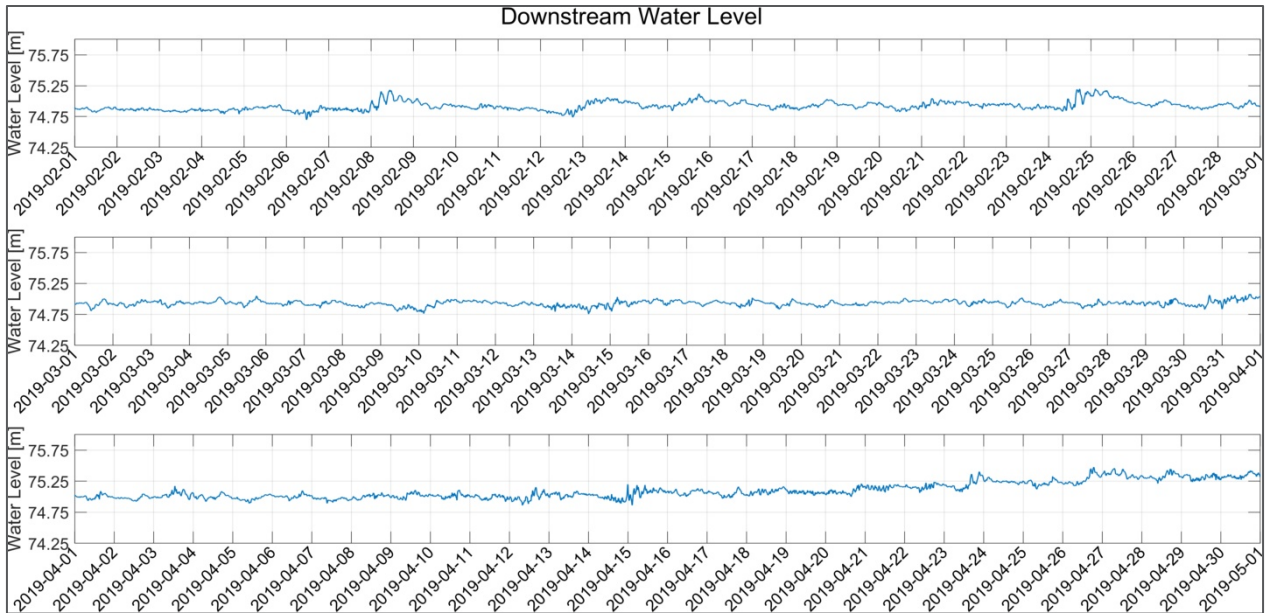
# Appendix 1-3

Water Level

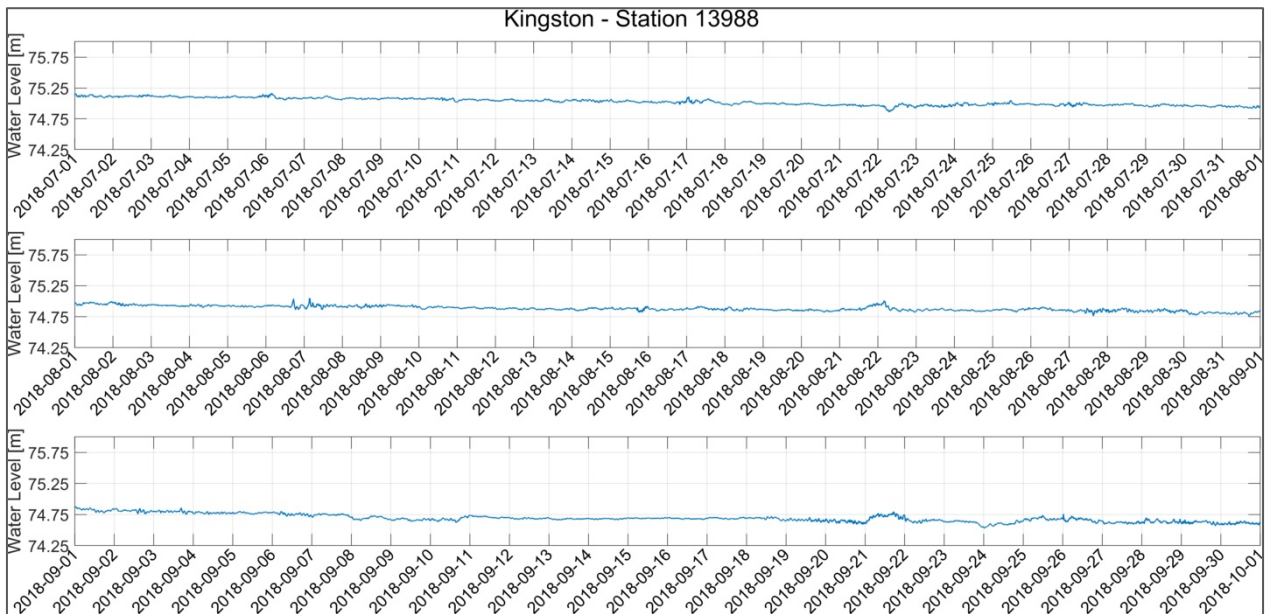
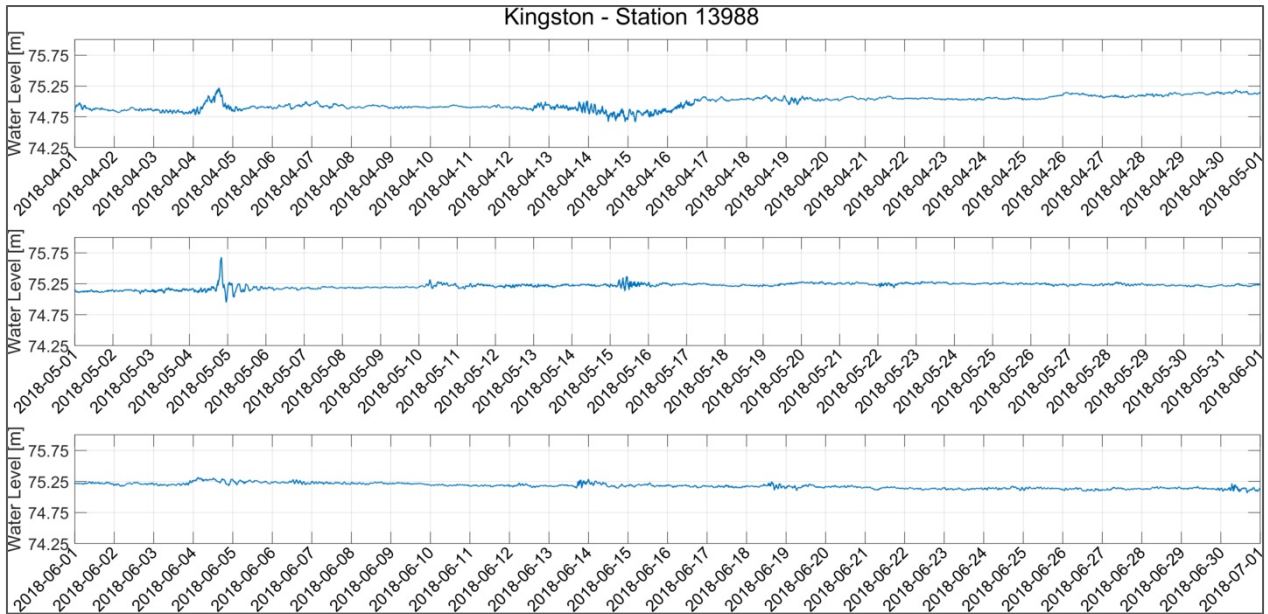


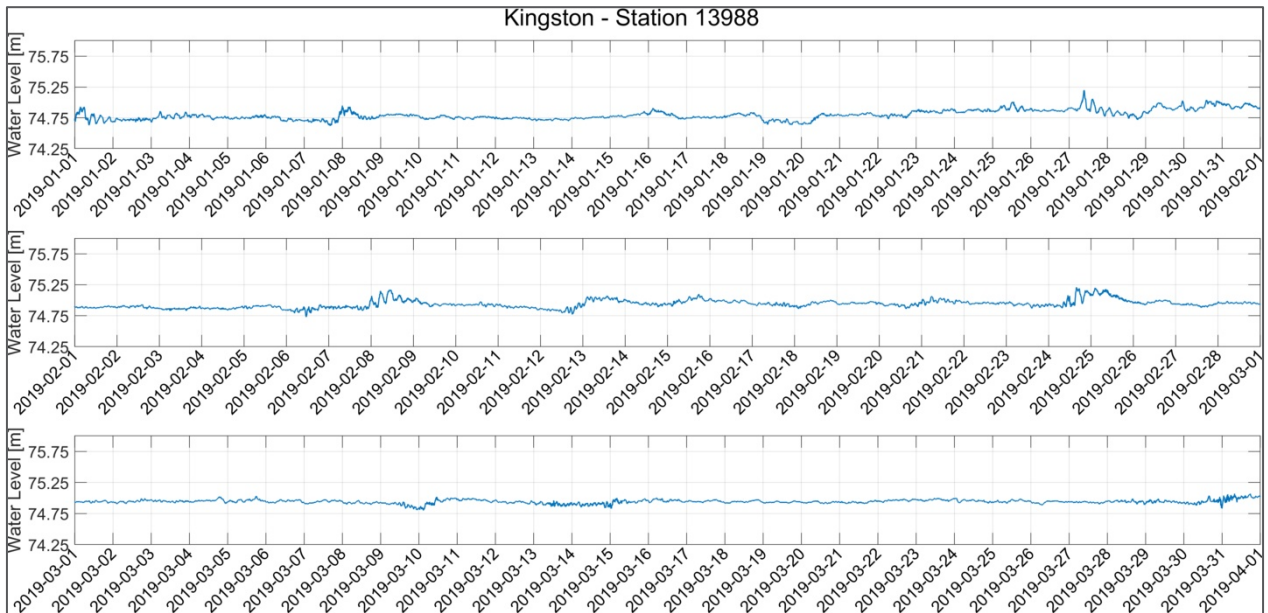
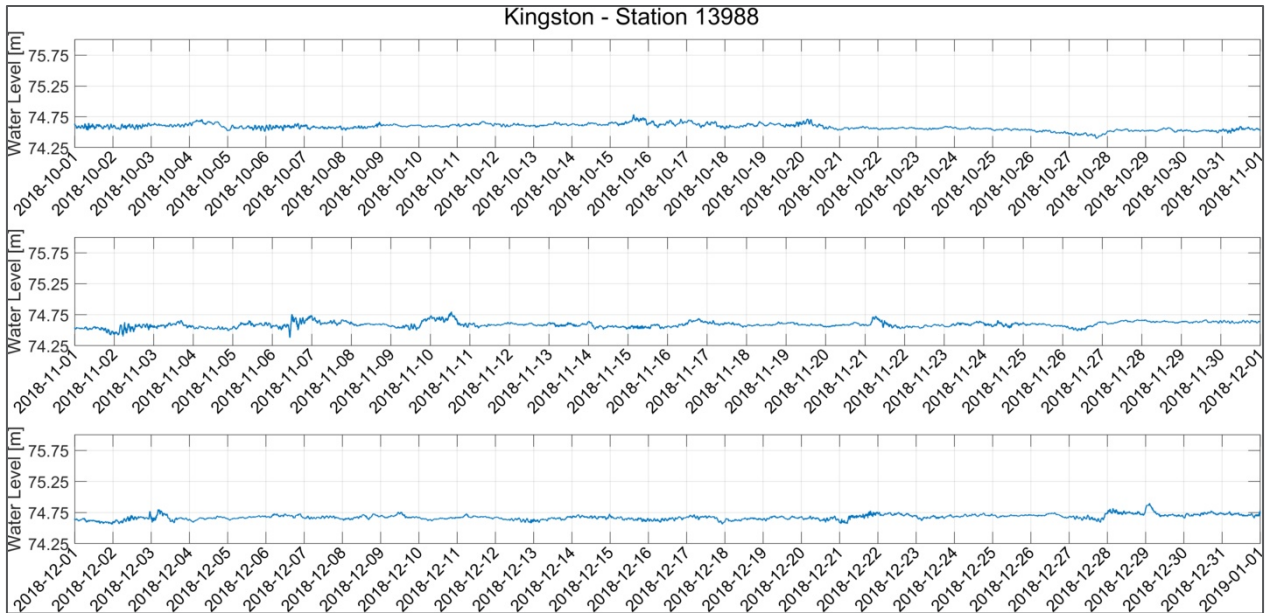
## LaSalle Causeway station

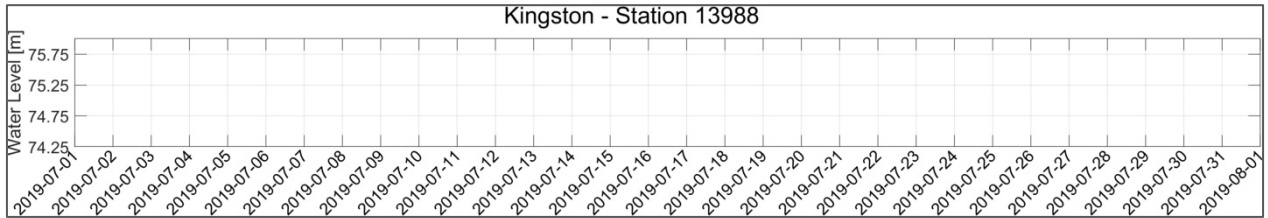
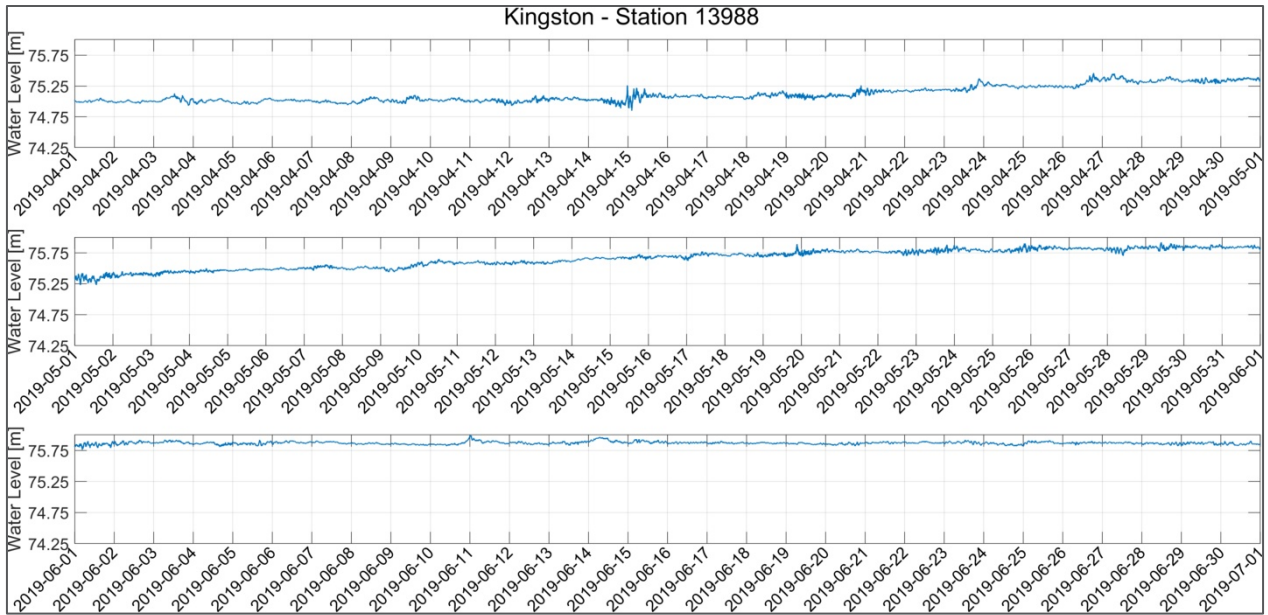




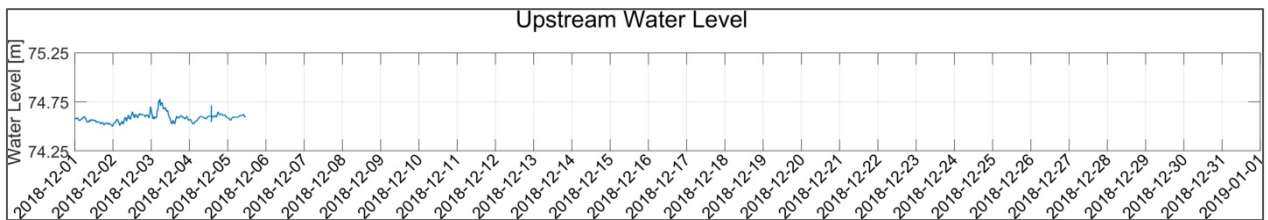
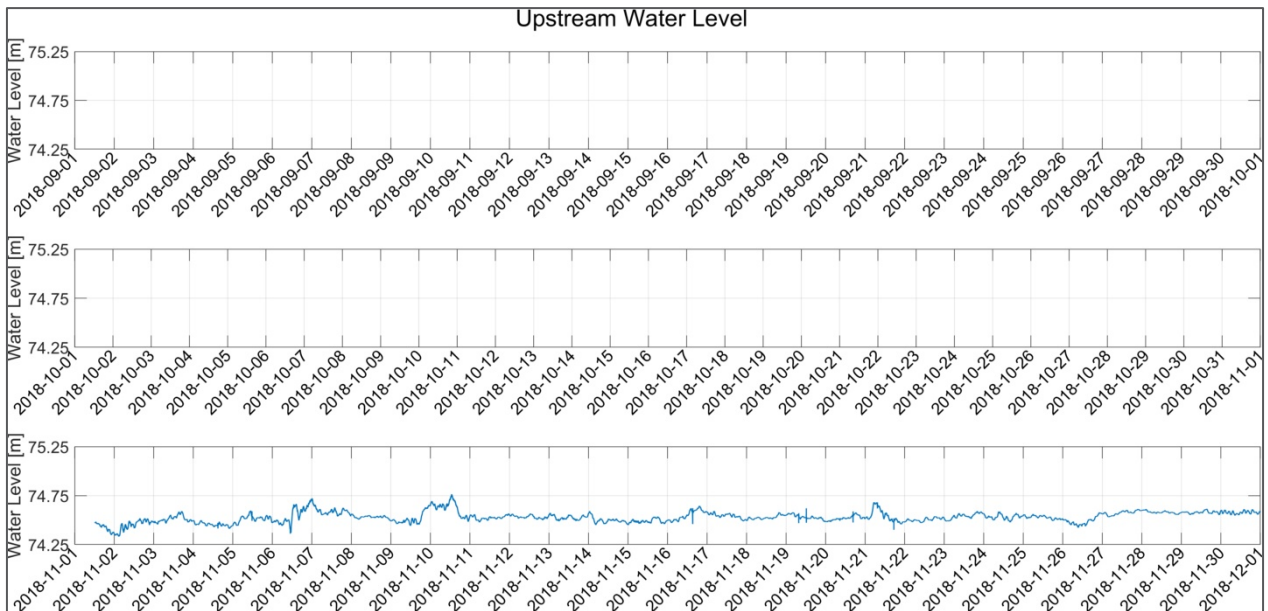
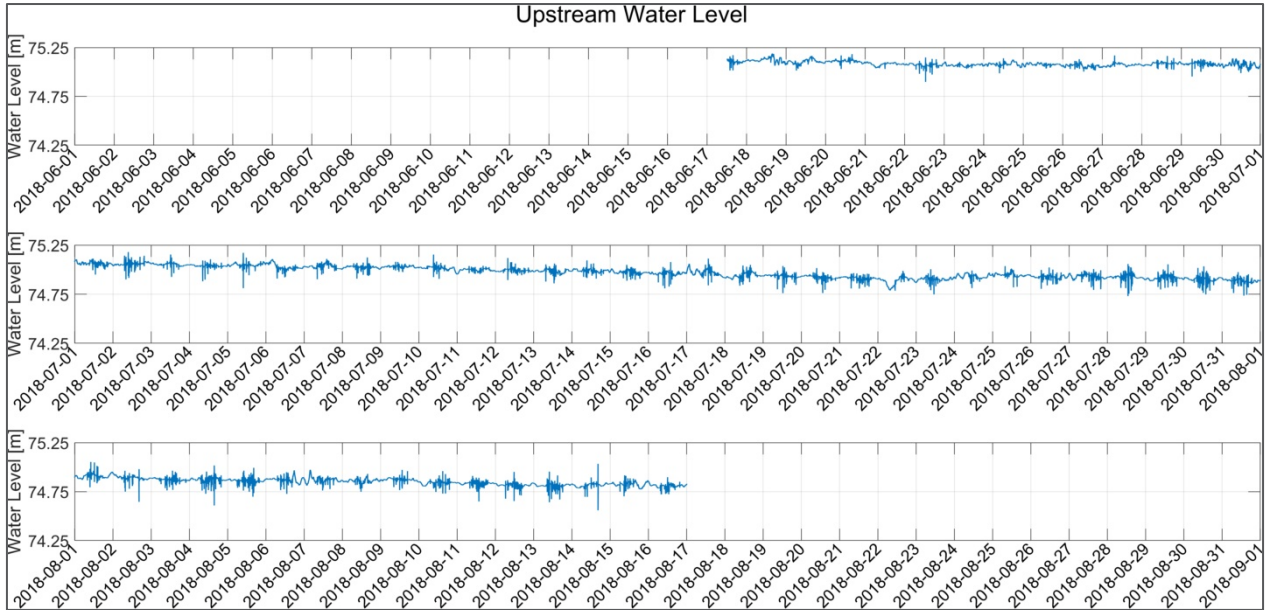
## Kingston Station





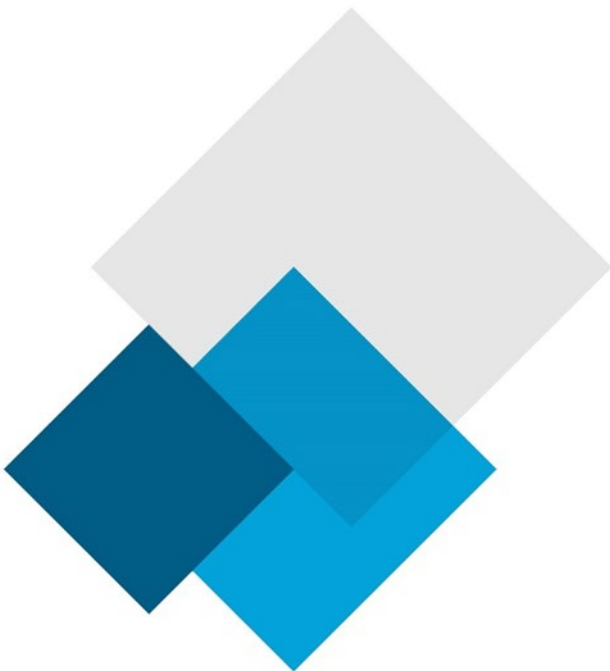


## Rideau Marina Station



# Appendix 2

Input parameters and validation CMS wave model



## Wind Waves modelling: CMS-Waves

### Inputs

- › Bathymetry: The bathymetry is a digitization of Navionics maps, data was cleaned and checked manually afterward with water depth data collected during the field surveys. At the causeway water depth is considered at basin depth until the toe edge of the causeway and not having a slope towards the toe of the structure.
- › Current: no currents was considered in this numerical modelling by river discharge or water elevation changes from oscillations in Lake Ontario.

### Numerical Grid

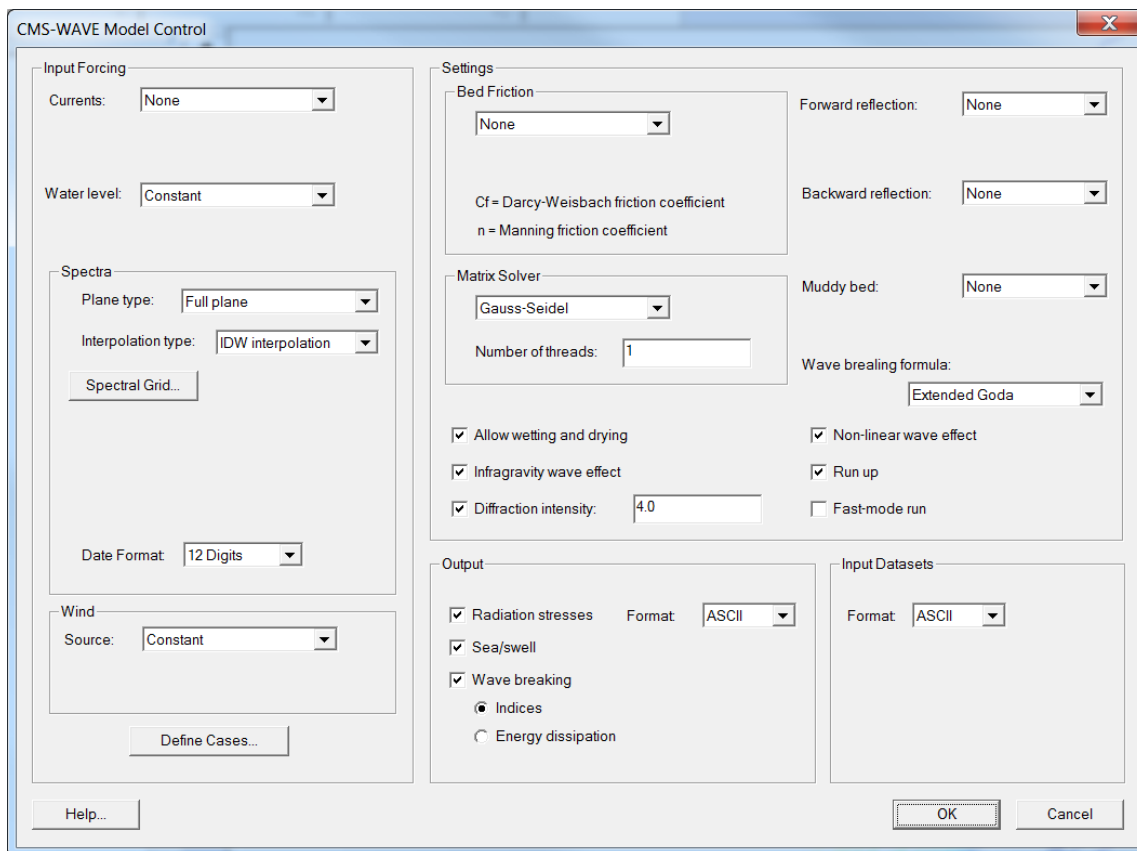
- › Domain grid size 1 x 1m

### Boundaries conditions

- › Waves are generated and propagated over the domain for 9 different cases of wind.

### CMS-Wave Parameter

Figure A2-1 Screenshot of CMS-wave parameter settings used



## Model Validation

### Sensibility

Grid size sensibility: The extreme of the runs have been done with a bigger grid size (2x2m) and the waves characteristics were extracted and compared at the location given on Figure A2-2. The maximum difference was very small: 6mm for wave height, 0.08s for period and 0.8 degrees for direction.

### Qualitative Validation

Waves characteristics from the modelling was extracted at the same location of the wave's pressures sensor for purposes of numerical model validation. But given the poor quality of the digital terrain model, the assumption of no vegetation and the continuous wind for the wave generation, the validation of the model is mostly qualitative. Vegetation and direction varying wind would attenuate the waves.

Specific wind conditions that happened during the survey have been selected to be reproduced in CMS-waves model. The wind conditions in CMS-Waves was approximated:

1. During October 27<sup>th</sup>, the wind was coming from the 55 degN to 30degN direction and was growing from around 10km/h to 25km/h. The waves did grow from around 2.5cm to 10cm height. A constant wind of 25km/h coming from 30deg N was used in CMS-Wave.
2. October 26<sup>th</sup>, the wind did blow from the South-east direction during few hours at 10km/h maximum. We see wave during that time reaching about 5cm height.
3. September 21, the wind was strong (up to 62km/h) coming from the south, the waves was about 12cm high.

Case number	H(m) max	CMS Hs
1	0.10	0.19
2	0.05	0.03
3	0.12	0.14

Those results show that the waves height generated are close to the sensor measurement. The bigger differences for wind coming from 30degN is explained by the bigger vegetation surface the waves have to go through compare to waves coming from south for example.

# Appendix 3

Results of wave simulation

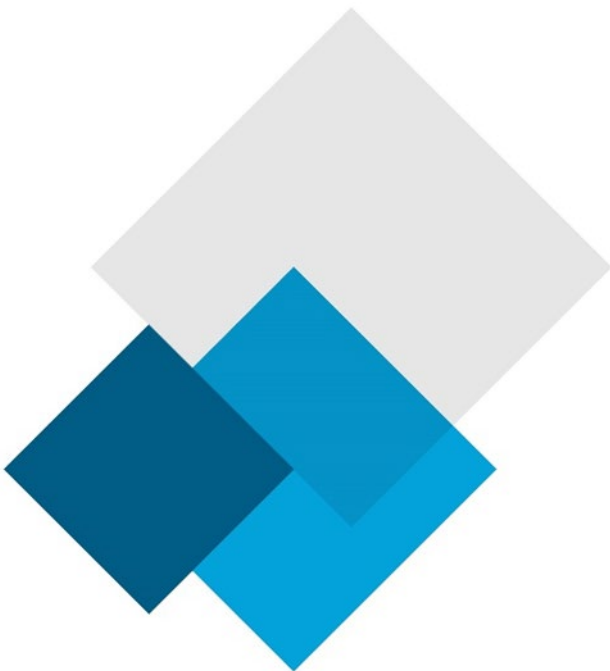


Figure A3-1 Wave height (a, b, c) and near bottom velocities (d, e, f) for Eastern winds with recurrence interval of 1 (a, d), 10 (b, e) and 50 (c, f) years.

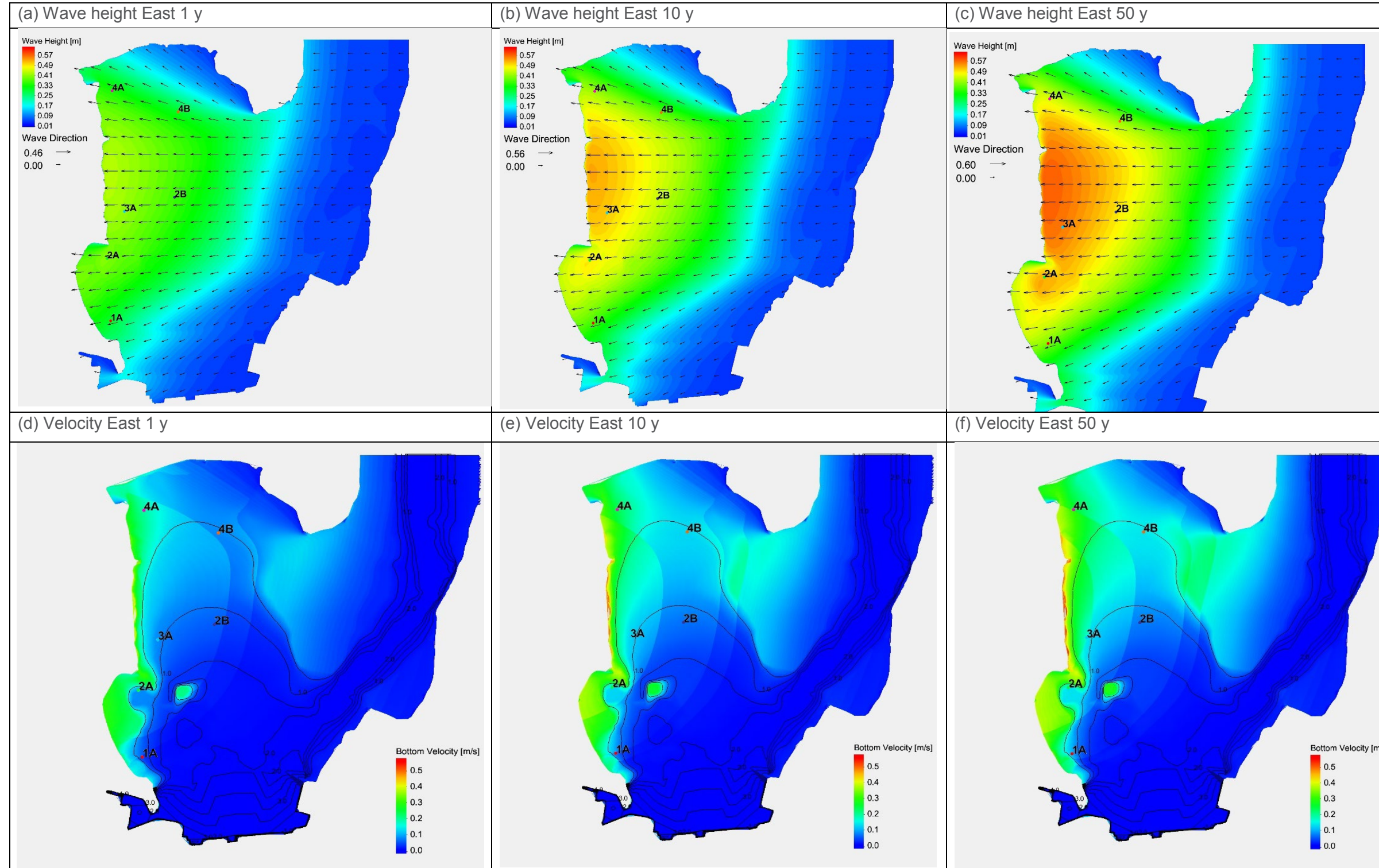


Figure A3-2 Wave height (a, b, c) and near bottom velocities (d, e, f) for South-East winds with recurrence interval of 1 (a, d), 10 (b, e) and 50 (c, f) years.

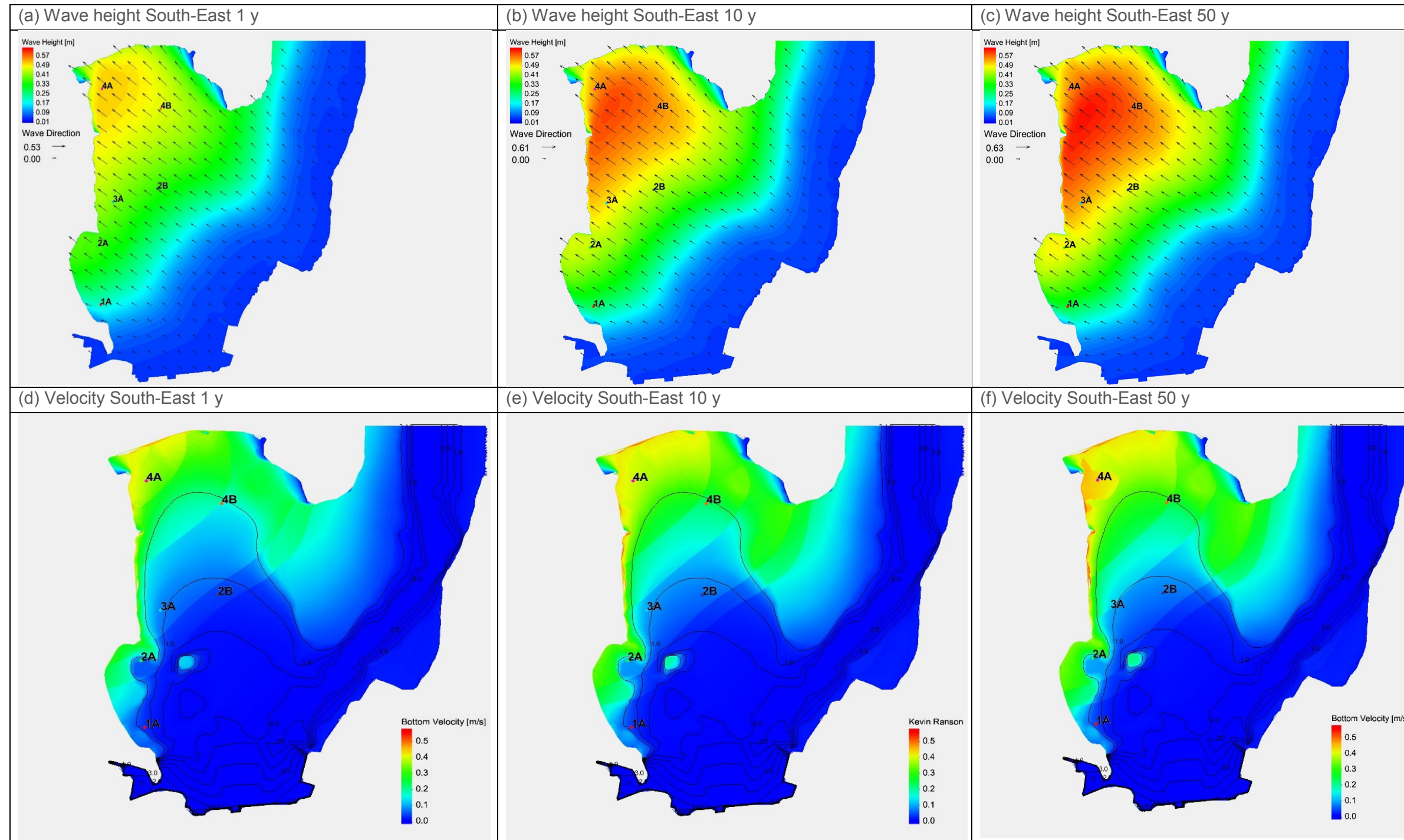
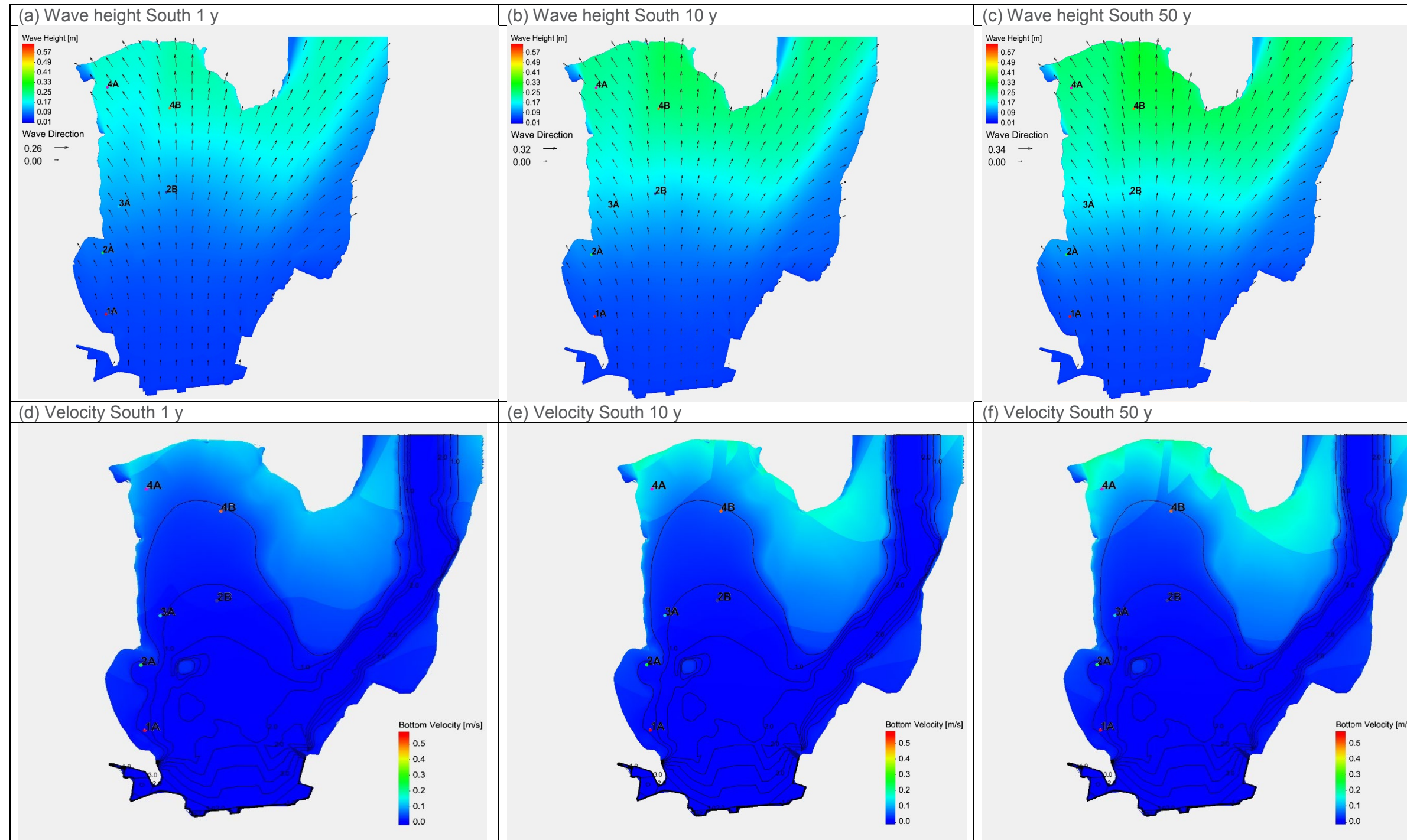


Figure A3-3 Wave height (a, b, c) and near bottom velocities (d, e, f) for Southern winds with recurrence interval of 1 (a, d), 10 (b, e) and 50 (c, f) years.



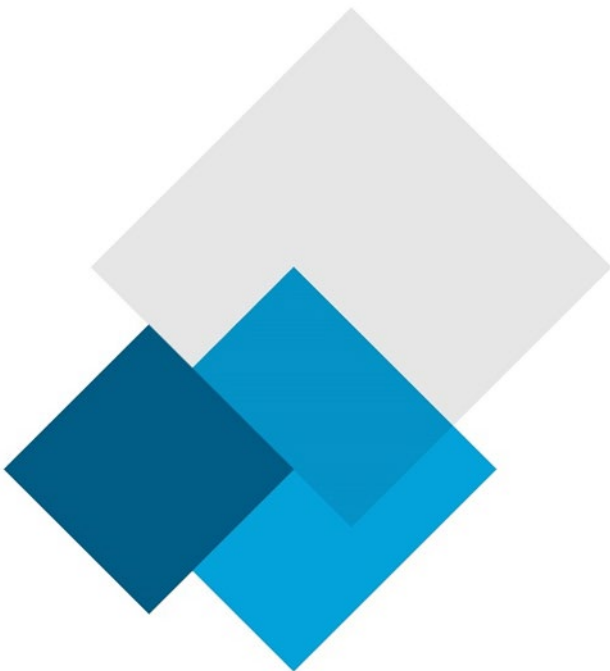
Tables A3-1 Waves characteristics at specific locations for different wind return period

Wind			Sample location	Waves			
Direction	Velocity	Return Period		Height	Period	Bottom Velocity	Energy
	[km/h]			[m]	[s]	[m/s]	[N] or [J/m]
South	53.5	1 year	1A	0.05	1.16	0.00	7
			2A	0.07	1.29	0.00	17
			2B	0.11	1.36	0.01	43
			3A	0.11	1.34	0.01	39
			4A	0.18	1.42	0.07	127
			4B	0.19	1.37	0.03	128
	63.5	10 years	1A	0.05	1.17	0.00	7
			2A	0.09	1.34	0.01	27
			2B	0.15	1.37	0.01	77
			3A	0.13	1.35	0.01	63
			4A	0.22	1.48	0.10	202
			4B	0.24	1.4	0.04	214
	68.0	50 years	1A	0.06	1.18	0.00	8
			2A	0.10	1.34	0.01	32
			2B	0.16	1.37	0.01	95
			3A	0.15	1.36	0.01	78
			4A	0.24	1.49	0.11	237
			4B	0.26	1.43	0.05	270
South-East	42.5	1 year	1A	0.19	1.37	0.02	135
			2A	0.36	1.49	0.05	541
			2B	0.35	1.49	0.03	511
			3A	0.40	1.56	0.06	739
			4A	0.50	1.82	0.37	1460
			4B	0.46	1.64	0.17	1047
	53.0	10 years	1A	0.26	1.37	0.03	241
			2A	0.44	1.56	0.07	907
			2B	0.43	1.56	0.05	868
			3A	0.49	1.64	0.10	1234
			4A	0.53	1.82	0.40	1653
			4B	0.55	1.72	0.23	1644
	57.5	50 years	1A	0.29	1.37	0.03	292
			2A	0.48	1.64	0.10	1154
			2B	0.47	1.56	0.06	1010
			3A	0.53	1.72	0.13	1558
			4A	0.54	1.92	0.44	1823
			4B	0.57	1.82	0.28	2008

Wind			Sample location	Waves			
Direction	Velocity	Return Period		Height	Period	Bottom Velocity	Energy
	[km/h]			[m]	[s]	[m/s]	[N] or [J/m]
East	33.0	1 year	1A	0.29	1.43	0.04	333
			2A	0.40	1.64	0.09	815
			2B	0.36	1.56	0.04	589
			3A	0.41	1.64	0.08	861
			4A	0.33	1.56	0.18	493
			4B	0.30	1.49	0.07	372
	40.5	10 years	1A	0.36	1.49	0.07	543
			2A	0.49	1.72	0.13	1324
			2B	0.45	1.64	0.07	1021
			3A	0.51	1.72	0.13	1436
			4A	0.41	1.64	0.25	837
			4B	0.37	1.56	0.11	637
	45.0	50 years	1A	0.39	1.56	0.09	715
			2A	0.52	1.72	0.14	1539
			2B	0.49	1.64	0.08	1237
			3A	0.56	1.82	0.18	1921
			4A	0.46	1.64	0.28	1016
			4B	0.41	1.64	0.15	850

# Appendix 4

Radio Isotopic Analysis Core 1A



# Interpretation of Pb-210, Ra-226 and Cs-137 Results

## Flett Research Ltd.

440 DeSalaberry Ave. Winnipeg, MB R2L 0Y7

Fax/Phone: (204) 667-2505

Email: [flett@flettresearch.ca](mailto:flett@flettresearch.ca) Webpage: <http://www.flettresearch.ca>

---

## Client: Lorrain, Stéphane

**Address:** SNC-LAVALIN GEM QUÉBEC INC., 455, boul. René-Lévesque ouest, Montréal (Québec) H2Z 1Z3

**Core ID:** 1A

**Transaction ID:** 882

**PO/Contract No.:** 653502-0028

**Date Received:** 20-Feb-19

**Analysis Dates:** February 25 - April 24, 2019

**Analysts:** L. Hesketh-Jost; X. Hu

**Sampling Date:** 9-Feb-19

**Project:** #653502

*Results authorized by Dr. Robert J. Flett, Chief Scientist*

---

## INTERPRETATION

### Observations:

The Pb-210 profile exhibits an irregular but approximately exponential decrease in total Pb-210 activity as a function of depth. The maximum activity of 9.05 DPM/g observed in section 6 - 7 cm is about 8 times the lowest activity of 1.07 DPM/g observed in section 50 - 51 cm (Pages 2 & 3). The Pb-210 activities in upper 2 sections (extrapolated depth 0 - 5 cm) are slightly lower than section 6 - 7 cm, and this probably represents increasing sediment accumulation rates, and/or physical mixing, and/or diffusion of Pb-210 across a redox gradient, and/or incomplete diagenesis of surface sediment, and/or incomplete ingrowth of the Po-210, granddaughter of Pb-210, actually being measured.

The dry bulk densities generally increase from the surface to section 24 (extrapolated depth 22.5 - 25 cm), ranging between 0.175 g/cm<sup>3</sup> and 0.357 g/cm<sup>3</sup>. The dry bulk densities then decrease beginning in section 27 (extrapolated depth 25 - 27.5 cm) from 0.289 g/cm<sup>3</sup> to 0.259 g/cm<sup>3</sup> at section 31 (extrapolated depth 29.5 - 33.5 cm). From section 37 (extrapolated depth 33.5 - 39 cm) to the bottom of the core the dry bulk densities increase rapidly, from 0.326 g/cm<sup>3</sup> to 0.664 g/cm<sup>3</sup> (Page 2 & 4).

Ra-226 was measured at 1.23, 1.31 and 1.05 DPM/g in sections 11 - 12 cm, 26 - 27 cm and 58 - 59 cm, respectively (Pages 5 - 8). The Pb-210 activity in the 50 - 51 cm section barely exceeds the Ra-226 activity measured in the 58 - 59 cm section, indicating that the background level of Pb-210 may have been achieved in this core.

Cs-137 was measured in 10 sections in the 0 - 31 cm core interval. Activities in the 0 - 29 cm portion of the core are significantly above background, ranging between 0.58 - 3.19 DPM/g (Pages 9 & 13). The shape of Cs-137 profile in the 0 - 27 cm core interval suggests that the majority of the Cs-137 is probably from external erosion sources (soils or sediments contaminated with bomb testing radionuclides). Below 27 cm, we expect to see the Cs-137 activity gradually decline with depth. This tailing of Cs-137 into deeper depths with Pb-210 dates prior to 1954 is commonly seen and is attributed to downward diffusion of the isotope. However, in this core the tailing into deeper depths is not seen, rather, we see a sharp and sudden decrease immediately below the highest Cs-137 activities and then a non detect at section 30 - 31 cm. This is unexpected and suggests that part of the Cs-137 profile may have been disturbed or is missing from the core.

### CRS model of Age at bottom of Extrapolated section in years vs. Depth of bottom edge of current section in cm:

The CRS model assumes constant input of Pb-210 and a core that is long enough to include all of the measurable atmospheric source Pb-210, i.e. it contains a complete Pb-210 inventory. If one assumes that the Pb-210 activity of 1.07 DPM/g (in the 50 - 51 cm section) is the background level, then it should be possible to apply the model.

When initially applied to the core, the CRS model predicted an age of 78 years at the bottom of the 26 - 27 cm section, an age too old to agree with the significant presence of Cs-137 in the same section. This leads to the assumption that the Pb-210 inventory is probably incomplete and the core cannot be processed by the CRS model.

### **Regression model of Unsupported Pb-210 activity vs. Cumulative Dry Weight (g/cm<sup>2</sup>):**

When applying the linear regression model, it is assumed that the input of Pb-210 and the sediment accumulation rate are constant. The shape of the Pb-210 profile suggests that these assumptions may be satisfied in the core interval of sections 7 - 22 (extrapolated depth 5 - 22.5 cm), and therefore the model was applied to this core interval to estimate the average sediment accumulation rate for this core interval.

When initially applied to the core interval of 5 - 22.5 cm (extrapolated depth), the regression model predicted ( $R^2 = 0.9496$ ) an average sediment accumulation rate of 0.0610 g/cm<sup>2</sup>/yr when the unsupported Pb-210 activity was calculated by subtracting the nearest neighbouring Ra-226 measurement from each total Pb-210 value. However, the regression model predicted an age of 102 years at the bottom of section 22, an age too old to agree with the significant presence of Cs-137 at this depth, and the continuing presence of significant Cs-137 activities into deeper depths.

Moreover, when the CRS model was applied it predicted that the sediment accumulation rates are variable throughout the core i.e. significant changes throughout the core length and increasing sediment accumulation rates towards the surface. Therefore, the assumption of constant sediment accumulation rate could not be satisfied, and it was concluded that the linear regression model should not be applied to this core.

### **Conclusion:**

The rapid decline in Cs-137 activity below 27 cm, combined with the sudden termination in exponential decay of Pb-210 at section 27 (extrapolated depth 25 - 27.5 cm) and the sharp decrease in dry bulk density in the same section, suggests that this core may have been disturbed or that a significant portion of the core may be missing.

However, with the significant presence of Cs-137 and unsupported Pb-210 found in the 0 - 27 cm core interval, we are able to conclude that in general all sediments in this core interval likely represent post 1966 sediment accumulation.

Overall, the analytical quality of radioisotope data (based upon the recovery of spike, the recovery of CRM, the results of repeat analyses and blanks) is considered good.

# Results of Pb-210 by Po-210 Analysis

Flett Research Ltd.

440 DeSalaberry Ave. Winnipeg, MB R2L 0Y7

Fax/Phone: (204) 667-2505

E-mail: flett@flettresearch.ca Webpage: http://www.flettresearch.ca

**Client: Lorrain, Stéphane**

Address: SNC-LAVALIN GEM QUÉBEC INC., 455, boul. René-Lévesque ouest, Montréal (Québec) H2Z 1Z3

Core ID: 1A

Date Received: 20-Feb-19

Sampling Date: 9-Feb-19

Project: #653502

Transaction ID: 882

PO/Contract No.: 653502-0028

Analysis Dates: February 25 - April 21, 2019

Analysts: L. Hesketh-Jost

Salt correction applied? No

Analytical Method: N20110 Determination of Lead-210 in Sediment, Soil and Peat by Alpha Spectrometry (Version 4)

Deviations from Method:

Comments:

**Detection Limit:** The method detection limit (MDL) for 0.25 - 0.5 g (dry wt.) sample is between 0.05 - 0.1 DPM Po-210/g dry sample at a 95% confidence level for 60,000 second counting time, and is based on greater than 20 method blanks. This can vary slightly and depends upon the amount of sample, detector and recovery efficiency of each sample.

**Estimated Uncertainty:** The estimated uncertainty for samples analyzed by this method (acid extraction) has been determined to be ± 11% at concentrations between 0.6 and 40 DPM/g at 95% confidence.

Results authorized by Dr. Robert J. Flett, Chief Scientist

Section Number	Sample ID	Upper Depth (cm)	Lower Depth (cm)	Extrapolated Upper Section Depth (cm)	Extrapolated Lower Section Depth (cm)	Dry Bulk Density (Dry wt./Wet vol.) (g/cm <sup>3</sup> )	% Loss on Drying	Mass in Extrapolated Section (g/cm <sup>2</sup> )	Cumulative Mass to Bottom of Current Section (g/cm <sup>2</sup> )	Plot-point of Cumulative Mass in Current Section (g/cm <sup>2</sup> )	Po-209 Counts Less Detector Background	Po-210 Counts Less Detector Background and Po-209 Spike Standard Blank	Weight of Sample Counted (g)	Count Time (sec)	Po-210 Total Activity (DPM/g)	Error Po-210 +/- 1 S.D. (DPM/g)	Ra-226 Activity (DPM/g dry wt.)	Error Ra-226 +/- 1 S.D. (DPM/g dry wt.)	Comments Code for Pb-210 Analysis
1	1A-2/2-1	0.0	1.0	0.00	2.00	0.175	84.14%	0.350	0.350	0.088					8.70	0.27			
4	1A-2/2-4	3.0	4.0	2.00	5.00	0.201	82.02%	0.604	0.954	0.652	2621	1248	0.507	60000	8.99	0.25			
7	1A-2/2-7	6.0	7.0	5.00	7.50	0.201	81.98%	0.503	1.458	1.256	2566	1155	0.476	60000	9.05	0.27			
9	1A-2/2-9	8.0	9.0	7.50	9.00	0.227	79.96%	0.340	1.798	1.685	1240	536	0.525	60000	7.88	0.34			
10	1A-2/2-10	9.0	10.0	9.00	10.50	0.242	78.73%	0.363	2.161	1.919	1195	468	0.483	60000	7.78	0.36			
12	1A-2/2-12	11.0	12.0	10.50	13.00	0.282	75.86%	0.705	2.866	2.443	1278	324	0.525	60000	4.62	0.26	1.23	0.03	
15	1A-2/2-15	14.0	15.0	13.00	15.50	0.329	72.59%	0.822	3.688	3.359	1696	319	0.556	60000	3.24	0.19			
17	1A-2/2-17	16.0	17.0	15.50	19.00	0.320	73.15%	1.119	4.807	4.008	2713	421	0.526	60000	2.82	0.14			
22	1A-2/2-22	21.0	22.0	19.00	22.50	0.357	70.62%	1.250	6.057	5.700	1153	146	0.547	60000	2.22	0.19			
24	1A-2/2-24	23.0	24.0	22.50	25.00	0.356	70.69%	0.890	6.947	6.413	1067	137	0.540	60000	2.29	0.20			
27	1A-2/2-27	26.0	27.0	25.00	27.50	0.289	75.07%	0.723	7.671	7.381	2091	286	0.489	60000	2.68	0.16	1.31	0.05	
29	1A-2/2-29	28.0	29.0	27.50	29.50	0.265	76.91%	0.530	8.201	7.936	1348	162	0.473	60000	2.44	0.20			
31	1A-2/2-31	30.0	31.0	29.50	33.50	0.259	77.42%	1.036	9.237	8.460	1387	175	0.562	60000	2.15	0.17			
37	1A-2/2-37	36.0	37.0	33.50	39.00	0.326	72.77%	1.796	11.032	10.216	1498	128	0.563	60000	1.45	0.14			
42	1A-2/2-42	41.0	42.0	39.00	46.00	0.422	66.40%	2.957	13.990	12.088	2278	148	0.506	60000	1.23	0.10			
51	1A-2/2-51	50.0	51.0	46.00	54.50	0.562	58.75%	4.781	18.770	16.521					1.07	0.12			
59	1A-2/2-59	58.0	59.0	54.50	59.00	0.664	53.41%	2.986	21.756	21.425	2549	183	0.516	60000	1.33	0.10	1.05	0.02	
Blank	Blank w/o Po-209 spike										-10	-3							
Blank	Blank w/ Po-209 spike										3026	-1							
Blank	Blank w/o Po-209 spike										0	0							
Blank	Blank w/ Po-209 spike										1495	-1							
1	1A-2/2-1	0.0	1.0			0.175	84.17%				2345	1033	0.484	60000	8.72	0.27			
1 Dup	1A-2/2-1 Duplicate	0.0	1.0			0.175	84.11%				2463	1090	0.488	60000	8.68	0.26			
51	1A-2/2-51	50.0	51.0								1579	98	0.514	60000	1.16	0.12			
51 Dup	1A-2/2-51 Duplicate	50.0	51.0								1740	88	0.494	60000	0.98	0.11			
CRM	IAEA 447										1655	1189	0.376	60000	18.29	0.53			Po-210 in CRM on counting date (DPM/g): 18.99 Recovery: 96.31%
CRM	IAEA 447										1223	943	0.455	60000	16.22	0.53			85.59%
CRM	IAEA 447										1284	751	0.343	60000	16.35	0.60			86.38%

**Dup (duplicate):** Two subsamples of the same sample were carried through the analytical procedure in an identical manner. **Rep (replicate):** Three or more subsamples of the same sample were carried through the analytical procedure in an identical manner.

This test report shall not be reproduced, except in full, without written approval of the laboratory.

Note: Results relate only to the items tested.

Q:\Clients A-L\Lorrain, Stéphane\2019\882\Radioisotopes\1A\Pb-210, Ra-226 and Cs-137 Lorrain Core 1A May 1-19 Final.xlsx

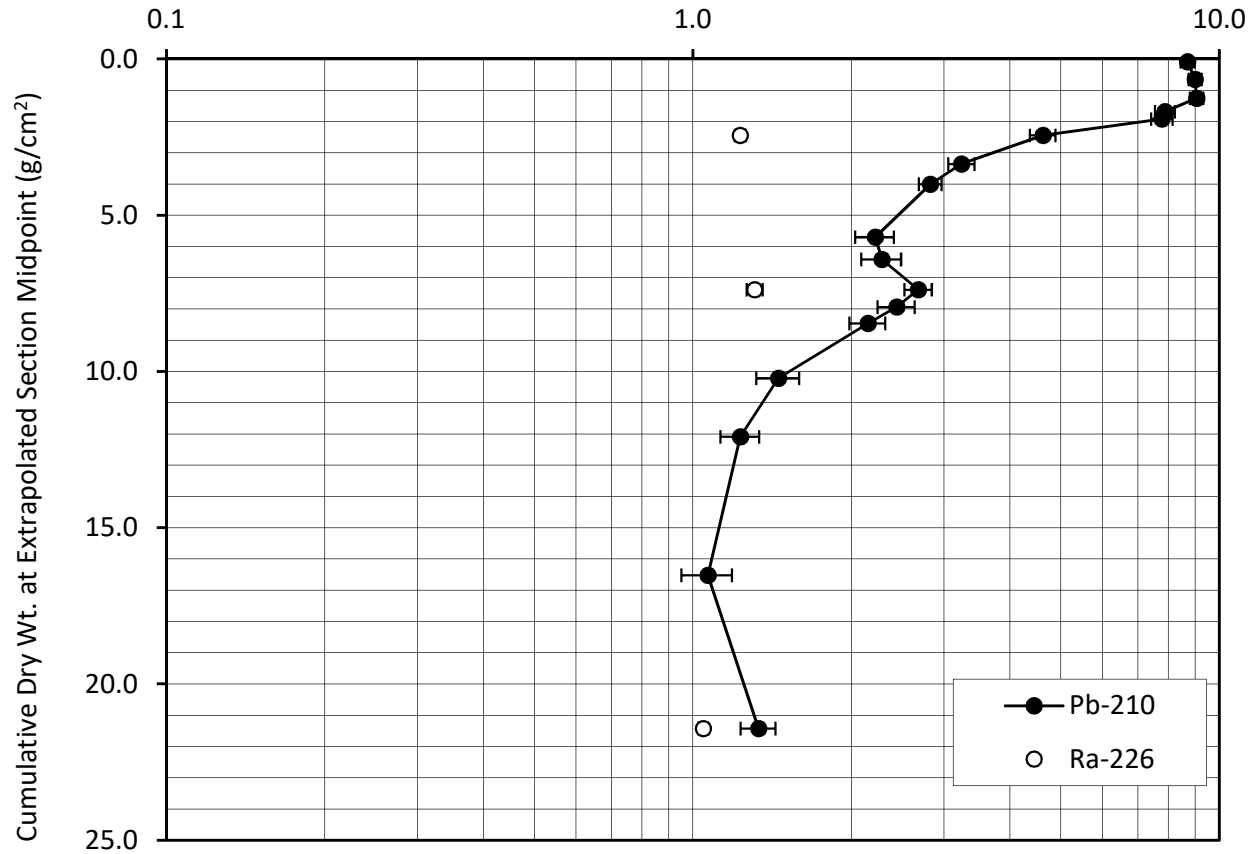
ISO / IEC 17025:2005 Accredited with the Canadian Association for Laboratory Accreditation (CALA Accreditation No. A3306)

Page 2 of 13

**Total Pb-210 Activity vs. Accumulated Sediment**

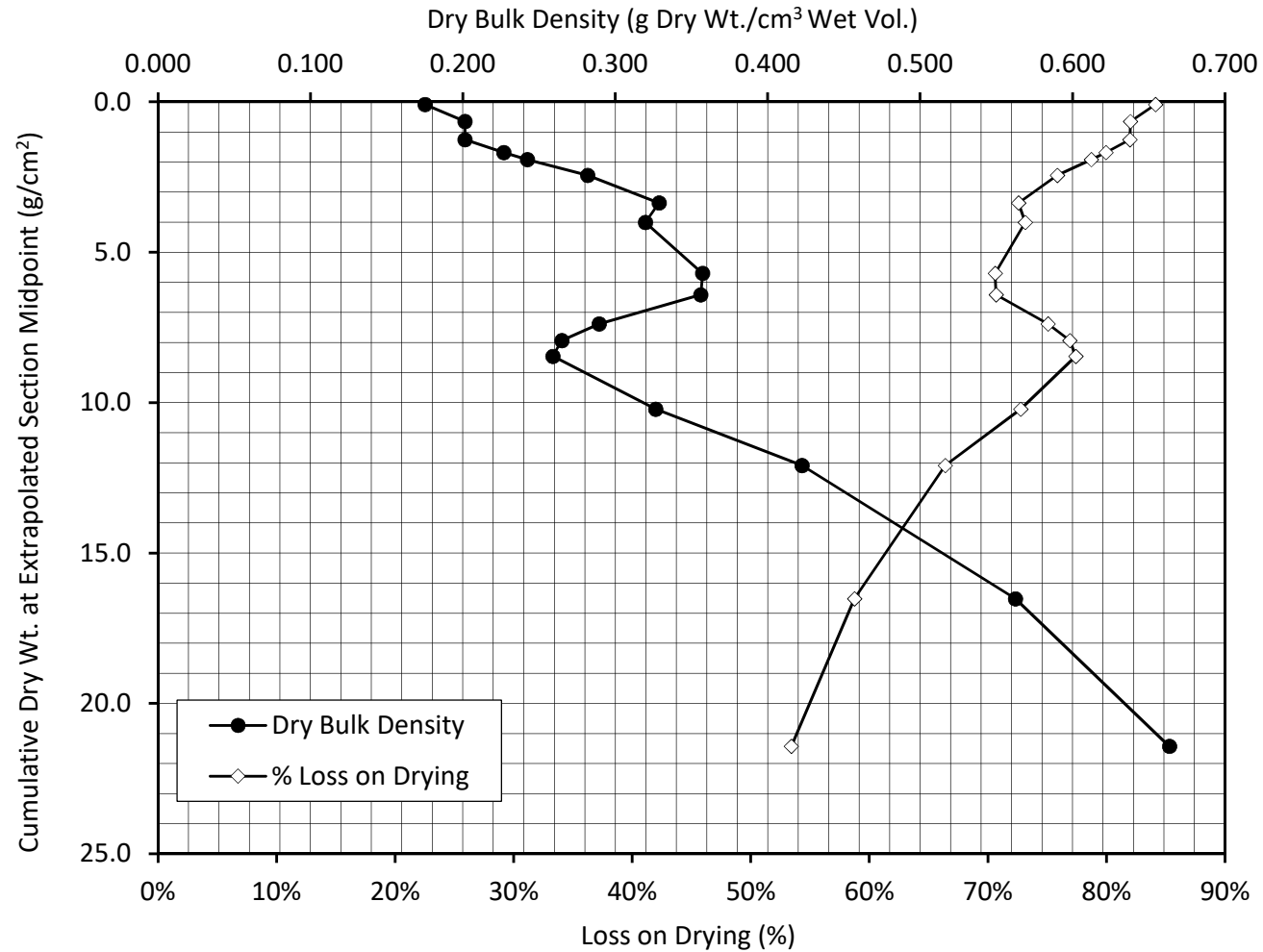
**1A**

Total Pb-210 Activity (DPM/g Dry Wt.)



**Dry Bulk Density and % Loss on Drying**  
**vs. Accumulated Sediment**

**1A**



# Results of Ra-226 Analysis by Rn-222 Emanation

Flett Research Ltd.

440 DeSalaberry Ave., Winnipeg, MB R2L 0Y7

Fax/Phone: (204) 667-2505

Email: flett@flettresearch.ca Webpage: http://www.flettresearch.ca

## Client: Lorrain, Stéphane

Address: SNC-LAVALIN GEM QUÉBEC INC., 455, boul. René-Lévesque ouest, Montréal (Québec) H2Z 1Z3

Core ID: 1A

Transaction ID: 882

Date Received: 20-Feb-19

PO/Contract No.: 653502-0028

Sampling Date: 9-Feb-19

Analysis Dates: February 25 - April 14, 2019

Project: #653502

Analysts: X. Hu; L. Hesketh-Jost

Salt Correction Applied? No

Analytical Method: N40110 Determination of Radium-226 in Sediment, Soil and Peat by Radon-222 Emanation (Version 3)

### Comments:

**Detection Limit:** The method detection limit (MDL) is dependent on the amount of sample analyzed. For a 60,000 second counting time the MDL at 95% confidence for 2 g of dry sample is 0.1 DPM/g and for 0.5 g of dry sample is 0.5 DPM/g.

**Estimated Uncertainty:** The estimate of uncertainty of measurement for this method in this laboratory is approximately ±12% at 95% confidence level (approximately 40,000 counts in 60,000 seconds).

Results authorized by Dr. Robert J. Flett, Chief Scientist

Core ID	Sample ID	Ra-226 Activity (DPM/g Dry Wt.)	Combined Error: 1 SD (DPM/g Dry Wt.)	Comments Code for Ra-226 Analysis
1A	1A-2/2-59	1.05	0.02	
1A	1A-2/2-12	1.23	0.03	
1A	1A-2/2-27	1.31	0.05	

Q:\Clients A-L\Lorrain, Stephane\2019(882)\Radioisotopes\1A\Pb-210, Ra-226 and Cs-137 Lorrain Core 1A May 1-19 Final.xlsm

**Duplicate:** Two subsamples of the same sample were carried through the analytical procedure in an identical manner.

**Re-count:** The sample bottle was re-sealed after the initial analysis, and was re-counted after 11 or more days of Rn-222 ingrowth. Repeat counting was chosen over duplicate analysis due to insufficient sample material provided.

This test report shall not be reproduced, except in full, without written approval of the laboratory.

Note: Results relate only to the items tested.

14-Apr-19

Page 5 of 13

ISO / IEC 17025:2005 Accredited with the Canadian Association for Laboratory Accreditation (CALA Accreditation No. A3306)

**Radium Analysis by Rn-222 Emanation**

Core ID	1A
Sample ID	1A-2/2-59
Lucas Cell No.	3
Number of days since Rn board last run	1
Dry weight of sample counted (g)	1.955
Total count in period	4986
Total count in period (carryover corrected)	n/a
Cell Blank count (CPM)	0.562
System Blank (DPM)	0.395
System Efficiency	0.839
Count duration (minutes)	1000

Typical carryover is about 1 - 2 % of the net counts (gross counts less system background) of the sample counted on the previous day. The carryover is subtracted from the gross counts of current sample. This correction is not required if the sample is run after a blank.

Carryover correction?	No
-----------------------	----

	Year	Month	Day	Hour	Minute	Second	Ingrowth time (Days)	Ingrowth factor	Decay correction
When sample last stripped	2019	2	26	16	57	0	11.03	0.86455	0.92494
When cell filled	2019	3	9	17	43	0			
Beginning time of count	2019	3	9	19	43	0			

Counts per minute	4.99
Gross CPM less Cell Blank (CPM)	4.42
CPM (decay during count corrected)	4.78
DPM Sample +System (efficiency corrected)	5.70
DPM sample	6.14
DPM/g	3.14
<b>Ra-226 DPM/g</b>	<b>1.05</b>
Ra-226 pCi/g	0.47

Error ± 1 sd    0.1325 DPM

**Error ± 1 sd    0.0226 DPM/g**

Error % =    2.2

Chemist	RF
PMT High Voltage +ve	770
HV Power supply	Spectrum Technologies
Alpha Counter	Spectrum Technologies
Region of Interest Ch.#s	28-1022
PMT	6655A - #1
Preamp	Canberra 2007P tube base
Amp Gain	1

**Radium Analysis by Rn-222 Emanation**

Core ID	1A
Sample ID	1A-2/2-12
Lucas Cell No.	3
Number of days since Rn board last run	1
Dry weight of sample counted (g)	1.415
Total count in period	4620
Total count in period (carryover corrected)	4593
Cell Blank count (CPM)	0.562
System Blank (DPM)	0.395
System Efficiency	0.839
Count duration (minutes)	1000

Typical carryover is about 1 - 2 % of the net counts (gross counts less system background) of the sample counted on the previous day. The carryover is subtracted from the gross counts of current sample. This correction is not required if the sample is run after a blank.

Carryover correction?	Yes	Mean of last 10 carryover measurements	1.02%
Gross counts of previous sample	3500	Mean of last 6 system background measurements	887
Counts carried over from previous sample	27		

	Year	Month	Day	Hour	Minute	Second	Ingrowth time (Days)	Ingrowth factor	Decay correction
When sample last stripped	2019	3	29	17	19	0	13.90	0.91950	0.92494
When cell filled	2019	4	12	15	0	0			
Beginning time of count	2019	4	12	17	0	0			

Counts per minute	4.59
Gross CPM less Cell Blank (CPM)	4.03
CPM (decay during count corrected)	4.36
DPM Sample +System (efficiency corrected)	5.19
DPM sample	5.22
DPM/g	3.69
<b>Ra-226 DPM/g</b>	<b>1.23</b>
Ra-226 pCi/g	0.55

Error ± 1 sd    0.1261 DPM

**Error ± 1 sd    0.0297 DPM/g**

Error % =    2.4

Chemist	XH
PMT High Voltage +ve	770
HV Power supply	Spectrum Technologies
Alpha Counter	Spectrum Technologies
Region of Interest Ch.#s	28-1022
PMT	6655A - #1
Preamp	Canberra 2007P tube base
Amp Gain	1

**Radium Analysis by Rn-222 Emanation**

Core ID	1A
Sample ID	1A-2/2-27
Lucas Cell No.	3
Number of days since Rn board last run	1
Dry weight of sample counted (g)	0.838
Total count in period	3296
Total count in period (carryover corrected)	3258
Cell Blank count (CPM)	0.562
System Blank (DPM)	0.395
System Efficiency	0.839
Count duration (minutes)	1000

Typical carryover is about 1 - 2 % of the net counts (gross counts less system background) of the sample counted on the previous day. The carryover is subtracted from the gross counts of current sample. This correction is not required if the sample is run after a blank.			
Carryover correction?	Yes	Mean of last 10 carryover measurements	1.02%
Gross counts of previous sample	4620	Mean of last 6 system background measurements	887
Counts carried over from previous sample	38		

	Year	Month	Day	Hour	Minute	Second	Ingrowth time (Days)	Ingrowth factor	Decay correction
When sample last stripped	2019	3	29	17	18	0	15.08	0.93496	0.92494
When cell filled	2019	4	13	19	13	0			
Beginning time of count	2019	4	13	21	13	0			

Counts per minute	3.26
Gross CPM less Cell Blank (CPM)	2.70
CPM (decay during count corrected)	2.91
DPM Sample +System (efficiency corrected)	3.47
DPM sample	3.29
DPM/g	3.93
<b>Ra-226 DPM/g</b>	<b>1.31</b>
Ra-226 pCi/g	0.59

Error ± 1 sd    0.1153 DPM

**Error ± 1 sd    0.0459 DPM/g**

Error % =    3.5

Chemist	RF
PMT High Voltage +ve	770
HV Power supply	Spectrum Technologies
Alpha Counter	Spectrum Technologies
Region of Interest Ch.#s	28-1022
PMT	6655A - #1
Preamp	Canberra 2007P tube base
Amp Gain	1

# Results of Cs-137 Analysis

Flett Research Ltd.

440 DeSalaberry Ave. Winnipeg, MB R2L 0Y7

Fax / Phone: (204) 667-2505

Email: flett@flettresearch.ca Webpage: http://www.flettresearch.ca

**Client: Lorrain, Stéphane**

**Address:** SNC-LAVALIN GEM QUÉBEC INC., 455, boul. René-Lévesque ouest, Montréal (Québec) H2Z 1Z3

**Core ID:** 1A

**Date Received:** 20-Feb-19

**Sampling Date:** 9-Feb-19

**Project:** #653502

**Transaction ID:** 882

**PO/Contract No.:** 653502-0028

**Analysis Dates:** April 4 - 24, 2019

**Analysts:** X. Hu; L. Hesketh-Jost

Salt Correction?	No
------------------	----

**Analytical Method:** N30120 Measurement of Gamma-Ray Emitting Radionuclides in Sediment/Soil Samples by Gamma Spectrometry Using HPGe Detectors (Version 2)

**Deviation from Method:**

**Comments:** <2SD: The measured Cs-137 activity is less than 2 counting errors (i.e. 2 SD), suggesting no significant presence of Cs-137 in this sample.

**Detection Limit:** The method detection limit (MDL) is 0.3 DPM/g for an 80,000 seconds counting period when measuring a 9 g of dry sample at a 95% confidence level. The method detection limit can be decreased to 0.1 DPM/g if 32 g of sample is used.

**Estimated Uncertainty:** The estimated uncertainty of this method has been determined to be: 10% at 95% confidence for samples with activities between 0.5 and 20 DPM/g, counting time 80,000 seconds and sample weights ranging from 9 to 32 grams. Method uncertainty can increase to 85% for samples with activities near detection limit (0.1 - 0.3 DPM/g).

Results authorized by Dr. Robert J. Flett, Chief Scientist

Sample ID	Upper Depth (cm)	Lower Depth (cm)	Day Sample Counted	Month Sample Counted	Year Sample Counted	Integral NET Cs-137 Peak	Counting Error 1 SD (Counts)	Count Time (seconds)	Dry Sample Weight (g)	Sample Thickness (mm)	CPM/g	Efficiency for Gammas Fractional	Gammas per min. per gram	Activity DPM/g (dry wt.) on Counting Date	Approx. Error DPM/g	Activity DPM/g (dry wt.) on Sampling Date	Approx. Error DPM/g	Activity pCi/g (dry wt.) on Sampling Date	Approx. Error pCi/g	Activity mBq/g (dry wt.) on Sampling Date	Approx. Error mBq/g	Detector Used	Comments Code for Cs-137 Analysis	
1A-2/2-1	0	1	19	4	2019	88	34	80000	2.275	1.30	0.0290	0.0455	0.6381	0.75	0.29	0.75	0.29	0.34	0.13	12.54	4.80	Canberra		
1A-2/2-12	11	12	4	4	2019	378	38	80000	6.216	2.00	0.0456	0.0294	1.5538	1.82	0.18	1.83	0.18	0.82	0.08	30.50	3.07	GMX		
1A-2/2-17	16	17	4	4	2019	610	45	80000	8.324	2.80	0.0550	0.0262	2.0974	2.46	0.18	2.47	0.18	1.11	0.08	41.17	3.04	GEM		
1A-2/2-22	21	22	5	4	2019	764	47	80000	9.070	2.80	0.0632	0.0262	2.4108	2.83	0.17	2.84	0.17	1.28	0.08	47.32	2.91	GEM		
1A-2/2-25	24	25	23	4	2019	1070	51	80000	11.552	3.65	0.0695	0.0256	2.7176	3.19	0.15	3.20	0.15	1.44	0.07	53.41	2.55	GEM		
1A-2/2-26	25	26	20	4	2019	668	43	80000	7.008	2.43	0.0715	0.0265	2.6983	3.17	0.20	3.18	0.20	1.43	0.09	53.02	3.41	GEM		
1A-2/2-27	26	27	9	4	2019	655	38	80000	7.034	2.40	0.0698	0.0265	2.6341	3.09	0.18	3.10	0.18	1.40	0.08	51.72	3.00	GEM		
1A-2/2-28	27	28	19	4	2019	154	35	80000	7.748	2.43	0.0149	0.0265	0.5627	0.66	0.15	0.66	0.15	0.30	0.07	11.05	2.51	GEM		
1A-2/2-29	28	29	19	4	2019	120	39	80000	6.192	2.05	0.0145	0.0293	0.4956	0.58	0.19	0.58	0.19	0.26	0.09	9.74	3.16	GMX		
1A-2/2-31	30	31	10	4	2019	-30	51	80000	6.822	2.30	-0.0033	0.0292	-0.1129	-0.13	0.23	-0.13	0.23	-0.06	0.10	-2.22	3.77	GMX	<2SD	
<b>Cs-137 Standards</b>																								
GMX 32g 10 mm			4	4	2019	19967	143	5000	32.00	10.0	7.4876	0.0237	315.7600	370.61	2.65	957.04								
GMX 24g 7.5mm			5	4	2019	16045	128	5000	24.00	7.5	8.0225	0.0254	315.7400	370.59	2.96	957.04								
GMX 15g 5mm			4	4	2019	10978	106	5000	15.00	5.0	8.7824	0.0278	315.7600	370.61	3.58	957.04								
GMX 9g 3mm			3	4	2019	6862	84	5000	9.00	3.0	9.1493	0.0290	315.7799	370.63	4.54	957.04								
GMX 2.85g 0.8mm			4	4	2019	2237	49	5000	2.854	0.8	9.4057	0.0298	315.7600	370.61	8.12	957.04								
GEM 32g 10 mm			4	4	2019	17960	139	5000	32.00	10.0	6.7350	0.0213	315.7600	370.61	2.87	957.04								
GEM 24g 7.5mm			4	4	2019	14367	124	5000	24.00	7.5	7.1835	0.0227	315.7600	370.61	3.20	957.04								
GEM 15g 5mm			3	4	2019	9822	102	5000	15.00	5.0	7.8576	0.0249	315.7799	370.63	3.85	957.04								
GEM 9g 3mm			4	4	2019	6102	79	5000	9.00	3.0	8.1360	0.0258	315.7600	370.61	4.80	957.04								
GEM 2.85g 0.8mm			4	4	2019	2093	48	5000	2.854	0.8	8.8003	0.0279	315.7600	370.61	8.50	957.04								
Canberra 32g 10 mm			11	4	2019	29236	172	5000	32.00	10.0	10.9635	0.0347	315.6205	370.45	2.19	957.04								
Canberra 24g 7.5mm			11	4	2019	23302	154	5000	24.00	7.5	11.6510	0.0369	315.6205	370.45	2.44	957.04								
Canberra 15g 5mm			10	4	2019	16207	128	5000	15.00	5.0	12.9656	0.0411	315.6404	370.47	2.93	957.04								
Canberra 9g 3mm			10	4	2019	10285	103	5000	9.00	3.0	13.7133	0.0434	315.6404	370.47	3.70	957.04								
Canberra 2.85g 0.8mm			10	4	2019	3449	60	5000	2.854	0.8	14.5018	0.0459	315.6404	370.47	6.45	957.04								

Q:\Clients A-L\Lorrain, Stephane\2019(882)\Radioisotopes\1A\Pb-210, Ra-226 and Cs-137 Lorrain Core 1A May 1-19 Final.xlsx

**Duplicate:** Two subsamples of the same sample were carried through the analytical procedure in an identical manner.

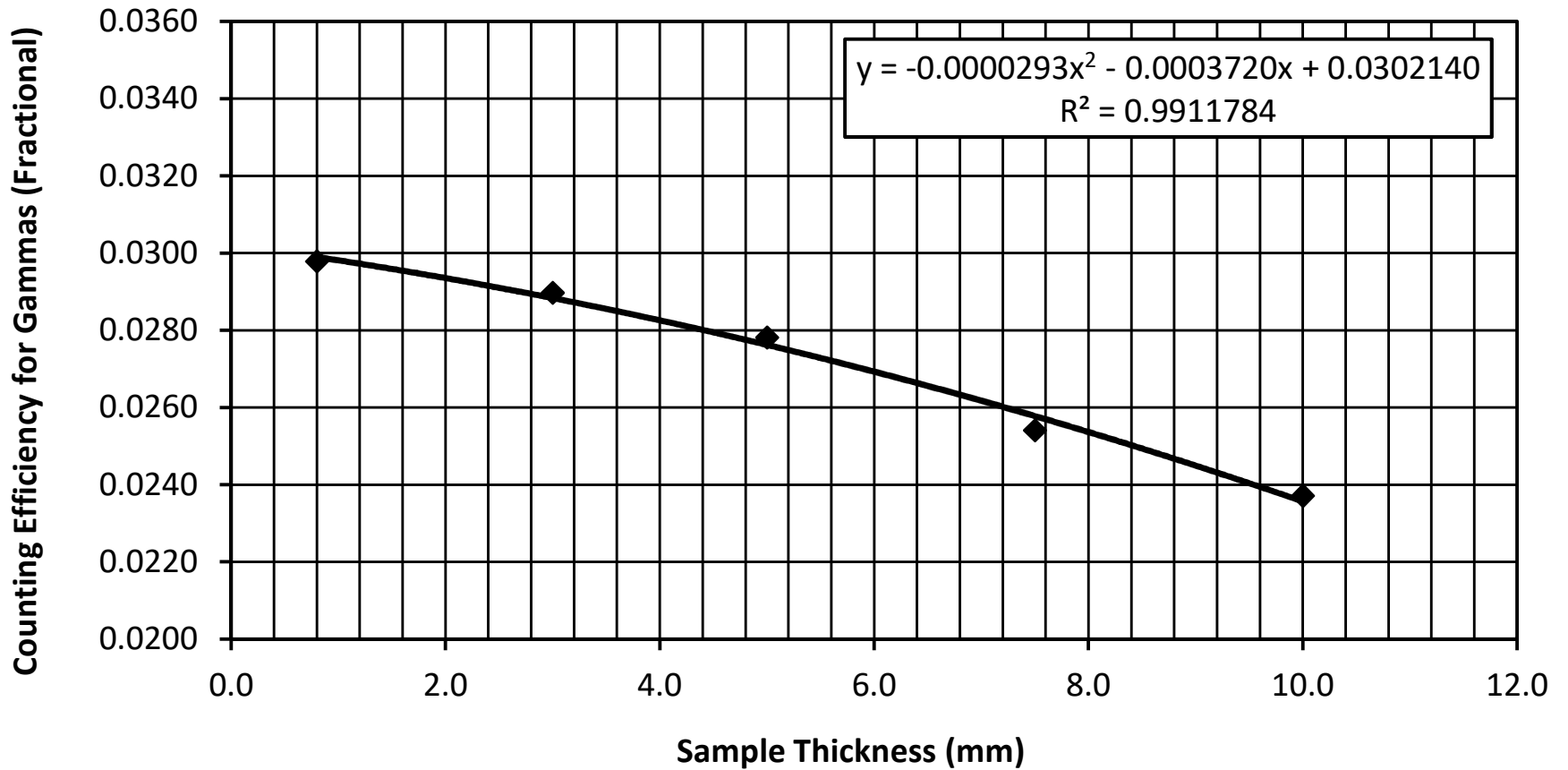
**Re-count:** The entire available dry sample material was used for making the sample pancake, and then this sample pancake was counted twice on a HPGe detector. Repeat counting was chosen over duplicate analysis due to insufficient sample material provided.

**This test report shall not be reproduced, except in full, without written approval of the laboratory.**

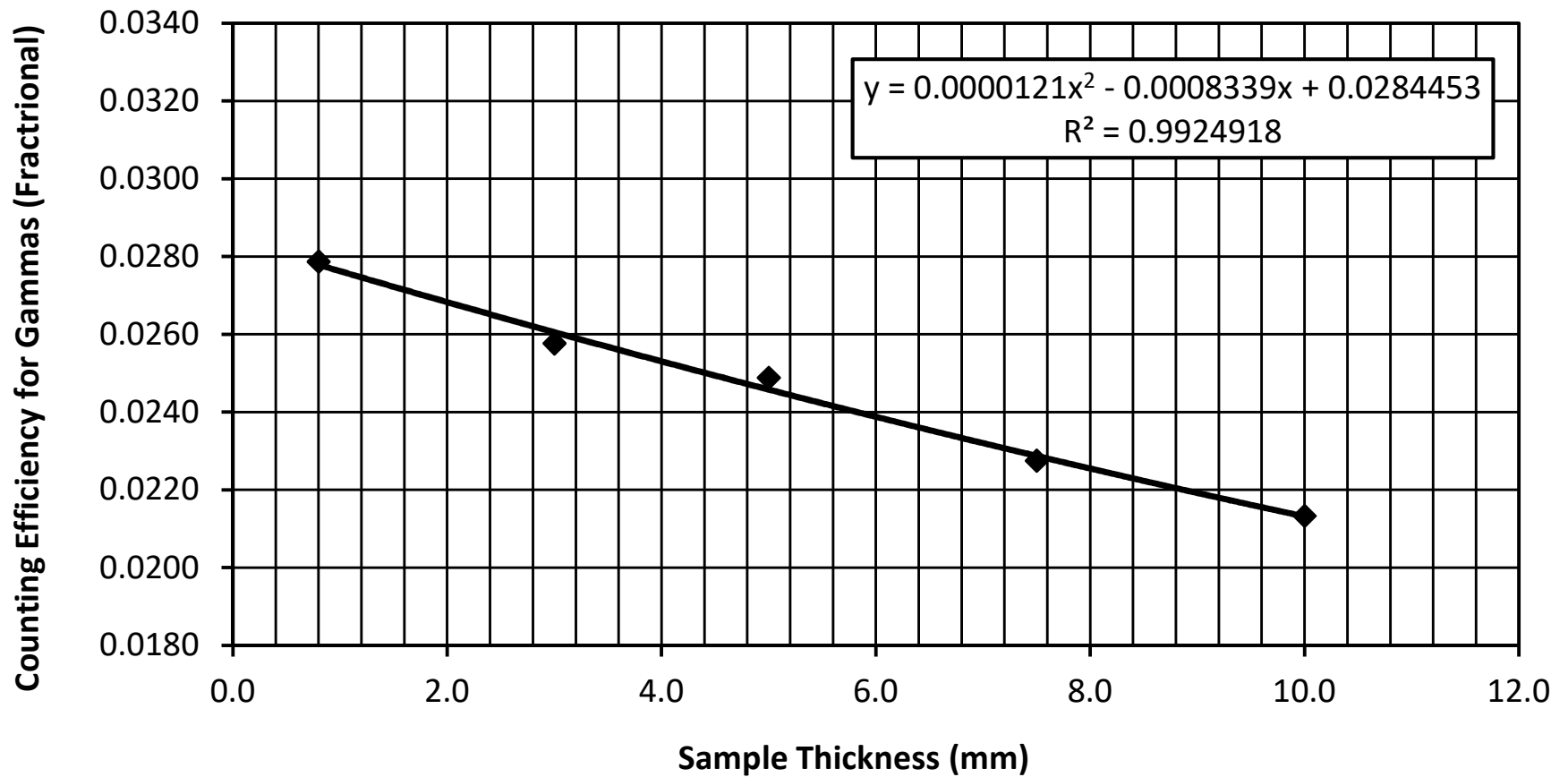
**Note:** Results relate only to the items tested.

ISO / IEC 17025:2005 Accredited with the Canadian Association for Laboratory Accreditation (CALA Accreditation No. A3306)

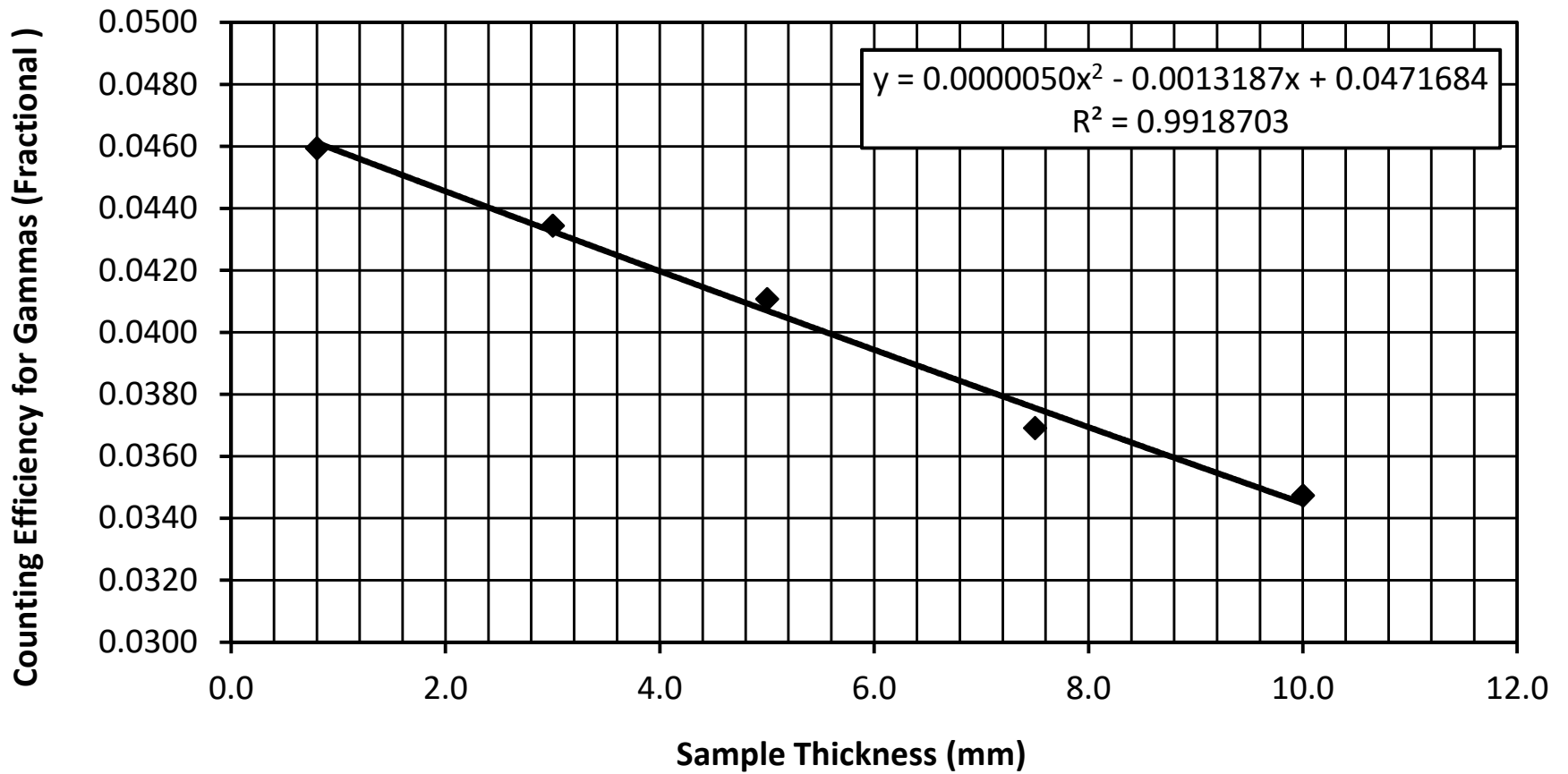
### Cs-137 Counting Efficiency of Gammas vs. Sample Thickness (mm) GMX 25% Detector (Apr 3-5, 2019)



### Cs-137 Counting Efficiency of Gammas vs. Sample Thickness (mm) GEM 19% Detector (Apr 3-4, 2019)



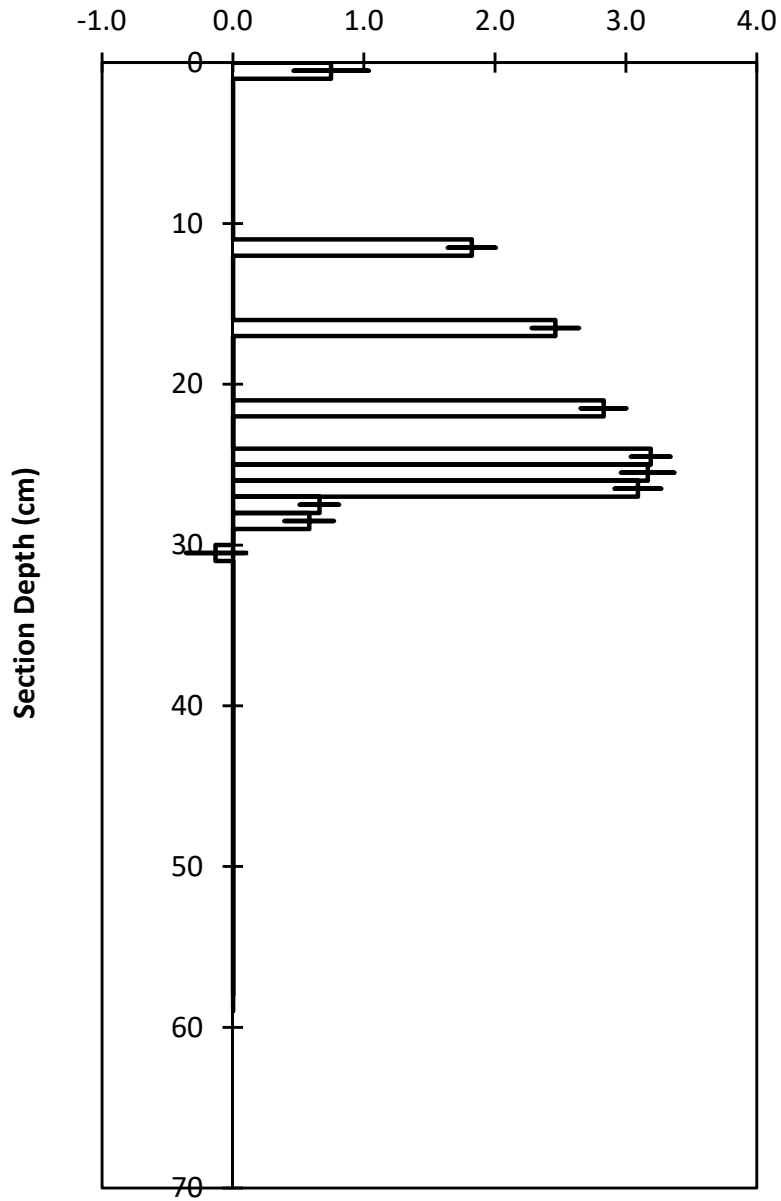
### Cs-137 Counting Efficiency of Gammas vs. Sample Thickness (mm) Canberra 29% Detector (Apr 10-11, 2019)



## Cs-137 in Sediments

### 1A

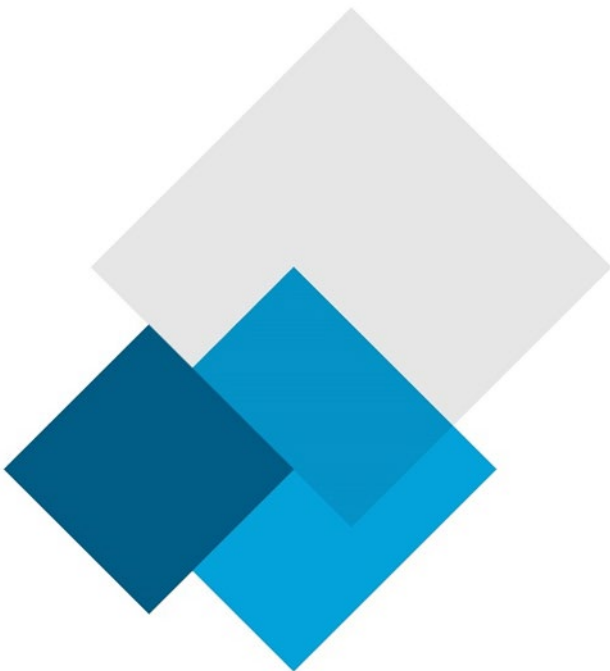
Cs-137 Activity on counting date (DPM/g dry wt.)



Note: The bar plotted at the midpoint depth of each section represents +/- 1 standard deviation of the Cs-137 counting error.

# Appendix 5

Radio Isotopic Analysis Core 2A



# Interpretation of Pb-210, Ra-226 and Cs-137 Results

## Flett Research Ltd.

440 DeSalaberry Ave. Winnipeg, MB R2L 0Y7

Fax/Phone: (204) 667-2505

Email: [flett@flettresearch.ca](mailto:flett@flettresearch.ca) Webpage: <http://www.flettresearch.ca>

---

## Client: Lorrain, Stéphane

**Address:** SNC-LAVALIN GEM QUÉBEC INC., 455, boul. René-Lévesque ouest, Montréal (Québec) H2Z 1Z3

**Core ID:** 2A

**Transaction ID:** 882

**PO/Contract No.:** 653502-0028

**Date Received:** 20-Feb-19

**Analysis Dates:** February 25 - April 29, 2019

**Analysts:** L. Hesketh-Jost, X. Hu

**Sampling Date:** 9-Feb-19

**Project:** #653502

*Results authorized by Dr. Robert J. Flett, Chief Scientist*

---

## INTERPRETATION

### Observations:

The Pb-210 profile exhibits an irregular but approximately exponential decrease in total Pb-210 activity as a function of depth. The maximum activity of 11.99 DPM/g observed in section 0 - 1 cm is about 8 times the lowest activity of 1.57 DPM/g observed in section 26 - 27 cm (Pages 2 & 3).

The dry bulk densities generally increase from the surface to section 11 (depth 10 - 11 cm), increasing from 0.019 g/cm<sup>3</sup> to 0.317 g/cm<sup>3</sup>. The dry bulk densities then decrease beginning in section 12 (extrapolated depth 11 - 13 cm) from 0.218 g/cm<sup>3</sup> to 0.207 g/cm<sup>3</sup> at section 15 (extrapolated depth 13 - 16 cm). From section 18 (extrapolated depth 16 - 20 cm) the dry bulk densities then generally increase with depth, ranging between 0.233 g/cm<sup>3</sup> and 0.431 g/cm<sup>3</sup> (Page 2 & 4).

Ra-226 was measured at 1.34, 1.22 and 1.48 DPM/g in sections 7 - 8 cm, 17 - 18 cm and 37 - 38 cm, respectively (Pages 8 - 11). The Pb-210 activity in the 22 - 23 cm section barely exceeds the Ra-226 activity measured in the 37 - 38 cm section, indicating that the background level of Pb-210 may have been achieved in this core.

Cs-137 was measured in core interval of 0 - 14 cm. The Cs-137 activities in this core interval are significantly above background in the upper 11 cm, ranging between 2.25 - 3.63 DPM/g. The shape of Cs-137 profile in the 0 - 11 cm core interval suggests that the majority of the Cs-137 is probably from external erosion sources (soils or sediments contaminated with bomb testing radionuclides). The Cs-137 activity then declines gradually with depth below 11 cm (Pages 12 & 16). The tailing of Cs-137 into deeper depths with Pb-210 dates prior to 1954 is commonly seen and is attributed to downward diffusion of the isotope.

### Regression model of Unsupported Pb-210 activity vs. Cumulative Dry Weight (g/cm<sup>2</sup>):

When applying the linear regression model, it is assumed that the input of Pb-210 and the sediment accumulation rate are constant. Due to the sudden decrease in total Pb-210 activity at section 10 - 11 cm and the rapid decrease in dry bulk density occurring in the 11 - 12 cm and 14 - 15 cm sections, it is concluded that these assumptions are not satisfied, and therefore the model cannot be applied to the core.

**CRS model of Age at bottom of Extrapolated section in years vs. Depth of bottom edge of current section in cm:**

The CRS model assumes constant input of Pb-210 and a core that is long enough to include all of the measurable atmospheric source Pb-210. If one assumes that the activity in section 23 (1.61 DPM/g) is at the background Pb-210 level, then the model can be applied.

The measured total activity results (DPM/g) are shown in column AF of the main data table on Page 2. The estimated age at the bottom of each section is shown in column AI, also shown on Page 2. The average sediment accumulation rate, from core surface to the extrapolated bottom depth of any section, can be calculated by dividing the cumulative dry mass at the bottom of the extrapolated section by the calculated age at that depth. For example, the average sediment accumulation rate, from the core surface to the bottom of section 10 (depth 10 cm) can be calculated as:  $1.459 / 41.4 = 0.0352 \text{ g/cm}^2/\text{yr}$ . The individual sedimentation rate for each section is shown in column AL on Page 2. Plots of age vs. depth, sediment accumulation rate vs. depth and sediment accumulation rate vs. age are seen in Pages 5, 6 and 7, respectively.

**Conclusion:**

In this core, the sediment accumulation rates are variable, ranging between  $0.0198 \text{ g/cm}^2/\text{yr}$  and  $0.0448 \text{ g/cm}^2/\text{yr}$ , with a large transient increase at section 11 (depth 10 - 11 cm) to  $0.0832 \text{ g/cm}^2/\text{yr}$  (by the CRS model) (Pages 2, 6 & 7).

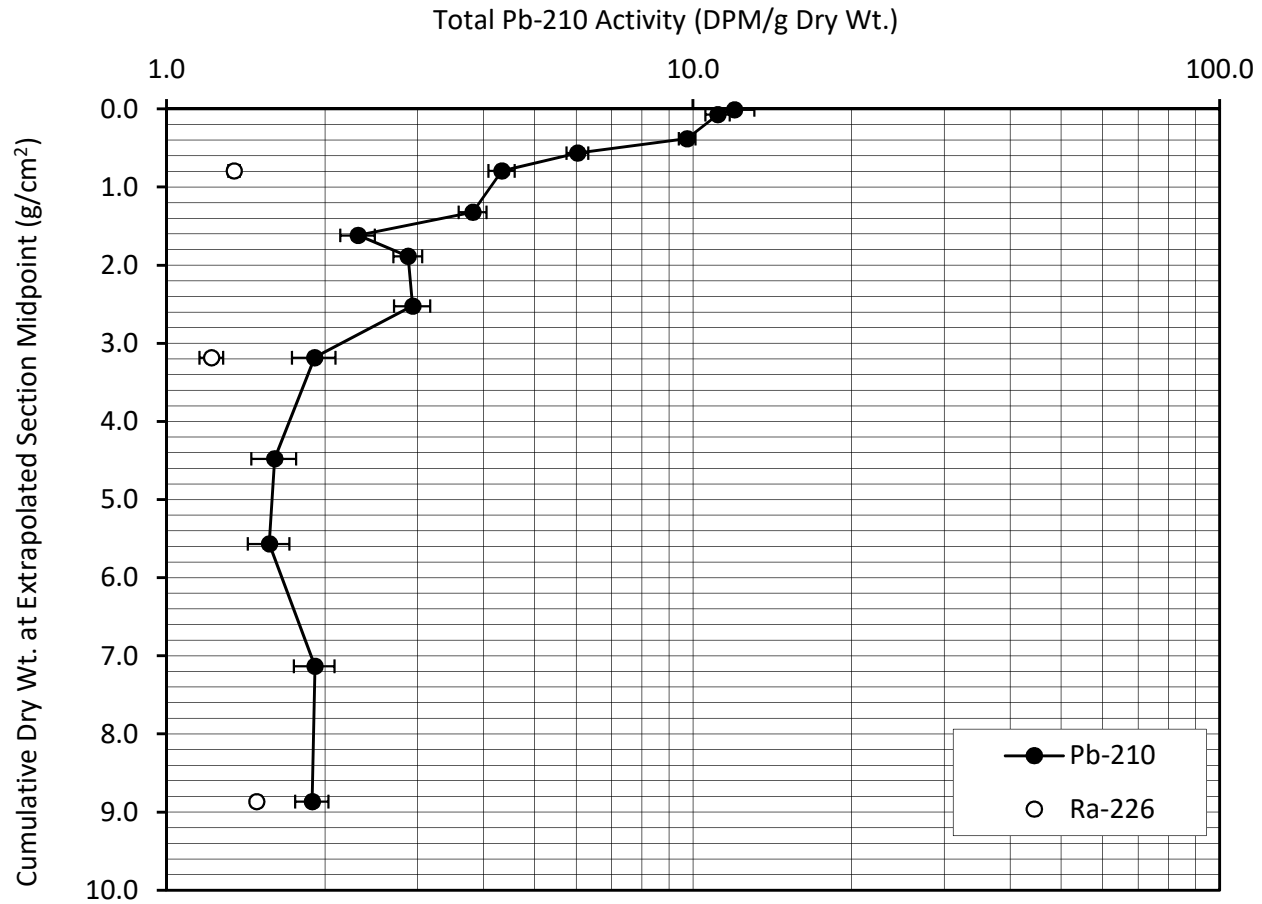
The elevated Cs-137 activities in the core interval of 0 - 12 cm suggests that the majority of the Cs-137 is probably from external erosion sources (soils or sediments contaminated with bomb testing radionuclides) rather than direct deposition from the atmosphere. It is assumed that the 10 - 11 cm section represents the attaining of maximum Cs-137 terrestrial inventory which occurred in 1966, 53 years before the core was obtained. To have confidence that the Pb-210 models are functioning correctly, we typically hope to see the age predicted for the Cs-137 maximum be within 5 years of its known 1966 deposition. In this core, the CRS model indicates an age of 45.3 yr at 11 cm depth. This age is about 7 years different from what we would expect when it is assumed that Cs-137 maximum inventory has been recorded at 10 -11 cm. Despite this difference and the uncertainty associated with the unknown sedimentary processes occurring in the 10 - 15 cm core interval, the CRS results are considered compatible with the Cs-137 results, and therefore, it is concluded that the CRS model is providing reasonable estimates of age in this core.

Overall, the analytical quality of radioisotope data (based upon the recovery of spike, the recovery of CRM, the results of repeat analyses and blanks) is considered good. It is cautioned that predicted ages greater than 80 years in this core are gross approximations only.



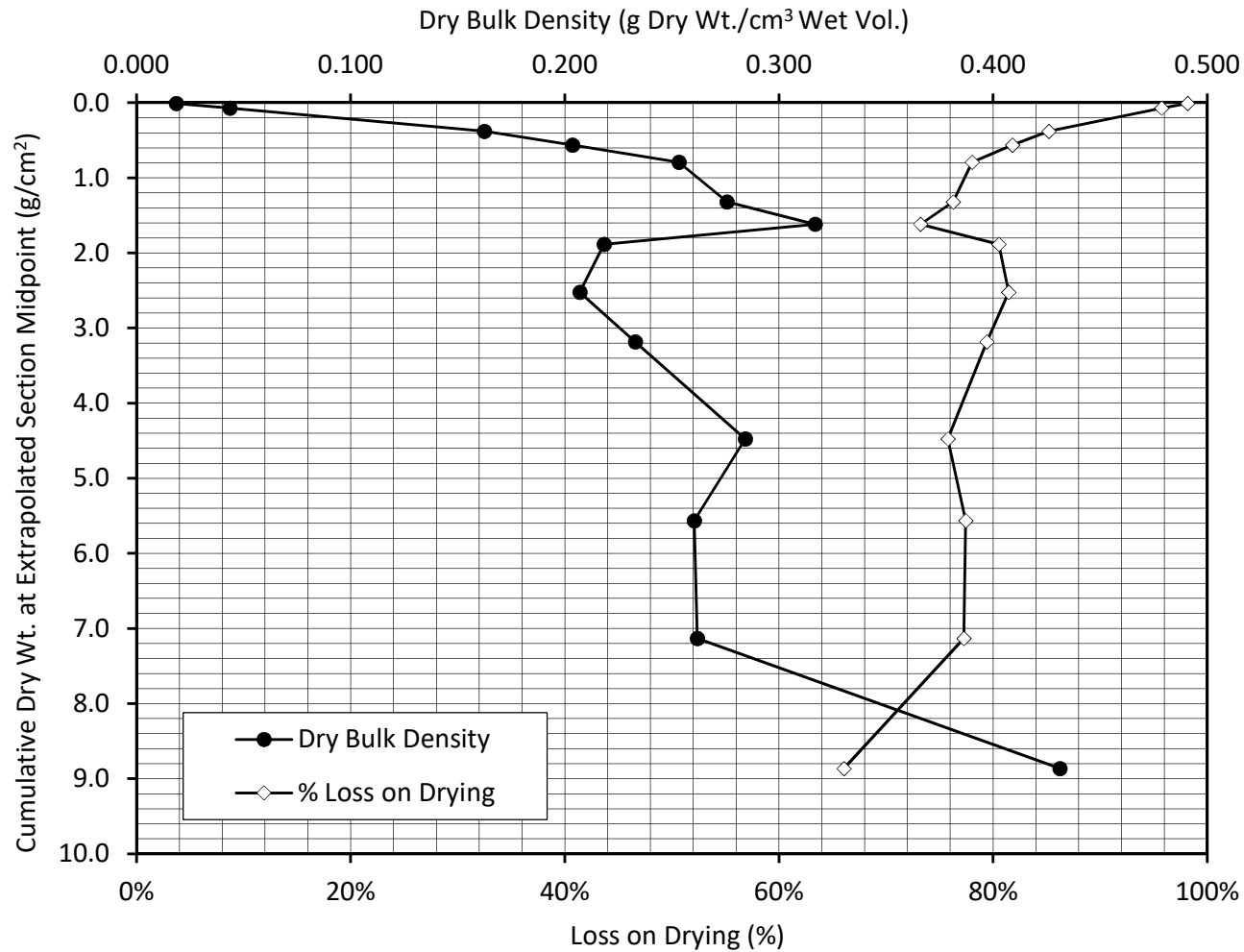
**Total Pb-210 Activity vs. Accumulated Sediment**

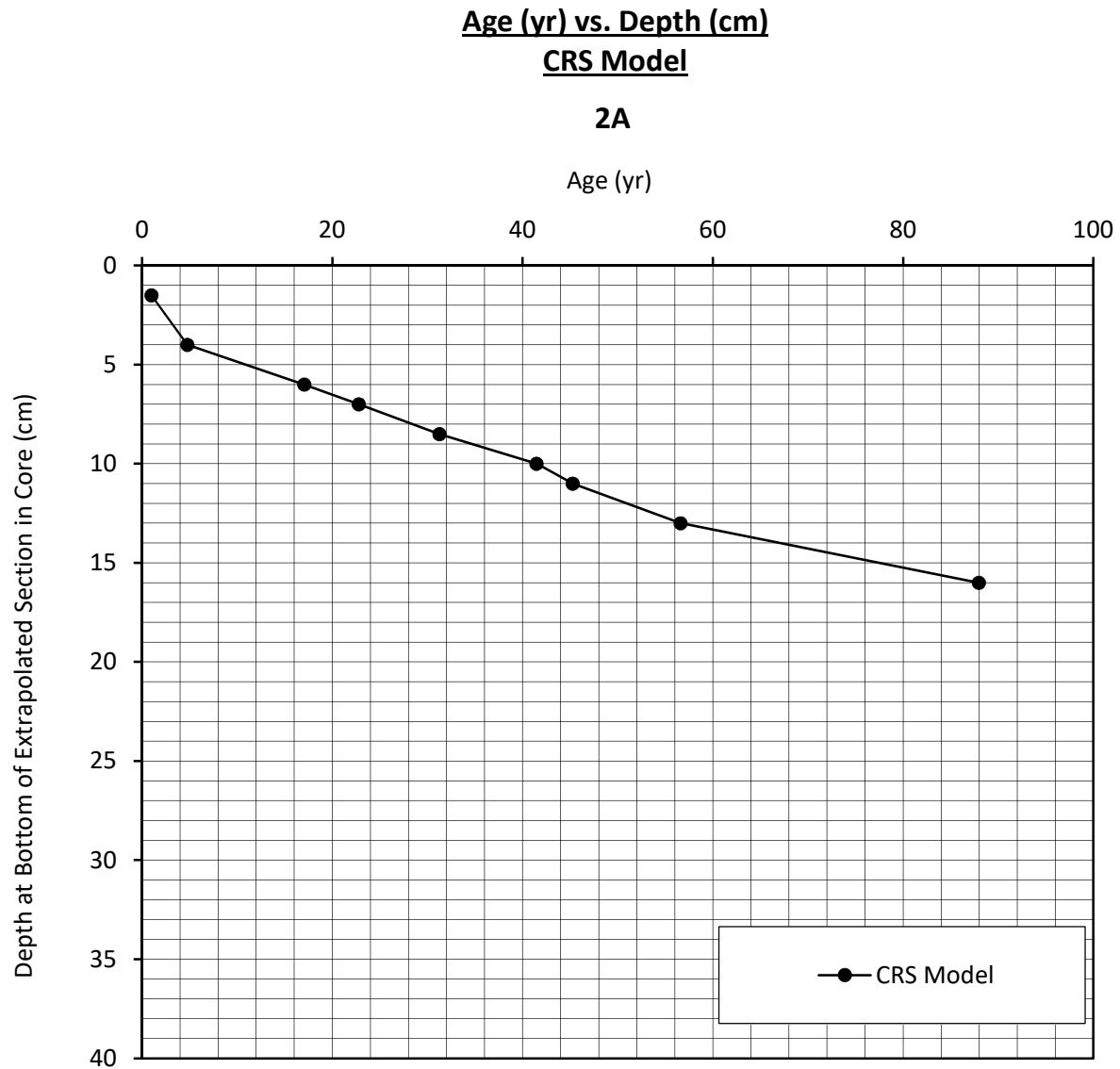
**2A**



**Dry Bulk Density and % Loss on Drying**  
**vs. Accumulated Sediment**

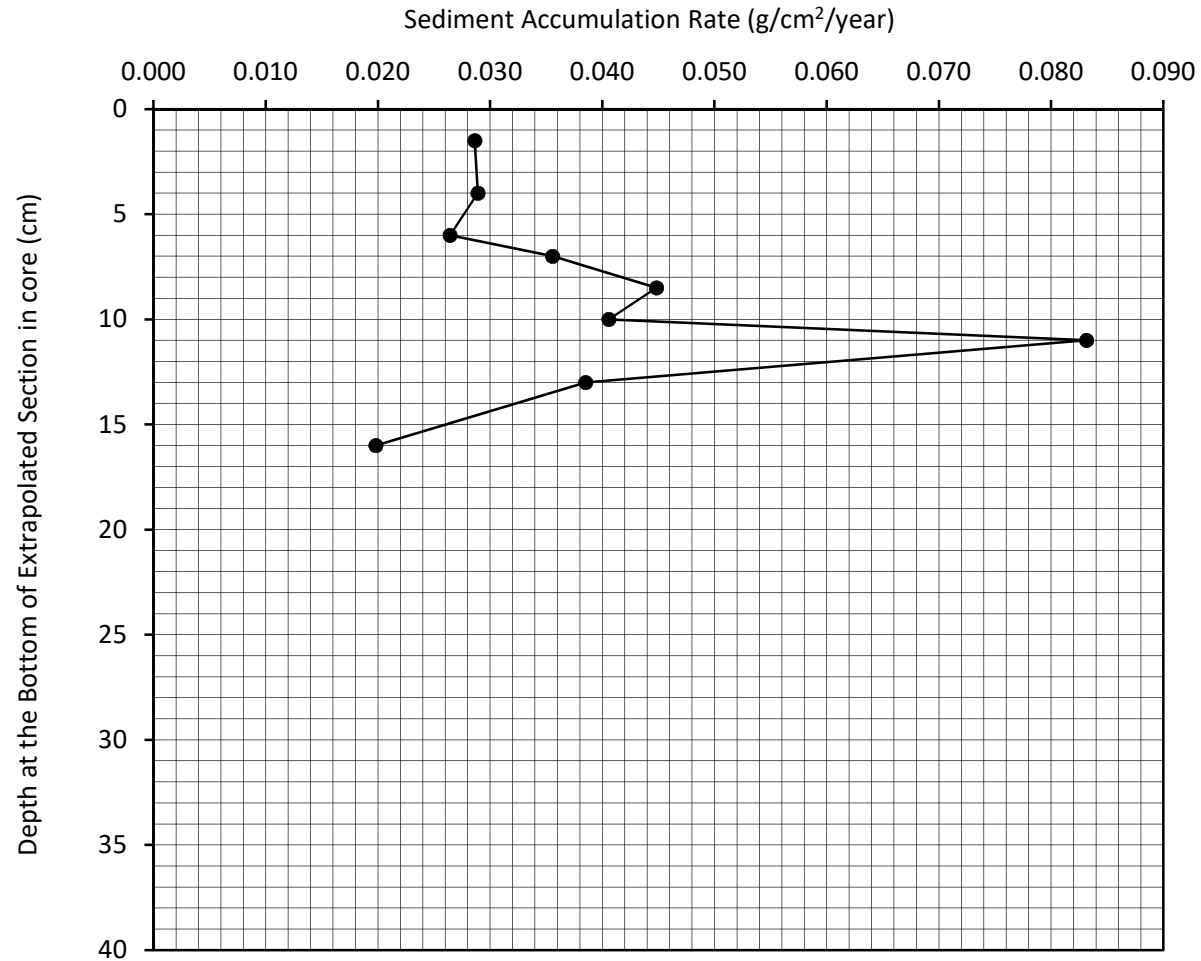
**2A**



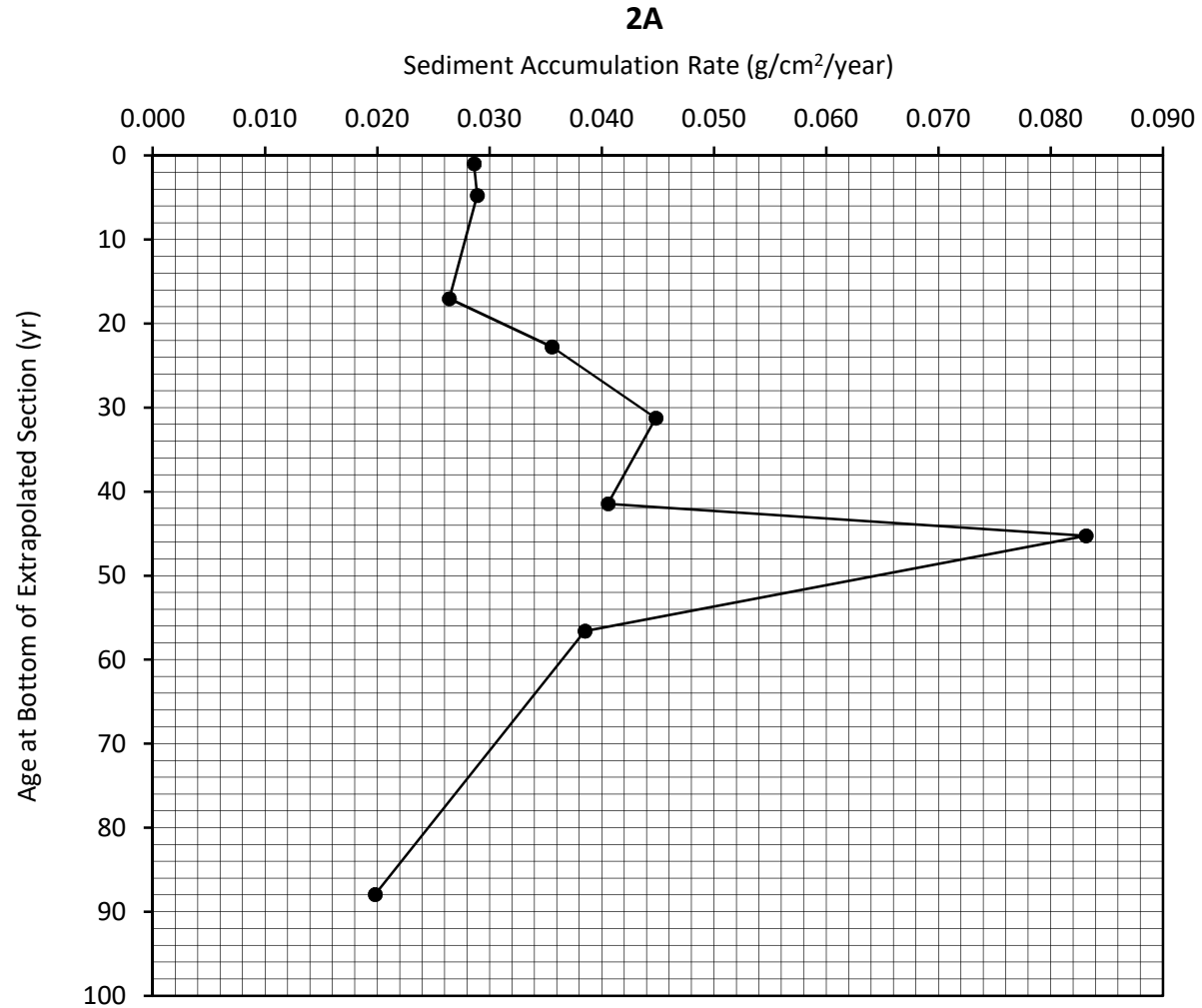


**CRS Sediment Accumulation Rate (g/cm<sup>2</sup>/year)**  
**vs. Depth at the Bottom of Extrapolated Section in Core (cm)**

**2A**



**CRS Sediment Accumulation Rate (g/cm<sup>2</sup>/year)**  
**vs. Age at Bottom of Extrapolated Section (yr)**



# Results of Ra-226 Analysis by Rn-222 Emanation

Flett Research Ltd.

440 DeSalaberry Ave., Winnipeg, MB R2L 0Y7

Fax/Phone: (204) 667-2505

Email: flett@flettresearch.ca Webpage: http://www.flettresearch.ca

## Client: Lorrain, Stéphane

Address: SNC-LAVALIN GEM QUÉBEC INC., 455, boul. René-Lévesque ouest, Montréal (Québec) H2Z 1Z3

Core ID: 2A

Transaction ID: 882

Date Received: 20-Feb-19

PO/Contract No.: 653502-0028

Sampling Date: 9-Feb-19

Analysis Dates: February 25 - April 18, 2019

Project: #653502

Analysts: X. Hu; L. Hesketh-Jost

Salt Correction Applied? No

Analytical Method: N40110 Determination of Radium-226 in Sediment, Soil and Peat by Radon-222 Emanation (Version 3)

### Comments:

**Detection Limit:** The method detection limit (MDL) is dependent on the amount of sample analyzed. For a 60,000 second counting time the MDL at 95% confidence for 2 g of dry sample is 0.1 DPM/g and for 0.5 g of dry sample is 0.5 DPM/g.

**Estimated Uncertainty:** The estimate of uncertainty of measurement for this method in this laboratory is approximately ±12% at 95% confidence level (approximately 40,000 counts in 60,000 seconds).

Results authorized by Dr. Robert J. Flett, Chief Scientist

Core ID	Sample ID	Ra-226 Activity (DPM/g Dry Wt.)	Combined Error: 1 SD (DPM/g Dry Wt.)	Comments Code for Ra-226 Analysis
2A	2A-2/2-38	1.48	0.02	
2A	2A-2/2-8	1.34	0.03	
2A	2A-2/2-18	1.22	0.06	

Q:\Clients A-L\Lorrain, Stephane\2019(882)\Radioisotopes\2A\Pb-210, Ra-226 and Cs-137 Lorrain Core 2A May 2-19 Final.xlsm

**Duplicate:** Two subsamples of the same sample were carried through the analytical procedure in an identical manner.

**Re-count:** The sample bottle was re-sealed after the initial analysis, and was re-counted after 11 or more days of Rn-222 ingrowth. Repeat counting was chosen over duplicate analysis due to insufficient sample material provided.

This test report shall not be reproduced, except in full, without written approval of the laboratory.

Note: Results relate only to the items tested.

18-Apr-19

Page 8 of 16

ISO / IEC 17025:2005 Accredited with the Canadian Association for Laboratory Accreditation (CALA Accreditation No. A3306)

**Radium Analysis by Rn-222 Emanation**

Core ID	2A
Sample ID	2A-2/2-38
Lucas Cell No.	3
Number of days since Rn board last run	1
Dry weight of sample counted (g)	2.019
Total count in period	7092
Total count in period (carryover corrected)	7050
Cell Blank count (CPM)	0.562
System Blank (DPM)	0.395
System Efficiency	0.839
Count duration (minutes)	1000

Typical carryover is about 1 - 2 % of the net counts (gross counts less system background) of the sample counted on the previous day. The carryover is subtracted from the gross counts of current sample. This correction is not required if the sample is run after a blank.			
Carryover correction?	Yes	Mean of last 10 carryover measurements	1.02%
Gross counts of previous sample	4986	Mean of last 6 system background measurements	887
Counts carried over from previous sample	42		

	Year	Month	Day	Hour	Minute	Second	Ingrowth time (Days)	Ingrowth factor	Decay correction
When sample last stripped	2019	2	26	16	56	0	12.01	0.88659	0.92490
When cell filled	2019	3	10	17	13	25			
Beginning time of count	2019	3	10	19	13	48			

Counts per minute	7.05
Gross CPM less Cell Blank (CPM)	6.49
CPM (decay during count corrected)	7.02
DPM Sample +System (efficiency corrected)	8.36
DPM sample	8.99
DPM/g	4.45
<b>Ra-226 DPM/g</b>	<b>1.48</b>
Ra-226 pCi/g	0.67

Error ± 1 sd    0.1462 DPM

**Error ± 1 sd    0.0241 DPM/g**

Error % =    1.6

Chemist	RF
PMT High Voltage +ve	770
HV Power supply	Spectrum Technologies
Alpha Counter	Spectrum Technologies
Region of Interest Ch.#s	28-1022
PMT	6655A - #1
Preamp	Canberra 2007P tube base
Amp Gain	1

**Radium Analysis by Rn-222 Emanation**

Core ID	2A
Sample ID	2A-2/2-8
Lucas Cell No.	3
Number of days since Rn board last run	1
Dry weight of sample counted (g)	1.211
Total count in period	4549
Total count in period (carryover corrected)	4510
Cell Blank count (CPM)	0.562
System Blank (DPM)	0.395
System Efficiency	0.839
Count duration (minutes)	1000

Typical carryover is about 1 - 2 % of the net counts (gross counts less system background) of the sample counted on the previous day. The carryover is subtracted from the gross counts of current sample. This correction is not required if the sample is run after a blank.

Carryover correction?	Yes	Mean of last 10 carryover measurements	1.02%
Gross counts of previous sample	4718	Mean of last 6 system background measurements	887
Counts carried over from previous sample	39		

	Year	Month	Day	Hour	Minute	Second	Ingrowth time (Days)	Ingrowth factor	Decay correction
When sample last stripped	2019	3	29	17	18	0	17.90	0.96101	0.92490
When cell filled	2019	4	16	14	59	0			
Beginning time of count	2019	4	16	16	59	23			

Counts per minute	4.51
Gross CPM less Cell Blank (CPM)	3.95
CPM (decay during count corrected)	4.27
DPM Sample +System (efficiency corrected)	5.09
DPM sample	4.88
DPM/g	4.03
<b>Ra-226 DPM/g</b>	<b>1.34</b>
Ra-226 pCi/g	0.61

Error ± 1 sd    0.1235 DPM

**Error ± 1 sd    0.0340 DPM/g**

Error % =    2.5

Chemist	XH
PMT High Voltage +ve	770
HV Power supply	Spectrum Technologies
Alpha Counter	Spectrum Technologies
Region of Interest Ch.#s	28-1022
PMT	6655A - #1
Preamp	Canberra 2007P tube base
Amp Gain	1

**Radium Analysis by Rn-222 Emanation**

Core ID	2A
Sample ID	2A-2/2-18
Lucas Cell No.	3
Number of days since Rn board last run	1
Dry weight of sample counted (g)	0.571
Total count in period	2471
Total count in period (carryover corrected)	2434
Cell Blank count (CPM)	0.562
System Blank (DPM)	0.395
System Efficiency	0.839
Count duration (minutes)	1000

Typical carryover is about 1 - 2 % of the net counts (gross counts less system background) of the sample counted on the previous day. The carryover is subtracted from the gross counts of current sample. This correction is not required if the sample is run after a blank.			
Carryover correction?	Yes	Mean of last 10 carryover measurements	1.02%
Gross counts of previous sample	4549	Mean of last 6 system background measurements	887
Counts carried over from previous sample	37		

	Year	Month	Day	Hour	Minute	Second	Ingrowth time (Days)	Ingrowth factor	Decay correction
When sample last stripped	2019	3	29	17	17	0	18.83	0.96706	0.92490
When cell filled	2019	4	17	13	18	42			
Beginning time of count	2019	4	17	15	19	5			

Counts per minute	2.43
Gross CPM less Cell Blank (CPM)	1.87
CPM (decay during count corrected)	2.02
DPM Sample +System (efficiency corrected)	2.41
DPM sample	2.09
DPM/g	3.65
<b>Ra-226 DPM/g</b>	<b>1.22</b>
Ra-226 pCi/g	0.55

Error ± 1 sd    0.1084 DPM

**Error ± 1 sd    0.0633 DPM/g**

Error % =    5.2

Chemist	XH
PMT High Voltage +ve	770
HV Power supply	Spectrum Technologies
Alpha Counter	Spectrum Technologies
Region of Interest Ch.#s	28-1022
PMT	6655A - #1
Preamp	Canberra 2007P tube base
Amp Gain	1

# Results of Cs-137 Analysis

Flett Research Ltd.

440 DeSalaberry Ave. Winnipeg, MB R2L 0Y7

Fax / Phone: (204) 667-2505

Email: flett@flettresearch.ca Webpage: http://www.flettresearch.ca

**Client: Lorrain, Stéphane**

**Address:** SNC-LAVALIN GEM QUÉBEC INC., 455, boul. René-Lévesque ouest, Montréal (Québec) H2Z 1Z3

**Core ID:** 2A  
**Date Received:** 20-Feb-19  
**Sampling Date:** 9-Feb-19  
**Project:** #653502

**Transaction ID:** 882  
**PO/Contract No.:** 653502-0028  
**Analysis Dates:** Apr 5 - 29, 2019  
**Analysts:** X. Hu; L. Hesketh-Jost

Salt Correction?	No
------------------	----

**Analytical Method:** N30120 Measurement of Gamma-Ray Emitting Radionuclides in Sediment/Soil Samples by Gamma Spectrometry Using HPGe Detectors (Version 2)

**Deviation from Method:**

**Comments:**

**Detection Limit:** The method detection limit (MDL) is 0.3 DPM/g for an 80,000 seconds counting period when measuring a 9 g of dry sample at a 95% confidence level. The method detection limit can be decreased to 0.1 DPM/g if 32 g of sample is used.

**Estimated Uncertainty:** The estimated uncertainty of this method has been determined to be ± 10% at 95% confidence for samples with activities between 0.5 and 20 DPM/g, counting time 80,000 seconds and sample weights ranging from 9 to 32 grams. Method uncertainty can increase to 85% for samples with activities near detection limit (0.1 - 0.3 DPM/g).

Results authorized by Dr. Robert J. Flett, Chief Scientist

Sample ID	Upper Depth (cm)	Lower Depth (cm)	Day Sample Counted	Month Sample Counted	Year Sample Counted	Integral NET Cs-137 Peak	Counting Error 1 SD (Counts)	Count Time (seconds)	Dry Sample Weight (g)	Sample Thickness (mm)	CPM/g	Efficiency for Gammas Fractional	Gammas per min. per gram	Activity DPM/g (dry wt.) on Counting Date	Approx. Error DPM/g	Activity DPM/g (dry wt.) on Sampling Date	Approx. Error DPM/g	Activity pCi/g (dry wt.) on Sampling Date	Approx. Error pCi/g	Activity mBq/g (dry wt.) on Sampling Date	Approx. Error mBq/g	Detector Used	Comments Code for Cs-137 Analysis
2A-2/2-1	0	1	26	4	2019	98	41	80000	0.795	0.80	0.0925	0.0299	3.0923	3.63	1.52	3.65	1.53	1.64	0.69	60.78	25.43	GMX	
2A-2/2-6	5	6	12	4	2019	351	37	80000	3.031	1.45	0.0869	0.0453	1.9187	2.25	0.23	2.26	0.24	1.02	0.11	37.68	3.92	Canberra	
2A-2/2-8	7	8	5	4	2019	351	46	80000	4.618	1.45	0.0570	0.0296	1.9250	2.26	0.30	2.27	0.30	1.02	0.13	37.79	4.95	GMX	
2A-2/2-9	8	9	20	4	2019	648	46	80000	8.159	2.55	0.0596	0.0291	2.0487	2.40	0.17	2.42	0.17	1.09	0.08	40.25	2.86	GMX	
2A-2/2-10	9	10	10	4	2019	604	41	80000	6.792	2.35	0.0667	0.0266	2.5119	2.95	0.20	2.96	0.20	1.33	0.09	49.32	3.35	GEM	
2A-2/2-11	10	11	20	4	2019	613	42	80000	4.499	1.55	0.1022	0.0451	2.2640	2.66	0.18	2.67	0.18	1.20	0.08	44.48	3.02	Canberra	
2A-2/2-12	11	12	7	4	2019	143	44	80000	3.986	1.55	0.0269	0.0296	0.9100	1.07	0.33	1.07	0.33	0.48	0.15	17.87	5.50	GMX	
2A-2/2-13	12	13												0.34	0.10	0.34	0.10	0.16	0.05	5.75	1.67	Canberra	
2A-2/2-14	13	14	28	4	2019	115	31	80000	6.821	2.03	0.0126	0.0445	0.2840	0.33	0.09	0.34	0.09	0.15	0.04	5.58	1.52	Canberra	
<b>Re-count</b>																							
2A-2/2-13	12	13	21	4	2019	115	34	80000	6.926	2.68	0.0125	0.0437	0.2851	0.33	0.10	0.34	0.10	0.15	0.04	5.60	1.66	Canberra	
2A-2/2-13 Re-count	12	13	22	4	2019	121	35	80000	6.926	2.68	0.0131	0.0437	0.3000	0.35	0.10	0.35	0.10	0.16	0.05	5.90	1.69	Canberra	
<b>Cs-137 Standards</b>																							
GMX 32g 10 mm			4	4	2019	19967	143	5000	32.00	10.0	7.4876	0.0237	315.7600	370.61	2.65	957.04							
GMX 24g 7.5mm			5	4	2019	16045	128	5000	24.00	7.5	8.0225	0.0254	315.7400	370.59	2.96	957.04							
GMX 15g 5mm			4	4	2019	10978	106	5000	15.00	5.0	8.7824	0.0278	315.7600	370.61	3.58	957.04							
GMX 9g 3mm			3	4	2019	6862	84	5000	9.00	3.0	9.1493	0.0290	315.7799	370.63	4.54	957.04							
GMX 2.85g 0.8mm			4	4	2019	2237	49	5000	2.854	0.8	9.4057	0.0298	315.7600	370.61	8.12	957.04							
GEM 32g 10 mm			4	4	2019	17960	139	5000	32.00	10.0	6.7350	0.0213	315.7600	370.61	2.87	957.04							
GEM 24g 7.5mm			4	4	2019	14367	124	5000	24.00	7.5	7.1835	0.0227	315.7600	370.61	3.20	957.04							
GEM 15g 5mm			3	4	2019	9822	102	5000	15.00	5.0	7.8576	0.0249	315.7799	370.63	3.85	957.04							
GEM 9g 3mm			4	4	2019	6102	79	5000	9.00	3.0	8.1360	0.0258	315.7600	370.61	4.80	957.04							
GEM 2.85g 0.8mm			4	4	2019	2093	48	5000	2.854	0.8	8.8003	0.0279	315.7600	370.61	8.50	957.04							
Canberra 32g 10 mm			11	4	2019	29236	172	5000	32.00	10.0	10.9635	0.0347	315.6205	370.45	2.19	957.04							
Canberra 24g 7.5mm			11	4	2019	23302	154	5000	24.00	7.5	11.6510	0.0369	315.6205	370.45	2.44	957.04							
Canberra 15g 5mm			10	4	2019	16207	128	5000	15.00	5.0	12.9656	0.0411	315.6404	370.47	2.93	957.04							
Canberra 9g 3mm			10	4	2019	10285	103	5000	9.00	3.0	13.7133	0.0434	315.6404	370.47	3.70	957.04							
Canberra 2.85g 0.8mm			10	4	2019	3449	60	5000	2.854	0.8	14.5018	0.0459	315.6404	370.47	6.45	957.04							

Duplicate: Two subsamples of the same sample were carried through the analytical procedure in an identical manner.

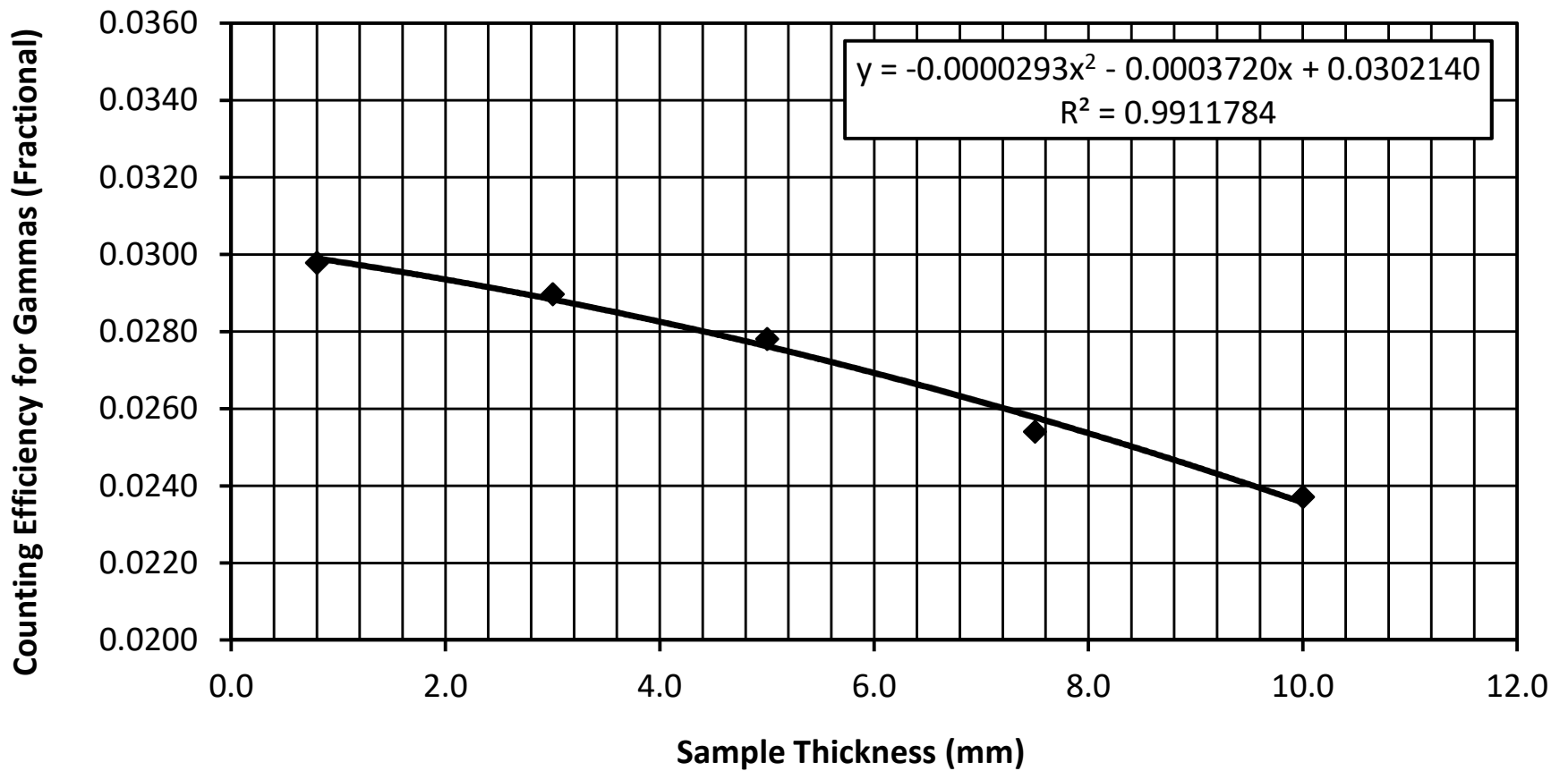
Re-count: The entire available dry sample material was used for making the sample pancake, and then this sample pancake was counted twice on a HPGe detector. Repeat counting was chosen over duplicate analysis due to insufficient sample material provided.

**This test report shall not be reproduced, except in full, without written approval of the laboratory.**

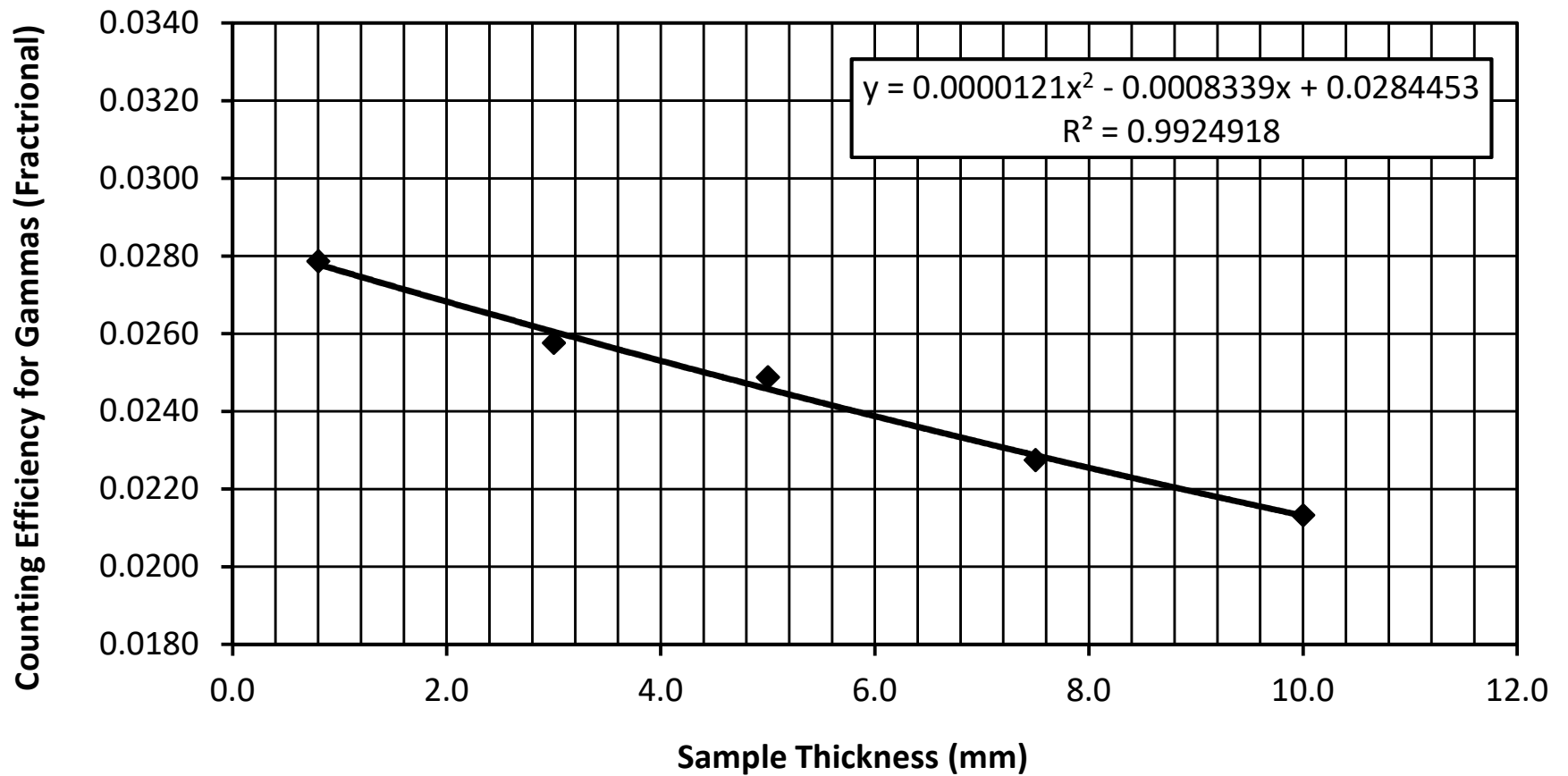
**Note: Results relate only to the items tested.**

ISO / IEC 17025:2005 Accredited with the Canadian Association for Laboratory Accreditation (CALA Accreditation No. A3306)

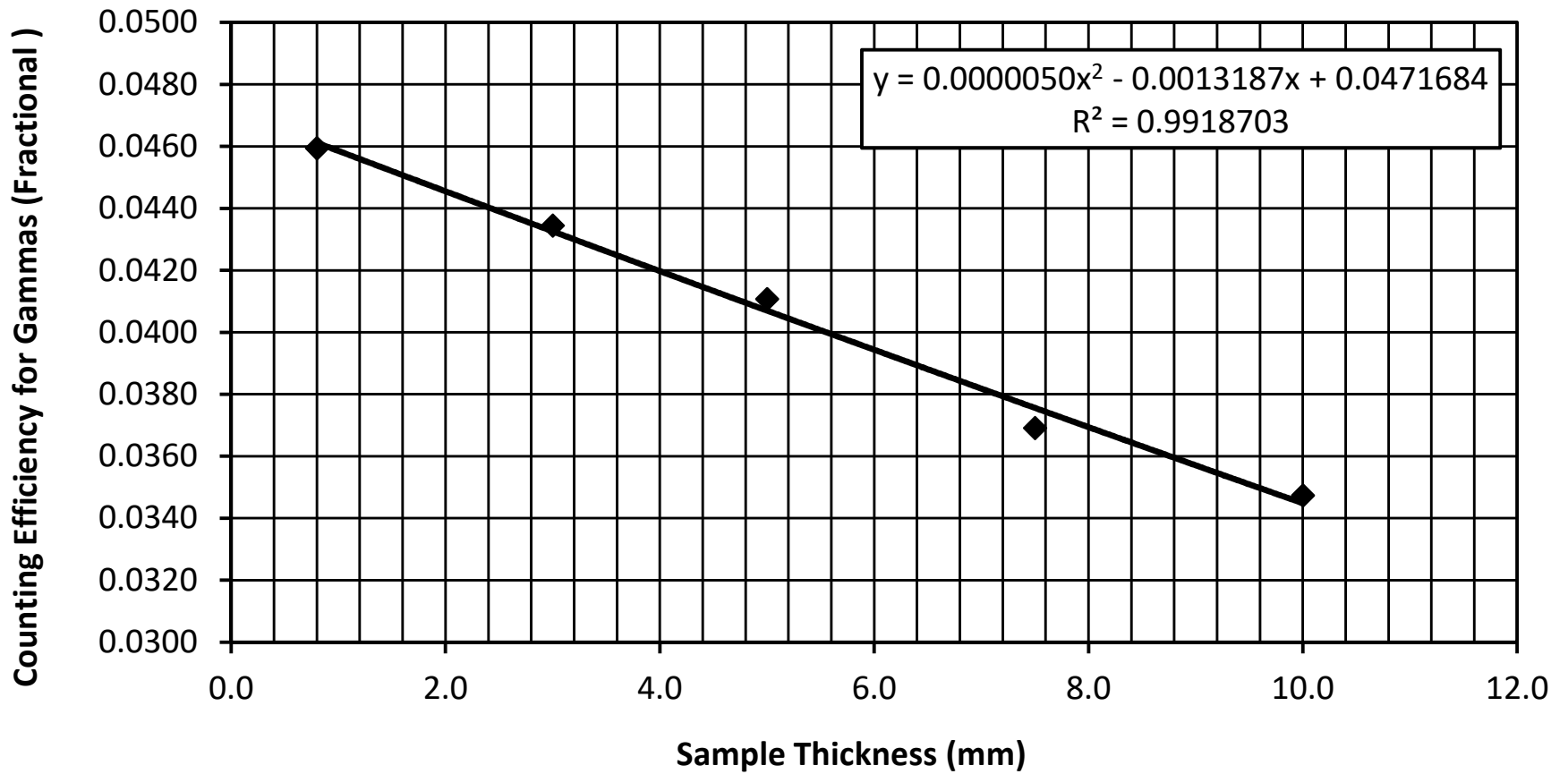
### Cs-137 Counting Efficiency of Gammas vs. Sample Thickness (mm) GMX 25% Detector (Apr 3 - 5, 2019)



### Cs-137 Counting Efficiency of Gammas vs. Sample Thickness (mm) GEM 19% Detector (Apr 3 - 4, 2019)



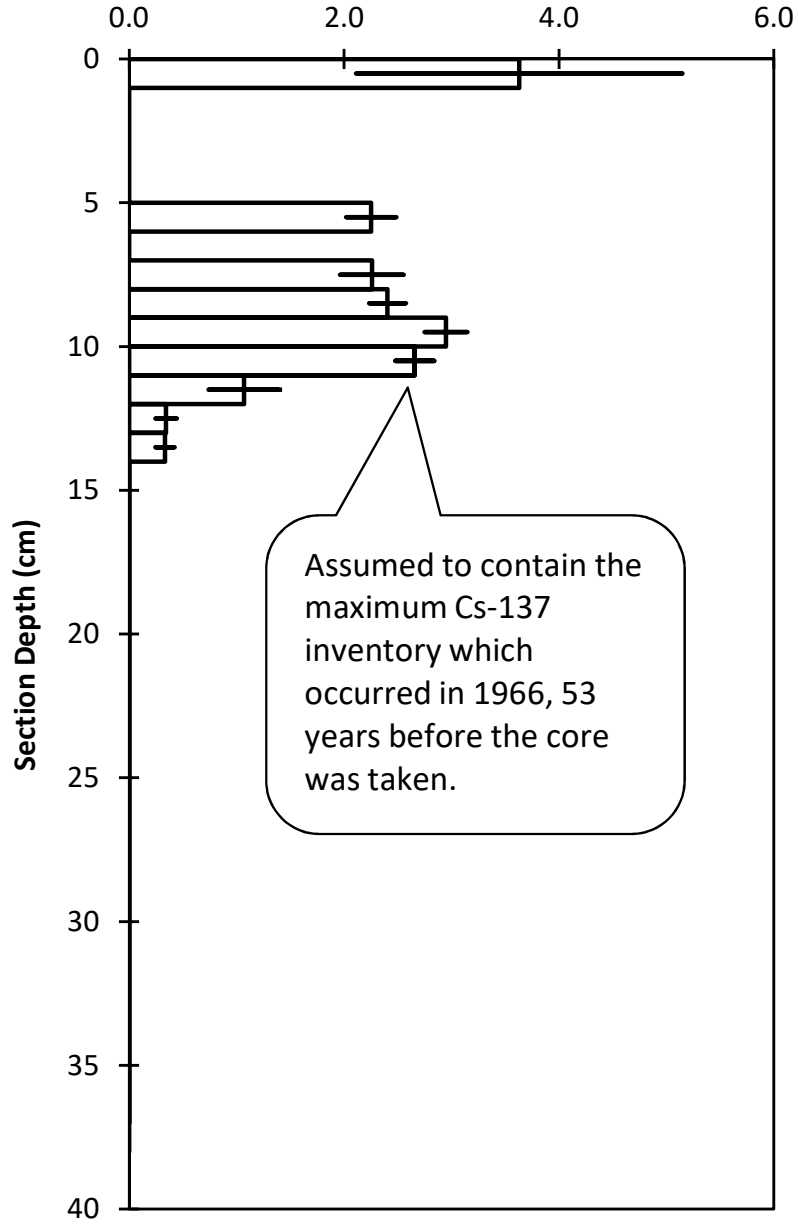
### Cs-137 Counting Efficiency of Gammas vs. Sample Thickness (mm) Canberra 29% Detector (Apr 10 - 11, 2019)



### Cs-137 in Sediments

#### 2A

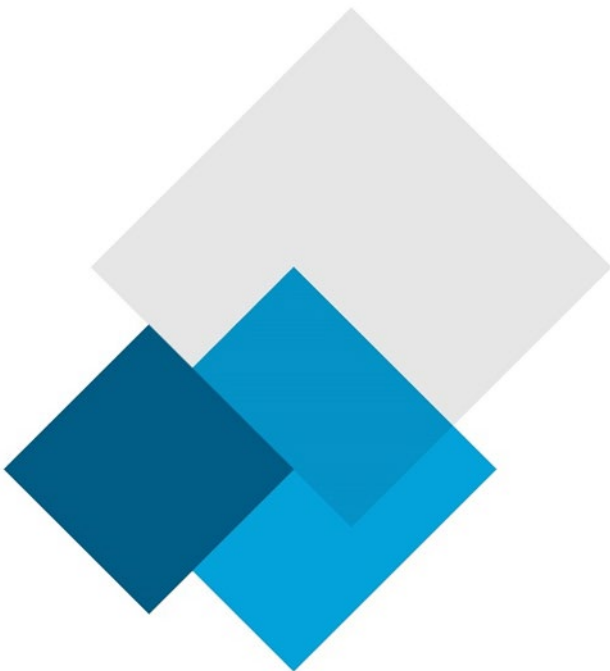
Cs-137 Activity on counting date (DPM/g dry wt.)



Note: The bar plotted at the midpoint depth of each section represents +/- 1 standard deviation of the Cs-137 counting error.

# Appendix 6

Radio Isotopic Analysis Core 3A



# Interpretation of Pb-210, Ra-226 and Cs-137 Results

## Flett Research Ltd.

440 DeSalaberry Ave. Winnipeg, MB R2L 0Y7

Fax/Phone: (204) 667-2505

Email: [flett@flettresearch.ca](mailto:flett@flettresearch.ca) Webpage: <http://www.flettresearch.ca>

---

## Client: Lorrain, Stéphane

**Address:** SNC-LAVALIN GEM QUÉBEC INC., 455, boul. René-Lévesque ouest, Montréal (Québec) H2Z 1Z3

**Core ID:** 3A1

**Transaction ID:** 882

**PO/Contract No.:** 653502-0028

**Date Received:** 20-Feb-19

**Analysis Dates:** March 1 - April 28, 2019

**Analysts:** L. Hesketh-Jost

**Sampling Date:** 9-Feb-19

**Project:** #653502

*Results authorized by Dr. Robert J. Flett, Chief Scientist*

---

## INTERPRETATION

### Observations:

The Pb-210 profile exhibits an irregular but approximately exponential decrease in total Pb-210 activity as a function of depth. The maximum activity of 9.07 DPM/g observed in the surface section is about 10 times the lowest activity of 0.91 DPM/g observed in section 19 - 20 cm (Pages 2 & 3).

The dry bulk densities gradually increase from the surface to section 18 (depth 17 - 18 cm), from 0.074 g/cm<sup>3</sup> to 0.381 g/cm<sup>3</sup>. The dry bulk densities then rapidly increase beginning in section 19 (depth 18 - 19 cm) to 0.832 g/cm<sup>3</sup>, peaking at 1.411 g/cm<sup>3</sup> at the bottom of the core (Page 2 & 4).

Ra-226 was measured at 1.24, 1.31 and 1.28 DPM/g in sections 7 - 8 cm, 17 - 18 cm and 20 - 21 cm, respectively (Pages 9 - 12). The Pb-210 activity in the 20 - 21 cm section is similar to the Ra-226 activity measured in the same section, indicating that the background level of Pb-210 has been achieved in this core.

Cs-137 was measured in 10 sections in the 1 - 20 cm core interval. Activities in the 1 - 18 cm portion of the core are all significantly above background, ranging between 0.92 - 2.03 DPM/g (Pages 13 & 17). Below 18 cm, the Cs-137 activity declines with depth. The shape of Cs-137 profile in the 1 - 18 cm core interval suggests that the majority of the Cs-137 is probably from external erosion sources (soils or sediments contaminated with bomb testing radionuclides).

### Regression model of Unsupported Pb-210 activity vs. Cumulative Dry Weight (g/cm<sup>2</sup>):

When applying the linear regression model, it is assumed that the input of Pb-210 and the sediment accumulation rate are constant. Although variation in the sediment accumulation rate is apparent, the linear regression model was applied to sections 1 - 18 (depth 0 - 18 cm), because it appears that the average sediment accumulation rate will be reasonably estimated. This estimate of sediment accumulation rate is used to calibrate the CRS model.

The regression results are seen in Page 5. The model predicts ( $R^2 = 0.9502$ ) an average sediment accumulation rate of 0.1185 g/cm<sup>2</sup>/yr when the unsupported Pb-210 activity was calculated by subtracting the nearest neighbouring Ra-226 measurement from each total Pb-210 value. The age at the bottom of any core section can be estimated by dividing the cumulative dry weight/cm<sup>2</sup> by the accumulation rate. For example, the age at the bottom of section 12 (extrapolated depth 12.5 cm) is calculated as 2.658 / 0.1185 = 22.4 yr. The age estimate at the bottom of each section is shown on Pages 2 (column AM) & 6.

### **CRS model of Age at bottom of Extrapolated section in years vs. Depth of bottom edge of current section in cm:**

The CRS model assumes constant input of Pb-210 and a core that is long enough to include all of the measurable atmospheric source Pb-210, i.e. it contains a complete Pb-210 inventory. The facts that 1) the suspicious sudden termination in exponential decay of the Pb-210 profile in section 19 (depth 18 - 19 cm), 2) the sudden and rapid increase in dry bulk density in the same section, are possible causes for us to discard the deeper portion of the core (i.e. truncate the core) due to the increasing uncertainty of the sedimentation process.

The Ra-226 activity indicates that the background Pb-210 activity level has not been achieved at 18 cm, leaving us with an incomplete truncated core that normally cannot be processed by the CRS model. In order to allow use of the CRS model, an artificial Pb-210 inventory of 32.105 DPM/cm<sup>2</sup> has been chosen such that the CRS model predicted exactly the same average sediment accumulation rate (0.1185 g/cm<sup>2</sup>/yr) as the linear regression model over the 0 - 18 cm segment of the core. With the CRS model calibrated, it has been used to calculate ages for the core interval of 0 - 18 cm.

The measured total activity results (DPM/g) are shown in column AF of the main data table on Page 2. The estimated age at the bottom of each section is shown in column AI, also shown on Page 2. The average sediment accumulation rate, from core surface to the extrapolated bottom depth of any section, can be calculated by dividing the cumulative dry mass at the bottom of the extrapolated section by the calculated age at that depth. For example, the average sediment accumulation rate, from the core surface to the bottom of section 12 (extrapolated depth 12.5 cm) can be calculated as:  $2.658 / 22.1 = 0.1203 \text{ g/cm}^2/\text{yr}$ . The individual sediment accumulation rate for each section is shown in column AL on Page 2. Plots of age vs. depth, sediment accumulation rate vs. depth and sediment accumulation rate vs. age are seen in Pages 6, 7 and 8, respectively.

### **Conclusion:**

The significant presence of Cs-137 in the 0 - 18 cm core interval indicates that these sections are less than 56 years old (post 1963). Based upon the shape of the Pb-210 and dry bulk density profiles and the ages predicted by the Pb-210 models, it is suspected that a portion of the core is missing and it is likely that the 1966 maximum Cs-137 inventory could be recorded in the suspected missing portions of the core. However, the CRS model indicates an age of 38.1 yr at 18 cm depth, an age compatible with the presence of Cs-137.

Over the entire core, the average sediment accumulation rate estimated by the CRS model has been forced to exactly coincide with the linear regression estimate of 0.1185 g/cm<sup>2</sup>/yr. Although the CRS calculated ages depend upon the results of the linear regression model, the CRS model is to be preferred because it should provide accurate age predictions at the bottom of each section even though the sediment accumulation rate is changing with time.

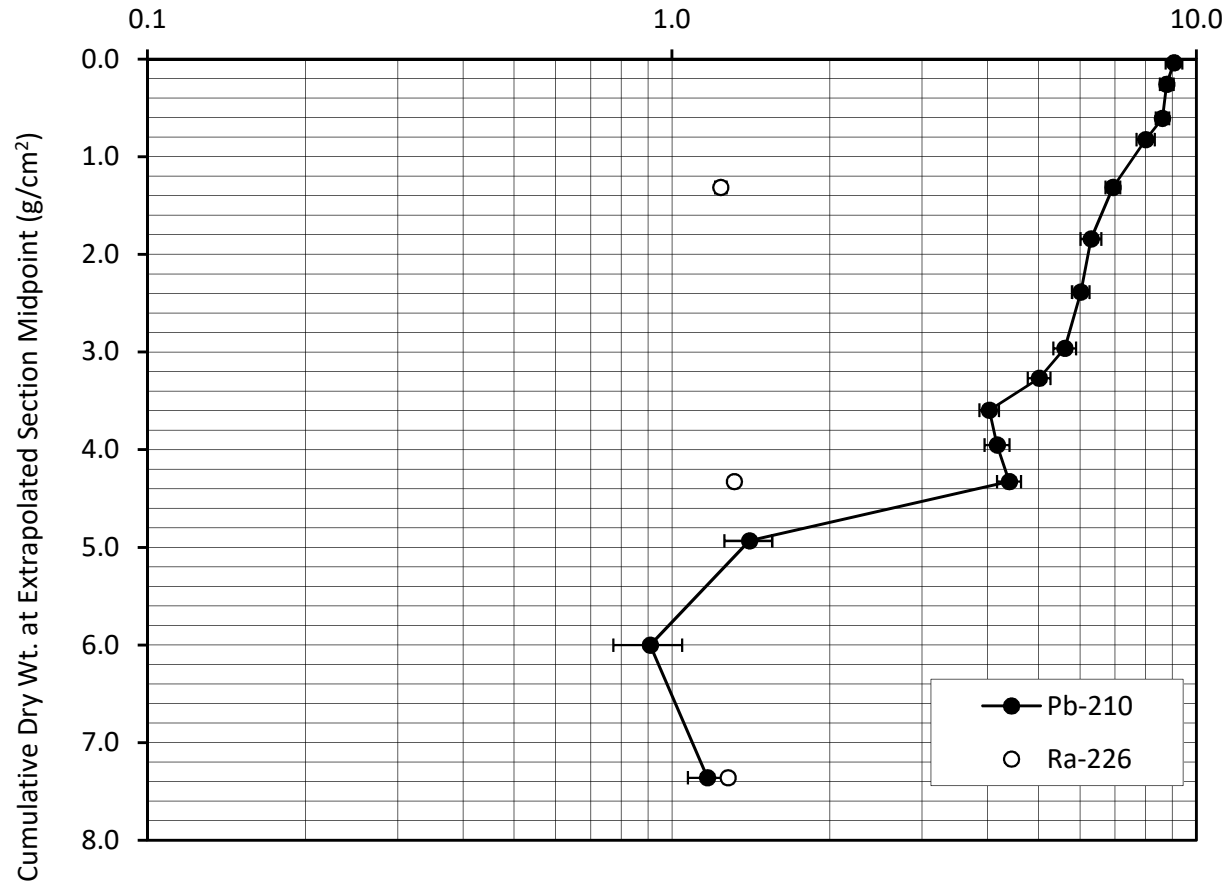
Overall, the analytical quality of radioisotope data (based upon the recovery of spike, the recovery of CRM, the results of repeat analyses and blanks) is considered good.



**Total Pb-210 Activity vs. Accumulated Sediment**

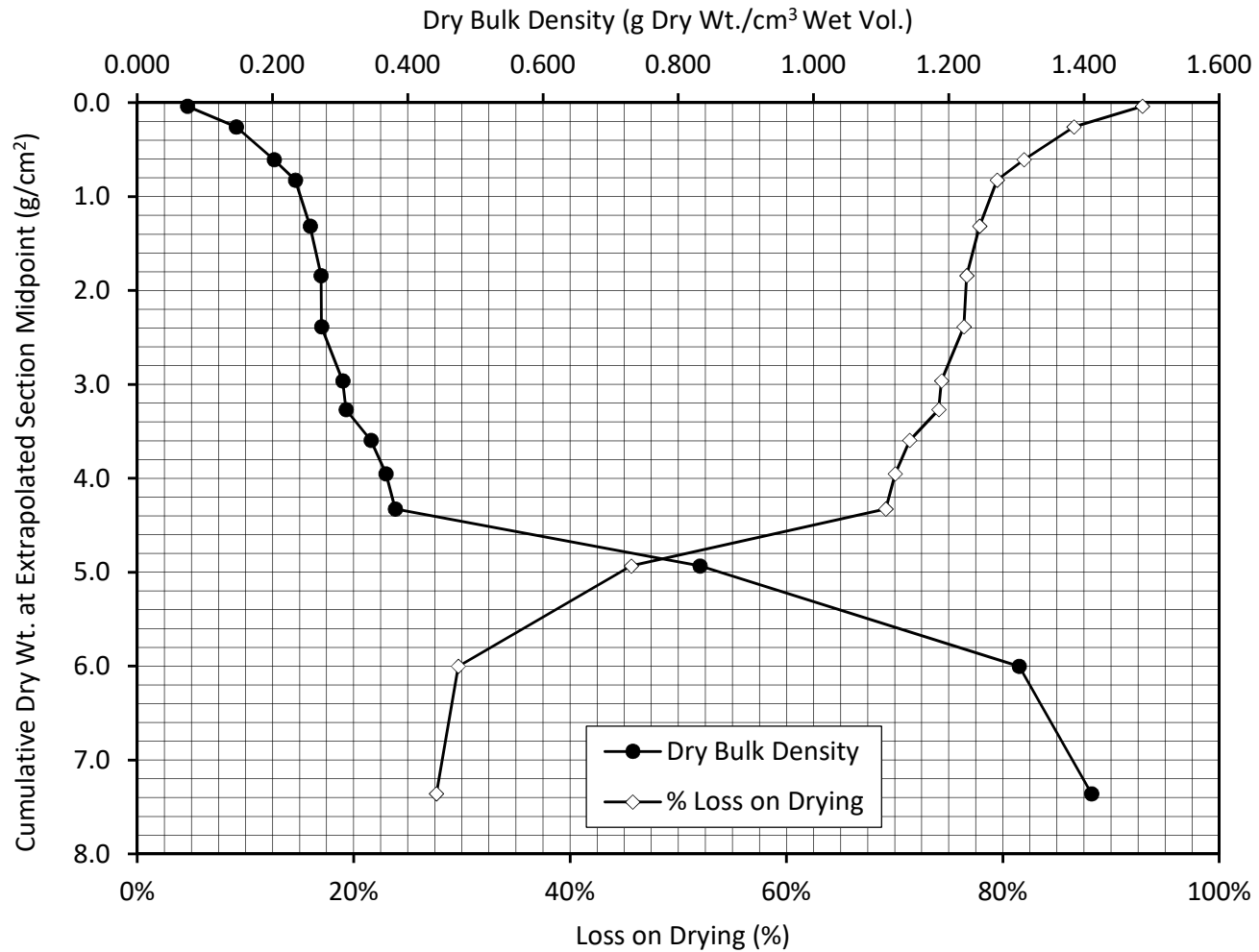
**3A1**

Total Pb-210 Activity (DPM/g Dry Wt.)



**Dry Bulk Density and % Loss on Drying**  
**vs. Accumulated Sediment**

**3A1**

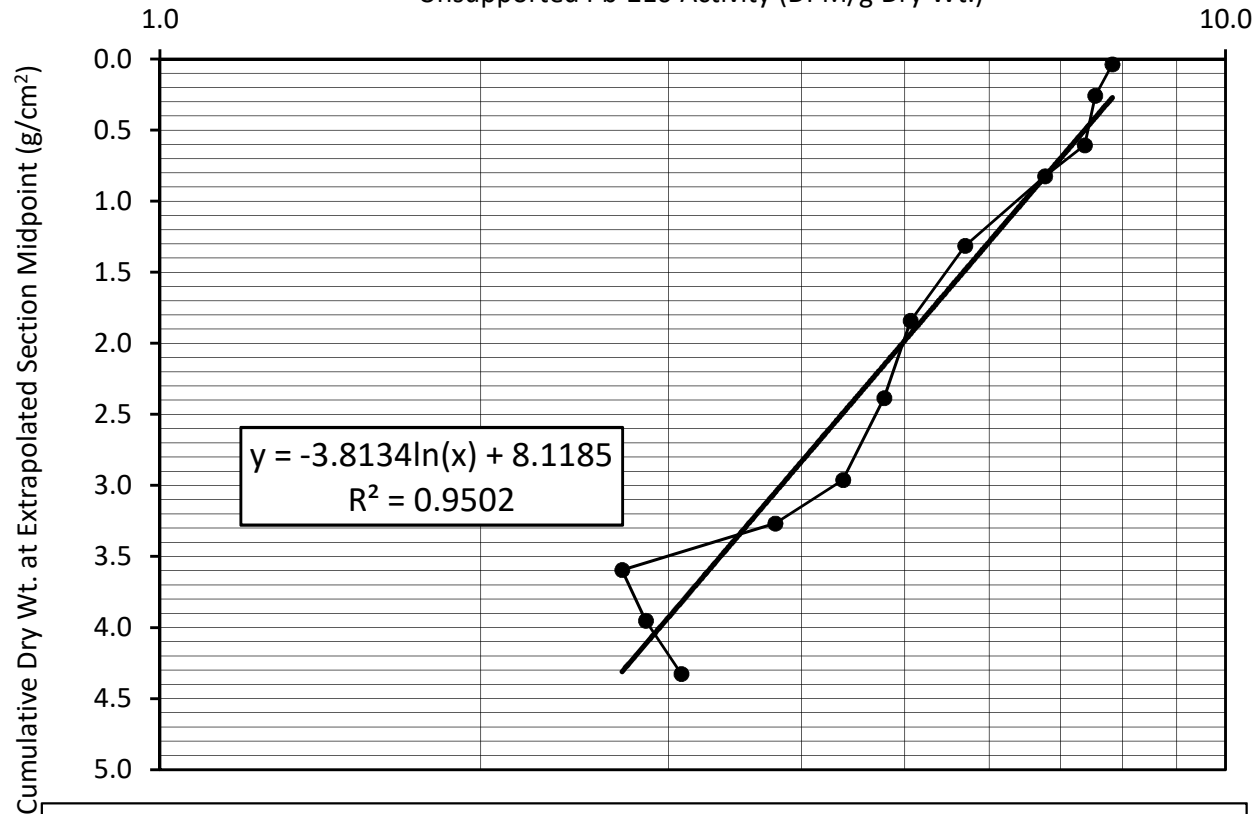


**Regression of Unsupported Pb-210 Activity  
vs. Accumulated Sediment**

(Unsupported activity calculated by subtracting the nearest neighbouring Ra-226 measurement from each total Pb-210 value)

**3A1**

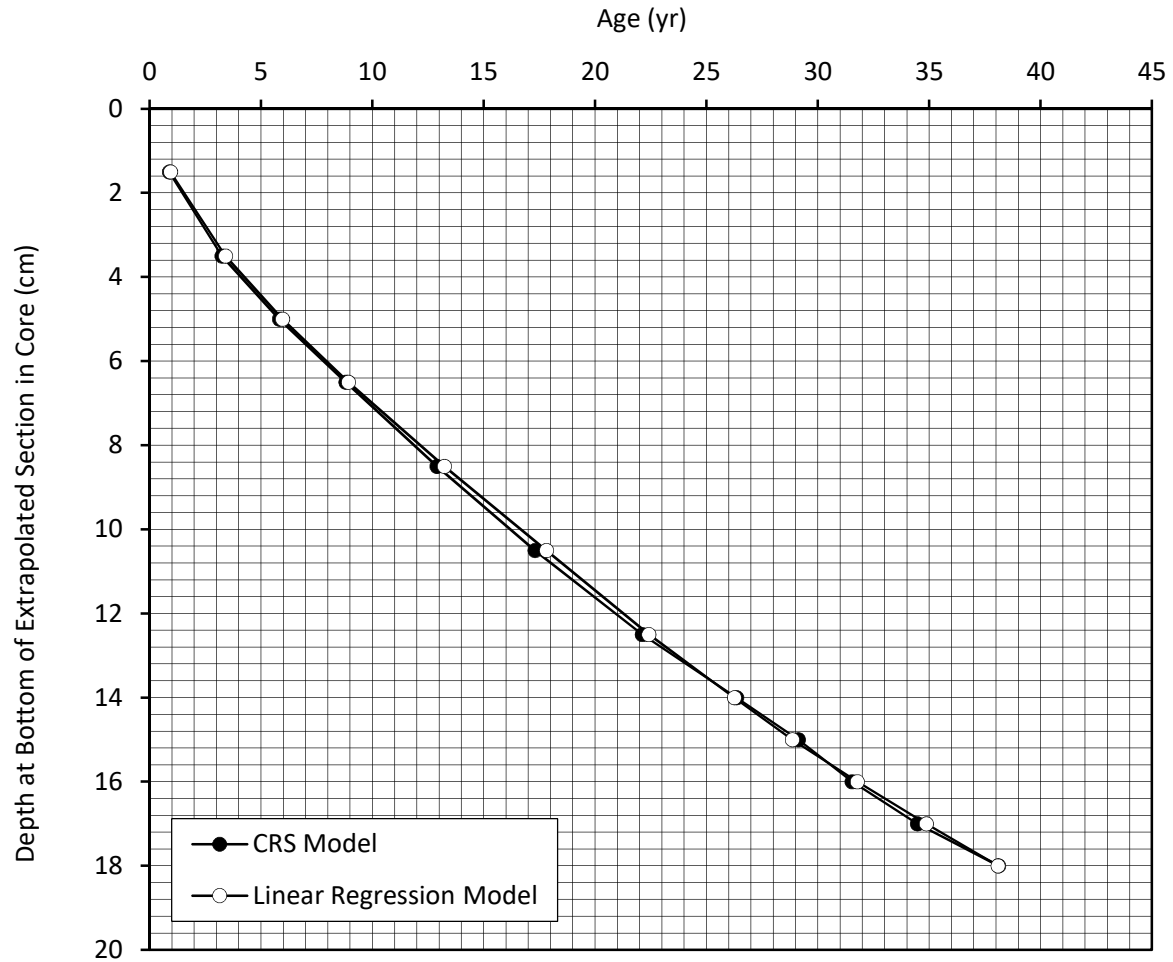
Unsupported Pb-210 Activity (DPM/g Dry Wt.)



**Sediment Accumulation Rate in sections 1 - 18**  
 $= (-3.8134) \times 0.6931 / (-22.3) = 0.1185 \text{ g/cm}^2/\text{yr}$

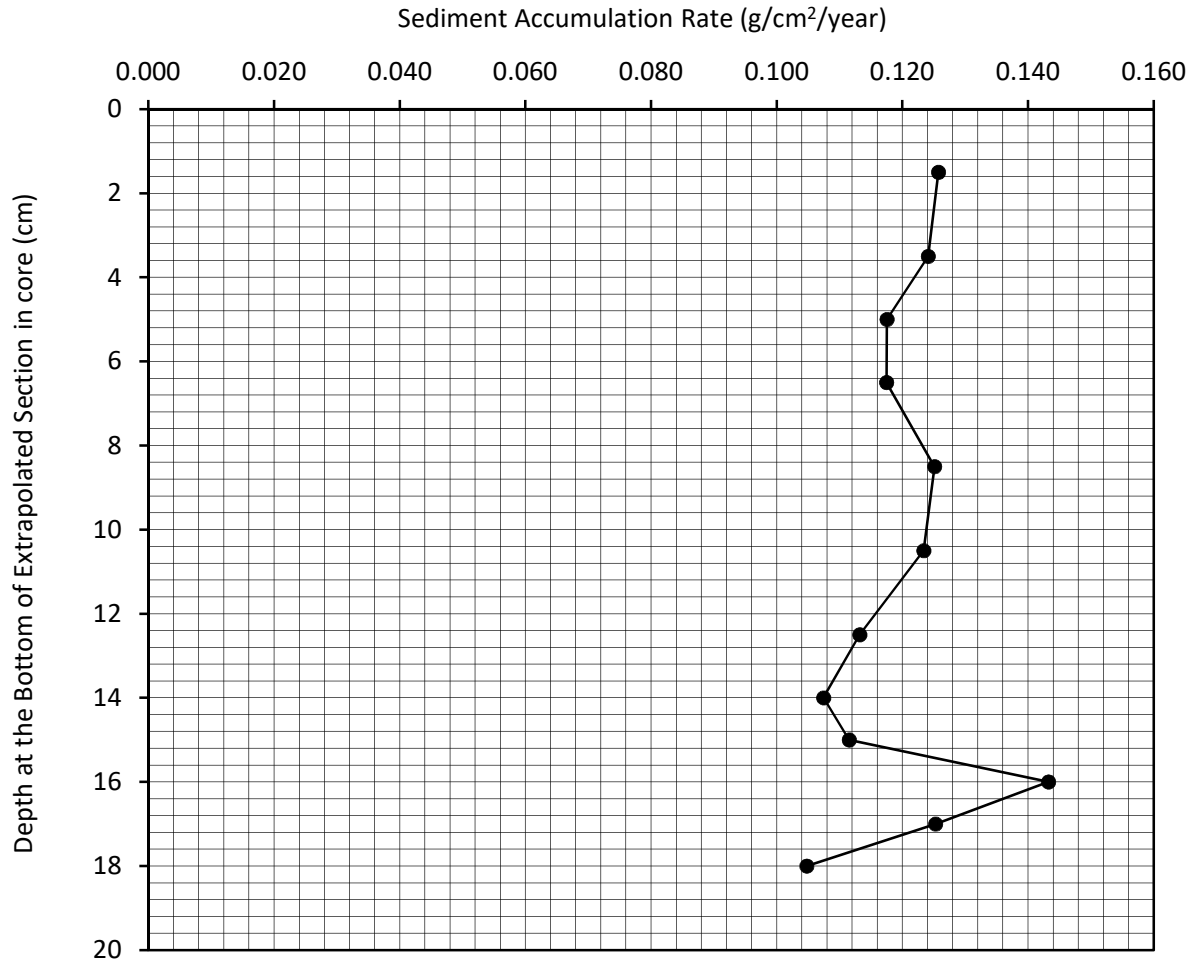
Age (yr) vs. Depth (cm)  
CRS Model vs. Linear Regression Model

3A1



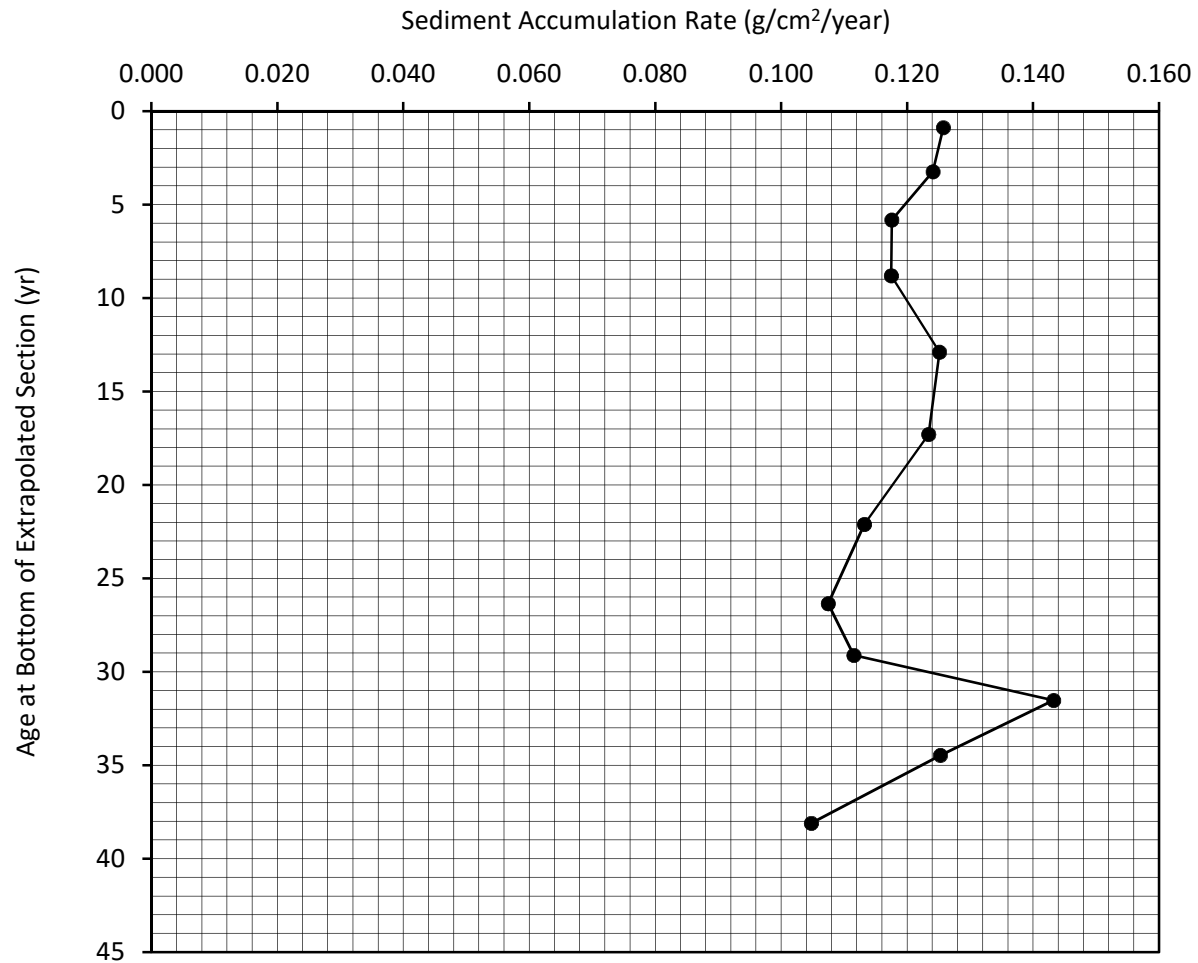
**CRS Sediment Accumulation Rate (g/cm<sup>2</sup>/year)**  
**vs. Depth at the Bottom of Extrapolated Section in Core (cm)**

**3A1**



**CRS Sediment Accumulation Rate (g/cm<sup>2</sup>/year)**  
**vs. Age at Bottom of Extrapolated Section (yr)**

**3A1**



# Results of Ra-226 Analysis by Rn-222 Emanation

Flett Research Ltd.

440 DeSalaberry Ave., Winnipeg, MB R2L 0Y7

Fax/Phone: (204) 667-2505

Email: flett@flettresearch.ca Webpage: http://www.flettresearch.ca

## Client: Lorrain, Stéphane

Address: SNC-LAVALIN GEM QUÉBEC INC., 455, boul. René-Lévesque ouest, Montréal (Québec) H2Z 1Z3

Core ID: 3A1

Transaction ID: 882

Date Received: 20-Feb-19

PO/Contract No.: 653502-0028

Sampling Date: 9-Feb-19

Analysis Dates: February 25 - April 20, 2019

Project: #653502

Analysts: X. Hu; L. Hesketh-Jost

Salt Correction Applied? No

Analytical Method: N40110 Determination of Radium-226 in Sediment, Soil and Peat by Radon-222 Emanation (Version 3)

### Comments:

**Detection Limit:** The method detection limit (MDL) is dependent on the amount of sample analyzed. For a 60,000 second counting time the MDL at 95% confidence for 2 g of dry sample is 0.1 DPM/g and for 0.5 g of dry sample is 0.5 DPM/g.

**Estimated Uncertainty:** The estimate of uncertainty of measurement for this method in this laboratory is approximately ±12% at 95% confidence level (approximately 40,000 counts in 60,000 seconds).

Results authorized by Dr. Robert J. Flett, Chief Scientist

Core ID	Sample ID	Ra-226 Activity (DPM/g Dry Wt.)	Combined Error: 1 SD (DPM/g Dry Wt.)	Comments Code for Ra-226 Analysis
3A1	3A1-2/2-21	1.28	0.02	
3A1	3A1-2/2-8	1.24	0.03	
3A1	3A1-2/2-18	1.31	0.03	

Q:\Clients A-L\Lorrain, Stephane\2019(882)\Radioisotopes\3A1\Pb-210, Ra-226 and Cs-137 Lorrain Core 3A1 May 3-19 Final.xlsm

**Duplicate:** Two subsamples of the same sample were carried through the analytical procedure in an identical manner.

**Re-count:** The sample bottle was re-sealed after the initial analysis, and was re-counted after 11 or more days of Rn-222 ingrowth. Repeat counting was chosen over duplicate analysis due to insufficient sample material provided.

This test report shall not be reproduced, except in full, without written approval of the laboratory.

Note: Results relate only to the items tested.

20-Apr-19

Page 9 of 17

ISO / IEC 17025:2005 Accredited with the Canadian Association for Laboratory Accreditation (CALA Accreditation No. A3306)

**Radium Analysis by Rn-222 Emanation**

Core ID	3A1
Sample ID	3A1-2/2-21
Lucas Cell No.	3
Number of days since Rn board last run	1
Dry weight of sample counted (g)	2.029
Total count in period	6397
Total count in period (carryover corrected)	6334
Cell Blank count (CPM)	0.562
System Blank (DPM)	0.395
System Efficiency	0.839
Count duration (minutes)	1000

Typical carryover is about 1 - 2 % of the net counts (gross counts less system background) of the sample counted on the previous day. The carryover is subtracted from the gross counts of current sample. This correction is not required if the sample is run after a blank.

Carryover correction?	Yes	Mean of last 10 carryover measurements	1.02%
Gross counts of previous sample	7092	Mean of last 6 system background measurements	887
Counts carried over from previous sample	63		

	Year	Month	Day	Hour	Minute	Second	Ingrowth time (Days)	Ingrowth factor	Decay correction
When sample last stripped	2019	2	26	16	56	0	12.95	0.90437	0.92490
When cell filled	2019	3	11	15	47	51			
Beginning time of count	2019	3	11	17	48	14			

Counts per minute	6.33
Gross CPM less Cell Blank (CPM)	5.77
CPM (decay during count corrected)	6.24
DPM Sample +System (efficiency corrected)	7.44
DPM sample	7.79
DPM/g	3.84
<b>Ra-226 DPM/g</b>	<b>1.28</b>
Ra-226 pCi/g	0.58

Error ± 1 sd    0.1396 DPM

**Error ± 1 sd    0.0229 DPM/g**

Error % =    1.8

Chemist	RF
PMT High Voltage +ve	770
HV Power supply	Spectrum Technologies
Alpha Counter	Spectrum Technologies
Region of Interest Ch.#s	28-1022
PMT	6655A - #1
Preamp	Canberra 2007P tube base
Amp Gain	1

**Radium Analysis by Rn-222 Emanation**

Core ID	3A1
Sample ID	3A1-2/2-8
Lucas Cell No.	3
Number of days since Rn board last run	1
Dry weight of sample counted (g)	1.315
Total count in period	4572
Total count in period (carryover corrected)	4556
Cell Blank count (CPM)	0.562
System Blank (DPM)	0.395
System Efficiency	0.839
Count duration (minutes)	1000

Typical carryover is about 1 - 2 % of the net counts (gross counts less system background) of the sample counted on the previous day. The carryover is subtracted from the gross counts of current sample. This correction is not required if the sample is run after a blank.

Carryover correction?	Yes	Mean of last 10 carryover measurements	1.02%
Gross counts of previous sample	2471	Mean of last 6 system background measurements	887
Counts carried over from previous sample	16		

	Year	Month	Day	Hour	Minute	Second	Ingrowth time (Days)	Ingrowth factor	Decay correction
When sample last stripped	2019	3	29	17	17	0	19.80	0.97236	0.92490
When cell filled	2019	4	18	12	31	31			
Beginning time of count	2019	4	18	14	31	54			

Counts per minute	4.56
Gross CPM less Cell Blank (CPM)	3.99
CPM (decay during count corrected)	4.32
DPM Sample +System (efficiency corrected)	5.15
DPM sample	4.89
DPM/g	3.72
<b>Ra-226 DPM/g</b>	<b>1.24</b>
Ra-226 pCi/g	0.56

Error ± 1 sd    0.1234 DPM

**Error ± 1 sd    0.0313 DPM/g**

Error % =    2.5

Chemist	XH
PMT High Voltage +ve	770
HV Power supply	Spectrum Technologies
Alpha Counter	Spectrum Technologies
Region of Interest Ch.#s	28-1022
PMT	6655A - #1
Preamp	Canberra 2007P tube base
Amp Gain	1

**Radium Analysis by Rn-222 Emanation**

Core ID	3A1
Sample ID	3A1-2/2-18
Lucas Cell No.	3
Number of days since Rn board last run	1
Dry weight of sample counted (g)	1.725
Total count in period	6067
Total count in period (carryover corrected)	6029
Cell Blank count (CPM)	0.562
System Blank (DPM)	0.395
System Efficiency	0.839
Count duration (minutes)	1000

Typical carryover is about 1 - 2 % of the net counts (gross counts less system background) of the sample counted on the previous day. The carryover is subtracted from the gross counts of current sample. This correction is not required if the sample is run after a blank.			
Carryover correction?	Yes	Mean of last 10 carryover measurements	1.02%
Gross counts of previous sample	4572	Mean of last 6 system background measurements	887
Counts carried over from previous sample	38		

	Year	Month	Day	Hour	Minute	Second	Ingrowth time (Days)	Ingrowth factor	Decay correction
When sample last stripped	2019	3	29	17	17	0	20.93	0.97748	0.92494
When cell filled	2019	4	19	15	40	0			
Beginning time of count	2019	4	19	17	40	0			

Counts per minute	6.03
Gross CPM less Cell Blank (CPM)	5.47
CPM (decay during count corrected)	5.91
DPM Sample +System (efficiency corrected)	7.05
DPM sample	6.80
DPM/g	3.94
<b>Ra-226 DPM/g</b>	<b>1.31</b>
Ra-226 pCi/g	0.59

Error ± 1 sd    0.1328 DPM

**Error ± 1 sd    0.0257 DPM/g**

Error % =    2.0

Chemist	LHJ
PMT High Voltage +ve	770
HV Power supply	Spectrum Technologies
Alpha Counter	Spectrum Technologies
Region of Interest Ch.#s	28-1022
PMT	6655A - #1
Preamp	Canberra 2007P tube base
Amp Gain	1

# Results of Cs-137 Analysis

Flett Research Ltd.

440 DeSalaberry Ave. Winnipeg, MB R2L 0Y7

Fax / Phone: (204) 667-2505

Email: flett@flettresearch.ca Webpage: http://www.flettresearch.ca

**Client: Lorrain, Stéphane**

**Address:** SNC-LAVALIN GEM QUÉBEC INC., 455, boul. René-Lévesque ouest, Montréal (Québec) H2Z 1Z3

**Core ID:** 3A1  
**Date Received:** 20-Feb-19  
**Sampling Date:** 9-Feb-19  
**Project:** #653502

**Transaction ID:** 882  
**PO/Contract No.:** 653502-0028  
**Analysis Dates:** April 6 - 28, 2019  
**Analysts:** X. Hu; L. Hesketh-Jost

Salt Correction?	No
------------------	----

**Analytical Method:** N30120 Measurement of Gamma-Ray Emitting Radionuclides in Sediment/Soil Samples by Gamma Spectrometry Using HPGe Detectors (Version 2)

**Deviation from Method:**

**Comments:**

**Detection Limit:** The method detection limit (MDL) is 0.3 DPM/g for an 80,000 seconds counting period when measuring a 9 g of dry sample at a 95% confidence level. The method detection limit can be decreased to 0.1 DPM/g if 32 g of sample is used.

**Estimated Uncertainty:** The estimated uncertainty of this method has been determined to be ± 10% at 95% confidence for samples with activities between 0.5 and 20 DPM/g, counting time 80,000 seconds and sample weights ranging from 9 to 32 grams. Method uncertainty can increase to 85% for samples with activities near detection limit (0.1 - 0.3 DPM/g).

Results authorized by Dr. Robert J. Flett, Chief Scientist

Sample ID	Upper Depth (cm)	Lower Depth (cm)	Day Sample Counted	Month Sample Counted	Year Sample Counted	Integral NET Cs-137 Peak	Counting Error 1 SD (Counts)	Count Time (seconds)	Dry Sample Weight (g)	Sample Thickness (mm)	CPM/g	Efficiency for Gammas Fractional	Gammas per min. per gram	Activity DPM/g (dry wt.) on Counting Date	Approx. Error DPM/g	Activity DPM/g (dry wt.) on Sampling Date	Approx. Error DPM/g	Activity pCi/g (dry wt.) on Sampling Date	Approx. Error pCi/g	Activity mBq/g (dry wt.) on Sampling Date	Approx. Error mBq/g	Detector Used	Comments Code for Cs-137 Analysis
3A1-2/2-2	1	2	27	4	2019	194	34	80000	3.390	1.30	0.0429	0.0455	0.9441	1.11	0.20	1.11	0.20	0.50	0.09	18.56	3.28	Canberra	
3A1-2/2-5	4	5	24	4	2019	114	32	80000	4.003	1.60	0.0214	0.0271	0.7869	0.92	0.26	0.93	0.26	0.42	0.12	15.47	4.34	GEM	
3A1-2/2-10	9	10	6	4	2019	275	39	80000	6.561	2.03	0.0314	0.0268	1.1727	1.38	0.20	1.38	0.20	0.62	0.09	23.02	3.26	GEM	
3A1-2/2-12	11	12	11	4	2019	497	40	80000	6.561	2.30	0.0568	0.0442	1.2865	1.51	0.12	1.52	0.12	0.68	0.05	25.26	2.03	Canberra	
3A1-2/2-14	13	14	6	4	2019	438	44	80000	6.473	2.13	0.0507	0.0293	1.7326	2.03	0.20	2.04	0.21	0.92	0.09	34.01	3.42	GMX	
3A1-2/2-16	15	16	11	4	2019	423	46	80000	7.244	2.30	0.0438	0.0292	1.4996	1.76	0.19	1.77	0.19	0.80	0.09	29.45	3.20	GMX	
3A1-2/2-17	16	17	25	4	2019	383	37	80000	8.680	2.53	0.0331	0.0264	1.2527	1.47	0.14	1.48	0.14	0.67	0.06	24.62	2.38	GEM	
3A1-2/2-18	17	18	7	4	2019	346	37	80000	6.309	2.00	0.0411	0.0268	1.5333	1.80	0.19	1.81	0.19	0.81	0.09	30.10	3.22	GEM	
3A1-2/2-19	18	19												0.63	0.09	0.63	0.09	0.29	0.04	10.55	1.50	GMX	
3A1-2/2-20	19	20												0.15	0.05	0.16	0.05	0.07	0.02	2.59	0.85	GEM	
<b>Re-count</b>																							
3A1-2/2-19	18	19	21	4	2019	328	46	80000	15.774	4.30	0.0156	0.0281	0.5555	0.65	0.09	0.65	0.09	0.30	0.04	10.92	1.53	GMX	
3A1-2/2-19 Re-count	18	19	22	4	2019	306	44	80000	15.774	4.30	0.0145	0.0281	0.5183	0.61	0.09	0.61	0.09	0.28	0.04	10.18	1.46	GMX	
3A1-2/2-20	19	20	21	4	2019	93	27	80000	22.989	6.18	0.0030	0.0238	0.1277	0.15	0.04	0.15	0.04	0.07	0.02	2.51	0.73	GEM	
3A1-2/2-20 Re-count	19	20	22	4	2019	99	36	80000	22.989	6.18	0.0032	0.0238	0.1360	0.16	0.06	0.16	0.06	0.07	0.03	2.67	0.97	GEM	
<b>Cs-137 Standards</b>																							
GMX 32g 10 mm			4	4	2019	19967	143	5000	32.00	10.0	7.4876	0.0237	315.7600	370.61	2.65	957.04							
GMX 24g 7.5mm			5	4	2019	16045	128	5000	24.00	7.5	8.0225	0.0254	315.7400	370.59	2.96	957.04							
GMX 15g 5mm			4	4	2019	10978	106	5000	15.00	5.0	8.7824	0.0278	315.7600	370.61	3.58	957.04							
GMX 9g 3mm			3	4	2019	6862	84	5000	9.00	3.0	9.1493	0.0290	315.7799	370.63	4.54	957.04							
GMX 2.85g 0.8mm			4	4	2019	2237	49	5000	2.854	0.8	9.4057	0.0298	315.7600	370.61	8.12	957.04							
GEM 32g 10 mm			4	4	2019	17960	139	5000	32.00	10.0	6.7350	0.0213	315.7600	370.61	2.87	957.04							
GEM 24g 7.5mm			4	4	2019	14367	124	5000	24.00	7.5	7.1835	0.0227	315.7600	370.61	3.20	957.04							
GEM 15g 5mm			3	4	2019	9822	102	5000	15.00	5.0	7.8576	0.0249	315.7799	370.63	3.85	957.04							
GEM 9g 3mm			4	4	2019	6102	79	5000	9.00	3.0	8.1360	0.0258	315.7600	370.61	4.80	957.04							
GEM 2.85g 0.8mm			4	4	2019	2093	48	5000	2.854	0.8	8.8003	0.0279	315.7600	370.61	8.50	957.04							
Canberra 32g 10 mm			11	4	2019	29236	172	5000	32.00	10.0	10.9635	0.0347	315.6205	370.45	2.19	957.04							
Canberra 24g 7.5mm			11	4	2019	23302	154	5000	24.00	7.5	11.6510	0.0369	315.6205	370.45	2.44	957.04							
Canberra 15g 5mm			10	4	2019	16207	128	5000	15.00	5.0	12.9656	0.0411	315.6404	370.47	2.93	957.04							
Canberra 9g 3mm			10	4	2019	10285	103	5000	9.00	3.0	13.7133	0.0434	315.6404	370.47	3.70	957.04							
Canberra 2.85g 0.8mm			10	4	2019	3449	60	5000	2.854	0.8	14.5018	0.0459	315.6404	370.47	6.45	957.04							

Q:\Clients A-1\Lorrain, Stephane\2019\882\Radioisotopes\3A1\Pb-210, Ra-226 and Cs-137 Lorrain Core 3A1 May 3-19 Final.xlsx

**Duplicate:** Two subsamples of the same sample were carried through the analytical procedure in an identical manner.

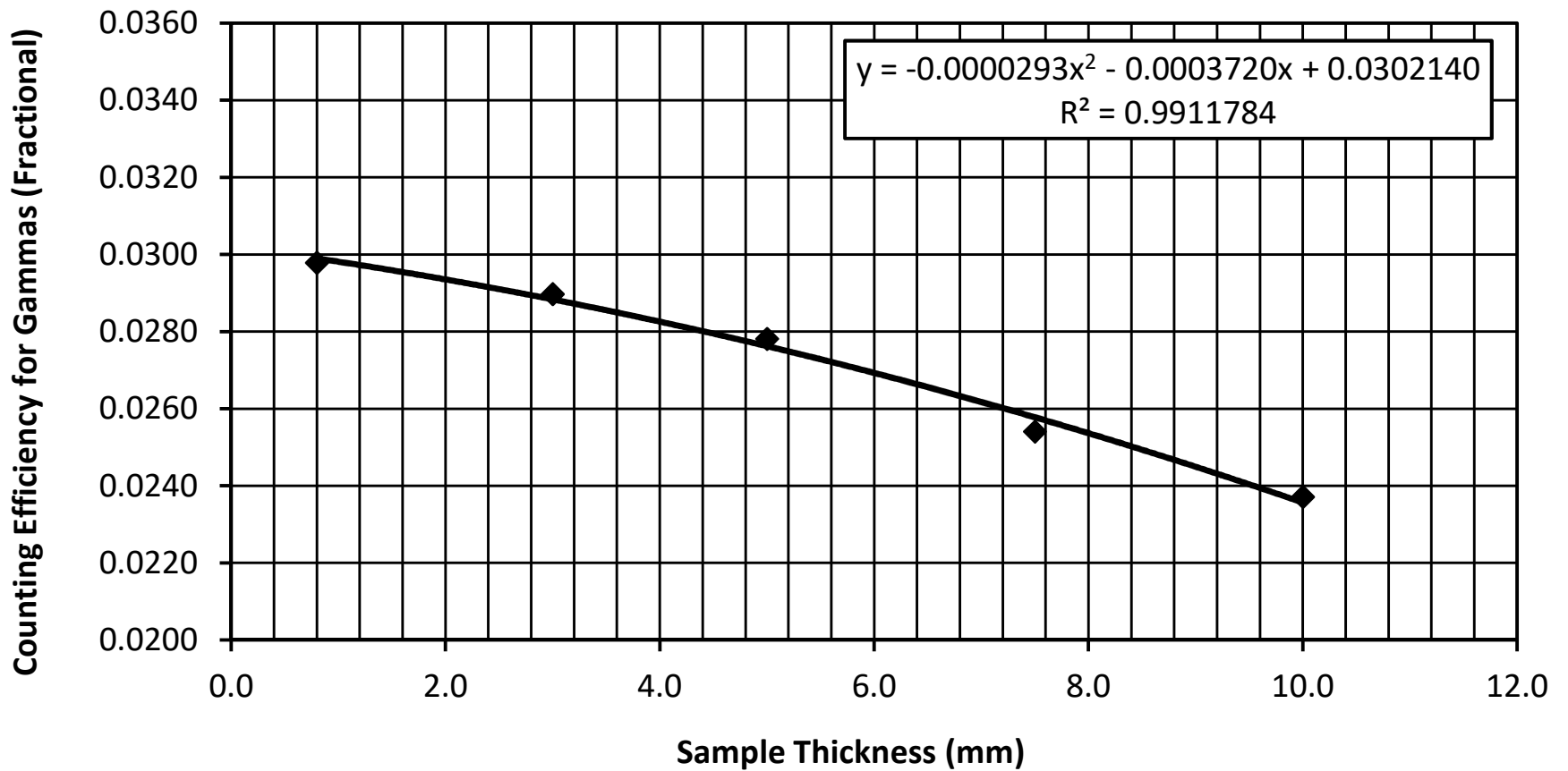
**Re-count:** The entire available dry sample material was used for making the sample pancake, and then this sample pancake was counted twice on a HPGe detector. Repeat counting was chosen over duplicate analysis due to insufficient sample material provided.

**This test report shall not be reproduced, except in full, without written approval of the laboratory.**

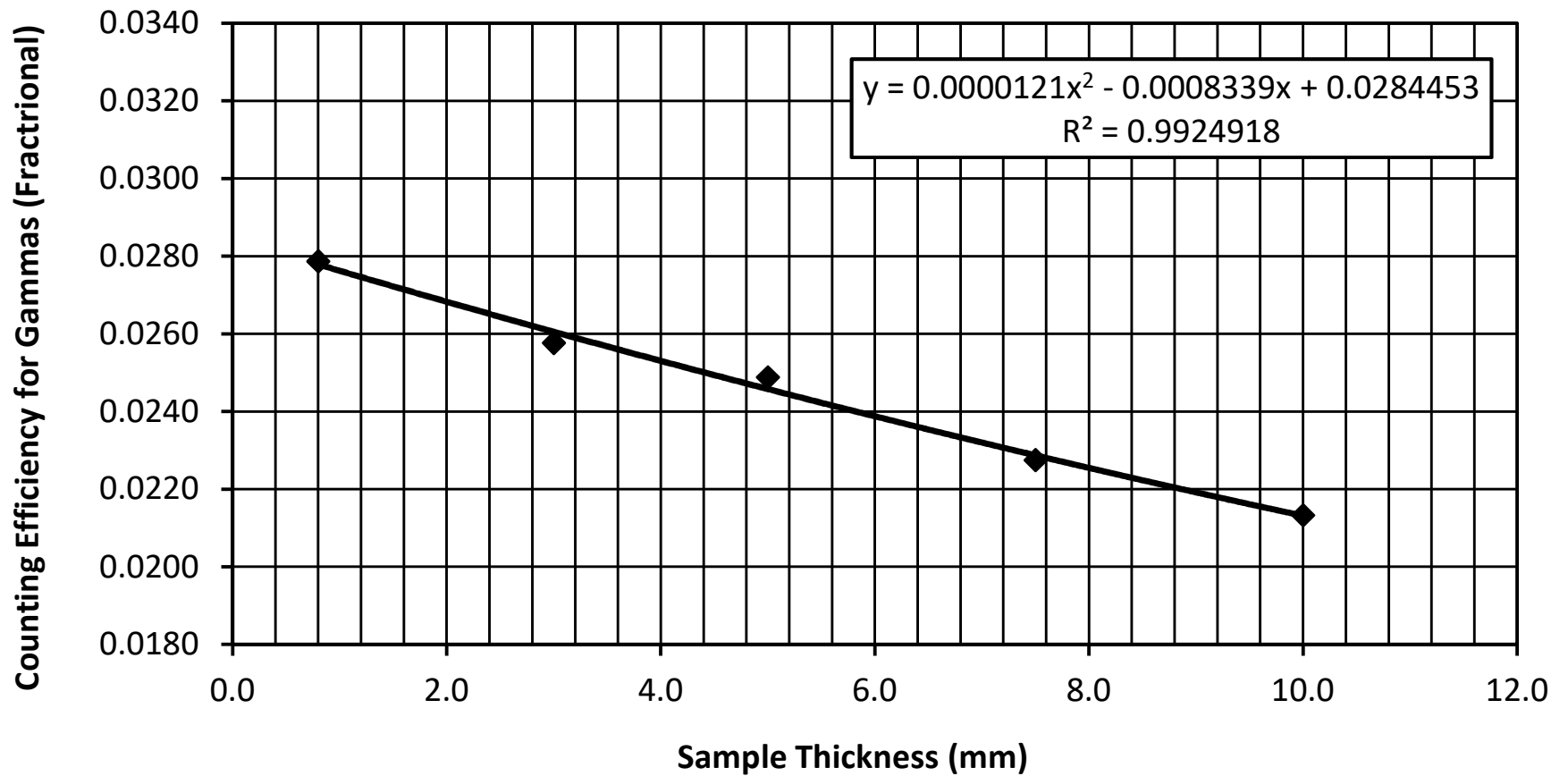
**Note:** Results relate only to the items tested.

ISO / IEC 17025:2005 Accredited with the Canadian Association for Laboratory Accreditation (CALA Accreditation No. A3306)

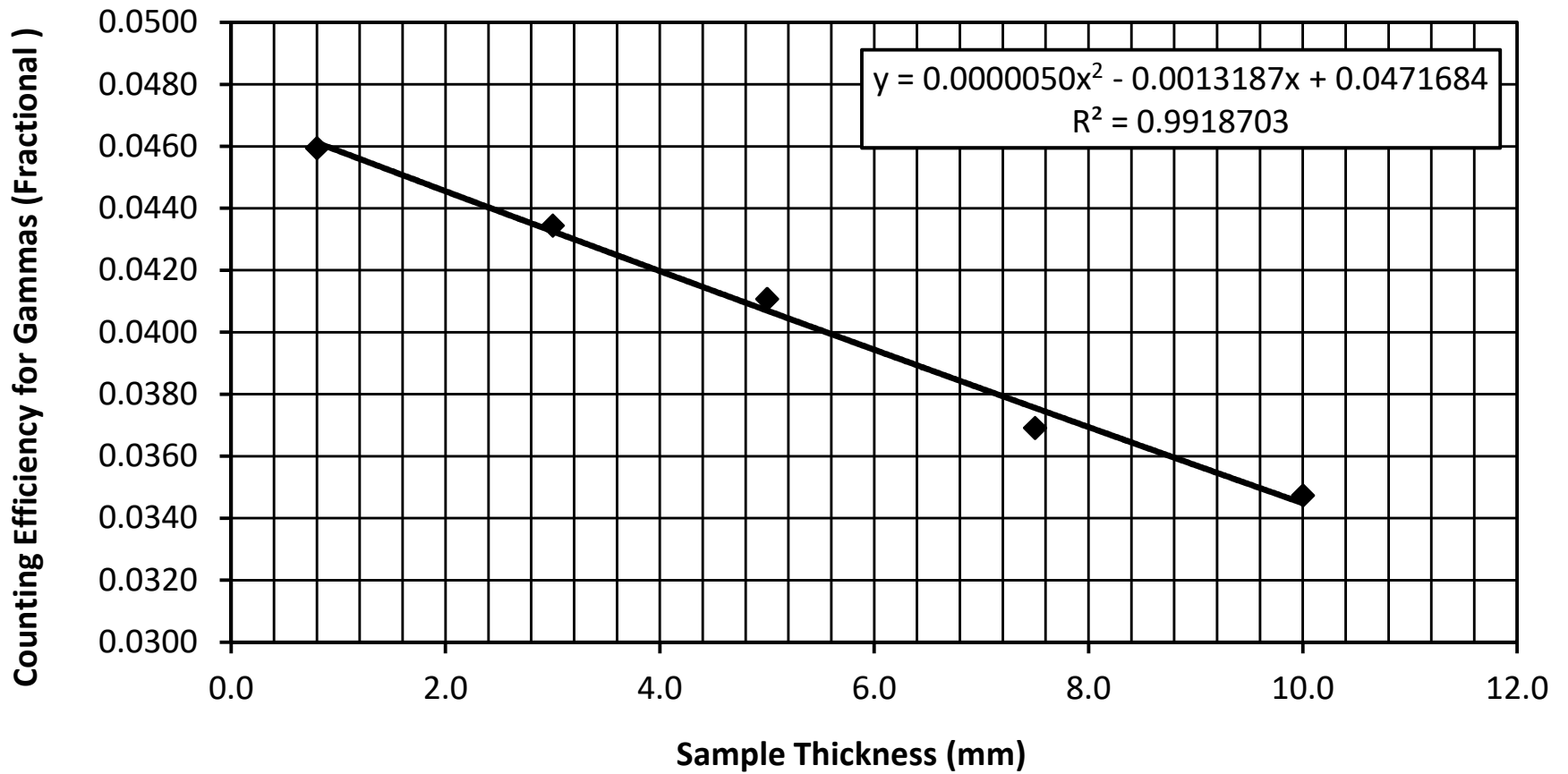
### Cs-137 Counting Efficiency of Gammas vs. Sample Thickness (mm) GMX 25% Detector (Apr 3 - 5, 2019)



### Cs-137 Counting Efficiency of Gammas vs. Sample Thickness (mm) GEM 19% Detector (Apr 3 - 4, 2019)

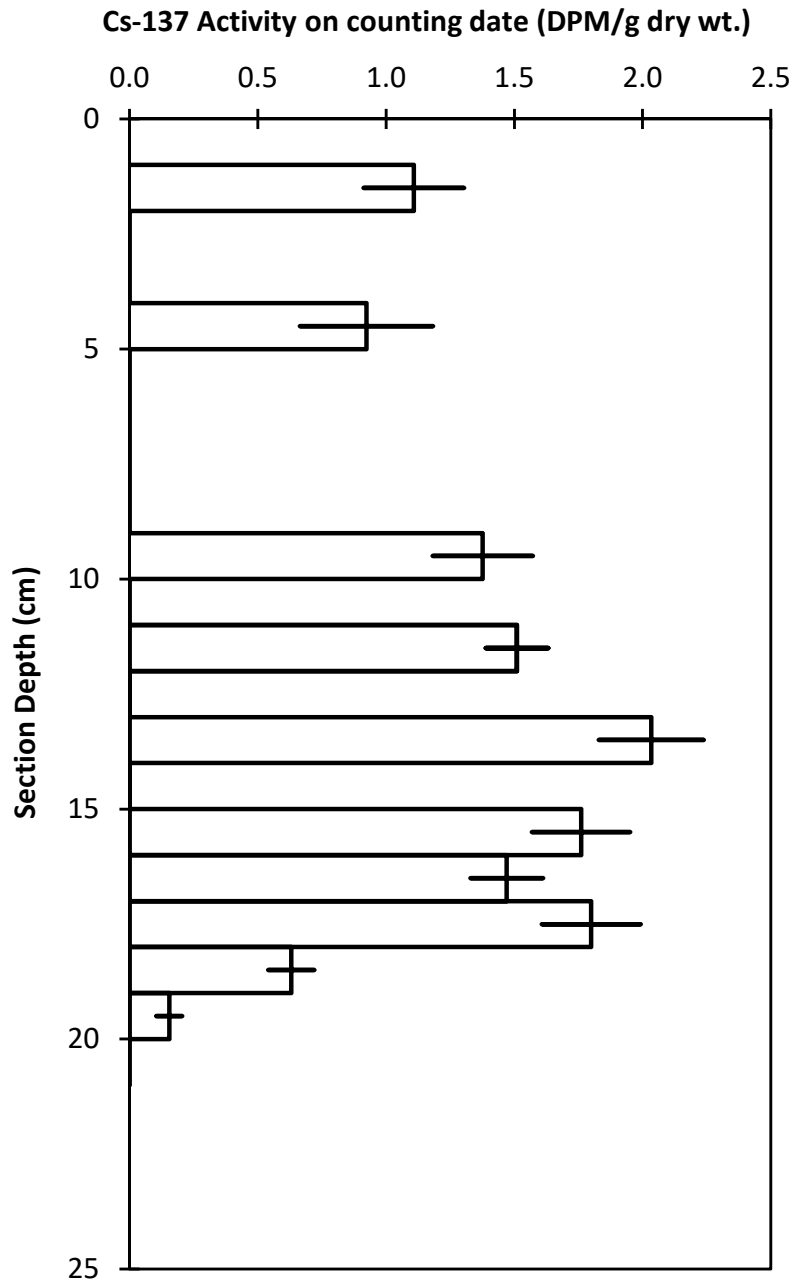


### Cs-137 Counting Efficiency of Gammas vs. Sample Thickness (mm) Canberra 29% Detector (Apr 10 - 11, 2019)



### Cs-137 in Sediments

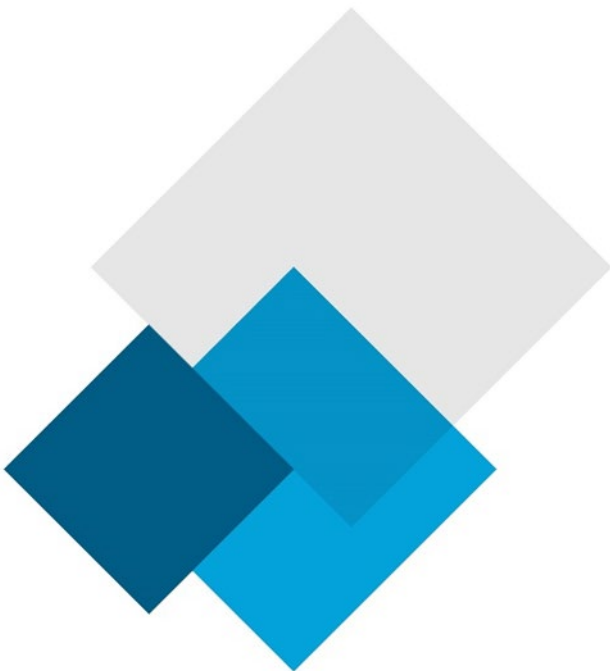
#### 3A1



Note: The bar plotted at the midpoint depth of each section represents +/- 1 standard deviation of the Cs-137 counting error.

# Appendix 7

Radio Isotopic Analysis Core 4A



# Interpretation of Pb-210, Ra-226 and Cs-137 Results

## Flett Research Ltd.

440 DeSalaberry Ave. Winnipeg, MB R2L 0Y7

Fax/Phone: (204) 667-2505

Email: [flett@flettresearch.ca](mailto:flett@flettresearch.ca) Webpage: <http://www.flettresearch.ca>

---

## Client: Lorrain, Stéphane

**Address:** SNC-LAVALIN GEM QUÉBEC INC., 455, boul. René-Lévesque ouest, Montréal (Québec) H2Z 1Z3

**Core ID:** 4A

**Transaction ID:** 882

**PO/Contract No.:** 653502-0028

**Date Received:** 20-Feb-19

**Analysis Dates:** February 25 - April 28, 2019

**Analysts:** L. Hesketh-Jost; X. Hu

**Sampling Date:** 10-Feb-19

**Project:** #653502

*Results authorized by Dr. Robert J. Flett, Chief Scientist*

---

## INTERPRETATION

### Observations:

The Pb-210 profile exhibits an irregular but approximately exponential decrease in total Pb-210 activity as a function of depth. The maximum activity of 11.20 DPM/g observed in the surface section (extrapolated depth 0 - 1.5 cm) is about 35 times the lowest activity of 0.32 DPM/g observed in section 38 - 39 cm (Pages 2 & 3).

The dry bulk densities gradually increase from 0.162 g/cm<sup>3</sup> at the surface to 0.454 g/cm<sup>3</sup> at section 31 (depth 30 - 31 cm). Below 31 cm depth the dry bulk densities rapidly decrease from 0.390 g/cm<sup>3</sup> at section 32 (depth 31 - 32 cm) to 0.146 g/cm<sup>3</sup> at the bottom of the core (Page 2 & 4).

Ra-226 was measured at 0.83, 0.91 and 0.20 DPM/g in sections 5 - 6 cm, 17 - 18 cm and 38 - 39 cm, respectively (Pages 9 - 12). The Pb-210 activity in the 38 - 39 cm section barely exceeds the Ra-226 activity measured in the same section, indicating that the background level of Pb-210 has been achieved in this core.

Cs-137 was measured in 10 sections in the 0 - 34 cm core interval. Activities in the 14 - 33 cm portion of the core are all significantly above background, ranging between 0.45 - 1.33 DPM/g (Pages 13 & 17). Below 31 cm, the Cs-137 activity declines with depth.

### Regression model of Unsupported Pb-210 activity vs. Cumulative Dry Weight (g/cm<sup>2</sup>):

When applying the linear regression model, it is assumed that the input of Pb-210 and the sediment accumulation rate are constant. Although variation in the sediment accumulation rate is apparent, the linear regression model was applied to sections 1 - 30 (depth 0 - 30 cm), because it appears that the average sediment accumulation rate will be reasonably estimated. This estimate of sediment accumulation rate is used to validate the CRS model.

The regression results are seen in Page 5. The model predicts ( $R^2 = 0.9485$ ) an average sediment accumulation rate of 0.2037 g/cm<sup>2</sup>/yr when the unsupported Pb-210 activity was calculated by subtracting the nearest neighbouring Ra-226 measurement from each total Pb-210 value. The age at the bottom of any core section can be estimated by dividing the cumulative dry weight/cm<sup>2</sup> by the accumulation rate. For example, the age at the bottom of section 15 (extrapolated depth 16 cm) is calculated as 4.842 / 0.2037 = 23.8 yr. The age estimate at the bottom of each section is shown on Pages 2 (column AM) & 6.

### CRS model of Age at bottom of Extrapolated section in years vs. Depth of bottom edge of current section in cm:

The CRS model assumes constant input of Pb-210 and a core that is long enough to include all of the measurable atmospheric source Pb-210, i.e. it contains a complete Pb-210 inventory. The facts that 1) the rapid decrease in dry bulk density at section 32 (depth 31- 32 m), and 2) the significant change in Ra-226 activity at the bottom of the core, are possible causes for us to discard the deeper portion of the core (i.e. truncate the core) due to the increasing uncertainty of the sedimentation process. The Ra-226 activities indicate that the background Pb-210 activity level has not been achieved at 31 cm, leaving us with an incomplete truncated core that normally cannot be processed by the CRS model.

However, in this core it is possible to calibrate the CRS model against the 1963 maximum Cs-137 input, and therefore allow the CRS model to be used. The total atmospheric Pb-210 inventory (DPM/cm<sup>2</sup>), required in the CRS model calculation, has been chosen (79.451 DPM/cm<sup>2</sup>) such that the CRS model correctly assigned an age of 2019 - 1963 = 56 years to the midpoint depth (30.5 cm) of the 30 - 31 cm section. The calculation is done as follows:

$$(\ln(I_T/I_1))/k = 56 \text{ years}$$

Where

$$k = \ln 2/t_{1/2} = \ln 2/22.3 = 0.0310828$$

$I_1$  is the Pb-210 inventory (DPM/cm<sup>2</sup>) below depth 30.5 cm

$$I_1 = I_T - 65.515 \text{ (the Pb-210 inventory above 30.5 cm)}$$

$I_T$  is the total Pb-210 inventory (DPM/cm<sup>2</sup>) in core (artificial) required for the CRS model to predict 56 yrs at 30.5 cm;

[see cell AK63 on sheet 'Pb-210 and Dry Bulk Density']

then

$$(\ln(I_T/(I_T - 65.515)))/0.0310828 = 56$$

$$I_T/(I_T - 65.515) = e^{56 \times 0.0310828} = 5.701$$

$$I_T = 5.701 I_T - 5.701 * 65.515$$

$$I_T = (5.701 * 65.515) / (5.701 - 1) = 79.451$$

With the CRS model calibrated, it has been used to calculate age for each section in the upper 31 cm of the core. The sections below 31 cm were excluded in the CRS model data set due to the significant uncertainty of dating.

The measured total activity results (DPM/g) are shown in column AF of the main data table on Page 2. The estimated age at the bottom of each section is shown in column AI, also shown on Page 2. The average sediment accumulation rate, from core surface to the extrapolated bottom depth of any section, can be calculated by dividing the cumulative dry mass at the bottom of the extrapolated section by the calculated age at that depth. For example, the average sediment accumulation rate, from the core surface to the bottom of section 15 (extrapolated depth 16 cm) can be calculated as: 4.842 / 24.3 = 0.1993 g/cm<sup>2</sup>/yr. The individual sedimentation rate for each section is shown in column AL on Page 2. Plots of age vs. depth, sediment accumulation rate vs. depth and sediment accumulation rate vs. age are seen in Pages 6, 7 and 8 respectively.

### **Conclusion:**

It is assumed that the 1963 peak input of atmospheric Cs-137 has been recorded in the 30 - 31 cm section (Pages 13 and 17), where the maximum Cs-137 activity of 1.33 DPM/g was observed. The CRS model has been forced to predict an age of 56 years to the midpoint depth of this section (30.5 cm). With the CRS model calibrated, section ages down to a depth of 31 cm have been calculated.

Over the interval of sections 1 - 30 (depth 0 - 30 cm), the CRS model predicts an average sediment accumulation rate of 0.1894 g/cm<sup>2</sup>/yr, while the regression model predicts an average rate of 0.2037 g/cm<sup>2</sup>/yr. These results are relatively close and suggest that the CRS model is functioning correctly. In general, the CRS model is to be preferred because it can provide valid predictions over the entire length of the modelled core, even though the sediment accumulation rate is changing with time.

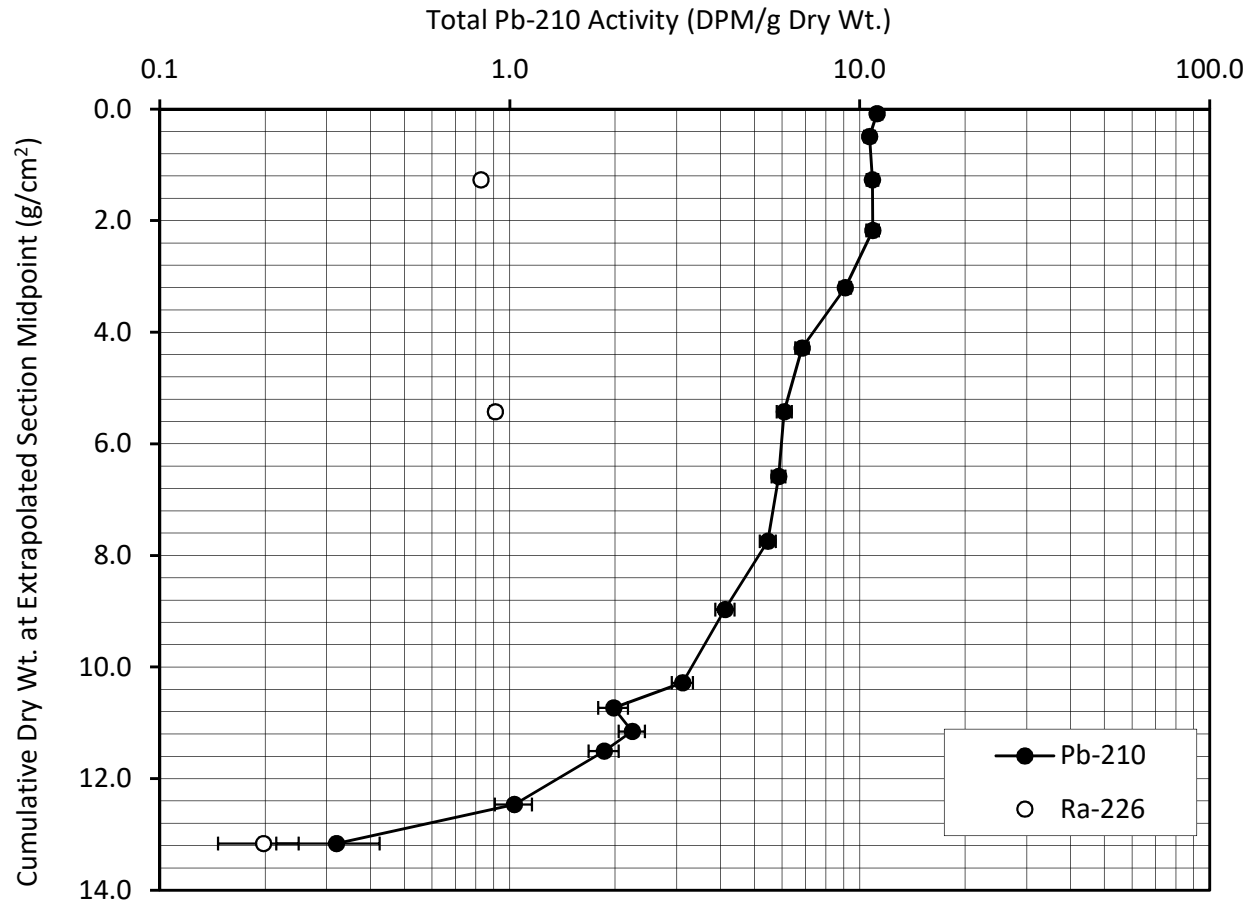
The sediment accumulation rates are variable in this core, ranging between 0.1558 g/cm<sup>2</sup>/yr and 0.2343 g/cm<sup>2</sup>/yr in 0 - 30 cm core interval, with a large increase at section 31 (depth 30 - 31 cm) increasing to 0.4041 g/cm<sup>2</sup>/yr (by the CRS model) (Pages 2, 3 & 7).

Overall, the analytical quality of radioisotope data (based upon the recovery of spike, the recovery of CRM, the results of repeat analyses and blanks) is considered good.



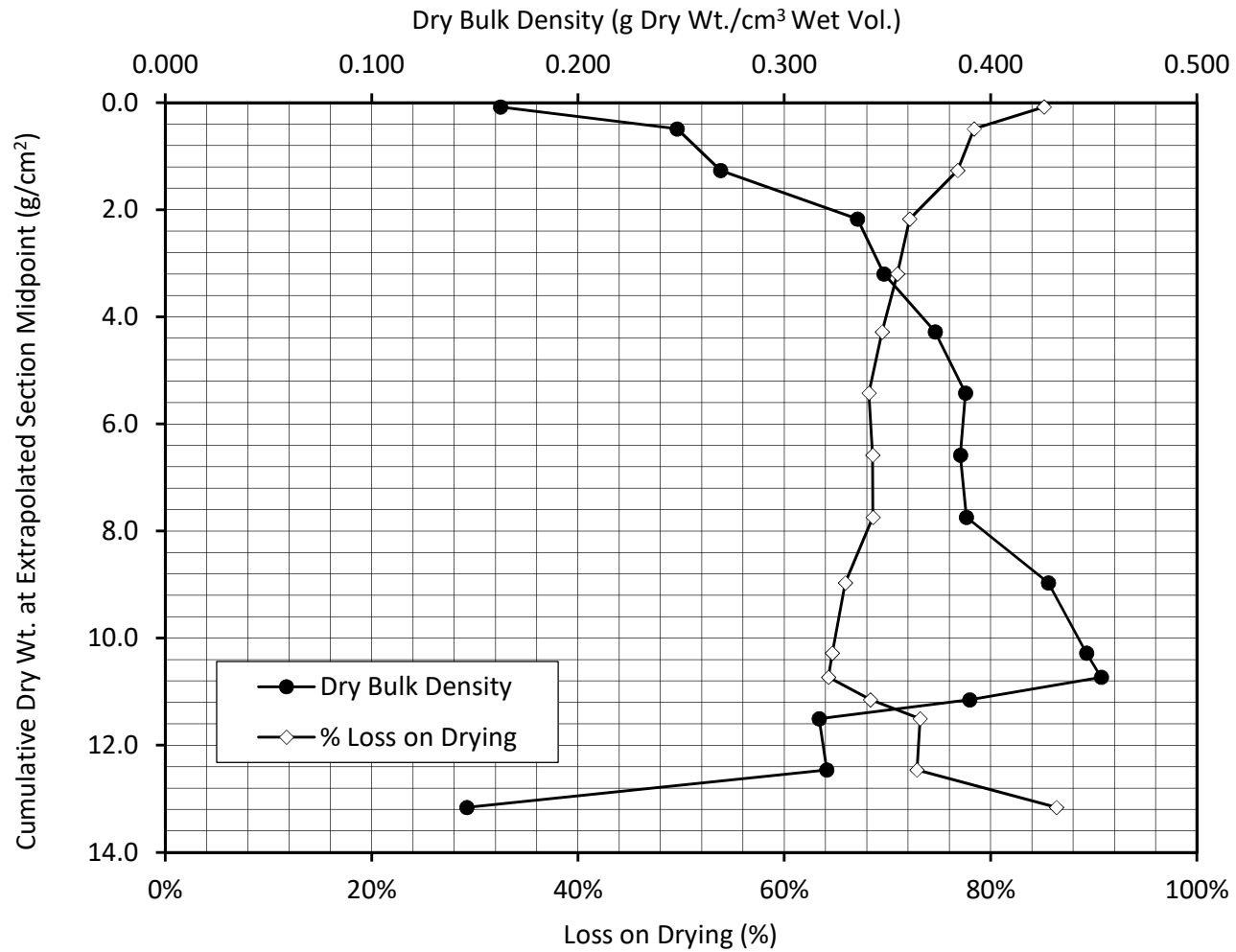
**Total Pb-210 Activity vs. Accumulated Sediment**

**4A**



**Dry Bulk Density and % Loss on Drying**  
**vs. Accumulated Sediment**

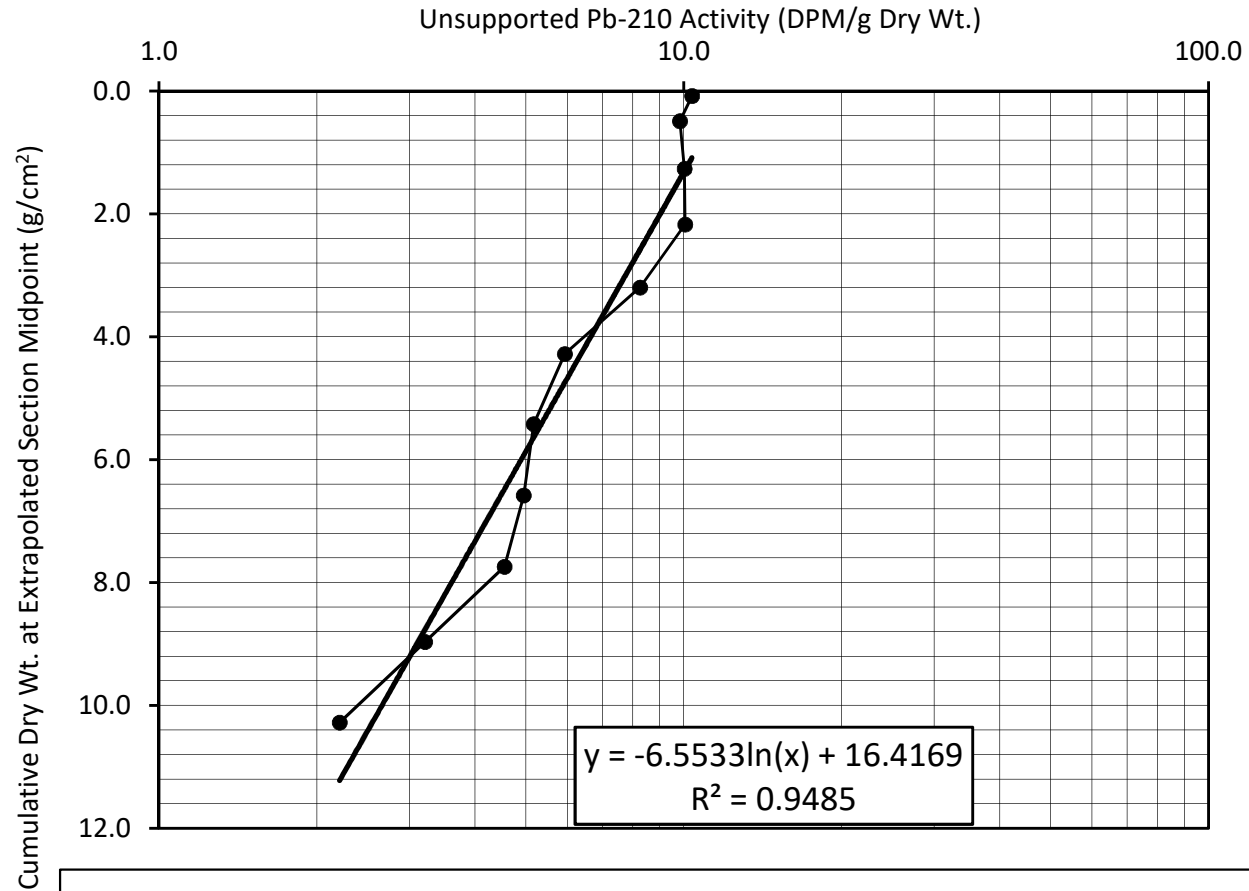
**4A**



**Regression of Unsupported Pb-210 Activity  
vs. Accumulated Sediment**

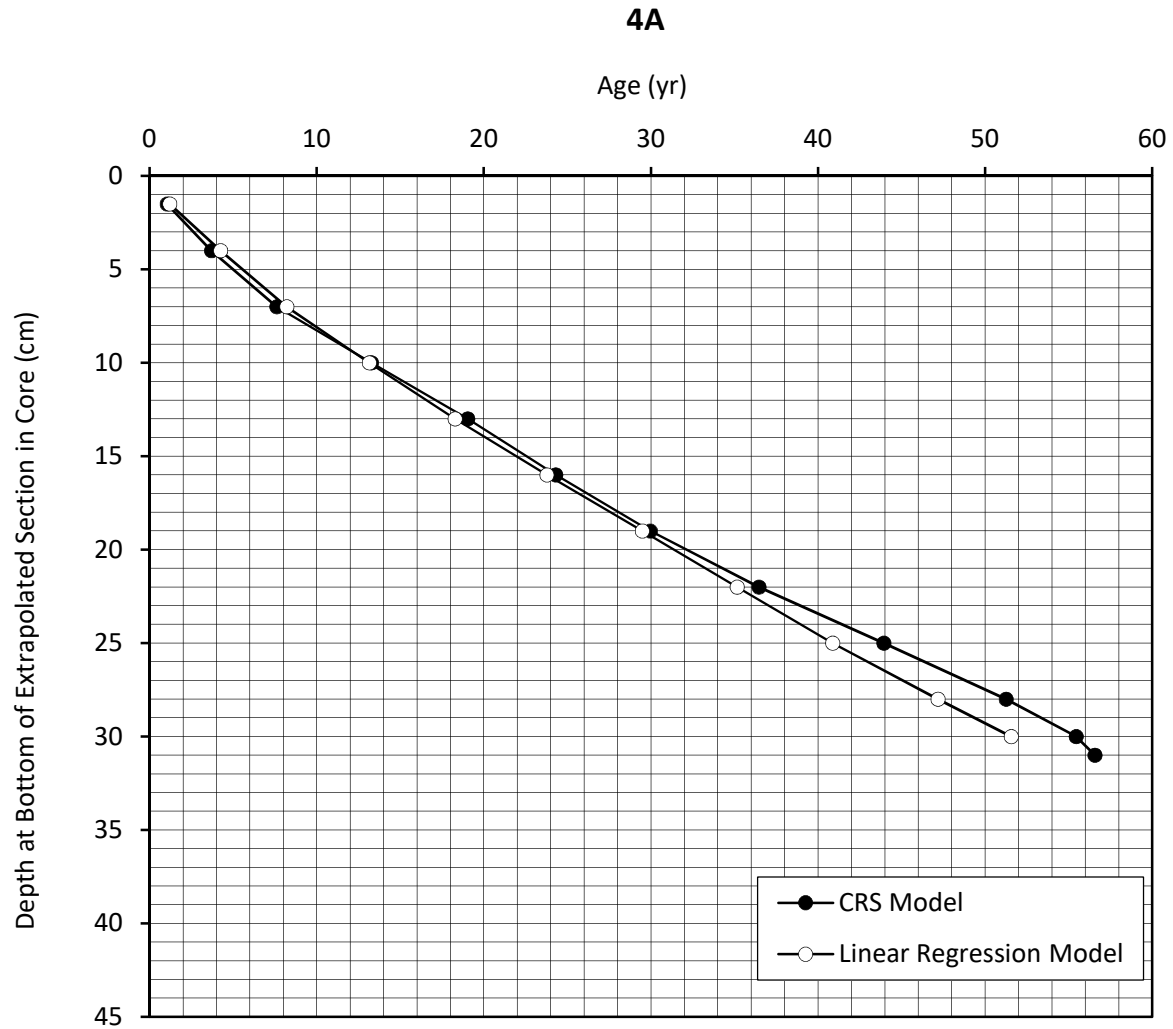
(Unsupported activity calculated by subtracting the nearest neighbouring Ra-226 measurement from each total Pb-210 value)

**4A**



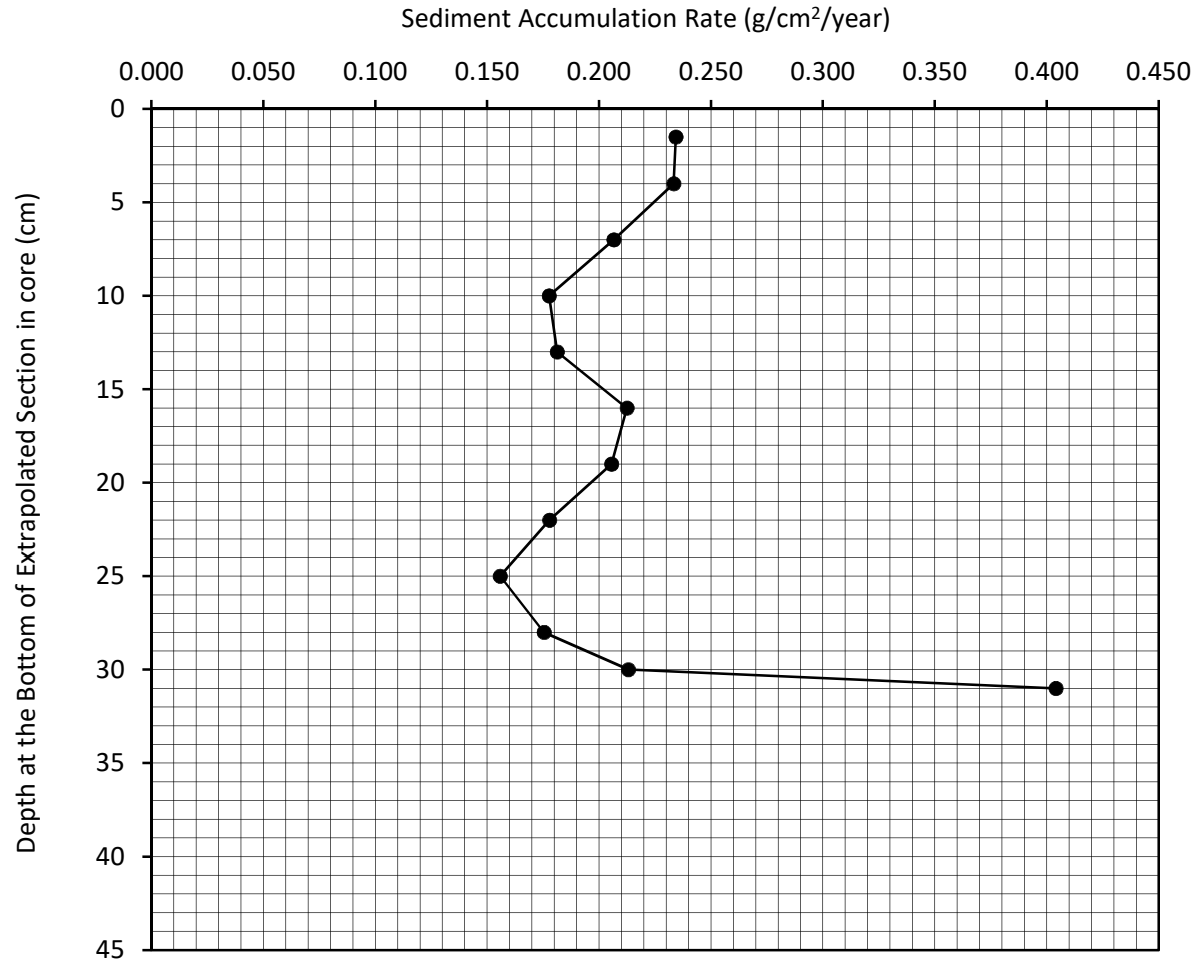
**Sediment Accumulation Rate in sections 1 - 30**  
 $= (-6.5533) \times 0.6931 / (-22.3) = 0.2037 \text{ g/cm}^2/\text{yr}$

Age (yr) vs. Depth (cm)  
CRS Model vs. Linear Regression Model

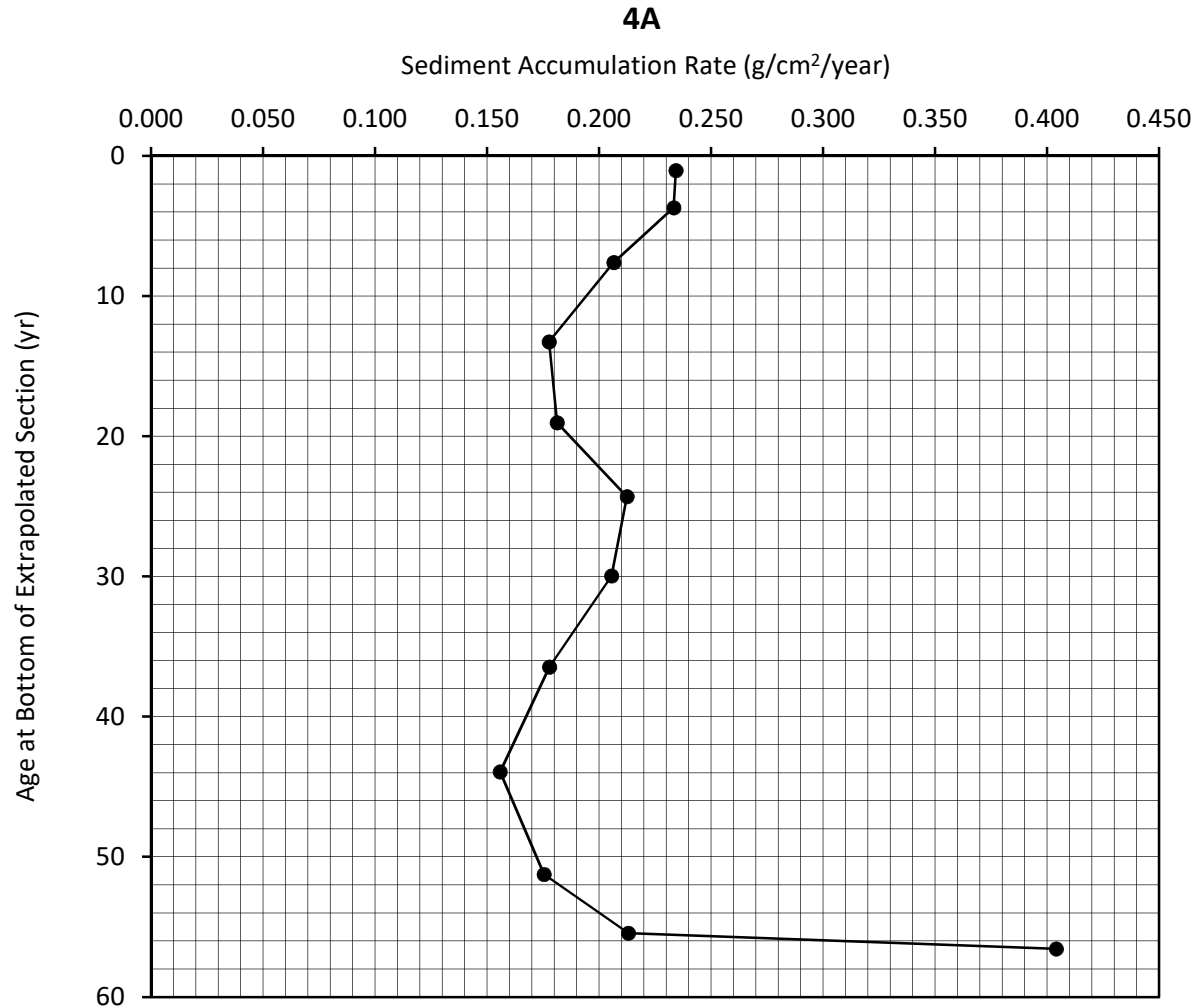


**CRS Sediment Accumulation Rate (g/cm<sup>2</sup>/year)**  
**vs. Depth at the Bottom of Extrapolated Section in Core (cm)**

**4A**



**CRS Sediment Accumulation Rate (g/cm<sup>2</sup>/year)**  
**vs. Age at Bottom of Extrapolated Section (yr)**



# Results of Ra-226 Analysis by Rn-222 Emanation

Flett Research Ltd.

440 DeSalaberry Ave., Winnipeg, MB R2L 0Y7

Fax/Phone: (204) 667-2505

Email: flett@flettresearch.ca Webpage: http://www.flettresearch.ca

## Client: Lorrain, Stéphane

Address: SNC-LAVALIN GEM QUÉBEC INC., 455, boul. René-Lévesque ouest, Montréal (Québec) H2Z 1Z3

Core ID: 4A

Transaction ID: 882

Date Received: 20-Feb-19

PO/Contract No.: 653502-0028

Sampling Date: 10-Feb-19

Analysis Dates: February 25 - April 13, 2019

Project: #653502

Analysts: X. Hu; L. Hesketh-Jost

Salt Correction Applied? No

Analytical Method: N40110 Determination of Radium-226 in Sediment, Soil and Peat by Radon-222 Emanation (Version 3)

**Comments:**

**Detection Limit:** The method detection limit (MDL) is dependent on the amount of sample analyzed. For a 60,000 second counting time the MDL at 95% confidence for 2 g of dry sample is 0.1 DPM/g and for 0.5 g of dry sample is 0.5 DPM/g.

**Estimated Uncertainty:** The estimate of uncertainty of measurement for this method in this laboratory is approximately ±12% at 95% confidence level (approximately 40,000 counts in 60,000 seconds).

Results authorized by Dr. Robert J. Flett, Chief Scientist

Core ID	Sample ID	Ra-226 Activity (DPM/g Dry Wt.)	Combined Error: 1 SD (DPM/g Dry Wt.)	Comments Code for Ra-226 Analysis
4A	4A-2/2-39	0.20	0.05	
4A	4A-2/2-6	0.83	0.03	
4A	4A-2/2-18	0.91	0.03	

Q:\Clients A-L\Lorrain, Stephane\2019(882)\Radioisotopes\4A\Pb-210, Ra-226 and Cs-137 Lorrain Core 4A May 6-19 Final.xlsm

**Duplicate:** Two subsamples of the same sample were carried through the analytical procedure in an identical manner.

**Re-count:** The sample bottle was re-sealed after the initial analysis, and was re-counted after 11 or more days of Rn-222 ingrowth. Repeat counting was chosen over duplicate analysis due to insufficient sample material provided.

This test report shall not be reproduced, except in full, without written approval of the laboratory.

Note: Results relate only to the items tested.

13-Apr-19

Page 9 of 16

ISO / IEC 17025:2005 Accredited with the Canadian Association for Laboratory Accreditation (CALA Accreditation No. A3306)

**Radium Analysis by Rn-222 Emanation**

Core ID	4A
Sample ID	4A-2/2-39
Lucas Cell No.	3
Number of days since Rn board last run	1
Dry weight of sample counted (g)	0.656
Total count in period	1150
Total count in period (carryover corrected)	n/a
Cell Blank count (CPM)	0.562
System Blank (DPM)	0.395
System Efficiency	0.839
Count duration (minutes)	1000

Typical carryover is about 1 - 2 % of the net counts (gross counts less system background) of the sample counted on the previous day. The carryover is subtracted from the gross counts of current sample. This correction is not required if the sample is run after a blank.

Carryover correction?	No
-----------------------	----

	Year	Month	Day	Hour	Minute	Second	Ingrowth time (Days)	Ingrowth factor	Decay correction
When sample last stripped	2019	2	26	16	55	0	14.83	0.93190	0.92490
When cell filled	2019	3	13	12	44	56			
Beginning time of count	2019	3	13	14	45	19			

Counts per minute	1.15
Gross CPM less Cell Blank (CPM)	0.59
CPM (decay during count corrected)	0.64
DPM Sample +System (efficiency corrected)	0.76
DPM sample	0.39
DPM/g	0.59
<b>Ra-226 DPM/g</b>	<b>0.20</b>
Ra-226 pCi/g	0.09

Error ± 1 sd    0.1007 DPM

**Error ± 1 sd    0.0511 DPM/g**

Error % =    25.9

Chemist	XH
PMT High Voltage +ve	770
HV Power supply	Spectrum Technologies
Alpha Counter	Spectrum Technologies
Region of Interest Ch.#s	28-1022
PMT	6655A - #1
Preamp	Canberra 2007P tube base
Amp Gain	1

**Radium Analysis by Rn-222 Emanation**

Core ID	4A
Sample ID	4A-2/2-6
Lucas Cell No.	3
Number of days since Rn board last run	1
Dry weight of sample counted (g)	1.525
Total count in period	3726
Total count in period (carryover corrected)	n/a
Cell Blank count (CPM)	0.562
System Blank (DPM)	0.395
System Efficiency	0.839
Count duration (minutes)	1000

Typical carryover is about 1 - 2 % of the net counts (gross counts less system background) of the sample counted on the previous day. The carryover is subtracted from the gross counts of current sample. This correction is not required if the sample is run after a blank.

Carryover correction?	No
-----------------------	----

	Year	Month	Day	Hour	Minute	Second	Ingrowth time (Days)	Ingrowth factor	Decay correction
When sample last stripped	2019	3	21	15	31	0	20.02	0.97343	0.92490
When cell filled	2019	4	10	15	58	59			
Beginning time of count	2019	4	10	17	59	22			

Counts per minute	3.73
Gross CPM less Cell Blank (CPM)	3.16
CPM (decay during count corrected)	3.42
DPM Sample +System (efficiency corrected)	4.08
DPM sample	3.78
DPM/g	2.48
<b>Ra-226 DPM/g</b>	<b>0.83</b>
Ra-226 pCi/g	0.37

Error ± 1 sd    0.1176 DPM

**Error ± 1 sd    0.0257 DPM/g**

Error % =    3.1

Chemist	XH
PMT High Voltage +ve	770
HV Power supply	Spectrum Technologies
Alpha Counter	Spectrum Technologies
Region of Interest Ch.#s	28-1022
PMT	6655A - #1
Preamp	Canberra 2007P tube base
Amp Gain	1

**Radium Analysis by Rn-222 Emanation**

Core ID	4A
Sample ID	4A-2/2-18
Lucas Cell No.	3
Number of days since Rn board last run	1
Dry weight of sample counted (g)	1.258
Total count in period	3500
Total count in period (carryover corrected)	3471
Cell Blank count (CPM)	0.562
System Blank (DPM)	0.395
System Efficiency	0.839
Count duration (minutes)	1000

Typical carryover is about 1 - 2 % of the net counts (gross counts less system background) of the sample counted on the previous day. The carryover is subtracted from the gross counts of current sample. This correction is not required if the sample is run after a blank.			
Carryover correction?	Yes	Mean of last 10 carryover measurements	1.02%
Gross counts of previous sample	3726	Mean of last 6 system background measurements	887
Counts carried over from previous sample	29		

	Year	Month	Day	Hour	Minute	Second	Ingrowth time (Days)	Ingrowth factor	Decay correction
When sample last stripped	2019	3	21	15	28	0	21.01	0.97778	0.92490
When cell filled	2019	4	11	15	37	41			
Beginning time of count	2019	4	11	17	38	4			

Counts per minute	3.47
Gross CPM less Cell Blank (CPM)	2.91
CPM (decay during count corrected)	3.15
DPM Sample +System (efficiency corrected)	3.75
DPM sample	3.43
DPM/g	2.73
<b>Ra-226 DPM/g</b>	<b>0.91</b>
Ra-226 pCi/g	0.41

Error ± 1 sd    0.1156 DPM

**Error ± 1 sd    0.0306 DPM/g**

Error % =    3.4

Chemist	XH
PMT High Voltage +ve	770
HV Power supply	Spectrum Technologies
Alpha Counter	Spectrum Technologies
Region of Interest Ch.#s	28-1022
PMT	6655A - #1
Preamp	Canberra 2007P tube base
Amp Gain	1

# Results of Cs-137 Analysis

Flett Research Ltd.

440 DeSalaberry Ave. Winnipeg, MB R2L 0Y7

Fax / Phone: (204) 667-2505

Email: flett@flettresearch.ca Webpage: http://www.flettresearch.ca

**Client: Lorrain, Stéphane**

**Address:** SNC-LAVALIN GEM QUÉBEC INC., 455, boul. René-Lévesque ouest, Montréal (Québec) H2Z 1Z3

**Core ID:** 4A  
**Date Received:** 20-Feb-19  
**Sampling Date:** 10-Feb-19  
**Project:** #653502

**Transaction ID:** 882  
**PO/Contract No.:** 653502-0028  
**Analysis Dates:** April 8 - 28, 2019  
**Analysts:** X. Hu; L. Hesketh-Jost

Salt Correction?	No
------------------	----

**Analytical Method:** N30120 Measurement of Gamma-Ray Emitting Radionuclides in Sediment/Soil Samples by Gamma Spectrometry Using HPGe Detectors (Version 2)

**Deviation from Method:**

**Comments:** <2SD: The measured Cs-137 activity is less than 2 counting errors (i.e. 2 SD), suggesting no significant presence of Cs-137 in this sample.

**Detection Limit:** The method detection limit (MDL) is 0.3 DPM/g for an 80,000 seconds counting period when measuring a 9 g of dry sample at a 95% confidence level. The method detection limit can be decreased to 0.1 DPM/g if 32 g of sample is used.

**Estimated Uncertainty:** The estimated uncertainty of this method has been determined to be ± 10% at 95% confidence for samples with activities between 0.5 and 20 DPM/g, counting time 80,000 seconds and sample weights ranging from 9 to 32 grams. Method uncertainty can increase to 85% for samples with activities near detection limit (0.1 - 0.3 DPM/g).

Results authorized by Dr. Robert J. Flett, Chief Scientist

Sample ID	Upper Depth (cm)	Lower Depth (cm)	Day Sample Counted	Month Sample Counted	Year Sample Counted	Integral NET Cs-137 Peak	Counting Error 1 SD (Counts)	Count Time (seconds)	Dry Sample Weight (g)	Sample Thickness (mm)	CPM/g	Efficiency for Gammas Fractional	Gammas per min. per gram	Activity DPM/g (dry wt.) on Counting Date	Approx. Error DPM/g	Activity DPM/g (dry wt.) on Sampling Date	Approx. Error DPM/g	Activity pCi/g (dry wt.) on Sampling Date	Approx. Error pCi/g	Activity mBq/g (dry wt.) on Sampling Date	Approx. Error mBq/g	Detector Used	Comments Code for Cs-137 Analysis
4A-2/2-1	0	1	26	4	2019	-7	31	80000	1.654	0.98	-0.0032	0.0276	-0.1148	-0.13	0.60	-0.14	0.60	-0.06	0.27	-2.26	9.99	GEM	<2SD
4A-2/2-6	5	6	27	4	2019	13	43	80000	7.278	2.30	0.0013	0.0292	0.0459	0.05	0.18	0.05	0.18	0.02	0.08	0.90	2.98	GEM	<2SD
4A-2/2-15	14	15	27	4	2019	126	30	80000	8.613	2.55	0.0110	0.0264	0.4156	0.49	0.12	0.49	0.12	0.22	0.05	8.17	1.95	GEM	
4A-2/2-21	20	21	8	4	2019	195	41	80000	8.681	2.85	0.0168	0.0289	0.5826	0.68	0.14	0.69	0.14	0.31	0.06	11.44	2.40	GMX	
4A-2/2-27	26	27	8	4	2019	199	37	80000	9.199	2.93	0.0162	0.0261	0.6214	0.73	0.14	0.73	0.14	0.33	0.06	12.20	2.27	GEM	
4A-2/2-30	29	30	11	4	2019	311	36	80000	12.718	4.08	0.0183	0.0252	0.7264	0.85	0.10	0.86	0.10	0.39	0.04	14.26	1.65	GEM	
4A-2/2-31	30	31	23	4	2019	453	44	80000	10.505	3.68	0.0323	0.0285	1.1367	1.33	0.13	1.34	0.13	0.60	0.06	22.34	2.17	GMX	
4A-2/2-32	31	32	24	4	2019	287	46	80000	8.462	2.83	0.0254	0.0289	0.8793	1.03	0.17	1.04	0.17	0.47	0.07	17.28	2.77	GMX	
4A-2/2-33	32	33	9	4	2019	113	51	80000	7.589	2.65	0.0112	0.0290	0.3848	0.45	0.20	0.45	0.20	0.20	0.09	7.55	3.41	GMX	
4A-2/2-34	33	34	25	4	2019	53	41	80000	9.432	3.30	0.0042	0.0287	0.1470	0.17	0.13	0.17	0.13	0.08	0.06	2.89	2.24	GMX	<2SD
<b>Cs-137 Standards</b>																							
GMX 32g 10 mm			4	4	2019	19967	143	5000	32.00	10.0	7.4876	0.0237	315.7600	370.61	2.65	957.04							
GMX 24g 7.5mm			5	4	2019	16045	128	9000	24.00	7.5	8.0225	0.0254	315.7400	370.59	2.96	957.04							
GMX 15g 5mm			4	4	2019	10978	106	5000	15.00	5.0	8.7824	0.0278	315.7600	370.61	3.58	957.04							
GMX 9g 3mm			3	4	2019	6862	84	5000	9.00	3.0	9.1493	0.0290	315.7799	370.63	4.54	957.04							
GMX 2.85g 0.8mm			4	4	2019	2237	49	5000	2.854	0.8	9.4057	0.0298	315.7600	370.61	8.12	957.04							
GEM 32g 10 mm			4	4	2019	17960	139	5000	32.00	10.0	6.7350	0.0213	315.7600	370.61	2.87	957.04							
GEM 24g 7.5mm			4	4	2019	14367	124	5000	24.00	7.5	7.1835	0.0227	315.7600	370.61	3.20	957.04							
GEM 15g 5mm			3	4	2019	9822	102	5000	15.00	5.0	7.8576	0.0249	315.7799	370.63	3.85	957.04							
GEM 9g 3mm			4	4	2019	6102	79	5000	9.00	3.0	8.1360	0.0258	315.7600	370.61	4.80	957.04							
GEM 2.85g 0.8mm			4	4	2019	2093	48	5000	2.854	0.8	8.8003	0.0279	315.7600	370.61	8.50	957.04							

Q:\Clients A-L\Lorrain, Stephane\2019(882)\Radioisotopes\4A\Pb-210, Ra-226 and Cs-137 Lorrain Core 4A May 6-19 Final.xlsm

**Duplicate:** Two subsamples of the same sample were carried through the analytical procedure in an identical manner.

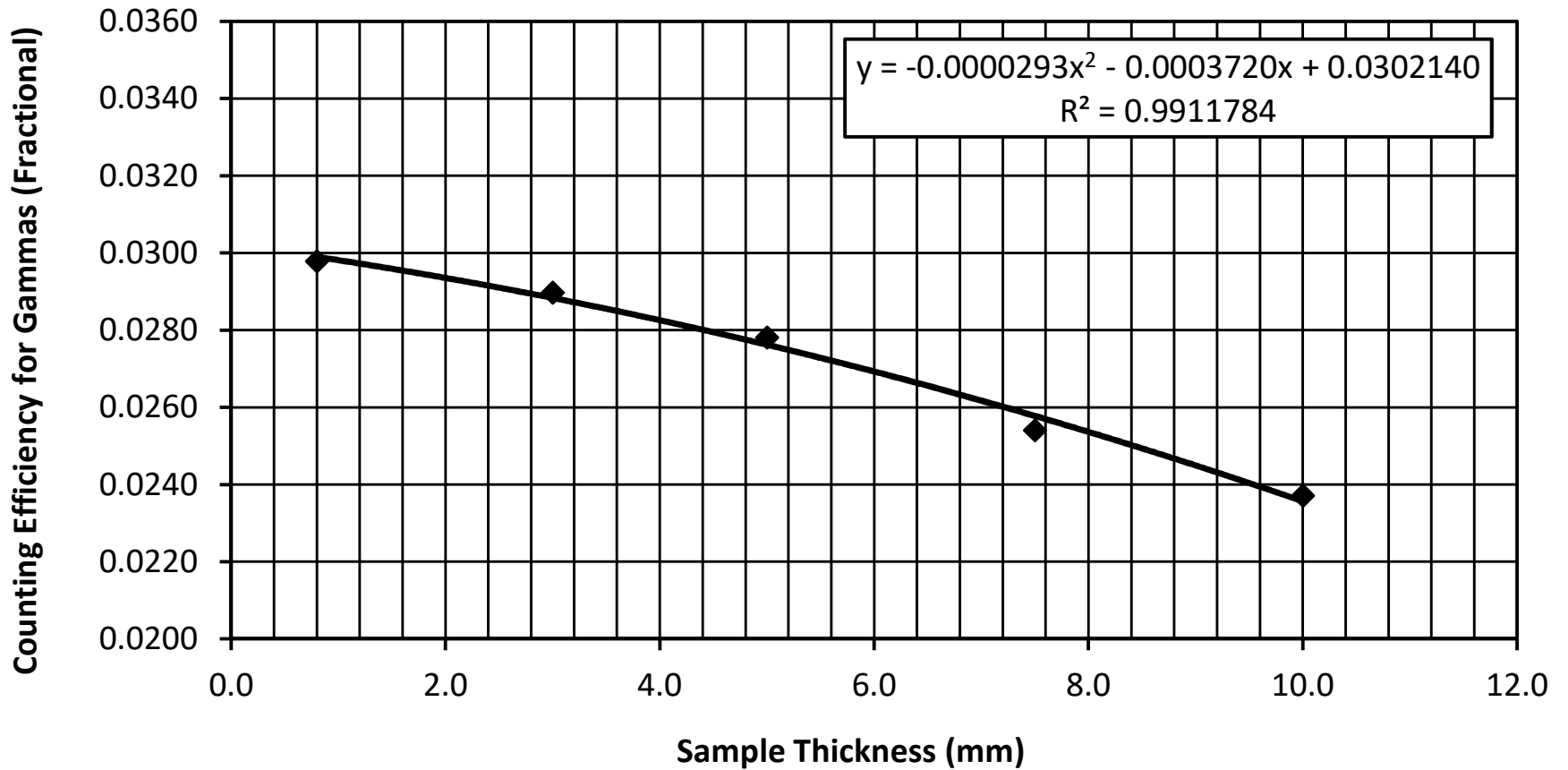
**Re-count:** The entire available dry sample material was used for making the sample pancake, and then this sample pancake was counted twice on a HPGe detector. Repeat counting was chosen over duplicate analysis due to insufficient sample material provided.

**This test report shall not be reproduced, except in full, without written approval of the laboratory.**

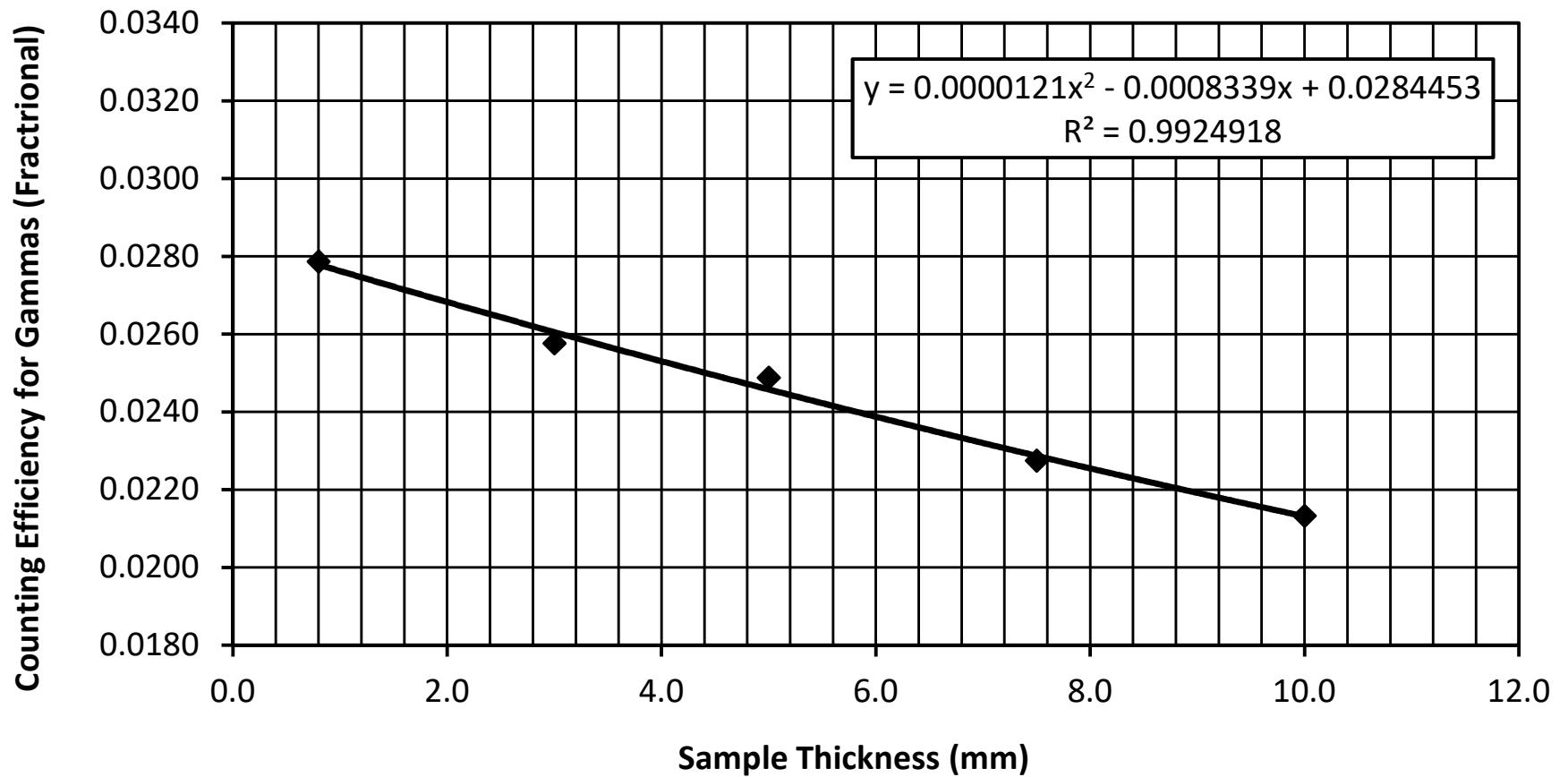
**Note:** Results relate only to the items tested.

ISO / IEC 17025:2005 Accredited with the Canadian Association for Laboratory Accreditation (CALA Accreditation No. A3306)

### Cs-137 Counting Efficiency of Gammas vs. Sample Thickness (mm) GMX 25% Detector (Apr 3 - 5, 2019)



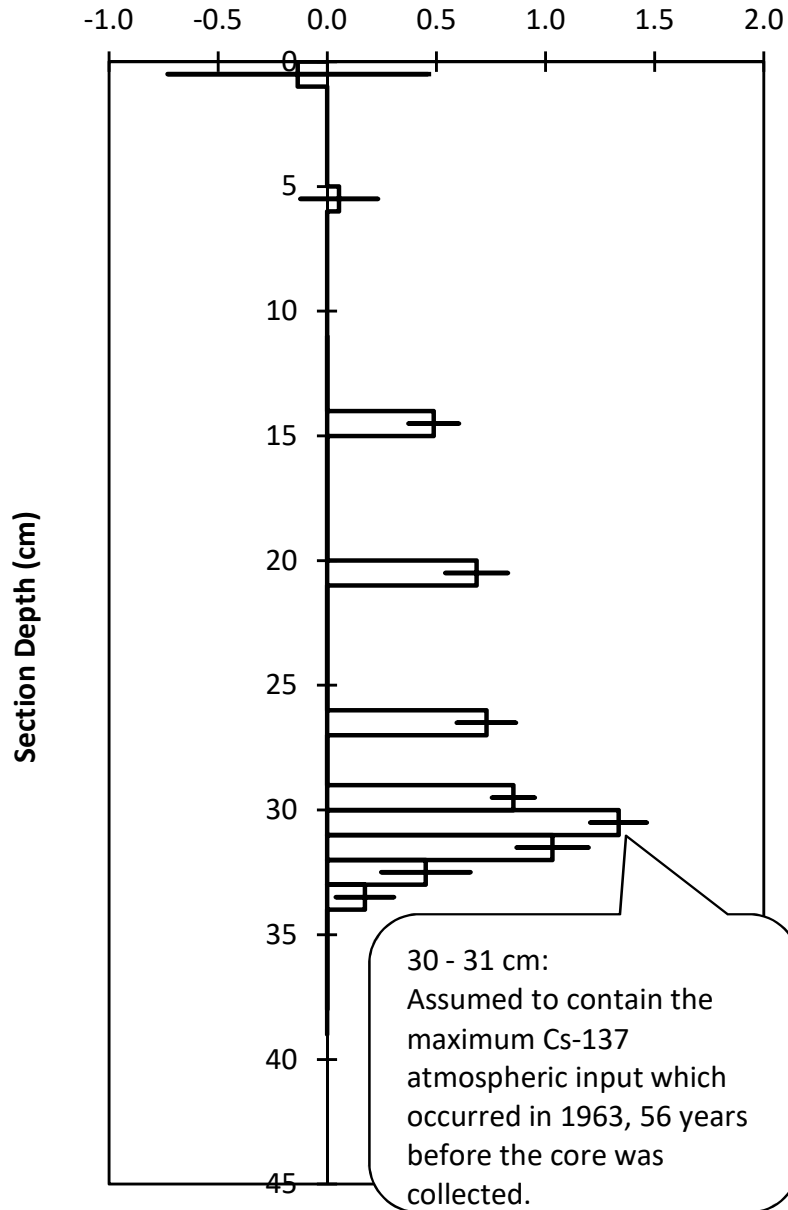
### Cs-137 Counting Efficiency of Gammas vs. Sample Thickness (mm) GEM 19% Detector (Apr 3 - 4, 2019)



### Cs-137 in Sediments

#### 4A

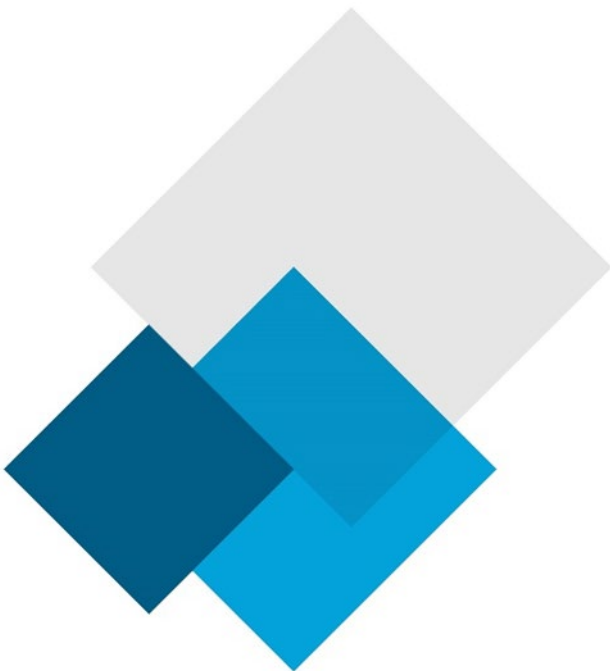
Cs-137 Activity on counting date (DPM/g dry wt.)



Note: The bar plotted at the midpoint depth of each section represents +/- 1 standard deviation of the Cs-137 counting error.

# Appendix 8

Radio Isotopic Analysis Core 2B



# Interpretation of Pb-210, Ra-226 and Cs-137 Results

## Flett Research Ltd.

440 DeSalaberry Ave. Winnipeg, MB R2L 0Y7

Fax/Phone: (204) 667-2505

Email: [flett@flettresearch.ca](mailto:flett@flettresearch.ca) Webpage: <http://www.flettresearch.ca>

## Client: Lorrain, Stéphane

**Address:** SNC-LAVALIN GEM QUÉBEC INC., 455, boul. René-Lévesque ouest, Montréal (Québec) H2Z 1Z3

**Core ID:** 2B

**Transaction ID:** 882

**PO/Contract No.:** 653502-0028

**Date Received:** 20-Feb-19

**Analysis Dates:** April 16 - June 17, 2019

**Analysts:** L. Hesketh-Jost; X. Hu

**Sampling Date:** 9-Feb-19

**Project:** #653502

*Results authorized by Dr. Robert J. Flett, Chief Scientist*

## INTERPRETATION

### Observations:

The Pb-210 profile exhibits an irregular but approximately exponential decrease in total Pb-210 activity as a function of depth. The maximum activity of 12.23 DPM/g observed in section 3 (extrapolated depth 1.5 - 3.5 cm) is about 15 times the lowest activity of 0.84 DPM/g observed in section 51 (extrapolated depth 47.5 - 54.5 cm) (Pages 2 & 3). The Pb-210 activity in the surface section (extrapolated depth 0 - 1.5 cm) is slightly lower than the Pb-210 activity in section 3 (extrapolated depth 1.5 - 3.5 cm), and this probably represents increasing sediment accumulation rates, and/or physical mixing, and/or diffusion of Pb-210 across a redox gradient, and/or incomplete diagenesis of surface sediment, and/or incomplete ingrowth of the Po-210, granddaughter of Pb-210, actually being measured.

The dry bulk densities generally increase with depth, beginning at the surface and increasing down to section 17 (extrapolated depth 15.5 - 17.5 cm), increasing from 0.101 g/cm<sup>3</sup> to 0.267 g/cm<sup>3</sup>, with a large transient increase to 0.277 g/cm<sup>3</sup> at section 7 (extrapolated depth 5.5 - 7.5 cm). Below section 17, beginning in section 19 (extrapolated depth 17.5 - 19.5 cm) the dry bulk densities gradually decrease, reaching 0.206 g/cm<sup>3</sup> at section 25 (extrapolated depth 23.5 - 26.5 cm). The dry bulk densities then increase reaching a maximum of 0.924 g/cm<sup>3</sup> at section 51 (extrapolated depth 47.5 - 54.5 cm); after section 51 the dry bulk densities decrease again to 0.519 g/cm<sup>3</sup> and 0.660 g/cm<sup>3</sup>, in sections 58 - 59 cm and 67 - 68 cm, respectively.

Ra-226 was measured at 1.36, 1.62 and 1.62 DPM/g in sections 6 - 7 cm, 28 - 29 cm and 67 - 68 cm, respectively (Pages 10 - 13). Net unsupported Pb-210 activity in core interval of 0 - 17.5 cm was calculated by subtracting the Ra-226 activity measured at 6 - 7 cm section from each total Pb-210 value. The Pb-210 activity in the 67 - 68 cm section is less than the Ra-226 activity measured in the same section, indicating that the background level of Pb-210 has been achieved in this core.

Cs-137 was measured in 7 sections in the 12 - 21 cm core interval. Activities in this portion of the core are all significantly above background, ranging between 0.43 - 2.53 DPM/g (Pages 14 & 18). Below 17 cm, the Cs-137 activity declines with depth. The shape of Cs-137 profile in the 12 - 17 cm core interval suggests that the majority of the Cs-137 is probably from external erosion sources (soils or sediments contaminated with bomb testing radionuclides).

### Regression model of Unsupported Pb-210 activity vs. Cumulative Dry Weight (g/cm<sup>2</sup>):

When applying the linear regression model, it is assumed that the input of Pb-210 and the sediment accumulation rate are constant. Although variation in the sediment accumulation rate is apparent, the linear regression model was applied to sections 1 - 17 (extrapolated depth 0 - 17.5 cm), because it appears that the average sediment accumulation rate will be reasonably estimated. This estimate of sediment accumulation rate is used to calibrate the CRS model over the same core interval.

The regression results are seen in Pages 5 & 6. The model predicts ( $R^2 = 0.9715$ ) an average sediment accumulation rate of 0.0803 g/cm<sup>2</sup>/yr when a Pb-210 background of 1.3608 DPM/g (closest to the Ra-226 activity of 1.36 DPM/g measured in the 6 - 7 cm section) is chosen from the regression table. The age at the bottom of any core section can be estimated by dividing the cumulative dry weight/cm<sup>2</sup> by the accumulation rate. For example, the age at the bottom of section 11 (extrapolated depth 11.5 cm) is calculated as 2.150 / 0.0803 = 26.8 yr. The age estimate at the bottom of each section is shown on Pages 2 (column AM) & 7.

**CRS model of Age at bottom of Extrapolated section in years vs. Depth of bottom edge of current section in cm:**

The CRS model assumes constant input of Pb-210 and a core that is long enough to include all of the measurable atmospheric source Pb-210, i.e. it contains a complete Pb-210 inventory. The facts that 1) the suspicious sudden termination in exponential decay of the Pb-210 profile in section 19 (extrapolated depth 17.5 - 19.5 cm), 2) the sudden decrease in dry bulk density beginning at section 19 and the continuing decrease in dry bulk density down to section 25, are possible causes for us to discard the deeper portion of the core (i.e. truncate the core) due to the increasing uncertainty of the sedimentation process.

The Ra-226 activity indicates that the background Pb-210 activity level has not been achieved at 17.5 cm (extrapolated depth), leaving us with an incomplete truncated core that normally cannot be processed by the CRS model. In order to allow use of the CRS model, an artificial Pb-210 inventory of 30.740 DPM/cm<sup>2</sup> has been chosen such that the CRS model predicted exactly the same average sediment accumulation rate (0.0803 g/cm<sup>2</sup>/yr) as the linear regression model over the 0 - 17.5 cm (extrapolated depth) segment of the core. With the CRS model calibrated, it has been used to calculate ages for the core interval of 0 - 17.5 cm (extrapolated depth).

The measured total activity results (DPM/g) are shown in column AF of the main data table on Page 2. The estimated age at the bottom of each section is shown in column AI, also shown on Page 2. The average sediment accumulation rate, from core surface to the extrapolated bottom depth of any section, can be calculated by dividing the cumulative dry mass at the bottom of the extrapolated section by the calculated age at that depth. For example, the average sediment accumulation rate, from the core surface to the bottom of section 11 (extrapolated depth 11.5 cm) can be calculated as: 2.150 / 27.0 = 0.0796 g/cm<sup>2</sup>/yr. The individual sediment accumulation rate for each section is shown in column AL on Page 2. Plots of age vs. depth, sediment accumulation rate vs. depth and sediment accumulation rate vs. age are seen in Pages 7, 8 and 9, respectively.

**Conclusion:**

The significant presence of Cs-137 in the 12 - 17 cm core interval indicates that these sections are less than 56 years old (post 1963). Based upon the shape of the Pb-210 and dry bulk density profiles and the ages predicted by the Pb-210 models, it is suspected that a portion of the core is missing and it is likely that the 1966 maximum Cs-137 inventory could be recorded in the suspected missing portions of the core (below 17.5 cm, extrapolated depth). However, the CRS model indicates an age of 45.6 yr at 17.5 cm extrapolated depth, an age compatible with the presence of Cs-137.

The water level at Kingston Harbour monitor station dropped to an historic low level of -0.47 m below datum on January 23, 1965. [See worksheet 'water level Kingston H'.] It is possible that this low water level may be related to the disturbance of the shallow water sediments, from which this core was obtained. The modeling results indicate that the disturbance probably occurred about 46 years ago (i.e. in 1973). This is compatible with our belief that a number of years of sediment may be missing from the core below 17.5 cm (extrapolated depth) prior to 1973.

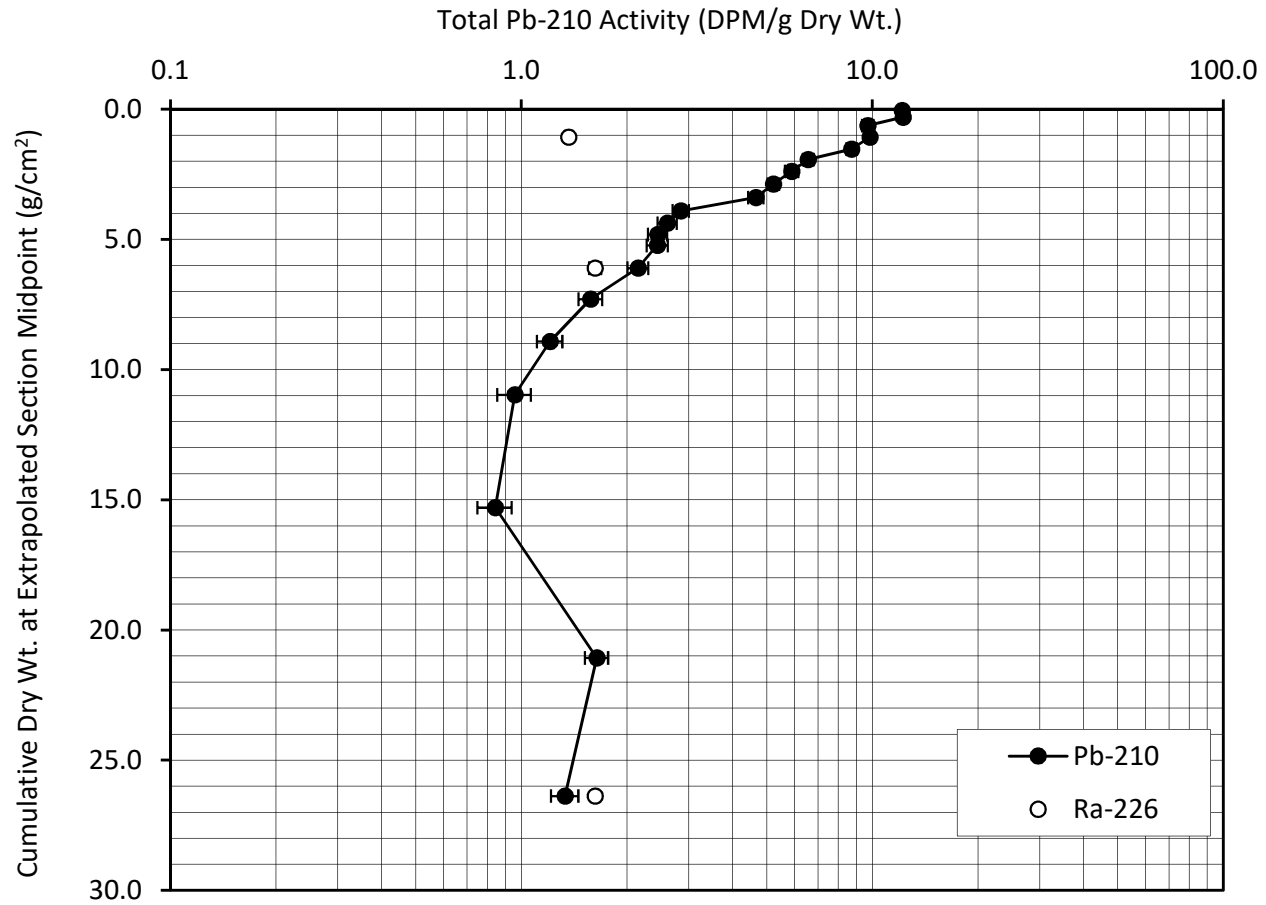
Over the core interval of 0 - 17.5 cm (extrapolated depth), the average sediment accumulation rate estimated by the CRS model has been forced to exactly coincide with the linear regression estimate of 0.0803 g/cm<sup>2</sup>/yr. Although the CRS calculated ages depend upon the results of the linear regression model, the CRS model is to be preferred because it should provide accurate age predictions at the bottom of each section even though the sediment accumulation rate is changing with time.

Overall, the analytical quality of radioisotope data (based upon the recovery of spike, the recovery of CRM, the results of repeat analyses and blanks) is considered good.



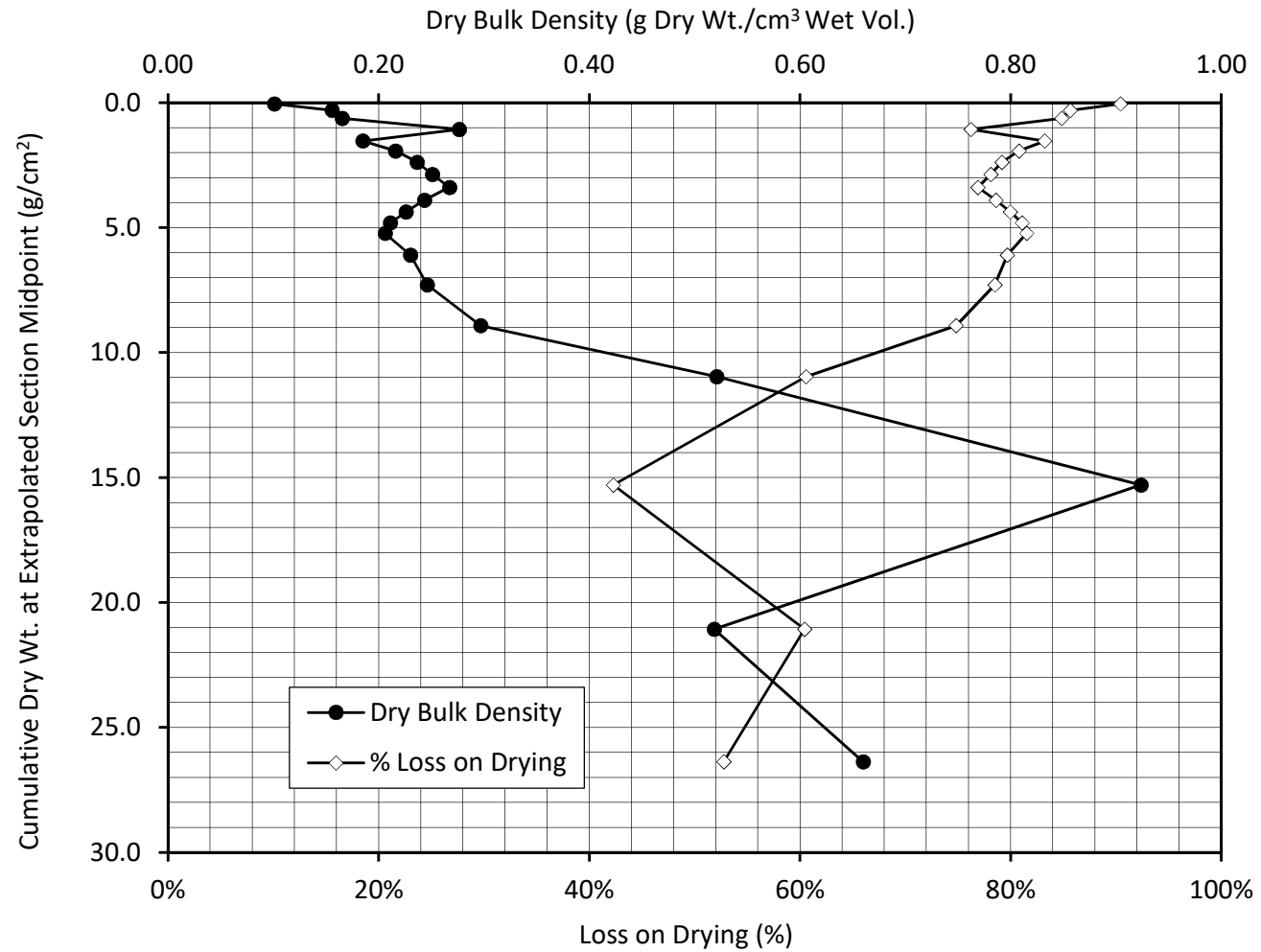
**Total Pb-210 Activity vs. Accumulated Sediment**

**2B**



**Dry Bulk Density and % Loss on Drying**  
**vs. Accumulated Sediment**

**2B**



**R<sup>2</sup> fit as a function of background subtracted**

Background (DPM/g)	R <sup>2</sup>	Sediment Accumulation Rate (g/cm <sup>2</sup> /yr)	Slope 'm'	Y intercept 'b'
0.0000	0.9703	0.0986	-3.171	8.119
0.1508	0.9704	0.0966	-3.107	7.923
0.3020	0.9706	0.0946	-3.042	7.727
0.4533	0.9707	0.0925	-2.978	7.532
0.6045	0.9709	0.0905	-2.913	7.338
0.7558	0.9711	0.0885	-2.847	7.144
0.9070	0.9712	0.0865	-2.782	6.951
1.0583	0.9713	0.0844	-2.716	6.759
1.2095	0.9714	0.0824	-2.650	6.568
1.3608	0.9715	0.0803	-2.584	6.377
1.5120	0.9716	0.0782	-2.517	6.187
1.6633	0.9717	0.0761	-2.450	5.997
1.8145	0.9717	0.0740	-2.382	5.809
1.9658	0.9717	0.0719	-2.314	5.621
2.1170	0.9717	0.0698	-2.245	5.433
2.2683	0.9716	0.0676	-2.175	5.246
2.4195	0.9715	0.0654	-2.105	5.059
2.5708	0.9712	0.0632	-2.034	4.873
2.7220	0.9709	0.0610	-1.962	4.687
2.8733	0.9704	0.0587	-1.889	4.501
3.0245	0.9698	0.0564	-1.815	4.315

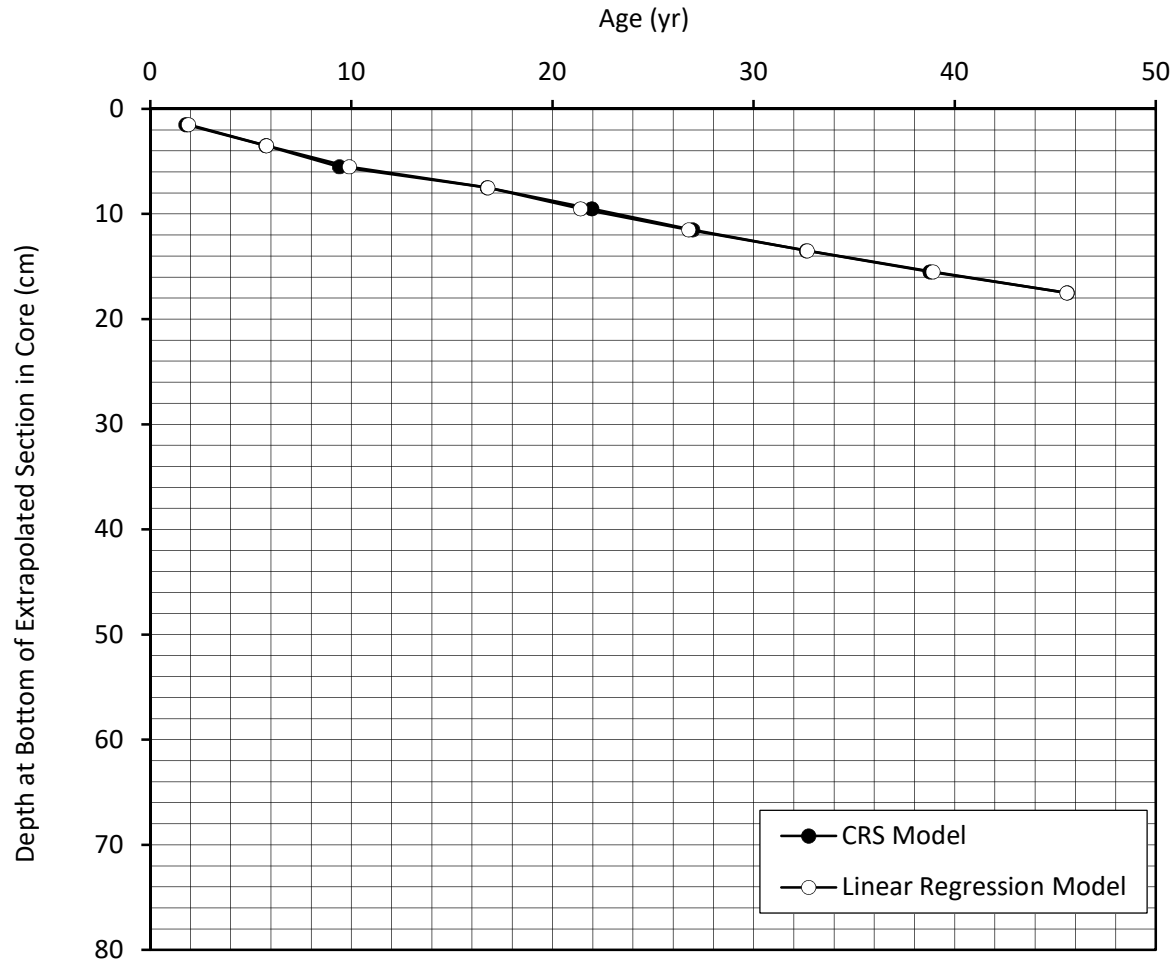
Note: Used column **BJ** for background subtraction.

Q:\Clients A-L\Lorrain, Stephane\2019(882)\Radioisotopes\2B\Pb-210, Ra-226 and Cs-137  
Lorrain Core 2B Jun 21-19 Final.xlsm



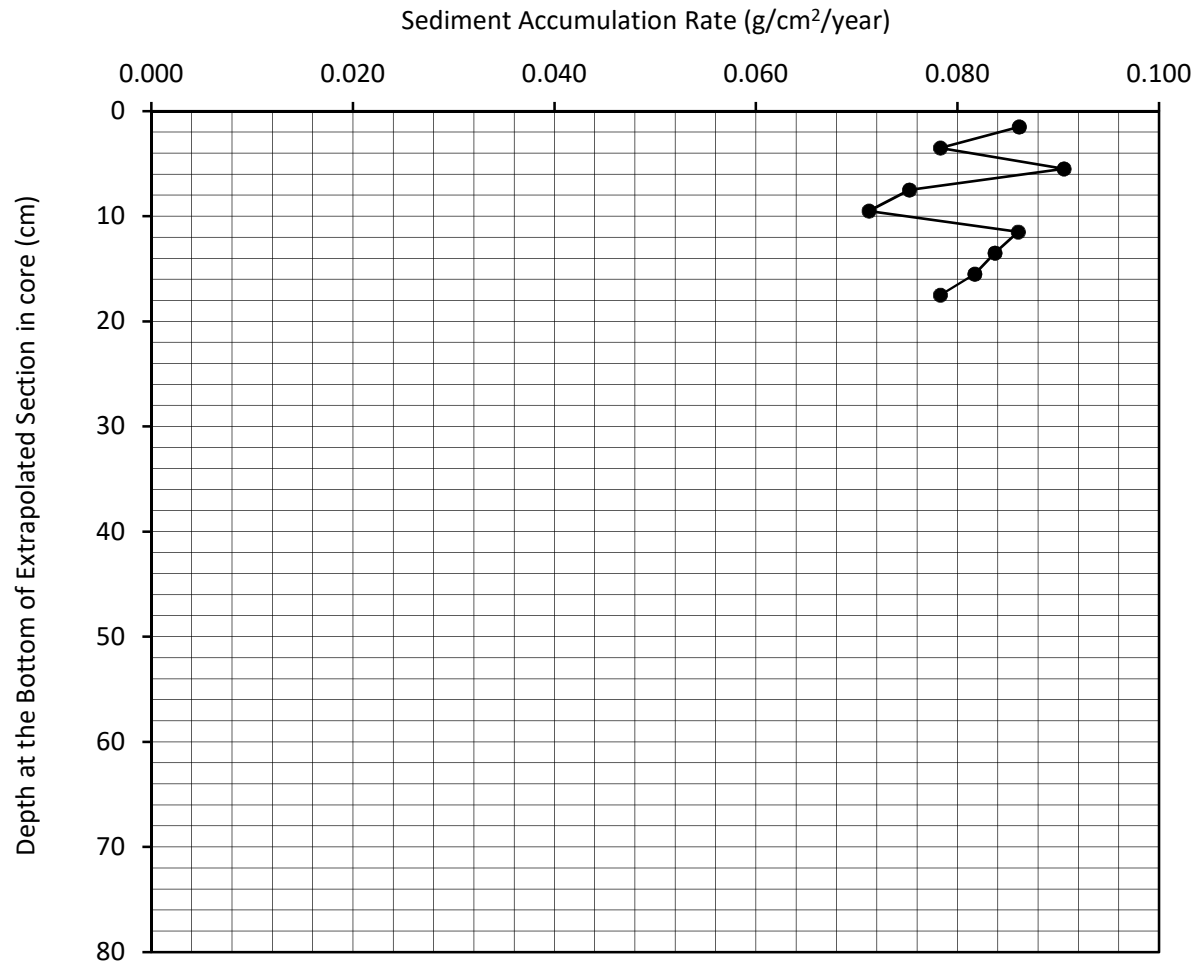
**Age (yr) vs. Depth (cm)**  
**CRS Model vs. Linear Regression Model**

**2B**

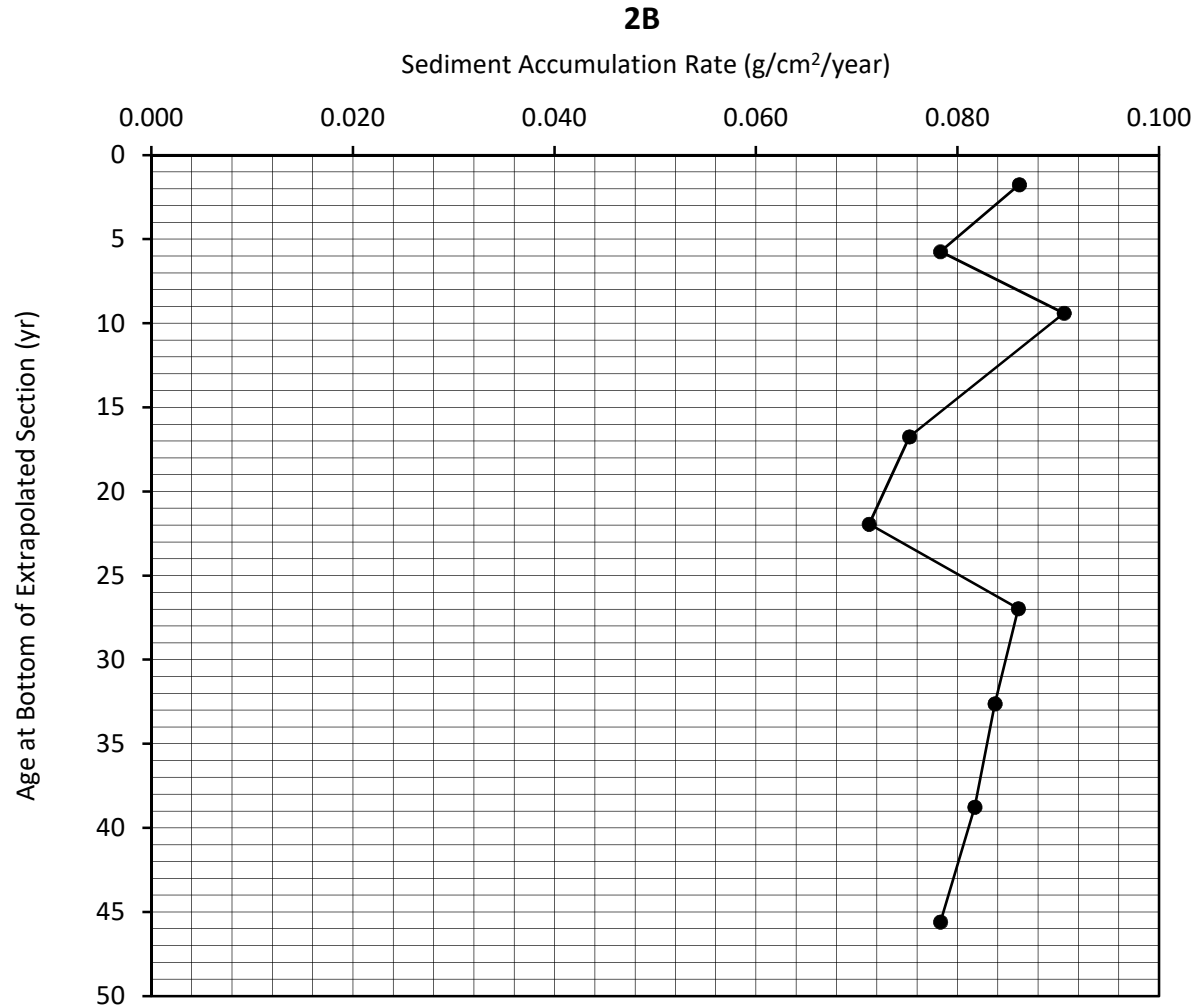


**CRS Sediment Accumulation Rate (g/cm<sup>2</sup>/year)**  
**vs. Depth at the Bottom of Extrapolated Section in Core (cm)**

**2B**



**CRS Sediment Accumulation Rate (g/cm<sup>2</sup>/year)**  
**vs. Age at Bottom of Extrapolated Section (yr)**



# Results of Ra-226 Analysis by Rn-222 Emanation

## Flett Research Ltd.

440 DeSalaberry Ave., Winnipeg, MB R2L 0Y7

Fax/Phone: (204) 667-2505

Email: flett@flettresearch.ca Webpage: <http://www.flettresearch.ca>

### Client: Lorrain, Stéphane

Address: SNC-LAVALIN GEM QUÉBEC INC., 455, boul. René-Lévesque ouest, Montréal (Québec) H2Z 1Z3

Core ID: **2B**

Transaction ID: 882

Date Received: 20-Feb-19

PO/Contract No.: 653502-0028

Sampling Date: 9-Feb-19

Analysis Dates: April 16 - June 17, 2019

Project: #653502

Analysts: L. Hesketh-Jost; X. Hu

Salt Correction Applied? No

Analytical Method: N40110 Determination of Radium-226 in Sediment, Soil and Peat by Radon-222 Emanation (Version 3)

#### Comments:

**Detection Limit:** The method detection limit (MDL) is dependent on the amount of sample analyzed. For a 60,000 second counting time the MDL at 95% confidence for 2 g of dry sample is 0.1 DPM/g and for 0.5 g of dry sample is 0.5 DPM/g.

**Estimated Uncertainty:** The estimate of uncertainty of measurement for this method in this laboratory is approximately  $\pm 12\%$  at 95% confidence level (approximately 40,000 counts in 60,000 seconds).

Results authorized by Dr. Robert J. Flett, Chief Scientist

Core ID	Sample ID	Ra-226 Activity (DPM/g Dry Wt.)	Combined Error: 1 SD (DPM/g Dry Wt.)	Comments Code for Ra-226 Analysis
2B	2B-2/2-68	1.62	0.02	
2B	2B-2/2-7	1.36	0.04	
2B	2B-2/2-29	1.62	0.06	

Q:\Clients A-L\Lorrain, Stephane\2019(882)\Radioisotopes\2B\Pb-210, Ra-226 and Cs-137 Lorrain Core 2B Jun 21-19 Final.xlsm

**Duplicate:** Two subsamples of the same sample were carried through the analytical procedure in an identical manner.

**Re-count:** The sample bottle was re-sealed after the initial analysis, and was re-counted after 11 or more days of Rn-222 ingrowth. Repeat counting was chosen over duplicate analysis due to insufficient sample material provided.

This test report shall not be reproduced, except in full, without written approval of the laboratory.

Note: Results relate only to the items tested.

17-Jun-19

Page 10 of 18

ISO / IEC 17025:2005 Accredited with the Canadian Association for Laboratory Accreditation (CALA Accreditation No. A3306)

**Radium Analysis by Rn-222 Emanation**

Core ID	2B
Sample ID	2B-2/2-68
Lucas Cell No.	3
Number of days since Rn board last run	1
Dry weight of sample counted (g)	2.744
Total count in period	10681
Total count in period (carryover corrected)	10674
Cell Blank count (CPM)	0.562
System Blank (DPM)	0.395
System Efficiency	0.839
Count duration (minutes)	1000

Typical carryover is about 1 - 2 % of the net counts (gross counts less system background) of the sample counted on the previous day. The carryover is subtracted from the gross counts of current sample. This correction is not required if the sample is run after a blank.			
Carryover correction?	Yes	Mean of last 10 carryover measurements	1.02%
Gross counts of previous sample	1594	Mean of last 6 system background measurements	887
Counts carried over from previous sample	7		

	Year	Month	Day	Hour	Minute	Second	Ingrowth time (Days)	Ingrowth factor	Decay correction
When sample last stripped	2019	4	18	15	18	0	16.14	0.94629	0.92494
When cell filled	2019	5	4	18	35	0			
Beginning time of count	2019	5	4	20	35	0			

Counts per minute	10.67
Gross CPM less Cell Blank (CPM)	10.11
CPM (decay during count corrected)	10.93
DPM Sample +System (efficiency corrected)	13.03
DPM sample	13.35
DPM/g	4.87
<b>Ra-226 DPM/g</b>	<b>1.62</b>
Ra-226 pCi/g	0.73

Error ± 1 sd    0.1634 DPM

**Error ± 1 sd    0.0198 DPM/g**

Error % =    1.2

Chemist	RF
PMT High Voltage +ve	770
HV Power supply	Spectrum Technologies
Alpha Counter	Spectrum Technologies
Region of Interest Ch.#s	28-1022
PMT	6655A - #1
Preamp	Canberra 2007P tube base
Amp Gain	1

**Radium Analysis by Rn-222 Emanation**

Core ID	2B
Sample ID	2B-2/2-7
Lucas Cell No.	3
Number of days since Rn board last run	1
Dry weight of sample counted (g)	0.992
Total count in period	3836
Total count in period (carryover corrected)	n/a
Cell Blank count (CPM)	0.547
System Blank (DPM)	0.389
System Efficiency	0.840
Count duration (minutes)	1000

Typical carryover is about 1 - 2 % of the net counts (gross counts less system background) of the sample counted on the previous day. The carryover is subtracted from the gross counts of current sample. This correction is not required if the sample is run after a blank.

Carryover correction?	No
-----------------------	----

	Year	Month	Day	Hour	Minute	Second	Ingrowth time (Days)	Ingrowth factor	Decay correction
When sample last stripped	2019	5	31	13	0	0	16.27	0.94756	0.92490
When cell filled	2019	6	16	19	26	20			
Beginning time of count	2019	6	16	21	26	44			

Counts per minute	3.84
Gross CPM less Cell Blank (CPM)	3.29
CPM (decay during count corrected)	3.56
DPM Sample +System (efficiency corrected)	4.23
DPM sample	4.06
DPM/g	4.09
<b>Ra-226 DPM/g</b>	<b>1.36</b>
Ra-226 pCi/g	0.61

Error ± 1 sd    0.1195 DPM

**Error ± 1 sd    0.0402 DPM/g**

Error % =    2.9

Chemist	RF
PMT High Voltage +ve	770
HV Power supply	Spectrum Technologies
Alpha Counter	Spectrum Technologies
Region of Interest Ch.#s	28-1022
PMT	6655A - #1
Preamp	Canberra 2007P tube base
Amp Gain	1

**Radium Analysis by Rn-222 Emanation**

Core ID	2B
Sample ID	2B-2/2-29
Lucas Cell No.	3
Number of days since Rn board last run	1
Dry weight of sample counted (g)	0.593
Total count in period	2904
Total count in period (carryover corrected)	2877
Cell Blank count (CPM)	0.547
System Blank (DPM)	0.389
System Efficiency	0.840
Count duration (minutes)	1000

Typical carryover is about 1 - 2 % of the net counts (gross counts less system background) of the sample counted on the previous day. The carryover is subtracted from the gross counts of current sample. This correction is not required if the sample is run after a blank.			
Carryover correction?	Yes	Mean of last 10 carryover measurements	0.96%
Gross counts of previous sample	3720	Mean of last 6 system background measurements	874
Counts carried over from previous sample	27		

	Year	Month	Day	Hour	Minute	Second	Ingrowth time (Days)	Ingrowth factor	Decay correction
When sample last stripped	2019	5	17	12	33	0	12.97	0.90468	0.92490
When cell filled	2019	5	30	11	51	21			
Beginning time of count	2019	5	30	13	51	44			

Counts per minute	2.88
Gross CPM less Cell Blank (CPM)	2.33
CPM (decay during count corrected)	2.52
DPM Sample +System (efficiency corrected)	3.00
DPM sample	2.88
DPM/g	4.86
<b>Ra-226 DPM/g</b>	<b>1.62</b>
Ra-226 pCi/g	0.73

Error ± 1 sd    0.1134 DPM

**Error ± 1 sd    0.0638 DPM/g**

Error % =    3.9

Chemist	XH
PMT High Voltage +ve	770
HV Power supply	Spectrum Technologies
Alpha Counter	Spectrum Technologies
Region of Interest Ch.#s	28-1022
PMT	6655A - #1
Preamp	Canberra 2007P tube base
Amp Gain	1

# Results of Cs-137 Analysis

Flett Research Ltd.

440 DeSalaberry Ave. Winnipeg, MB R2L 0Y7

Fax / Phone: (204) 667-2505

Email: flett@flettresearch.ca Webpage: http://www.flettresearch.ca

**Client: Lorrain, Stéphane**

**Address:** SNC-LAVALIN GEM QUÉBEC INC., 455, boul. René-Lévesque ouest, Montréal (Québec) H2Z 1Z3

**Core ID:** 2B  
**Date Received:** 20-Feb-19  
**Sampling Date:** 9-Feb-19  
**Project:** #653502

**Transaction ID:** 882  
**PO/Contract No.:** 653502-0028  
**Analysis Dates:** May 24 - 30, 2019  
**Analysts:** X. Hu

Salt Correction?	No
------------------	----

**Analytical Method:** N30120 Measurement of Gamma-Ray Emitting Radionuclides in Sediment/Soil Samples by Gamma Spectrometry Using HPGe Detectors (Version 2)

**Deviation from Method:**

**Comments:**

**Detection Limit:** The method detection limit (MDL) is 0.3 DPM/g for an 80,000 seconds counting period when measuring a 9 g of dry sample at a 95% confidence level. The method detection limit can be decreased to 0.1 DPM/g if 32 g of sample is used.

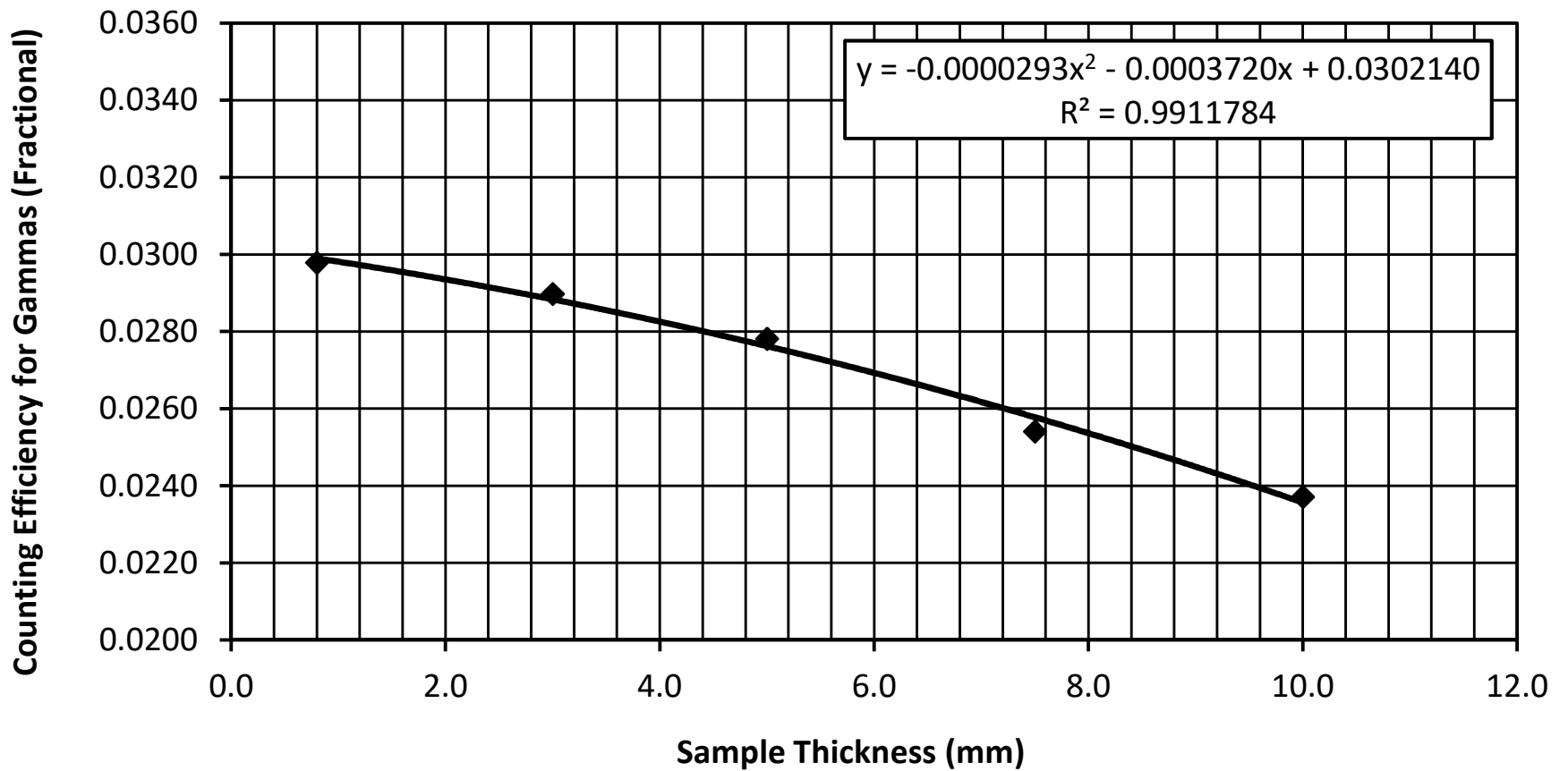
**Estimated Uncertainty:** The estimated uncertainty of this method has been determined to be ± 10% at 95% confidence for samples with activities between 0.5 and 20 DPM/g, counting time 80,000 seconds and sample weights ranging from 9 to 32 grams. Method uncertainty can increase to 85% for samples with activities near detection limit (0.1 - 0.3 DPM/g).

Results authorized by Dr. Robert J. Flett, Chief Scientist

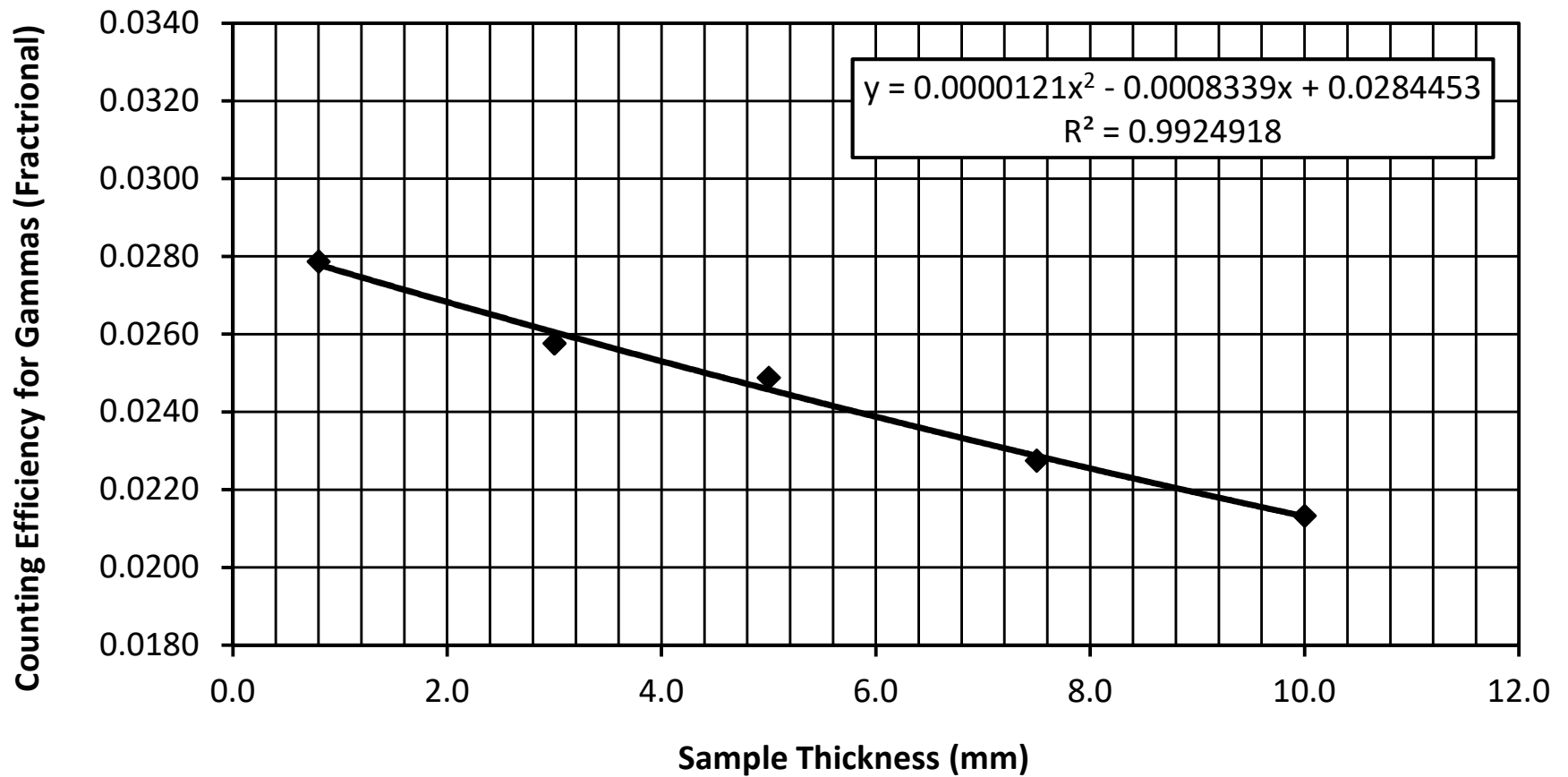
Sample ID	Upper Depth (cm)	Lower Depth (cm)	Day Sample Counted	Month Sample Counted	Year Sample Counted	Integral NET Cs-137 Peak	Counting Error 1 SD (Counts)	Count Time (seconds)	Dry Sample Weight (g)	Sample Thickness (mm)	CPM/g	Efficiency for Gammas Fractional	Gammas per min. per gram	Activity DPM/g (dry wt.) on Counting Date	Approx. Error DPM/g	Activity DPM/g (dry wt.) on Sampling Date	Approx. Error DPM/g	Activity pCi/g (dry wt.) on Sampling Date	Approx. Error pCi/g	Activity mBq/g (dry wt.) on Sampling Date	Approx. Error mBq/g	Detector Used	Comments Code for Cs-137 Analysis
2B-2/2-13	12	13												2.53	0.28	2.54	0.28	1.15	0.13	42.38	4.71	GMX	
2B-2/2-15	14	15	25	5	2019	598	41	80000	5.723	2.80	0.0784	0.0435	1.8009	2.11	0.14	2.13	0.14	0.96	0.07	35.46	2.41	Canberra	
2B-2/2-16	15	16												2.36	0.17	2.38	0.17	1.07	0.08	39.64	2.81	GEM	
2B-2/2-17	16	17	24	5	2019	503	38	80000	6.806	2.05	0.0554	0.0268	2.0693	2.43	0.18	2.44	0.18	1.10	0.08	40.75	3.08	GEM	
2B-2/2-18	17	18	27	5	2019	635	39	80000	9.012	2.88	0.0528	0.0434	1.2171	1.43	0.09	1.44	0.09	0.65	0.04	23.97	1.46	Canberra	
2B-2/2-19	18	19	24	5	2019	162	50	80000	6.871	2.30	0.0177	0.0292	0.6055	0.71	0.22	0.72	0.22	0.32	0.10	11.92	3.68	GMX	
2B-2/2-21	20	21	24	5	2019	138	31	80000	6.313	2.08	0.0164	0.0445	0.3688	0.43	0.10	0.44	0.10	0.20	0.04	7.26	1.66	Canberra	
<b>Re-count</b>																							
2B-2/2-13	12	13	28	5	2019	402	51	80000	5.203	1.68	0.0579	0.0295	1.9637	2.30	0.29	2.32	0.29	1.05	0.13	38.68	4.91	GMX	
2B-2/2-13 Re-count	12	13	29	5	2019	479	47	80000	5.203	1.68	0.0690	0.0295	2.3399	2.75	0.27	2.77	0.27	1.25	0.12	46.09	4.52	GMX	
2B-2/2-16	15	16	28	5	2019	542	40	80000	7.865	2.10	0.0517	0.0267	1.9323	2.27	0.17	2.28	0.17	1.03	0.08	38.06	2.81	GEM	
2B-2/2-16 Re-count	15	16	29	5	2019	587	40	80000	7.865	2.10	0.0560	0.0267	2.0928	2.46	0.17	2.47	0.17	1.11	0.08	41.22	2.81	GEM	
<b>Cs-137 Standards</b>																							
GMX 32g 10 mm			4	4	2019	19967	143	5000	32.00	10.0	7.4876	0.0237	315.7600	370.61	2.65	957.04							
GMX 24g 7.5mm			5	4	2019	16045	128	5000	24.00	7.5	8.0225	0.0254	315.7400	370.59	2.96	957.04							
GMX 15g 5mm			4	4	2019	10978	106	5000	15.00	5.0	8.7824	0.0278	315.7600	370.61	3.58	957.04							
GMX 9g 3mm			3	4	2019	6862	84	5000	9.00	3.0	9.1493	0.0290	315.7799	370.63	4.54	957.04							
GMX 2.85g 0.8mm			4	4	2019	2237	49	5000	2.854	0.8	9.4057	0.0298	315.7600	370.61	8.12	957.04							
GEM 32g 10 mm			4	4	2019	17960	139	5000	32.00	10.0	6.7350	0.0213	315.7600	370.61	2.87	957.04							
GEM 24g 7.5mm			4	4	2019	14367	124	5000	24.00	7.5	7.1835	0.0227	315.7600	370.61	3.20	957.04							
GEM 15g 5mm			3	4	2019	9822	102	5000	15.00	5.0	7.8576	0.0249	315.7799	370.63	3.85	957.04							
GEM 9g 3mm			4	4	2019	6102	79	5000	9.00	3.0	8.1360	0.0258	315.7600	370.61	4.80	957.04							
GEM 2.85g 0.8mm			4	4	2019	2093	48	5000	2.854	0.8	8.8003	0.0279	315.7600	370.61	8.50	957.04							
Canberra 32g 10 mm			11	4	2019	29236	172	5000	32.00	10.0	10.9635	0.0347	315.6205	370.45	2.19	957.04							
Canberra 24g 7.5mm			11	4	2019	23302	154	5000	24.00	7.5	11.6510	0.0369	315.6205	370.45	2.44	957.04							
Canberra 15g 5mm			10	4	2019	16207	128	5000	15.00	5.0	12.9656	0.0411	315.6404	370.47	2.93	957.04							
Canberra 9g 3mm			10	4	2019	10285	103	5000	9.00	3.0	13.7133	0.0434	315.6404	370.47	3.70	957.04							



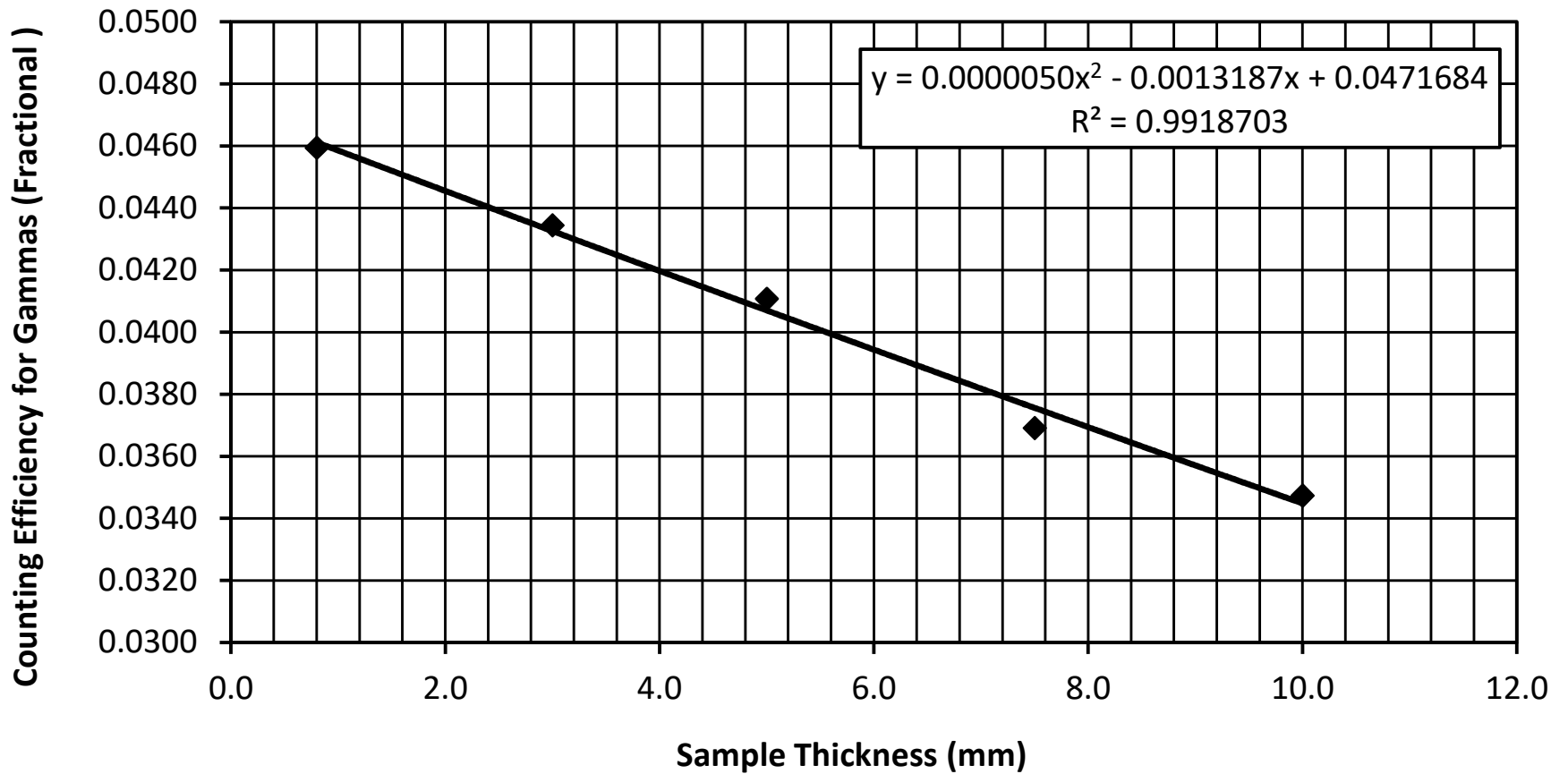
### Cs-137 Counting Efficiency of Gammas vs. Sample Thickness (mm) GMX 25% Detector (Apr 3 - 5, 2019)



### Cs-137 Counting Efficiency of Gammas vs. Sample Thickness (mm) GEM 19% Detector (Apr 3 - 4, 2019)



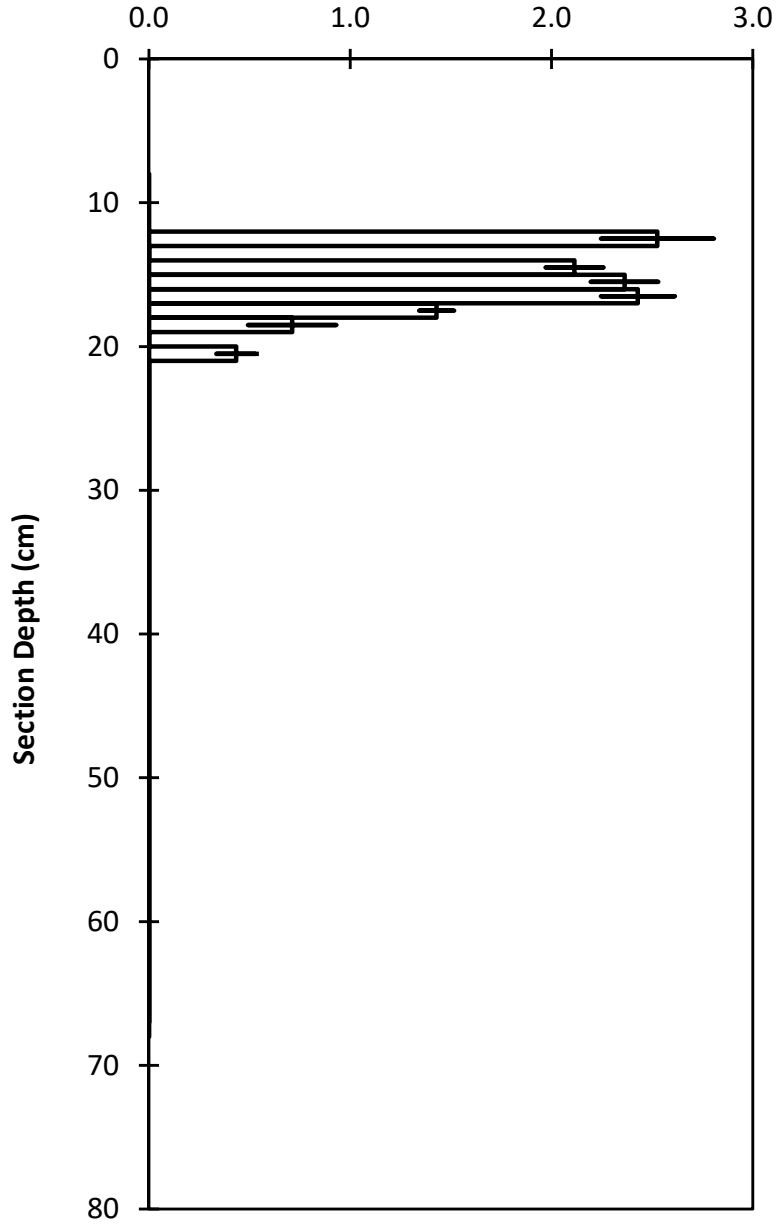
### Cs-137 Counting Efficiency of Gammas vs. Sample Thickness (mm) Canberra 29% Detector (Apr 10 - 11, 2019)



### Cs-137 in Sediments

#### 2B

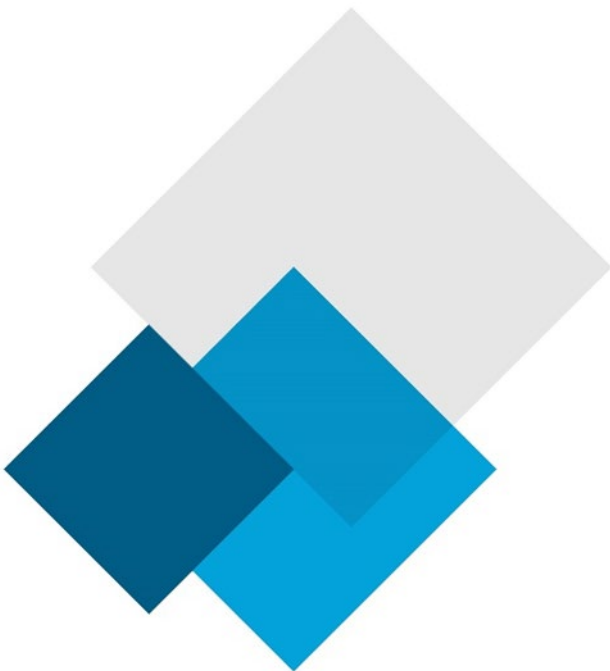
Cs-137 Activity on counting date (DPM/g dry wt.)



Note: The bar plotted at the midpoint depth of each section represents +/- 1 standard deviation of the Cs-137 counting error.

# Appendix 9

Radio Isotopic Analysis Core 4B



# Interpretation of Pb-210, Ra-226 and Cs-137 Results

## Flett Research Ltd.

440 DeSalaberry Ave. Winnipeg, MB R2L 0Y7

Fax/Phone: (204) 667-2505

Email: [flett@flettresearch.ca](mailto:flett@flettresearch.ca) Webpage: <http://www.flettresearch.ca>

## Client: Lorrain, Stéphane

**Address:** SNC-LAVALIN GEM QUÉBEC INC., 455, boul. René-Lévesque ouest, Montréal (Québec) H2Z 1Z3

**Core ID:** 4B

**Transaction ID:** 882

**PO/Contract No.:** 653502-0028

**Date Received:** 20-Feb-19

**Analysis Dates:** April 16 - June 22, 2019

**Analysts:** L. Hesketh-Jost; X. Hu

**Sampling Date:** 9-Feb-19

**Project:** #653502

*Results authorized by Dr. Robert J. Flett, Chief Scientist*

## INTERPRETATION

### Observations:

The Pb-210 profile exhibits an irregular but approximately exponential decrease in total Pb-210 activity as a function of depth. The maximum activity of 9.63 DPM/g observed in section 5 (extrapolated depth 3.5 - 5.5 cm) is about 30 times the lowest activity of 0.32 DPM/g observed in section 31 (extrapolated depth 29 - 31 cm) (Pages 2 & 3). The Pb-210 activities in sections 1 and 3 (extrapolated depth 0 - 3.5 cm) are slightly lower than the Pb-210 activity in section 5 (extrapolated depth 3.5 - 5.5 cm), and this probably represents increasing sediment accumulation rates, and/or physical mixing, and/or diffusion of Pb-210 across a redox gradient, and/or incomplete diagenesis of surface sediment, and/or incomplete ingrowth of the Pb-210, granddaughter of Pb-210, actually being measured.

The dry bulk densities generally increase with depth, from 0.117 g/cm<sup>3</sup> at the surface to 0.934 g/cm<sup>3</sup> at section 21 (extrapolated depth 19.5 - 21 cm). Below section 21, the dry bulk densities then decrease, reaching 0.178 g/cm<sup>3</sup> at the bottom of the core (Pages 2 & 4).

Ra-226 was measured at 1.07, 1.05, 0.93, 0.52, 0.50, 0.47 and 0.35 DPM/g in sections 6 - 7 cm, 16 - 17 cm, 18 - 19 cm, 20 - 21 cm, 21 - 22 cm, 23 - 24 cm and 30 - 31 cm, respectively (Pages 9 - 16). Net unsupported Pb-210 activity in core interval of 0 - 24.5 cm (extrapolated depth) was calculated by subtracting the nearest neighbouring Ra-226 activity from each total Pb-210 value, unless noted otherwise. The Pb-210 activity in the 30 - 31 cm section is very close to the Ra-226 activity measured in the same section, indicating that the background level of Pb-210 has been achieved in this core.

Cs-137 was measured in 10 sections in the 14 - 28 cm core interval. Activities in the 14 - 26 cm core interval are all significantly above background, ranging between 0.40 - 1.24 DPM/g (Pages 17 & 21). Below 23 cm, the Cs-137 activity declines with depth. The shape of Cs-137 profile in the 14 - 24 cm core interval suggests that the majority of the Cs-137 is probably from external erosion sources (soils or sediments contaminated with bomb testing radionuclides).

### Regression model of Unsupported Pb-210 activity vs. Cumulative Dry Weight (g/cm<sup>2</sup>):

When applying the linear regression model, it is assumed that the input of Pb-210 and the sediment accumulation rate are constant. Although variation in the sediment accumulation rate is apparent, the linear regression model was applied to sections 5 - 17 (extrapolated depth 3.5 - 17.5 cm), because it appears that the average sediment accumulation rate will be reasonably estimated. This estimate of sediment accumulation rate is used to calibrate the CRS model over the same core interval.

The regression results are seen in Page 5. The model predicts ( $R^2 = 0.9667$ ) an average sediment accumulation rate of 0.1121 g/cm<sup>2</sup>/yr when the unsupported Pb-210 activity was calculated by subtracting the nearest neighbouring Ra-226 measurement from each total Pb-210 value. The age at the bottom of any core section can be estimated by dividing the cumulative dry weight/cm<sup>2</sup> by the accumulation rate. However, it must be added to the age of 3.7 years previously calculated for the bottom of section 3 (extrapolated depth 3.5 cm) by the CRS model. For example, the age at the bottom of section 9 (extrapolated depth 10 cm) is calculated as  $3.7 + (1.856 - 0.499) / 0.1121 = 15.8$  yr. The age estimate at the bottom of each section is shown on Pages 2 (column AM) & 6.

**CRS model of Age at bottom of Extrapolated section in years vs. Depth of bottom edge of current section in cm:**

The CRS model assumes constant input of Pb-210 and a core that is long enough to include all of the measurable atmospheric source Pb-210, i.e. it contains a complete Pb-210 inventory. The Pb-210 activities in sections 25 - 26 cm, 27 - 28 cm and 30 - 31 cm are not significantly different from the Ra-226 activities measured in sections 23 - 24 cm and 30 - 31 cm, and therefore, it is suspected that the bottom 3 sections are likely an older basement sediment overlaid with different more recent sediment accumulation. This is possible cause for us to exclude the sections below 25 cm from the CRS calculation, due to the increasing uncertainty of the sedimentation process.

The Ra-226 activity indicates that the background Pb-210 activity level has not been achieved at 24.5 cm (extrapolated depth), leaving us with an incomplete truncated core that normally cannot be processed by the CRS model. In order to allow use of the CRS model, an artificial Pb-210 inventory of 35.740 DPM/cm<sup>2</sup> has been chosen such that the CRS model predicted exactly the same average sediment accumulation rate (0.1121 g/cm<sup>2</sup>/yr) as the linear regression model over the 3.5 - 24.5 cm (extrapolated depth) segment of the core. With the CRS model calibrated, it has been used to calculate ages for the core interval of 0 - 24.5 cm (extrapolated depth).

The measured total activity results (DPM/g) are shown in column AF of the main data table on Page 2. The estimated age at the bottom of each section is shown in column AI, also shown on Page 2. The average sediment accumulation rate, from core surface to the extrapolated bottom depth of any section, can be calculated by dividing the cumulative dry mass at the bottom of the extrapolated section by the calculated age at that depth. For example, the average sediment accumulation rate, from the core surface to the bottom of section 9 (extrapolated depth 10 cm) can be calculated as: 1.856 / 15.4 = 0.1205 g/cm<sup>2</sup>/yr. The individual sediment accumulation rate for each section is shown in column AL on Page 2. Plots of age vs. depth, sediment accumulation rate vs. depth and sediment accumulation rate vs. age are seen in Pages 6, 7 and 8, respectively.

**Conclusion:**

In this core, the sediment accumulation rates remain relatively constant in section 1 - 17 (extrapolated depth 0 - 17.5 cm), ranging between 0.1026 g/cm<sup>2</sup>/yr and 0.1400 g/cm<sup>2</sup>/yr. Below 17.5 cm the sediment accumulation rates start to increase with depth, peaking at 0.6029 g/cm<sup>2</sup>/yr in section 22 (extrapolated depth 22.5 cm), and then decrease to 0.3462 g/cm<sup>2</sup>/yr in section 24 (extrapolated depth 22.5 - 24.5 cm (by the CRS model) (Pages 2, 6 & 7).

The elevated Cs-137 activities in the core interval of 14 - 24 cm suggests that the majority of the Cs-137 is probably from external erosion sources (soils or sediments contaminated with bomb testing radionuclides) rather than direct deposition from the atmosphere. It is assumed that the 23 - 24 cm section represents the attaining of maximum Cs-137 terrestrial inventory which occurred in 1966, 53 years before the core was obtained. To have confidence that the Pb-210 models are functioning correctly, we typically hope to see the age predicted for the Cs-137 maximum be within 5 years of its known 1966 deposition. In this core, the CRS model indicates an age of 52.9 yr at 24.5 cm (extrapolated depth). This age is very close to what we would expect when it is assumed that Cs-137 maximum inventory has been recorded at 23 -24 cm. Despite the small difference and the uncertainty associated with the unknown sedimentary processes occurring below 24.5 cm (extrapolated depth), the CRS results are considered compatible with the Cs-137 results, and therefore, it is concluded that the CRS model is providing reasonable estimates of age in this core.

Over the core interval of 3.5 - 17.5 cm (extrapolated depth), the average sediment accumulation rate estimated by the CRS model has been forced to exactly coincide with the linear regression estimate of 0.1121 g/cm<sup>2</sup>/yr. Although the CRS calculated ages depend upon the results of the linear regression model, the CRS model is to be preferred because it should provide accurate age predictions at the bottom of each section even though the sediment accumulation rate is changing with time.

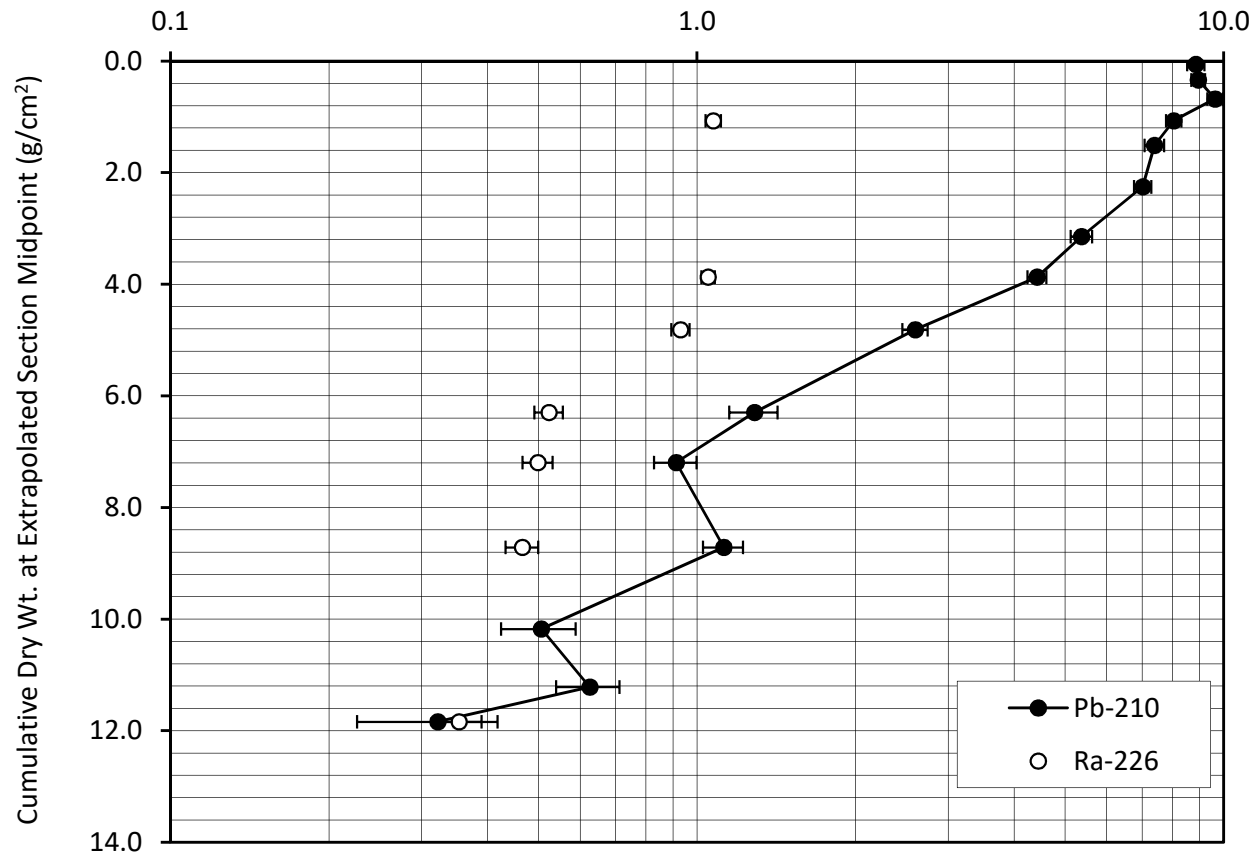
Overall, the analytical quality of radioisotope data (based upon the recovery of spike, the recovery of CRM, the results of repeat analyses and blanks) is considered good.



**Total Pb-210 Activity vs. Accumulated Sediment**

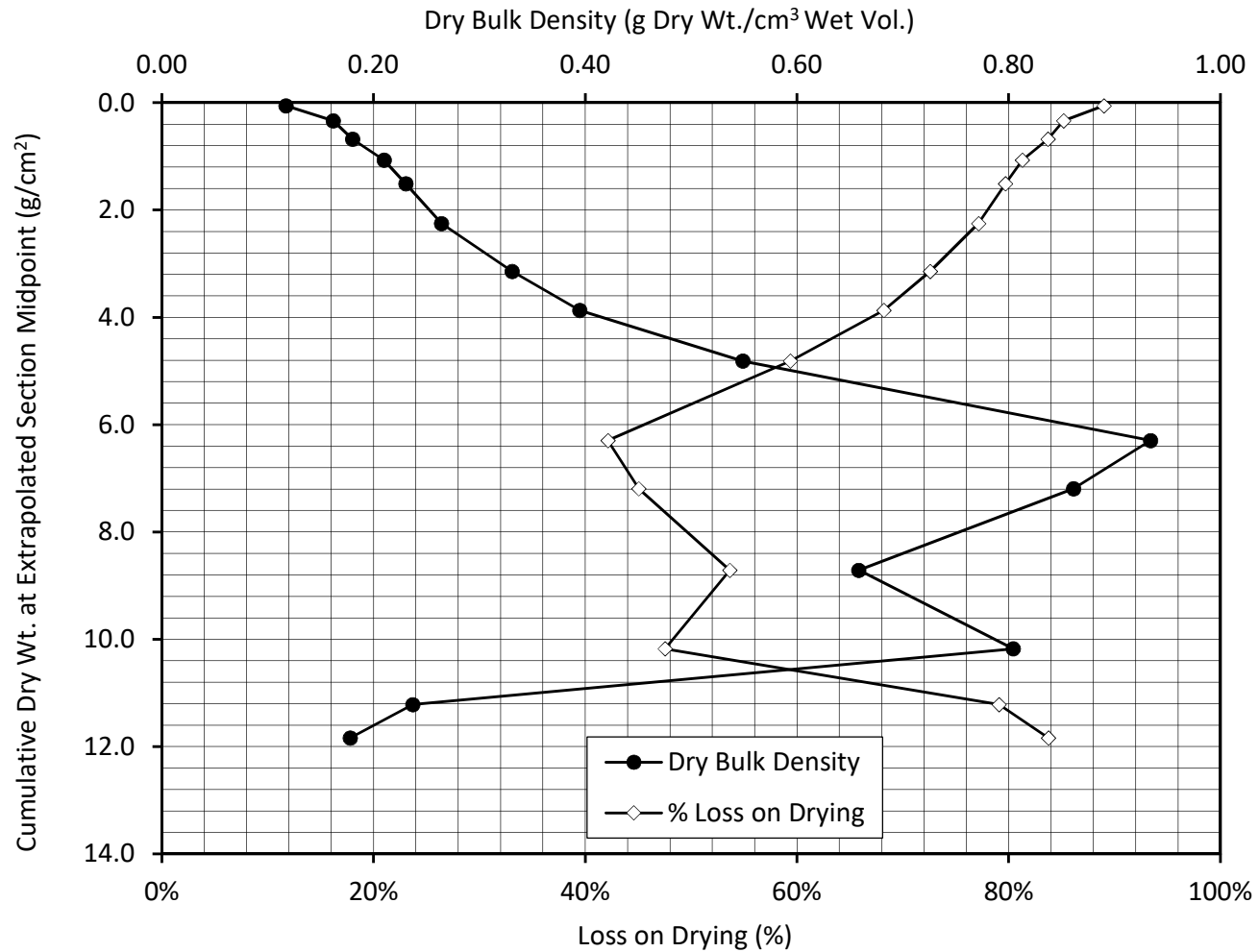
**4B**

Total Pb-210 Activity (DPM/g Dry Wt.)



**Dry Bulk Density and % Loss on Drying**  
**vs. Accumulated Sediment**

**4B**

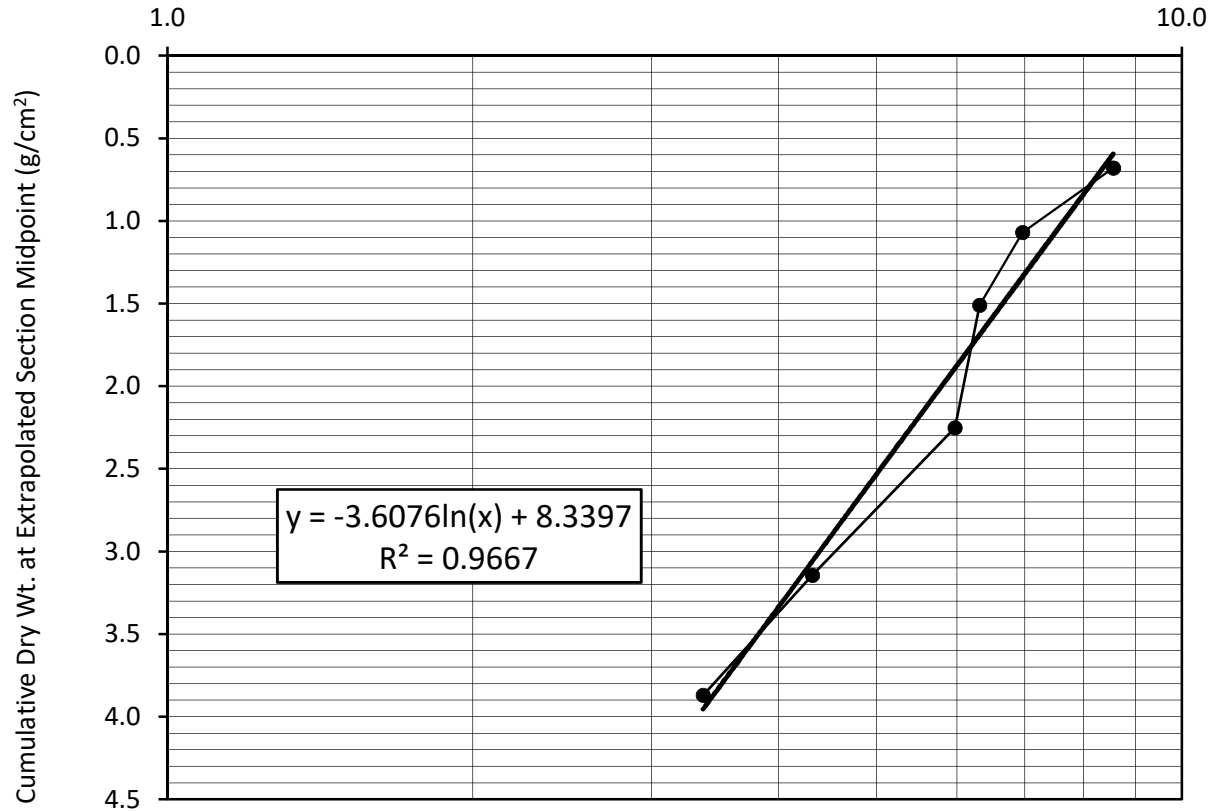


**Regression of Unsupported Pb-210 Activity  
vs. Accumulated Sediment**

(Unsupported activity calculated by subtracting the nearest neighbouring Ra-226 measurement from each total Pb-210 value)

**4B**

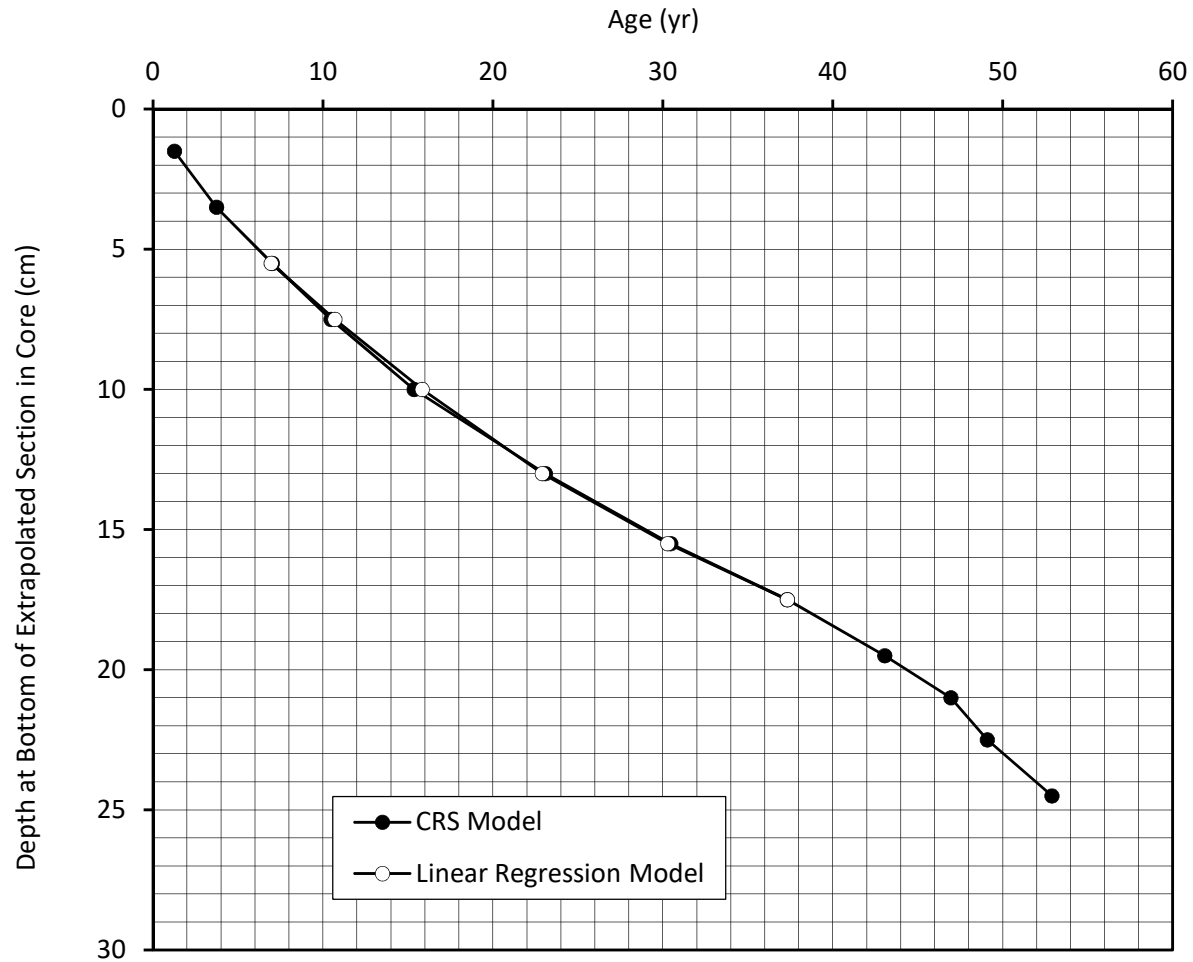
Unsupported Pb-210 Activity (DPM/g Dry Wt.)



**Sediment Accumulation Rate in sections 5 - 17**  
 $= (-3.6076) \times 0.6931 / (-22.3) = 0.1121 \text{ g/cm}^2/\text{yr}$

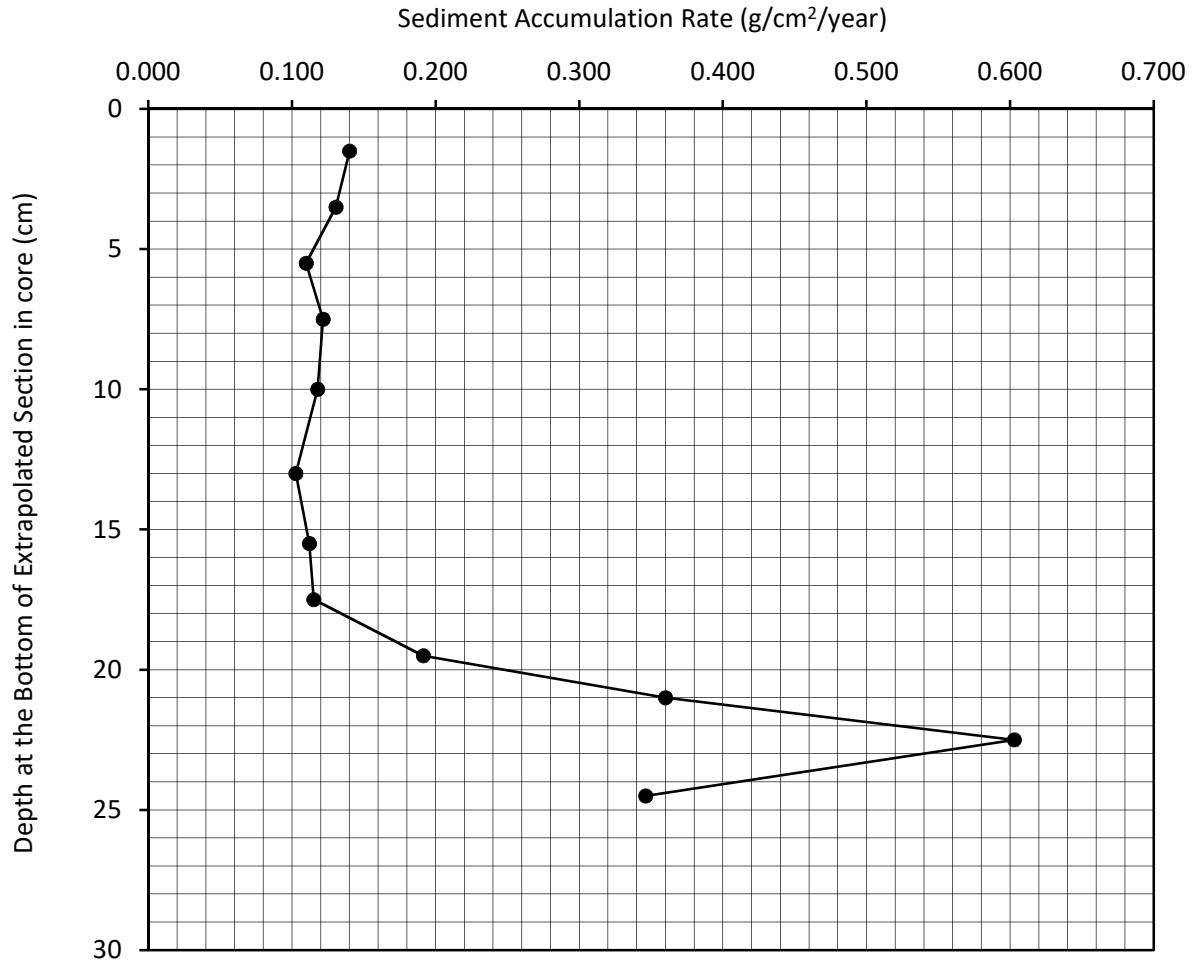
Age (yr) vs. Depth (cm)  
CRS Model vs. Linear Regression Model

4B



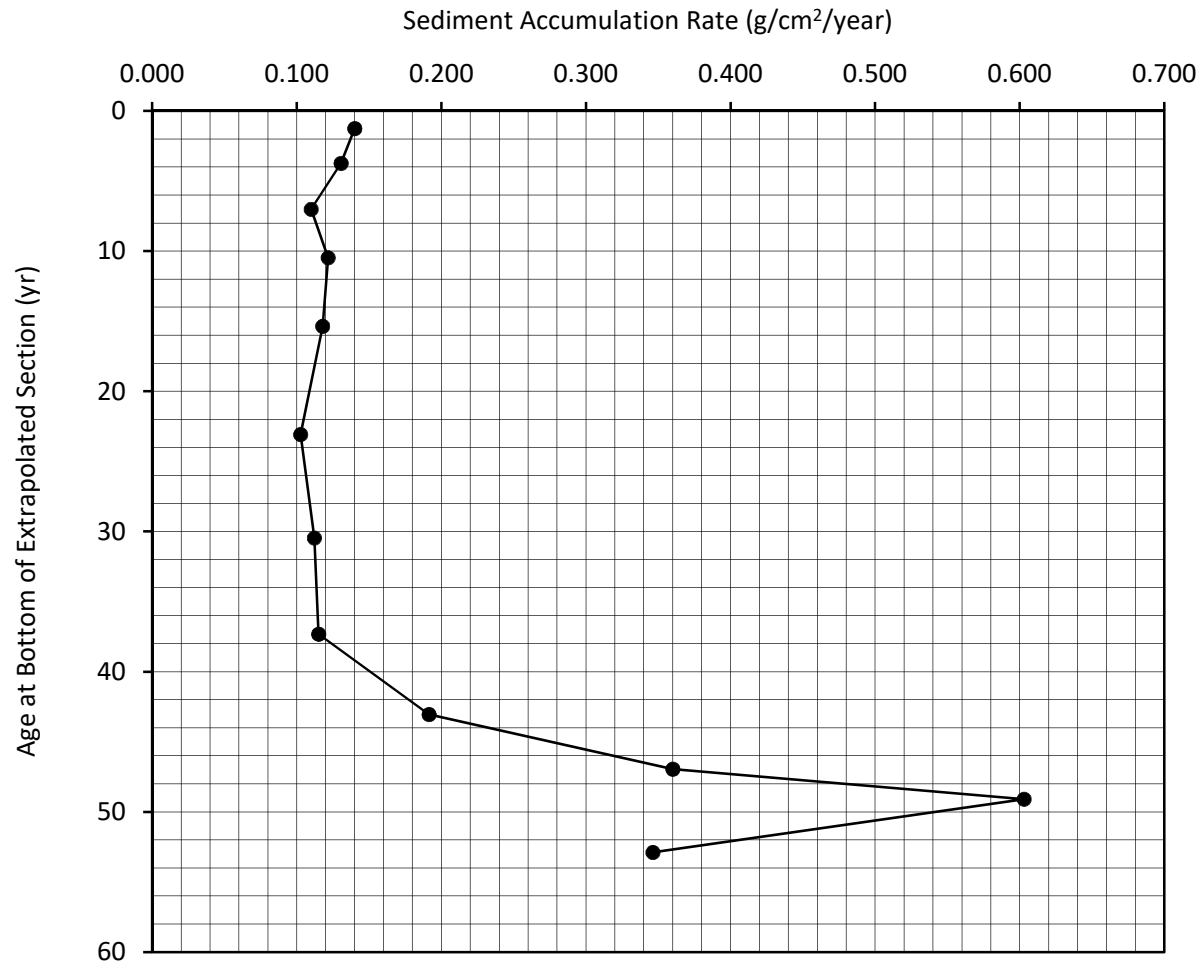
**CRS Sediment Accumulation Rate (g/cm<sup>2</sup>/year)**  
**vs. Depth at the Bottom of Extrapolated Section in Core (cm)**

**4B**



**CRS Sediment Accumulation Rate (g/cm<sup>2</sup>/year)**  
**vs. Age at Bottom of Extrapolated Section (yr)**

**4B**



# Results of Ra-226 Analysis by Rn-222 Emanation

## Flett Research Ltd.

440 DeSalaberry Ave., Winnipeg, MB R2L 0Y7

Fax/Phone: (204) 667-2505

Email: flett@flettresearch.ca Webpage: http://www.flettresearch.ca

### Client: Lorrain, Stéphane

Address: SNC-LAVALIN GEM QUÉBEC INC., 455, boul. René-Lévesque ouest, Montréal (Québec) H2Z 1Z3

Core ID: **4B**

Transaction ID: 882

Date Received: 20-Feb-19

PO/Contract No.: 653502-0028

Sampling Date: 9-Feb-19

Analysis Dates: April 16 - June 22, 2019

Project: #653502

Analysts: L. Hesketh-Jost; X. Hu

Salt Correction Applied? No

Analytical Method: N40110 Determination of Radium-226 in Sediment, Soil and Peat by Radon-222 Emanation (Version 3)

#### Comments:

**Detection Limit:** The method detection limit (MDL) is dependent on the amount of sample analyzed. For a 60,000 second counting time the MDL at 95% confidence for 2 g of dry sample is 0.1 DPM/g and for 0.5 g of dry sample is 0.5 DPM/g.

**Estimated Uncertainty:** The estimate of uncertainty of measurement for this method in this laboratory is approximately  $\pm 12\%$  at 95% confidence level (approximately 40,000 counts in 60,000 seconds).

Results authorized by Dr. Robert J. Flett, Chief Scientist

Core ID	Sample ID	Ra-226 Activity (DPM/g Dry Wt.)	Combined Error: 1 SD (DPM/g Dry Wt.)	Comments Code for Ra-226 Analysis
4B	4B-2/2-31	0.35	0.04	
4B	4B-2/2-7	1.07	0.04	
4B	4B-2/2-17	1.05	0.03	
4B	4B-2/2-19	0.93	0.04	
4B	4B-2/2-21	0.52	0.03	
4B	4B-2/2-22	0.50	0.03	
4B	4B-2/2-24	0.47	0.03	

Q:\Clients A-L\Lorrain, Stephane\2019(882)\Radioisotopes\4B\Pb-210, Ra-226 and Cs-137 Lorrain Core 4B Jun 27-19 Final.xlsm

**Duplicate:** Two subsamples of the same sample were carried through the analytical procedure in an identical manner.

**Re-count:** The sample bottle was re-sealed after the initial analysis, and was re-counted after 11 or more days of Rn-222 ingrowth. Repeat counting was chosen over duplicate analysis due to insufficient sample material provided.

This test report shall not be reproduced, except in full, without written approval of the laboratory.

22-Jun-19

Note: Results relate only to the items tested.

Page 9 of 21

ISO / IEC 17025:2005 Accredited with the Canadian Association for Laboratory Accreditation (CALA Accreditation No. A3306)

**Radium Analysis by Rn-222 Emanation**

Core ID	4B
Sample ID	4B-2/2-31
Lucas Cell No.	3
Number of days since Rn board last run	1
Dry weight of sample counted (g)	0.946
Total count in period	1594
Total count in period (carryover corrected)	n/a
Cell Blank count (CPM)	0.562
System Blank (DPM)	0.395
System Efficiency	0.839
Count duration (minutes)	1000

Typical carryover is about 1 - 2 % of the net counts (gross counts less system background) of the sample counted on the previous day. The carryover is subtracted from the gross counts of current sample. This correction is not required if the sample is run after a blank.

Carryover correction?	No
-----------------------	----

	Year	Month	Day	Hour	Minute	Second	Ingrowth time (Days)	Ingrowth factor	Decay correction
When sample last stripped	2019	4	18	15	19	0	14.88	0.93260	0.92494
When cell filled	2019	5	3	12	31	0			
Beginning time of count	2019	5	3	14	31	0			

Counts per minute	1.59
Gross CPM less Cell Blank (CPM)	1.03
CPM (decay during count corrected)	1.12
DPM Sample +System (efficiency corrected)	1.33
DPM sample	1.00
DPM/g	1.06
<b>Ra-226 DPM/g</b>	<b>0.35</b>
Ra-226 pCi/g	0.16

Error ± 1 sd    0.1031 DPM

**Error ± 1 sd    0.0363 DPM/g**

Error % =    10.3

Chemist	XH
PMT High Voltage +ve	770
HV Power supply	Spectrum Technologies
Alpha Counter	Spectrum Technologies
Region of Interest Ch.#s	28-1022
PMT	6655A - #1
Preamp	Canberra 2007P tube base
Amp Gain	1

**Radium Analysis by Rn-222 Emanation**

Core ID	4B
Sample ID	4B-2/2-7
Lucas Cell No.	3
Number of days since Rn board last run	1
Dry weight of sample counted (g)	1.075
Total count in period	3179
Total count in period (carryover corrected)	n/a
Cell Blank count (CPM)	0.547
System Blank (DPM)	0.389
System Efficiency	0.840
Count duration (minutes)	1000

Typical carryover is about 1 - 2 % of the net counts (gross counts less system background) of the sample counted on the previous day. The carryover is subtracted from the gross counts of current sample. This correction is not required if the sample is run after a blank.

Carryover correction?	No
-----------------------	----

	Year	Month	Day	Hour	Minute	Second	Ingrowth time (Days)	Ingrowth factor	Decay correction
When sample last stripped	2019	5	17	12	32	0	11.10	0.86630	0.92490
When cell filled	2019	5	28	15	1	10			
Beginning time of count	2019	5	28	17	1	34			

Counts per minute	3.18
Gross CPM less Cell Blank (CPM)	2.63
CPM (decay during count corrected)	2.85
DPM Sample +System (efficiency corrected)	3.39
DPM sample	3.46
DPM/g	3.22
<b>Ra-226 DPM/g</b>	<b>1.07</b>
Ra-226 pCi/g	0.48

Error ± 1 sd    0.1173 DPM

**Error ± 1 sd    0.0364 DPM/g**

Error % =    3.4

Chemist	XH
PMT High Voltage +ve	770
HV Power supply	Spectrum Technologies
Alpha Counter	Spectrum Technologies
Region of Interest Ch.#s	28-1022
PMT	6655A - #1
Preamp	Canberra 2007P tube base
Amp Gain	1

**Radium Analysis by Rn-222 Emanation**

Core ID	4B
Sample ID	4B-2/2-17
Lucas Cell No.	3
Number of days since Rn board last run	1
Dry weight of sample counted (g)	1.313
Total count in period	3720
Total count in period (carryover corrected)	3698
Cell Blank count (CPM)	0.547
System Blank (DPM)	0.389
System Efficiency	0.840
Count duration (minutes)	1000

Typical carryover is about 1 - 2 % of the net counts (gross counts less system background) of the sample counted on the previous day. The carryover is subtracted from the gross counts of current sample. This correction is not required if the sample is run after a blank.			
Carryover correction?	Yes	Mean of last 10 carryover measurements	0.96%
Gross counts of previous sample	3179	Mean of last 6 system background measurements	874
Counts carried over from previous sample	22		

	Year	Month	Day	Hour	Minute	Second	Ingrowth time (Days)	Ingrowth factor	Decay correction
When sample last stripped	2019	5	17	12	32	0	12.03	0.88701	0.92490
When cell filled	2019	5	29	13	18	49			
Beginning time of count	2019	5	29	15	19	12			

Counts per minute	3.70
Gross CPM less Cell Blank (CPM)	3.15
CPM (decay during count corrected)	3.41
DPM Sample +System (efficiency corrected)	4.06
DPM sample	4.13
DPM/g	3.15
<b>Ra-226 DPM/g</b>	<b>1.05</b>
Ra-226 pCi/g	0.47

Error ± 1 sd    0.1208 DPM

**Error ± 1 sd    0.0307 DPM/g**

Error % =    2.9

Chemist	XH
PMT High Voltage +ve	770
HV Power supply	Spectrum Technologies
Alpha Counter	Spectrum Technologies
Region of Interest Ch.#s	28-1022
PMT	6655A - #1
Preamp	Canberra 2007P tube base
Amp Gain	1

**Radium Analysis by Rn-222 Emanation**

Core ID	4B
Sample ID	4B-2/2-19
Lucas Cell No.	3
Number of days since Rn board last run	1
Dry weight of sample counted (g)	1.011
Total count in period	2766
Total count in period (carryover corrected)	2753
Cell Blank count (CPM)	0.547
System Blank (DPM)	0.389
System Efficiency	0.840
Count duration (minutes)	1000

Typical carryover is about 1 - 2 % of the net counts (gross counts less system background) of the sample counted on the previous day. The carryover is subtracted from the gross counts of current sample. This correction is not required if the sample is run after a blank.

Carryover correction?	Yes	Mean of last 10 carryover measurements	0.96%
Gross counts of previous sample	2214	Mean of last 6 system background measurements	874
Counts carried over from previous sample	13		

	Year	Month	Day	Hour	Minute	Second	Ingrowth time (Days)	Ingrowth factor	Decay correction
When sample last stripped	2019	6	7	11	52	0	11.20	0.86854	0.92490
When cell filled	2019	6	18	16	35	41			
Beginning time of count	2019	6	18	18	36	5			

Counts per minute	2.75
Gross CPM less Cell Blank (CPM)	2.21
CPM (decay during count corrected)	2.39
DPM Sample +System (efficiency corrected)	2.84
DPM sample	2.82
DPM/g	2.79
<b>Ra-226 DPM/g</b>	<b>0.93</b>
Ra-226 pCi/g	0.42

Error ± 1 sd    0.1135 DPM

**Error ± 1 sd    0.0374 DPM/g**

Error % =    4.0

Chemist	XH
PMT High Voltage +ve	770
HV Power supply	Spectrum Technologies
Alpha Counter	Spectrum Technologies
Region of Interest Ch.#s	28-1022
PMT	6655A - #1
Preamp	Canberra 2007P tube base
Amp Gain	1

Q:\Clients A-L\Lorrain, Stephane\2019(882)\Radioisotopes\4B\Pb-210, Ra-226 and Cs-137 Lorrain Core 4B Jun 27-19 Final.xlsm

19-Jun-19

Page 13 of 21

**Radium Analysis by Rn-222 Emanation**

Core ID	4B
Sample ID	4B-2/2-21
Lucas Cell No.	3
Number of days since Rn board last run	1
Dry weight of sample counted (g)	1.089
Total count in period	2048
Total count in period (carryover corrected)	2030
Cell Blank count (CPM)	0.547
System Blank (DPM)	0.389
System Efficiency	0.840
Count duration (minutes)	1000

Typical carryover is about 1 - 2 % of the net counts (gross counts less system background) of the sample counted on the previous day. The carryover is subtracted from the gross counts of current sample. This correction is not required if the sample is run after a blank.

Carryover correction?	Yes	Mean of last 10 carryover measurements	0.96%
Gross counts of previous sample	2766	Mean of last 6 system background measurements	874
Counts carried over from previous sample	18		

	Year	Month	Day	Hour	Minute	Second	Ingrowth time (Days)	Ingrowth factor	Decay correction
When sample last stripped	2019	6	7	11	52	0	12.12	0.88880	0.92490
When cell filled	2019	6	19	14	45	25			
Beginning time of count	2019	6	19	16	45	48			

Counts per minute	2.03
Gross CPM less Cell Blank (CPM)	1.48
CPM (decay during count corrected)	1.60
DPM Sample +System (efficiency corrected)	1.91
DPM sample	1.71
DPM/g	1.57
<b>Ra-226 DPM/g</b>	<b>0.52</b>
Ra-226 pCi/g	0.24

Error ± 1 sd    0.1069 DPM

**Error ± 1 sd    0.0327 DPM/g**

Error % =    6.3

Chemist	XH
PMT High Voltage +ve	770
HV Power supply	Spectrum Technologies
Alpha Counter	Spectrum Technologies
Region of Interest Ch.#s	28-1022
PMT	6655A - #1
Preamp	Canberra 2007P tube base
Amp Gain	1

**Radium Analysis by Rn-222 Emanation**

Core ID	4B
Sample ID	4B-2/2-22
Lucas Cell No.	3
Number of days since Rn board last run	1
Dry weight of sample counted (g)	1.078
Total count in period	1996
Total count in period (carryover corrected)	1985
Cell Blank count (CPM)	0.547
System Blank (DPM)	0.389
System Efficiency	0.840
Count duration (minutes)	1000

Typical carryover is about 1 - 2 % of the net counts (gross counts less system background) of the sample counted on the previous day. The carryover is subtracted from the gross counts of current sample. This correction is not required if the sample is run after a blank.			
Carryover correction?	Yes	Mean of last 10 carryover measurements	0.96%
Gross counts of previous sample	2048	Mean of last 6 system background measurements	874
Counts carried over from previous sample	11		

	Year	Month	Day	Hour	Minute	Second	Ingrowth time (Days)	Ingrowth factor	Decay correction
When sample last stripped	2019	6	7	11	51	0	13.07	0.90642	0.92490
When cell filled	2019	6	20	13	35	50			
Beginning time of count	2019	6	20	15	36	13			

Counts per minute	1.98
Gross CPM less Cell Blank (CPM)	1.44
CPM (decay during count corrected)	1.55
DPM Sample +System (efficiency corrected)	1.85
DPM sample	1.61
DPM/g	1.50
<b>Ra-226 DPM/g</b>	<b>0.50</b>
Ra-226 pCi/g	0.22

Error ± 1 sd    0.1063 DPM

**Error ± 1 sd    0.0329 DPM/g**

Error % =    6.6

Chemist	XH
PMT High Voltage +ve	770
HV Power supply	Spectrum Technologies
Alpha Counter	Spectrum Technologies
Region of Interest Ch.#s	28-1022
PMT	6655A - #1
Preamp	Canberra 2007P tube base
Amp Gain	1

**Radium Analysis by Rn-222 Emanation**

Core ID	4B
Sample ID	4B-2/2-24
Lucas Cell No.	3
Number of days since Rn board last run	1
Dry weight of sample counted (g)	1.056
Total count in period	1916
Total count in period (carryover corrected)	1905
Cell Blank count (CPM)	0.547
System Blank (DPM)	0.389
System Efficiency	0.840
Count duration (minutes)	1000

Typical carryover is about 1 - 2 % of the net counts (gross counts less system background) of the sample counted on the previous day. The carryover is subtracted from the gross counts of current sample. This correction is not required if the sample is run after a blank.			
Carryover correction?	Yes	Mean of last 10 carryover measurements	0.96%
Gross counts of previous sample	1996	Mean of last 6 system background measurements	874
Counts carried over from previous sample	11		

	Year	Month	Day	Hour	Minute	Second	Ingrowth time (Days)	Ingrowth factor	Decay correction
When sample last stripped	2019	6	7	11	51	0	14.01	0.92103	0.92490
When cell filled	2019	6	21	12	3	55			
Beginning time of count	2019	6	21	14	4	18			

Counts per minute	1.91
Gross CPM less Cell Blank (CPM)	1.36
CPM (decay during count corrected)	1.47
DPM Sample +System (efficiency corrected)	1.75
DPM sample	1.48
DPM/g	1.40
<b>Ra-226 DPM/g</b>	<b>0.47</b>
Ra-226 pCi/g	0.21

Error ± 1 sd    0.1055 DPM

**Error ± 1 sd    0.0333 DPM/g**

Error % =    7.2

Chemist	XH
PMT High Voltage +ve	770
HV Power supply	Spectrum Technologies
Alpha Counter	Spectrum Technologies
Region of Interest Ch.#s	28-1022
PMT	6655A - #1
Preamp	Canberra 2007P tube base
Amp Gain	1

# Results of Cs-137 Analysis

Flett Research Ltd.

440 DeSalaberry Ave. Winnipeg, MB R2L 0Y7

Fax / Phone: (204) 667-2505

Email: flett@flettresearch.ca Webpage: http://www.flettresearch.ca

**Client: Lorrain, Stéphane**

**Address:** SNC-LAVALIN GEM QUÉBEC INC., 455, boul. René-Lévesque ouest, Montréal (Québec) H2Z 1Z3

**Core ID:** 4B  
**Date Received:** 20-Feb-19  
**Sampling Date:** 9-Feb-19  
**Project:** #653502

**Transaction ID:** 882  
**PO/Contract No.:** 653502-0028  
**Analysis Dates:** May 23 - June 11, 2019  
**Analysts:** X. Hu

Salt Correction?	No
------------------	----

**Analytical Method:** N30120 Measurement of Gamma-Ray Emitting Radionuclides in Sediment/Soil Samples by Gamma Spectrometry Using HPGe Detectors (Version 2)

**Deviation from Method:**

**Comments:** <2SD: The measured Cs-137 activity is less than 2 counting errors (i.e. 2 SD), suggesting no significant presence of Cs-137 in this sample.

**Detection Limit:** The method detection limit (MDL) is 0.3 DPM/g for an 80,000 seconds counting period when measuring a 9 g of dry sample at a 95% confidence level. The method detection limit can be decreased to 0.1 DPM/g if 32 g of sample is used.

**Estimated Uncertainty:** The estimated uncertainty of this method has been determined to be: 10% at 95% confidence for samples with activities between 0.5 and 20 DPM/g, counting time 80,000 seconds and sample weights ranging from 9 to 32 grams. Method uncertainty can increase to 85% for samples with activities near detection limit (0.1 - 0.3 DPM/g).

Results authorized by Dr. Robert J. Flett, Chief Scientist

Sample ID	Upper Depth (cm)	Lower Depth (cm)	Day Sample Counted	Month Sample Counted	Year Sample Counted	Integral NET Cs-137 Peak	Counting Error 1 SD (Counts)	Count Time (seconds)	Dry Sample Weight (g)	Sample Thickness (mm)	CPM/g	Efficiency for Gammas Fractional	Gammas per min. per gram	Activity DPM/g (dry wt.) on Counting Date	Approx. Error DPM/g	Activity DPM/g (dry wt.) on Sampling Date	Approx. Error DPM/g	Activity pCi/g (dry wt.) on Sampling Date	Approx. Error pCi/g	Activity mBq/g (dry wt.) on Sampling Date	Approx. Error mBq/g	Detector Used	Comments Code for Cs-137 Analysis
4B-2/2-15	14	15	23	5	2019	313	36	80000	7.914	2.48	0.0297	0.0439	0.6751	0.79	0.09	0.80	0.09	0.36	0.04	13.29	1.52	Canberra	
4B-2/2-17	16	17	23	5	2019	299	47	80000	9.932	3.23	0.0226	0.0287	0.7864	0.92	0.15	0.93	0.15	0.42	0.07	15.48	2.43	GMX	
4B-2/2-19	18	19	23	5	2019	278	38	80000	13.716	3.83	0.0152	0.0254	0.5977	0.70	0.10	0.71	0.10	0.32	0.04	11.77	1.61	GEM	
4B-2/2-21	20	21	25	5	2019	243	49	80000	14.690	3.80	0.0124	0.0284	0.4372	0.51	0.10	0.52	0.10	0.23	0.05	8.61	1.74	GMX	
4B-2/2-22	21	22	25	5	2019	222	36	80000	10.476	3.18	0.0159	0.0259	0.6132	0.72	0.12	0.72	0.12	0.33	0.05	12.07	1.96	GEM	
4B-2/2-23	22	23												1.24	0.06	1.25	0.06	0.56	0.03	20.80	0.96	Canberra	
4B-2/2-24	23	24	27	5	2019	347	45	80000	10.504	2.85	0.0248	0.0289	0.8568	1.01	0.13	1.01	0.13	0.46	0.06	16.87	2.19	GMX	
4B-2/2-25	24	25	6	6	2019	269	31	80000	24.465	5.88	0.0082	0.0240	0.3441	0.40	0.05	0.41	0.05	0.18	0.02	6.78	0.78	GEM	
4B-2/2-26	25	26	27	5	2019	210	35	80000	16.679	4.60	0.0094	0.0249	0.3798	0.45	0.07	0.45	0.07	0.20	0.03	7.48	1.25	GEM	
4B-2/2-28	27	28	28	5	2019	24	32	80000	4.537	1.80	0.0040	0.0448	0.0885	0.10	0.14	0.10	0.14	0.05	0.06	1.74	2.30	Canberra	<2SD
<b>Re-count</b>																							
4B-2/2-23	22	23	6	6	2019	978	44	80000	16.386	4.30	0.0448	0.0416	1.0763	1.26	0.06	1.27	0.06	0.57	0.03	21.21	0.95	Canberra	
4B-2/2-23 Re-count	22	23	10	6	2019	940	44	80000	16.386	4.30	0.0430	0.0416	1.0345	1.21	0.06	1.22	0.06	0.55	0.03	20.39	0.96	Canberra	
<b>Cs-137 Standards</b>																							
GMX 32g 10 mm				4	4	2019	19967	143	5000	32.00	10.0	7.4876	0.0237	315.7600	370.61	2.65	957.04						
GMX 24g 7.5mm				5	4	2019	16045	128	5000	24.00	7.5	8.0225	0.0254	315.7400	370.59	2.96	957.04						
GMX 15g 5mm				4	4	2019	10978	106	5000	15.00	5.0	8.7824	0.0278	315.7600	370.61	3.58	957.04						
GMX 9g 3mm				3	4	2019	6862	84	5000	9.00	3.0	9.1493	0.0290	315.7799	370.63	4.54	957.04						
GMX 2.85g 0.8mm				4	4	2019	2237	49	5000	2.854	0.8	9.4057	0.0298	315.7600	370.61	8.12	957.04						
GEM 32g 10 mm				4	4	2019	17960	139	5000	32.00	10.0	6.7350	0.0213	315.7600	370.61	2.87	957.04						
GEM 24g 7.5mm				4	4	2019	14367	124	5000	24.00	7.5	7.1835	0.0227	315.7600	370.61	3.20	957.04						
GEM 15g 5mm				3	4	2019	9822	102	5000	15.00	5.0	7.8576	0.0249	315.7799	370.63	3.85	957.04						
GEM 9g 3mm				4	4	2019	6102	79	5000	9.00	3.0	8.1360	0.0258	315.7600	370.61	4.80	957.04						
GEM 2.85g 0.8mm				4	4	2019	2093	48	5000	2.854	0.8	8.8003	0.0279	315.7600	370.61	8.50	957.04						
Canberra 32g 10 mm				11	4	2019	29236	172	5000	32.00	10.0	10.9635	0.0347	315.6205	370.45	2.19	957.04						
Canberra 24g 7.5mm				11	4	2019	23302	154	5000	24.00	7.5	11.6510	0.0369	315.6205	370.45	2.44	957.04						
Canberra 15g 5mm				10	4	2019	16207	128	5000	15.00	5.0	12.9656	0.0411	315.6404	370.47	2.93	957.04						
Canberra 9g 3mm				10	4	2019	10285	103	5000	9.00	3.0	13.7133	0.0434	315.6404	370.47	3.70	957.04						
Canberra 2.85g 0.8mm				10	4	2019	3449	60	5000	2.854	0.8	14.5018	0.0459	315.6404	370.47	6.45	957.04						

Q:\Clients A-L\Lorrain, Stephane\2019\882\Radioisotopes\4B\Pb-210, Ra-226 and Cs-137 Lorrain Core 4B Jun 27-19 Final.xlsx

**Duplicate:** Two subsamples of the same sample were carried through the analytical procedure in an identical manner.

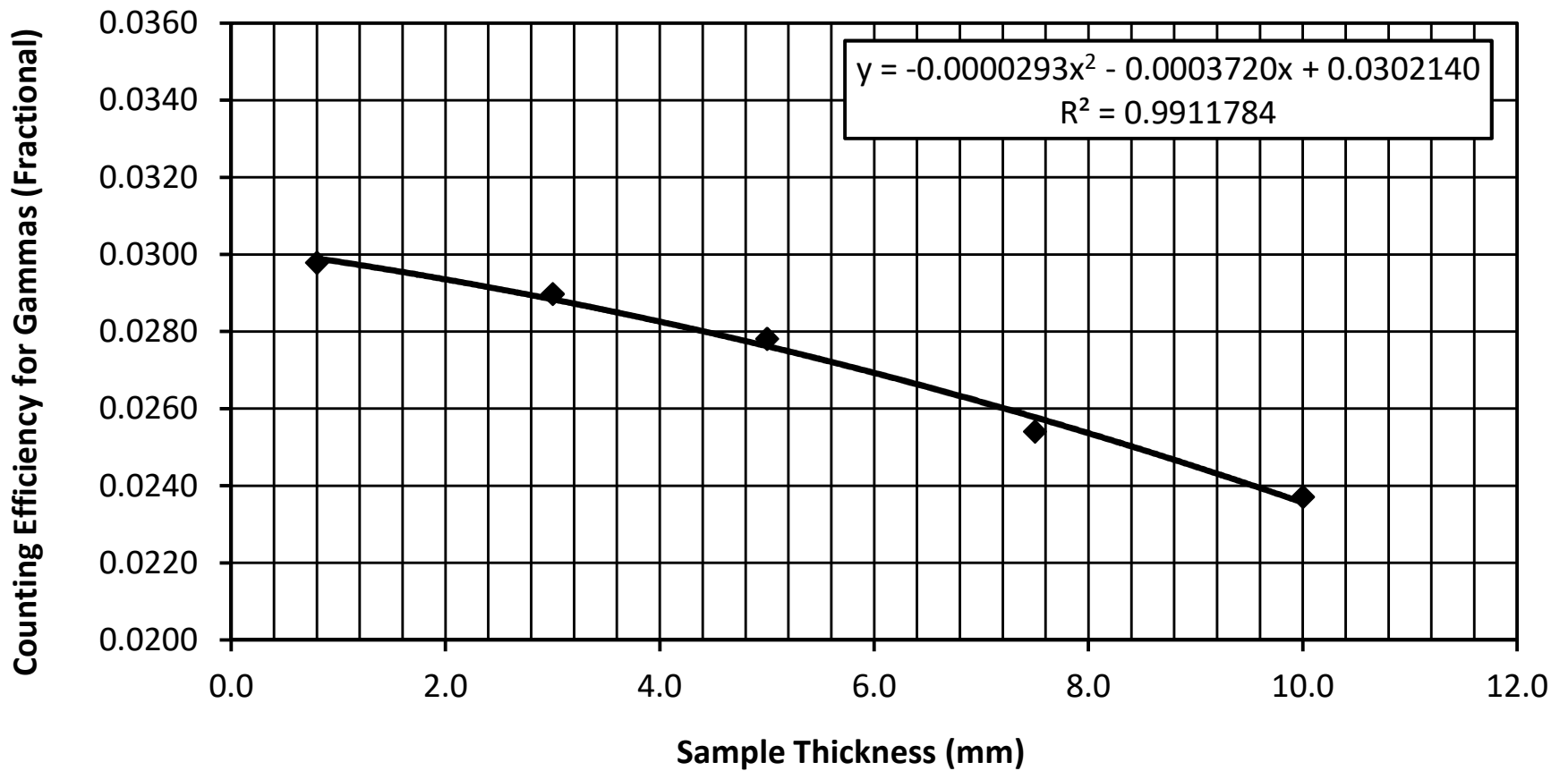
**Re-count:** The entire available dry sample material was used for making the sample pancake, and then this sample pancake was counted twice on a HPGe detector. Repeat counting was chosen over duplicate analysis due to insufficient sample material provided.

**This test report shall not be reproduced, except in full, without written approval of the laboratory.**

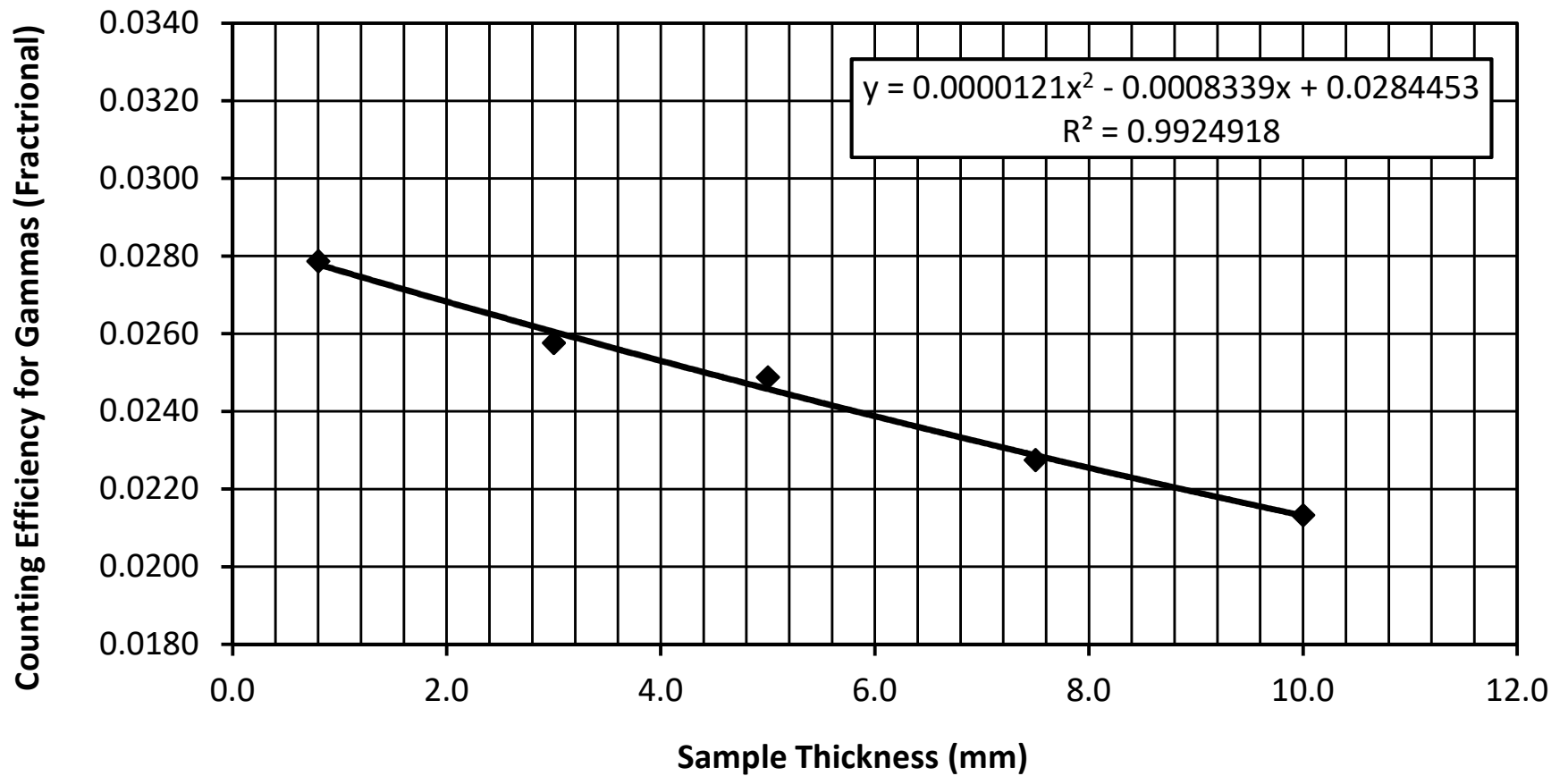
**Note:** Results relate only to the items tested.

ISO / IEC 17025:2005 Accredited with the Canadian Association for Laboratory Accreditation (CALA Accreditation No. A3306)

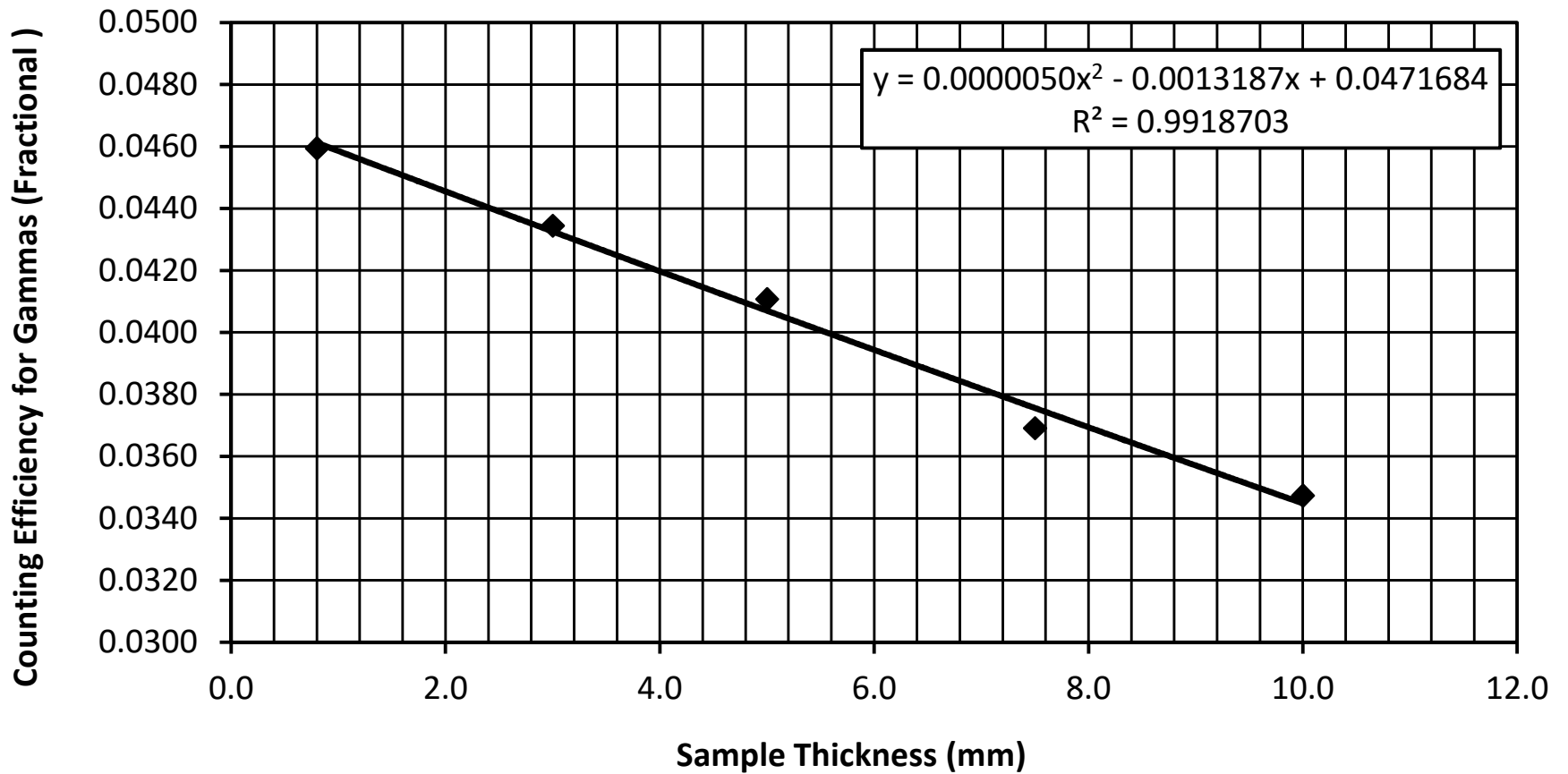
### Cs-137 Counting Efficiency of Gammas vs. Sample Thickness (mm) GMX 25% Detector (Apr 3 - 5 , 2019)



### Cs-137 Counting Efficiency of Gammas vs. Sample Thickness (mm) GEM 19% Detector (Apr 3 - 4 , 2019)



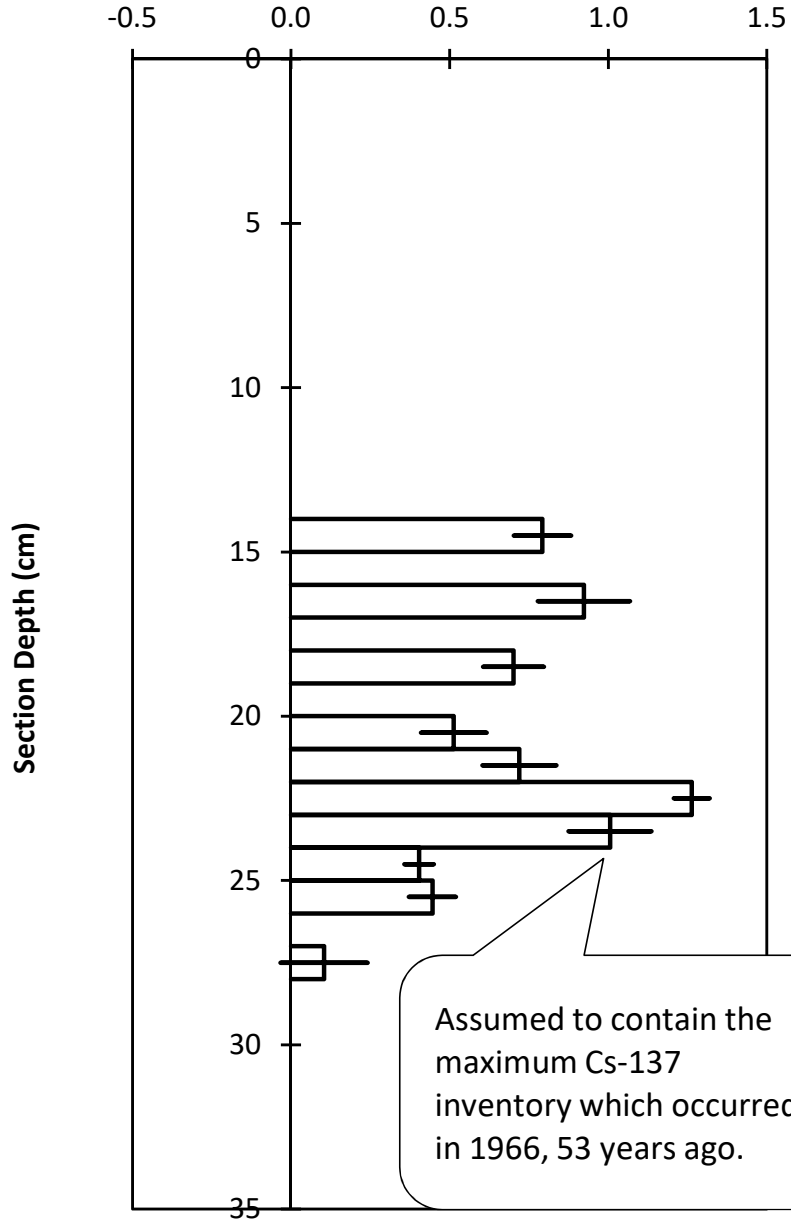
### Cs-137 Counting Efficiency of Gammas vs. Sample Thickness (mm) Canberra 29% Detector (Apr 10 - 11 , 2019)



### Cs-137 in Sediments

#### 4B

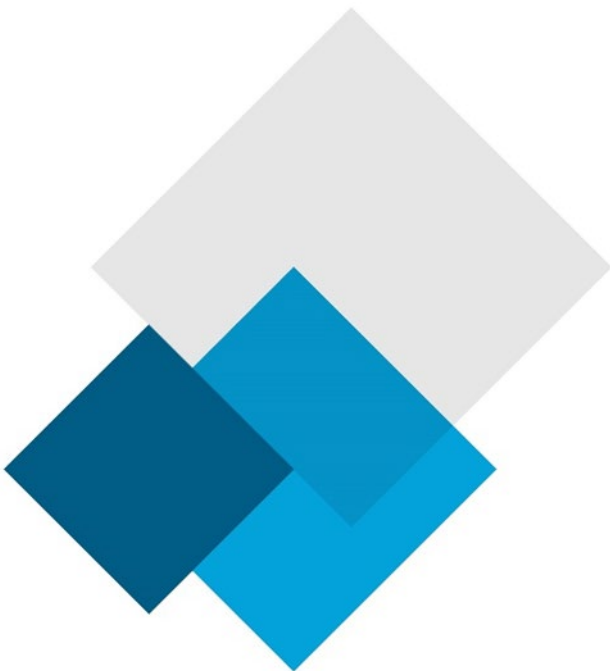
Cs-137 Activity on counting date (DPM/g dry wt.)



Note: The bar plotted at the midpoint depth of each section represents +/- 1 standard deviation of the Cs-137 counting error.

# Appendix 10

Core extraction forms and photos



Core	1A	Field technician
Sampled	2019-02-10 14h40	Pierre-David Beaudry
Collected	2019-02-09 10h40	Pierre-David Beaudry

Sample number	Interval [m]		Nature	Texture	Colour	Odour	Notes	Notes
	top	bottom						
1A-2/2-1	0.0	1.0	sand/silt	watery	brown		vegetation (little)	small shell fragments
1A-2/2-4	3.0	4.0	sand/silt	less watery	brown		vegetation (little)	small shell fragments
1A-2/2-7	6.0	7.0	sand/silt	less watery	brown		vegetation (little)	small shell fragments
1A-2/2-9	8.0	9.0	silt/sand	less watery	brown		vegetation (little)	small shell fragments
1A-2/2-10	9.0	10.0	silt/sand	less watery	brown		vegetation (little)	
1A-2/2-12	11.0	12.0	silt/sand	little thick	brown	smell hydrocarbon	of vegetation (little)	
1A-2/2-15	14.0	15.0	silt/sand	little thick	brown	smell hydrocarbon	of vegetation (little)	
1A-2/2-17	16.0	17.0	clay/sand	thick	brown	smell hydrocarbon	of	Iron oxide forming on bottom of container
1A-2/2-22	21.0	22.0	clay/sand	thick	brown	smell hydrocarbon	of	Iron oxide forming on bottom of container
1A-2/2-24	23.0	24.0	clay/sand	thick	brown	smell hydrocarbon	of	Iron oxide forming on bottom of container
1A-2/2-27	26.0	27.0	clay	thick	brown	smell hydrocarbon	of	Iron oxide forming on bottom of container
1A-2/2-29	28.0	29.0	clay	thick	brown	smell hydrocarbon	of	Iron oxide forming on bottom of container
1A-2/2-31	30.0	31.0	clay	thick	brown	strong smell hydrocarbon	of	Iron oxide forming on bottom of container
1A-2/2-37	36.0	37.0	clay	thick	brown			Iron oxide forming on bottom of container
1A-2/2-42	41.0	42.0	clay	thick	brown			
1A-2/2-51	50.0	51.0	clay	thick	brown			
1A-2/2-59	58.0	59.0	clay	thick	brown			



Core	2A	Field technician
Sampled	2019-02-11 08h30	Pierre-David Beaudry
Collected	2019-02-09 12h00	Pierre-David Beaudry

Sample number	Interval [m]		Nature	Texture	Colour	Odour	Notes	Notes
	top	bottom						
2A-2/2-1	0.0	1.0	silt	very watery	brown		vegetation (plenty)	Large quantity of vegetation
2A-2/2-3	2.0	3.0	silt	very watery	brown		vegetation (plenty)	Large quantity of vegetation
2A-2/2-6	5.0	6.0	silt/sand	less watery	brown		vegetation (little)	
2A-2/2-7	6.0	7.0	silt/sand	less watery	brown		vegetation (little)	
2A-2/2-8	7.0	8.0	silt/sand	less watery	brown			
2A-2/2-10	9.0	10.0	silt/sand	less watery	brown			
2A-2/2-11	10.0	11.0	clay/sand	little thick	brown	smell hydrocarbon	of	
2A-2/2-12	11.0	12.0	clay/sand	little thick	brown	smell hydrocarbon	of	
2A-2/2-15	14.0	15.0	clay/sand	little thick	brown	smell hydrocarbon	of	
2A-2/2-18	17.0	18.0	clay/sand	little thick	dark brown	faint smell hydrocarbon	of	
2A-2/2-23	22.0	23.0	clay/sand	little thick	dark brown	faint smell hydrocarbon	of	
2A-2/2-27	26.0	27.0	clay/sand	little thick	dark brown			vegetation (little)
2A-2/2-33	32.0	33.0	clay/sand	little thick	dark brown			
2A-2/2-38	37.0	38.0	clay/sand	little thick	dark brown			vegetation (little)



Core	3A	Field technician
Sampled	2019-02-11 14h00	Pierre-David Beaudry
Collected	2019-02-09 15h58	Pierre-David Beaudry

Sample number	Interval [m]		Nature	Texture	Colour	Odour	Notes	Notes
	top	bottom						
3A1-2/2-1	0.0	1.0	silt	very watery	light brown			
3A1-2/2-3	2.0	3.0	clay/silt	watery	light brown		vegetation (plenty)	
3A1-2/2-5	4.0	5.0	sand/clay	watery	light brown		vegetation (little)	
3A1-2/2-6	5.0	6.0	sand/clay	watery	light brown		vegetation (little)	Shell fragments
3A1-2/2-8	7.0	8.0	sand/clay	less watery	light brown		vegetation (little)	
3A1-2/2-10	9.0	10.0	sand/clay	less watery	light brown		vegetation (little)	
3A1-2/2-12	11.0	12.0	sand/clay	little thick	light brown			
3A1-2/2-14	13.0	14.0	sand/clay	little thick	light brown			
3A1-2/2-15	14.0	15.0	sand/clay	little thick	light brown			
3A1-2/2-16	15.0	16.0	sand/clay	little thick	light brown			
3A1-2/2-17	16.0	17.0	sand/clay	little thick	light brown			
3A1-2/2-18	17.0	18.0	sand/clay	little thick	light brown			
3A1-2/2-19	18.0	19.0	clay	very thick not much water	grey			
3A1-2/2-20	19.0	20.0	clay	very thick not much water	grey			
3A1-2/2-21	20.0	21.0	clay	very thick not much water	grey			



Core	4A	Field technician
Sampled	2019-02-11 17h00	Pierre-David Beaudry
Collected	2019-02-10 10h20	Pierre-David Beaudry

Sample number	Interval [m]		Nature	Texture	Colour	Odour	Notes	Notes
	top	bottom						
4A-2/2-1	0.0	1.0	silt	very watery	dark brown		vegetation (little)	
4A-2/2-3	2.0	3.0	silt/clay	less watery	dark brown	faint smell of decomposed vegetation	vegetation (little)	
4A-2/2-6	5.0	6.0	silt/clay	less watery	dark brown	See above	vegetation (little)	
4A-2/2-9	8.0	9.0	silt/clay	less watery	dark brown	See above		
4A-2/2-12	11.0	12.0	clay/silt	little thick	dark brown	See above		
4A-2/2-15	14.0	15.0	clay/silt	little thick	dark brown	See above		
4A-2/2-18	17.0	18.0	clay/silt	thick	dark brown			
4A-2/2-21	20.0	21.0	clay/silt	little thick	dark brown	See above		
4A-2/2-24	23.0	24.0	clay/silt	little thick	dark brown			
4A-2/2-27	26.0	27.0	clay/silt	thick	dark brown		shell (fragments)	
4A-2/2-30	29.0	30.0	clay/silt	thick	dark brown		shell (fragments)	
4A-2/2-31	30.0	31.0	clay/silt	thick	dark brown			
4A-2/2-32	31.0	32.0	clay/silt	thick	dark brown			
4A-2/2-33	32.0	33.0	clay/silt	thick	dark brown			
4A-2/2-36	35.0	36.0	silt	thick	black		vegetation (plenty)	Fluffy dark organic material, not a lot of water so fairly thick. Large pieces of wood present in sample. Tried to avoid when sub-sampling
4A-2/2-39	38.0	39.0	silt	thick	black		vegetation (plenty)	Fluffy dark organic material, not a lot of water so fairly thick



Core	2B	Field technician
Sampled	2019-02-11 10h00	Pierre-David Beaudry
Collected	2019-02-09 14h02	Pierre-David Beaudry

Sample number	Interval		Nature	Texture	Colour	Odour	Notes	Notes
	top	bottom						
2B-2/2-1	0.0	1.0	silt	very watery	dark brown		vegetation (little)	Shell fragments and vegetation.
2B-2/2-3	2.0	3.0	silt	very watery	dark brown		vegetation (little)	Shell fragments and vegetation.
2B-2/2-5	4.0	5.0	silt	very watery	dark brown		vegetation (little)	Shell fragments and vegetation.
2B-2/2-7	6.0	7.0	silt	little thick	dark brown		vegetation (little)	
2B-2/2-9	8.0	9.0	silt	watery	dark brown		vegetation (little)	
2B-2/2-11	10.0	11.0	silt	watery	dark brown		vegetation (little)	Shell fragments and vegetation.
2B-2/2-13	12.0	13.0	silt	watery	dark brown		vegetation (little)	
2B-2/2-15	14.0	15.0	silt	less watery	dark brown		vegetation (little)	
2B-2/2-17	16.0	17.0	silt	little thick	dark brown		vegetation (little)	
2B-2/2-19	18.0	19.0	silt	less watery	dark brown	smell of hydrocarbon		
2B-2/2-21	20.0	21.0	silt	less watery	dark brown	smell of hydrocarbon		
2B-2/2-23	22.0	23.0	silt	less watery	dark brown	smell of hydrocarbon		
2B-2/2-25	24.0	25.0	silt/sand	little thick	dark brown		vegetation (little)	
2B-2/2-29	28.0	29.0	silt	less watery	dark brown			
2B-2/2-34	33.0	34.0	silt	little thick	dark brown			
2B-2/2-40	39.0	40.0	silt	little thick	dark brown			
2B-2/2-45	44.0	45.0	clay/silt	little thick	light brown	not noticeable	shell (fragments)	
2B-2/2-51	50.0	51.0	clay/silt	little thick	light brown	not noticeable	shell (fragments)	
2B-2/2-59	58.0	59.0	clay/silt	little thick	light brown	not noticeable	shell (fragments)	
2B-2/2-68	67.0	68.0	clay	thick	grey/black	not noticeable		



Core	4B	Field technician
Sampled	2019-02-11 15h10	Pierre-David Beaudry
Collected	2019-02-10 09h15	Pierre-David Beaudry

Sample number	Interval [m]		Nature	Texture	Colour	Odour	Notes	Notes
	top	bottom						
4B-2/2-1	0.0	1.0	silt	very watery	brown	not noticeable	vegetation (plenty)	
4B-2/2-3	2.0	3.0	silt	very watery	brown	not noticeable	vegetation (plenty)	
4B-2/2-5	4.0	5.0	silt	very watery	brown	not noticeable	vegetation (plenty)	
4B-2/2-7	6.0	7.0	silt	very watery	brown	not noticeable	vegetation (plenty)	
4B-2/2-9	8.0	9.0	silt	less watery	brown	not noticeable	vegetation (plenty)	
4B-2/2-12	11.0	12.0	silt	watery	brown	not noticeable	vegetation (little)	
4B-2/2-15	14.0	15.0	silt	little thick	brown	not noticeable	vegetation (plenty)	
4B-2/2-17	16.0	17.0	silt/sand	little thick	brown	not noticeable	vegetation (plenty)	
4B-2/2-19	18.0	19.0	silt/sand	little thick	brown	not noticeable	shell (fragments)	
4B-2/2-21	20.0	21.0	silt/sand	thick	brown	not noticeable	shell (fragments)	Shell fragments
4B-2/2-22	21.0	22.0	silt/sand	thick	brown	not noticeable	shell (fragments)	Shell fragments
4B-2/2-24	23.0	24.0	silt/sand	thick	brown	not noticeable	shell (fragments)	Shell fragments
4B-2/2-26	25.0	26.0	silt	thick	brown	not noticeable	vegetation (plenty)	Shell fragments
4B-2/2-28	27.0	28.0	silt	thick	brown	not noticeable	vegetation (plenty)	
4B-2/2-31	30.0	31.0	silt	thick	brown	not noticeable	vegetation (plenty)	





**SNC • LAVALIN**

360, Saint-Jacques, 16<sup>th</sup> Floor  
Montreal (Quebec) J3Y 4R3  
514-393-1000 - 514-392-4758  
[www.snclavalin.com](http://www.snclavalin.com)

